UC Berkeley
UC Berkeley Electronic Theses and Dissertations

## Title

Transgenic and genomic analyses of an adaptive cis-regulatory variant in threespine stickleback

## Permalink

https://escholarship.org/uc/item/05g5n2t9

## Author

Stepaniak, Mark Douglas

## Publication Date

2021

Peer reviewed|Thesis/dissertation

eScholarship.org Powered by the California Digital Library
University of California

# Transgenic and genomic analyses of an adaptive cis-regulatory variant in threespine stickleback

by

Mark Douglas Stepaniak

A dissertation submitted in partial satisfaction of the

requirements for the degree of

Doctor of Philosophy

in

Molecular and Cell Biology

in the

Graduate Division

of the

University of California, Berkeley

Committee in charge:

Professor Craig Miller, Chair
Professor Richard Harland
Professor David Weisblat
Professor Noah Whiteman

Spring 2021

Abstract

Transgenic and genomic analyses of an adaptive cis-regulatory variant in threespine stickleback

by

Mark Douglas Stepaniak

Doctor of Philosophy in Molecular and Cell Biology

University of California, Berkeley

Professor Craig Miller, Chair

How populations adapt to their local environment has been a central question in evolutionary biology for the history of the field. Darwin's evolution by natural selection provided a means for how pressures such as predation or resource availability, can select for variations of traits. It was not until the rapid growth of the field of genetics that a mechanism for heritable variation could be identified.

The intersection of population genetics, developmental, evolutionary, and cell biology, allows researchers to probe the underlying means by which populations have been able to adapt. In countless species regions of the genome and genes have been identified that are responsible for evolution by looking for patterns within population genetic data. For example, regions that are highly divergent between populations may drive adaptation to either of the environments. In laboratory crosses quantitative trait loci (QTL) mapping can identify possible candidate genes in the evolution of a trait of interest. Species that have evolved a trait multiple times like armor plating reduction in the threespine stickleback (*Gasterosteus aculeatus*) spark the question: is the same gene, or allele of a specific gene, re-used each time, or does each instance of evolution have a unique genetic mechanism? While the answer is undoubtedly somewhere between the two extremes, where exactly the answer falls on the spectrum is constantly being re-evaluated.

The threespine stickleback is an ideal system to study how populations adapt. A small, marine species, found throughout the Northern Hemisphere, the stickleback has repeatedly colonized an incredible range of freshwater habitats. Following colonization, sticklebacks tend to evolve certain traits, most famously a loss or reduction of armor plating and pelvic spines. For the majority of traits in which candidate genes have been identified, it appears that changes in gene regulation is what drives the differences in phenotype between the ancestral marine and derived freshwater ecotypes, and often the same gene or even allele is re-used. Overall, very few cases have implicated coding changes in the evolution of specific traits.

The rarity of coding mutations underlying examples of stickleback evolution reflects a broader conversation in evolutionary biology. As genetics and molecular biology matured the incredible degree of homology between orthologous proteins across the tree of life led to the hypothesis that evolution can occur not only by mutations in coding regions, thereby changing the proteins, but by modifying where, when, and how genes, and subsequently proteins are expressed. *Cis*-regulatory elements control gene transcription, causing tissue and time specific expression of the gene, as well as modulating the intensity of expression. Changes in *cis*-

regulatory regions can reduce organism wide, or pleiotropic, effects, compared to coding changes, and target specific aspects of a gene's activity or function. Genes essential for development are controlled by multiple regulatory elements and so mutations in these elements can lead to evolutionary change.

The central focus of this dissertation serves as an example of each of the two previously stated concepts in evolutionary biology: 1) adaptation through the re-use of alleles and 2) adaptation through changes in the *cis*-regulation of developmental genes. Another trait that can evolve following colonization of freshwater environments by marine fish is an increase in pharyngeal tooth number, and is thought to be driven by *cis*-regulatory changes. The increase in tooth number is thought to be an adaptation to a newly available niche or resource.

When comparing a high toothed population from Paxton Lake and a low toothed marine population, the tooth numbers are similar in young fish but later in development a difference arises. Using QTL mapping, the candidate gene *Bmp6* was identified as potentially underlying evolved tooth gain, a result replicated in multiple freshwater populations. Allele specific expression data found differences in *Bmp6* expression between the marine and freshwater allele that occurred in a similar time frame as the tooth number difference, suggesting a change in regulation of the gene underlies the tooth number divergence. Comparing genomic sequence of chromosomes that had an effect on tooth number and those that did not yielded a set of six single nucleotide polymorphisms (SNPs) upstream of a tooth enhancer for *Bmp6* that co-occur with the presence of the QTL peak. I hypothesize the SNPs modulate the activity of the tooth enhancer, resulting in differences in *Bmp6* expression and thereby affecting tooth number. The six SNPs define a high-tooth associated haplotype which was identified in multiple QTL crosses with fish from different, geographically isolated populations and is, therefore, likely standing genetic variation. If the haplotype underlies the evolved tooth gain in multiple populations then it would be another example of evolution "re-using" alleles, and an example of evolution via changes in *cis*-regulation.

This dissertation can be broken down into three questions:

1. Do high and low tooth associated alleles of the *Bmp6* tooth enhancer drive different expression patterns?
2. Can the alleles be replaced through editing, exchanging a high-tooth associated allele with a low-tooth associated/marine allele in a freshwater fish?
3. Has the high-tooth associated allele experienced selection in wild populations?

The answers from the three questions can begin to address a larger question: Is the haplotype responsible for evolved tooth gain, and if so through what mechanism?

Chapter 1 explains the scope of the dissertation, the two big ideas that form the current model for potential adaptation through the haplotype: evolution via *cis*-regulatory changes in developmental genes and the use of standing genetic variation to drive local adaptation. In both instances, the threespine stickleback is an ideal system for both the repeated "natural experiments" and prevalence of *cis*-regulatory examples already characterized in the species. The chapter also details the history of the haplotype in research and the evidence, before this dissertation work, that supports *cis*-regulatory changes in the gene as driving evolved tooth gain.

Chapter 2 details expression pattern differences between a high-tooth haplotype containing and low-tooth haplotype containing alleles of the *Bmp6* tooth enhancer. Two methods were used, with independent transgenes for each enhancer/reporter, and a single bicistronic

construct that allows comparison of enhancers within a single organism, while controlling for positional insertion effects. Expression differences in both domains of the tooth enhancer, the condensed mesenchyme and the overlying epithelium of pre-eruption teeth, were identified. Patterns were consistent across multiple integrations and methods. Differences in the extent of expression domains, stages of fish, and tooth plates (ventral compared to dorsal), mirrors previous work such as the *Bmp6* allele specific expression result, suggesting the haplotypes may have a role in regulating *Bmp6* and subsequently, impacting tooth number.

In chapter 3, the CRISPR/Cas9 system is used to replace a high tooth associated allele in freshwater stock fish with a low tooth associated/marine allele. CRISPR/Cas9 has had success inducing insertions or deletions for gene knockout experiments and repairing small mutations. More rarely has it been used to replace large stretches of sequence, and in most instances where it has been used for that purpose, the sequences being exchanged are either non-homologous, or divergent orthologues. In this experiment, the sequences have high degrees of similarity making partial replacement a potential outcome. Multiple chimeric alleles were created, in some case containing just portions of replaced haplotype, while in other cases complete replacement appears to have occurred. As the replacement was demonstrated in $F_0$ fish a phenotypic effect of the replacement has not been determined. However, multiple partial or complete replacement alleles have been propagated and subsequent experiments could examine tooth number in the transgenic lineages, determining the impact of different chimeric alleles on the trait, and even potentially testing individual sites within the haplotype.

Lastly, in chapter 4, whole genome sequence data from a wild population, Fishtrap Creek, was scanned for signals of natural selection surrounding the haplotype. The creek was formed approximately 10,000 years ago and likely colonized soon after. The haplotype is segregating within the population and was found in other populations in the Pacific northwest, expanding the range of the allele and supporting the model it was present as standing genetic variation. Multiple metrics were calculated for the entire genome of the data set, including pairwise nucleotide diversity $\pi$, Tajima's D, iHS, and nSL. A relatively new method, using ancestral recombination graphs with the program Relate, was also performed. Overall, variation existed in the scores for the single site metrics (iHS, nSL, Relate) and consistently resulted in the same site having elevated scores compared to the others within the haplotype. The site creates a binding site for the transcription factor NFATc1 which has a role in maintaining stem cell quiescence in hair follicle stem cells. This result supports further experiments, such as those in chapters 1 and 2 that focus on this specific site as a potential causative mutation for the observations in chapter 1.

*For my family, Molly and Calder*

“One of the beautiful things about science is that it allows us to bumble along, getting it wrong time after time, and feel perfectly fine as long as we learn something each time.”
-Martin A. Schwartz

# Table of Contents

List of Figures ..... v
List of Tables ..... vii
Acknowledgments ..... viii

**Chapter 1: Introduction ..... 1**
1.1 The growth of Evo-Devo and the importance of gene regulation ..... 1
1.2 Sticklebacks as a model for evolutionary biology and local adaptation ..... 1
1.3 Evolved tooth gain in sticklebacks is driven by a *cis*-regulation of the gene *Bmp6* ..... 2
1.4 Standing genetic variation ..... 3
1.5 Overview of projects ..... 4
1.6 Dissertation scope and overview ..... 6
1.7 References ..... 6

**Chapter 2: Evolved *Bmp6* enhancer alleles drive spatial shifts in gene expression during tooth development ..... 15**
2.1 Abstract ..... 15
2.2 Introduction ..... 16
2.3 Materials and Methods ..... 18
2.4 Results ..... 20
2.5 Discussion ..... 32
2.6 References ..... 37
2.7 Supplemental Materials ..... 43

**Chapter 3: Replacement of population specific enhancer alleles in threespine stickleback using the CRISPR/Cas9 system ..... 56**
3.1 Abstract ..... 56
3.2 Introduction ..... 56
3.3 Methods ..... 58
3.4 Results ..... 64
3.5 Discussion ..... 70
3.6 References ..... 76
3.7 Supplemental Materials ..... 81

**Chapter 4: Population genetics of an adaptive *cis*-regulatory allele of the gene *Bmp6*..... 82**
4.1 Abstract..... 82
4.2 Introduction..... 82
4.3 Methods..... 86
4.4 Results..... 90
4.5 Conclusion..... 109
4.6 References..... 114

# List of Figures


Figure 2.1 An insulated bicistronic construct reports separate expression patterns from two different enhancers. ..... 23

Figure 2.2 A bicistronic construct using a genetic insulator separates the expression domains of the marine and freshwater alleles of the *Bmp6* tooth enhancer..... 24

Figure 2.3 Reduced mesenchymal and expanded epithelial expression of freshwater enhancer relative to marine enhancer in developing teeth. ..... 26

Figure 2.4 Marine and freshwater *Bmp6* enhancers drive more similar spatial patterns in younger fish. ..... 28

Figure 2.5 Differences in enhancer activity vary based on dorsal vs. ventral tooth field, fish total length, and epithelial vs. mesenchymal domain. ..... 30

Figure 2.6 In situ hybridization illustrates that *Bmp6* expression shifts mirror enhancer activity differences in marine and freshwater backgrounds. ..... 32

Figure 2.7 A model for the role of *Bmp6 cis*-regulatory changes in underlying evolved tooth gain in sticklebacks. ..... 34

Figure S 2.1 Sequence alignment of marine and freshwater alleles of *Bmp6* tooth enhancer. ..... 43

Figure S 2.2 *Col2a1a* enhancer drives reporter expression in craniofacial cartilage and notochord in developing stickleback embryos. ..... 44

Figure S 2.3 Marine and freshwater *Bmp6* enhancers drive different spatial patterns in dorsal pharyngeal replacement teeth..... 45

Figure S 2.4 Freshwater allele drives expression in more intersegmental joints of both pectoral and caudal fins compared to the marine allele. ..... 47

Figure S 2.5 Fin expression patterns of both alleles change over developmental time..... 48

Figure S 2.6 DAPI counterstain distinguishes between epithelial and mesenchymal tissues on thin sections. ..... 49

Figure 3.1 Donor plasmids and injection schemes for both freshwater (Fishtrap Creek) and marine (Rabbit Slough) backgrounds. ..... 61

Figure 3.2 Mutant alleles isolated from three $F_0$ injected Fishtrap Creek embryos demonstrate allele replacement using two guide RNAs and Cas9 protein..... 65

Figure 3.3 Multiple mutant alleles were created from the injection of $F_0$ fish with a single guide. ..... 67

Figure 3.4 Figure 3.4 Multiple alleles are present in the germline of an $F_0$ male injected with sgMDS11/sgMDS4 and Cas9 mRNA. ..... 69

Figure 4.1 Marine and freshwater populations show differing levels of overall genetic diversity. ..... 91
Figure 4.2 Chromosomes contained within the Fishtrap Creek population show differing patterns of nearby variation relative to the high tooth or non-high tooth associated haplotype. ..... 94
Figure 4.3 20kb window of chromosome XXI in Fishtrap Creek continues to show clustering of chromosomes with the high tooth associated haplotypes. ..... 95
Figure 4.4 Population specific differences exist in nucleotide diversity and Tajima's D. ..... 97
Figure 4.5 Extended haplotype homozygosity (EHH) graphs for each of the six haplotype defining sites. ..... 98
Figure 4.6 iHS and nSL values in the haplotype show differences across positions. ..... 100
Figure 4.7 Distribution of *P* values suggests an overestimation of selection. ..... 102
Figure 4.8 Positions within the haplotypes differ in their Relate Evidence of Selection *P* scores and shape of marginal trees ..... 103
Figure 4.9 Elevated scores for three metrics fall within a previously identified bone length QTL window. ..... 105
Figure 4.10 Marginal trees for a site near the haplotype and within a branchial bone length QTL window display differing patterns. ..... 106
Figure 4.11 Geographic distribution of the high-tooth associated haplotype in the Pacific Northwest reveals an expanded range. ..... 107
Figure 4.12 The high tooth associated haplotype is segregating in the Little Campbell marine population. ..... 108

# List of Tables


Table S 2.1 Insulator scores for each reporter positive domain in F0 fish with *Col2a1a:*mCh;*Bmp6* tooth enhancer:eGFP transgene..... 50

Table S 2.2 Insulator scores for each reporter positive domain in F0 fish with the *Col2a1a*:eGFP;*Bmp6* tooth enhancer:mCh transgene..... 50

Table S 2.3 Epithelial expression of enhancer by tooth plate, tooth stage, and genotype.. ..... 50

Table S 2.4 Mesenchymal bias of enhancer expression by tooth plate, tooth stage, and genotype. ..... 51

Table 3.1 Guide and Cas9 combinations used for allele replacement ..... 59

Table 3.2 Crosses of F0 injected Fishtrap Creek fish ..... 68

Table 3.3 Injection and replacement outcomes in a marine background..... 70

Table 4.1 Minor allele frequencies of Little Campbell and Fishtrap Creek populations..... 91

Table 4.2 Allele and genotype frequencies of the high-tooth associated haplotype in previously genotyped Fishtrap Creek fish ..... 92

Table 4.3 Allele frequency for each position within the haplotype..... 92

Table 4.4 K values and resulting CV error scores from the program ADMIXTURE for Fishtrap Creek ..... 96

## Acknowledgments

I would first like to express my deepest gratitude to my mentor, Craig Miller. You were patient when I needed you to be and you pushed me when I needed to be pushed. You've been incredibly understanding and supportive, helping me balance life inside and outside the lab. You are directly responsible for my growth as a scientist and I am truly grateful for the opportunity to be a part of the Miller lab.

To my committee, Richard Harland, David Weisblat, and Noah Whiteman, thank you for your support and guidance over the years. Your thesis meetings always helped me see my projects from new angles.

An advisor once told me when looking to join a lab, look at the current lab members, they are the measurement of the quality of the lab. With that in mind I want to thank the members of the Miller lab that made it a welcoming environment when I joined. To Nick Ellis and Priscilla Erickson, I wish I could've spent more time learning from both of you but I feel I learned so much in such a short period of time. It was inspiring to have two such amazing students at the end of their graduate school journey as models to strive for. To James Hart, who taught me nearly everything I know regarding bioinformatics, thank you for dealing with my, what I'm sure felt like, constant questions and self-doubt. You provided patient guidance, help, and re-assurance.

To my current lab mates, I am saddened to leave the people that have created an incredible work environment and family. To my bay mate Alyssa Borgmann, your outgoing and shining personality always brought a glow to everything. To Tyler Square, who always had insight and unique perspectives on my projects, thank you for your constant input during lab meetings and whenever I just had a question. To Sophie Archambeault, I feel like I could learn so much from you, and I'm excited for the future of the Miller lab with you on board.

To all the undergraduates I've had the fortune of mentoring, Mary Chan, John O'Hara Smith, James Wilson, Noelle Terrero, and Ana Shaughnessy, you have helped me grow as a scientist, educator, mentor, and a person. I think it is a hallmark of a great student when a mentor learns just as much from them, and that was undoubtedly the case.

To my close friends I've made here, Stefanie Engert, 'Jack' Tsai-Ching Hsi, and Austin Mudd, you helped keep me going by letting me know I wasn't alone in the struggles of grad school. Our game and movie nights were often the break I needed and always filled with laughs. Austin, also thank you for help and insight in everything computational.

To my undergraduate PI, George Gilchrist, thank you for giving me my first opportunity and sparking my interest in research.

To my mentors in the Office of Professional Development, Linda von Hoene and Linda Louie, thank you for helping me grow in graduate school outside of the research lab.

To my mother Jackie, you have always believed in me. Thank you for all the encouragement and conversations about any aspect of biology you came across, it helped me keep my broad passion in biology lit.

To my sister Lauren, you were probably the first person to call me a nerd, but also the first to tell me it was something to be proud of. You always watched out for me and I know that hasn't changed.

To my father Kurt, who always pushed me, thank you for the drive that makes me get out of my comfort zone. The little voice in my head that keeps me striving to go just a bit further can make all the difference.

To my son Calder, you have made the last year of graduate school into an even bigger adventure than it already was. Thank you for your endless smiles, laughs, and hugs which have been the best motivation I could ask for. I am so excited to see you continue to grow.

And finally to my wife Molly, you are my greatest source of support and my biggest advocate. You are truly my better half. Thank you for dealing with all the weekends in lab, help feeding the fish, and your patience and understanding when I had to check "just one more thing" on my computer in the middle of the night. I know, if not for your love, support, help, and encouragement, I would never had made it to graduate school or have completed it. I love you more than words can express.

Mark Stepaniak

# Chapter 1
## Introduction

### 1.1 The growth of Evo-Devo and the importance of gene regulation

For nearly all of recorded history, humans have tried to explain the diversity of life observable in nature (Mayr, 1982). The beginning of our current understanding began in the mid 1800's with Darwin's infamous voyage and rise to scientific prominence (Darwin, 1859; Quammen, 2006). At the time the mechanisms of inheritance were largely unknown and it was not until decades later that the initial form of the field of genetics began to take shape through the rediscovery of the work of Mendel (Mendel, 1865; J. Schwartz, 2008). The Modern Synthesis combined the understanding of the basic mechanisms of inheritance, in which heritable traits can be passed from one generation to the next, and how natural selection can favor specific traits, those that increase an organism's ability to survive and reproduce to form the basis of the current understanding of evolutionary biology (Huxley, 1942).

Later in time, progress in the field of genetics lead to the discovery of *cis*-regulatory elements (Jacob & Monod, 1961), non-coding regions that control the expression of a gene. Following the discovery of these elements and the high degree of homology of proteins between species, the result of coding regions (King & Wilson, 1975), the idea that evolution and development in part rely on where and when genes are expressed began gaining ground. Simultaneously, work began to illuminate how specific genes used in development are connected to phenotype (Gehring, 1998; Nüsslein-Volhard & Wieschaus, 1980). Mutations in these genes often lead to severe phenotypes as most genes used in controlling development are pleiotropic, and are redeployed at different times and in different areas during the process (Sabarís et al., 2019). Therefore, mutations affecting coding regions of these genes are likely to have global affects and be maladaptive, presenting a difficulty reconciling the then current understandings of genetic and evolution. If most induced changes in developmental genes are detrimental at an organism scale how can new morphologies arise?

Development is largely controlled by regulatory genes whose patterns of transcription are controlled by *cis*-regulatory elements, which bind transcription factors that then promote the transcription of the target gene in a specific time or place (Furlong & Levine, 2018; Gasperini et al., 2020). As mutations in regulatory regions are likely to have fewer pleiotropic effects, they would be better tolerated than coding mutations which would have affects over the entire expression domain of the gene (Carroll, 2008). Evolution through changes in the *cis*-regulatory regions of developmental genes has been well established (Rebeiz & Tsiantis, 2017; Wray, 2007) and represent a common method for morphological evolution.

### 1.2 Sticklebacks as a model for evolutionary biology and local adaptation

Threespine sticklebacks (*Gasterosteus aculeatus*) have rapidly become a model system for studying the genetics of local adaptation (Jones et al., 2012; Chan et al., 2010; Colosimo, 2005; Hohenlohe et al., 2010; Marques et al., 2017). The species is found in marine environments throughout the northern hemisphere and has colonized freshwater habitats repeatedly and independently (Bell & Foster, 1994; Jones et al., 2012; Mäkinen et al., 2006; McKinnon & Rundle, 2002). Anadromous marine fish travel to freshwater environments to spawn and can establish resident populations. Following colonization a suite of traits typically evolves,

including a reduction in armor plating (Colosimo, 2005; Cresko et al., 2004; Indjeian et al., 2016), body shape (Albert et al., 2008; Reid & Peichel, 2010; Walker, 1997; Walker & Bell, 2000), pelvic spines (Chan et al., 2010), pigmentation (Miller et al., 2007), and feeding structures such as branchial bone length (Erickson et al., 2016b), gill raker number (Glazer et al., 2014; Hagen, 1967) and pharyngeal teeth (Cleves et al., 2014; Ellis et al., 2015). Changes in feeding structures are likely adaptation to different diets of larger, benthic prey items in some freshwater environments (Bell & Foster, 1994; Gross & Anderson, 1984; Lavin & McPhail, 1986; Schluter & McPhail, 1992), allowing the exploitation of newly available niches.

The stickleback provides opportunities to study evolution not only due to the incredible number of "natural experiments", i.e. repeated colonization and adaption, but also because of its tractability as a model organism. Extensive resources and methods such as a fully sequenced genome that has been continuously refined (Jones et al., 2012; Glazer et al., 2015; Nath et al., 2021; Peichel et al., 2017), quantitative trait loci (QTL) mapping (Albert et al., 2008; Miller et al., 2014), and the application of transgenesis tools such as Tol2, CRISPR/Cas9, and BACs (Erickson et al., 2016; Erickson et al., 2015; Hart & Miller, 2017; Wucherpfennig et al., 2019), has allowed researchers to ask detailed questions regarding the underlying genetics of evolution and adaptation. The small fish can be maintained and bred easily in captivity, creating a steady supply of samples and a means to produce specific crosses, creating or propagating transgenes .

The genetics of many evolved traits have been identified, including both coding changes (Marques et al., 2017) and regulatory changes. *Cis*-regulatory changes have been implicated as underlying a reduction in armor plating (Colosimo, 2005; Indjeian et al., 2016), pelvic spines (Chan et al., 2010), and pigmentation (Miller et al., 2007), as well as increases in branchial bone length (Erickson et al., 2016b) and pharyngeal tooth number (Cleves et al., 2014; Cleves et al., 2018). It appears mutations affecting regulatory regions are the rule more often than not in stickleback evolution. When focusing on regions that are repeatedly used in the marine to freshwater adaptation, a majority were determined to fall within non-coding sequence, or likely non-coding sequence, with a small minority falling in coding regions with identifiable marine/freshwater non-synonymous substitutions (Jones et al., 2012).

### 1.3 Evolved tooth gain in sticklebacks is driven by a *cis*-regulation of the gene *Bmp6*

Following colonization and adaptation to new freshwater habitats, populations of sticklebacks have repeatedly evolved an increase in pharyngeal tooth number compared to marine populations (Cleves et al., 2014; Ellis et al., 2015). Sticklebacks contain two sets of pharyngeal tooth plates connected to the fifth ceratobranchial (Ellis et al. 2016). Changes in feeding structures are thought to be in response to changes in diet, allowing the new freshwater population to exploit a new niche, mainly consuming large benthic invertebrates, instead of feeding in the water column like marine fish (Gross & Anderson, 1984; Hagen, 1967; Lavin & McPhail, 1986; Schluter & McPhail, 1992). QTL mapping experiments using a high-toothed Paxton Lake fish and a low-toothed Japanese marine fish identified a peak on chromosome XXI responsible for approximately 30% of the variance between the populations (Cleves et al., 2014).

The peak contained the gene *Bone morphogenetic protein 6* (*Bmp6*), which through *in situ* hybridization, was shown to be dynamically expressed in developing teeth. *Bmp6* is first detected in the inner epithelium and underlying mesenchyme and as the tooth continues to develop, expression in the epithelium decreases until the tooth erupts and becomes a functional tooth (Cleves et al., 2014; Ellis et al., 2016). In addition to being expressed in teeth, allele specific expression (ASE) experiments further supported *Bmp6* as the candidate underlying the

tooth QTL. Tooth plates from $F_1$ hybrids of high-toothed Paxton benthic fish and low-toothed marine fish exhibited a 1.4 fold decrease in *Bmp6* expression in the freshwater allele compared to the marine allele. Further supporting the role of *Bmp6* is the mirroring of tooth number and ASE results. The tooth number difference between freshwater and marine fish arose later in development, in > 20 mm standard length fish, while the ASE difference also became significant at that time point (Cleves et al., 2014). Additional support for the hypothesis that *Bmp6* underlies the tooth number QLT comes from work in mice and fish that has demonstrated an essential role for BMPs in tooth development (Bei et al., 2000; Jia et al., 2013; Vainio et al., 1993; Wang et al., 2012).

Fine mapping of the tooth number QTL identified a haplotype defined by 10 single nucleotide polymorphisms (SNPs) that varied concordantly with the presence or absence of the tooth QTL within the fourth intron of *Bmp6* (Cleves et al., 2018). Following a comparison of chromosomes which had an overlapping chromosome XXI tooth number QTL and comparisons to multiple population, the 10 SNPs were narrowed to six that co-occurred perfectly with the QTL peak. The non-reference identities at the six sites create a high-tooth number QTL associated haplotype, from a Paxton benthic population, while the reference identities define a low-tooth number QTL associated haplotype from a marine population. Throughout the dissertation the different alleles of the haplotype are interchangeably called the high-tooth associated haplotype, freshwater haplotype, or D allele, as the original chromosome on which the haplotype was identified was labeled "D" in a genetic cross. The other allele is interchangeably referred to as the low-tooth associated haplotype, marine allele, or non-D. It should be noted, there are alleles of the haplotype, found in freshwater populations, that do not share identities at the six sites with the original high-tooth associated allele. The labels "freshwater" and "marine" for the haplotypes will only be used in juxtaposition to each other, when the only freshwater allele being discussed is the high-tooth associated allele.

The six SNPs lie upstream of a 511 bp *Bmp6* minimal tooth enhancer within the fourth intron of the gene (Cleves et al., 2018). The haplotype could modify the temporal and/or spatial activity of the minimal enhancer, with the two alleles having different effects, and underlie at least a portion of the allele specific expression result. The high-tooth associated haplotype creates a predicted NFATc1 binding site that is disrupted in the low-tooth associated allele. The transcription factor is expressed in developing stickleback teeth (Square et al., 2021) and is important in the balancing of quiescent and dividing stem cells in hair follicles (Horsley et al., 2008) which share homology with teeth (Ahn, 2015; Biggs & Mikkola, 2014; Pispa & Thesleff, 2003). Mutations within transcription factor binding sites can disrupt recognition by the transcription factor and subsequently transcription itself (Deplancke et al., 2016). Specific SNPs have been demonstrated to be important in transcription factor binding and subsequently gene expression regarding human disease (Huo et al., 2019; A. M. Schwartz et al., 2017). Therefore, it is reasonable to hypothesize that the haplotypes differ in their affinity for transcription factors, likely NFATc1, and so may have different effects on the immediately downstream enhancer.

## 1.4 Standing genetic variation

The high-tooth associated haplotype has been identified in multiple freshwater populations, Paxton and Priest Lake benthic populations from Texada Island, Enos Lake benthic from Vancouver Island, as well as Connor Creek and Fishtrap Creek from Washington (Cleves et al., 2018; Hart, 2018). The presence in geographically isolated populations suggests a model in which the allele was present in the ancestral marine population in the Pacific Northwest at low

frequency. The founding populations for each of the lakes or creeks contained the allele and it increased in frequency in the new environments, potentially due to a selective advantage of an increase in tooth number, if the haplotype is either causative or linked to a causative allele underlying tooth gain. An adaptive low plate allele of *eda*, associated with plate reduction in freshwater populations, was found in multiple marine populations at low frequency, between 0.2% and 3.8% (Colosimo, 2005), similar to the explanation for the distribution of the high-tooth associated haplotype.

One means populations can adapt to local conditions is through the use of standing genetic variation, in which alleles selected for in new environments are segregating in the ancestral population. Once the allele is introduced into a new environment, going from marine to freshwater for example, it can be adaptive and increase in frequency, driving evolution. The allele may or may not be adaptive in the ancestral population, and may even be selected against, however if selection is weak enough, it can be maintained through either gene flow from other populations or through drift (Barrett & Schluter, 2008; Hermisson & Pennings, 2005; Orr & Betancourt, 2001; Przeworski et al., 2005). Adaptation from standing genetic variation can occur rapidly as the adaptive alleles are likely present at higher frequencies than de novo mutation, allowing them to rise in frequency even faster (Innan & Kim, 2004). The adaptive allele also has potentially already been screened by selection in other populations and can lead to parallel evolution (Schluter et al., 2004). The higher initial frequency of an allele in the standing genetic variation model means that small affect alleles are more likely to increase in frequency as pre-existing variation rather than as de novo mutations, suggesting when small affect alleles are involved in adaptation, it is more likely to be as standing genetic variation (Hermisson & Pennings, 2005).

Sticklebacks have rapidly adapted to new environments following colonization (Bell, 2001; Lescak et al., 2015). Multiple population genetic studies have determined overlapping genomic regions are often re-used in independent colonization events, suggesting the same genes are involved in adaptation to similar environments, a hallmark of adaptation through standing variation (Jones et al., 2012; Hohenlohe et al., 2010). The study of some specific traits has shown that not only are the same genes involved, but the same allele is re-deployed in multiple colonization and adaptation events (Colosimo, 2005; Miller et al., 2007). QTL mapping also supports the role of standing genetic variation in stickleback adaptation and evolution, as there is enrichment of QTL peaks in regions associated with marine/freshwater ecotype divergence (Peichel & Marques, 2017). Rapid adaptation, overlapping signals of adaptation, and specific adaptive alleles found in multiple populations strongly support the model that stickleback adaptation and evolution is largely driven by standing genetic variation.

## 1.5 Overview of projects

The model in which the high-tooth associated haplotype modifies a tooth enhancer of *Bmp6*, affecting expression of the gene and therefore tooth number in multiple populations is both an example of the use of mutations in *cis*-regulatory regions to drive evolution and the use of standing genetic variation to rapidly adapt to a new habitat. In order to determine if the haplotype underlies freshwater evolved tooth gain, and if so, through what mechanism I have pursued three separate avenues: 1) marine vs. freshwater enhancer activity comparison through transgene reporters, 2) CRISPR/Cas9 induced and homology directed repair mediated replacement of the allele, and 3) whole genome sequencing of a wild population containing the high-tooth associated allele to scan for signals of selection around the region.

**Chapter 2: Evolved Bmp6 enhancer alleles drive spatial shifts in gene expression during tooth development**

Through the use of the tol2 transposase system (Kawakami, 2004) I have created bi-color transgenic lines containing both a marine, low-tooth associated allele of the enhancer and the high-tooth associated allele, each driving different reporters, eGFP and mCherry. Both pairings of enhancer/reporter were used to rule out effects the reporters may have in the appearance of a difference in activity. Two lines (marine:eGFP;freshwater:mCherry and marine:mCherry;freshwater:eGFP) were generated with individual enhancer/reporter pairs (i.e. two Tol2 plasmids were used to create each line). An alternative method was also used, in which a genetic insulator was placed between each enhancer/reporter pair in a single construct, a technique which has had success in zebrafish (Bessa et al., 2009; Shimizu & Shimizu, 2013). The independent methods yielded consistent results, in which the marine allele of the enhancer tended to have an expanded mesenchymal domain, while the freshwater allele tended to have a more robust epithelial domain. The biases towards the enhancers in each domain appears to become more dramatic later in development, similar to the allele specific expression and tooth number differences (Cleves et al., 2014), suggesting the enhancers may at least partially explain those observations.

**Chapter 3: Replacement of population specific enhancer alleles in threespine stickleback using the CRISPR/Cas9 system**

The CRISPR/Cas9 nuclease system can be used to make precise edits within the genome. The system uses a flexible 20bp guide RNA component to target specific regions and induce double stranded breaks (Jinek et al., 2012). Following a break, cell repair machinery commonly utilizes non-homologous end joining (NHEJ) in which the ends of the break are trimmed and ligated together, typically leaving a scar in the form of an insertion or deletion (Chang et al., 2017; Liu et al., 2012; Moore & Haber, 1996; Roth & Wilson, 1986). The system has successfully generated gene knockouts and reporter knock-ins in zebrafish (Hisano et al., 2015; Hoshijima et al., 2016) and replaced sequence at individual positions (Boel et al., 2018; Irion et al., 2014). Knock-in and sequence replacement typically rely on an alternative repair pathway to NHEJ. Cells can repair double stranded breaks and maintain sequence by using the homologous chromosome as a donor template through a process called homology directed repair (HDR) (Liang et al., 1998), which can be used to introduce new sequence in combination with a nuclease like Cas9 and a desired donor (Sansbury et al., 2019; Yoshimi et al., 2016; Zhang et al., 2017).

A subset of experiments has sought to replace an endogenous genomic sequence using the HDR pathway. Sequence from different species have been used as the donor template to answer questions regarding evolution of a gene or gene regulation through replacement of entire genes (Byrne et al., 2015; McDiarmid et al., 2018) or enhancers (Kvon et al., 2016; Xu et al., 2017). Similarly, in order to test the hypothesis that similar methods can be used to replace the haplotype, I used the CRISPR/Cas9 system and a plasmid donor in an attempt to swap the high-tooth associated haplotype in a freshwater background with a marine, low-tooth associated sequence. Multiple approaches were used, such as cutting with two guides, flanking the sequence to be replaced, or a single cut upstream of the haplotype. Sequencing data revealed multiple chimeric chromosomes were generated, including those which contained entire replaced haplotypes as well as subsets of replaced SNPs. The resulting transgenic fish can be used to test

the hypothesis the haplotype underlies evolved tooth gain, and the subsets of replaced SNPs may allow for increased resolution to determine the relative contribution of individual sites.

**Chapter 4: Population genetics of an adaptive *cis*-regulatory allele of the gene *Bmp6***
Fishtrap Creek, WA contains a highly derived population of sticklebacks with changes to armor plating, body shape, gill rakers (Hagen & Gilbertson, 1972), branchial bone length (Erickson et al., 2014) and pharyngeal tooth number (Hart, 2018). Both the high-tooth associated haplotype and chromosome XXI tooth number QTL peak were observed in previous crosses with fish from the population (Hart, 2018). As the haplotype is found in multiple freshwater populations and is associated with an evolved tooth gain, it is possible, if it underlies the increase in tooth number, that the haplotype is adaptive. If this is the case, then there would likely be certain patterns or features in the region surrounding the haplotype, for example a decrease in genetic diversity (Smith & Haigh, 1974) or extend regions of haplotype homozygosity (Sabeti et al., 2002; Voight et al., 2006) in population genomic data. As the haplotype was known to be present in Fishtrap Creek, whole genome sequencing was performed on wild fish from the population. A variety of methods were used to test for potential signals of selection specifically centered on the *Bmp6* intron 4 enhancer/haplotype. Methods such as iHS (Voight et al., 2006), nSL (Ferrer-Admetlla et al., 2014), and an ancestral recombination graph method, Relate (Speidel et al., 2019), allow for site level resolution and score calculation. Within the haplotype defining SNPs a specific position, chrXXI:8000169, consistently scored higher than the others, suggesting that site, which creates an NFATc1 binding motif, may have experienced some degree of selection compared to the others.

## 1.6 Dissertation scope and overview

This dissertation lies at the intersection of multiple disciplines of biology: development, genetics, gene editing, and population genetics. A multidisciplinary approach helps to independently validate broad conclusions from each project and can help to generate a more complete picture of the topic. In addition, the results of individual projects can lead to more questions, not just within the same realm but in others. For example, elevated signals of selection around specific sites within the haplotype, or chimeric alleles generated through CRISPR/Cas9 can be used to inspire new enhancer/reporter constructs to test the impact of individual sites. This dissertation also represents an attempt to step back and ask questions from different points of view in an attempt to more fully and deeply understand both a specific question, “What role does the haplotype potentially play in evolved tooth gain?” and a broad question that is central to evolutionary biology, “How do populations adapt to their local environment?”.

## 1.7 References

Ahn, Y. (2015). Signaling in Tooth, Hair, and Mammary Placodes. In *Current Topics in Developmental Biology* (Vol. 111, pp. 421–459). Elsevier. https://doi.org/10.1016/bs.ctdb.2014.11.013

Albert, A. Y. K., Sawaya, S., Vines, T. H., Knecht, A. K., Miller, C. T., Summers, B. R., Balabhadra, S., Kingsley, D. M., & Schluter, D. (2008). The genetics of adaptive shape shift in stickleback: Pleiotropy and effect size. *Evolution; International Journal of Organic Evolution*, *62*(1), 76–85. https://doi.org/10.1111/j.1558-5646.2007.00259.x

Barrett, R., & Schluter, D. (2008). Adaptation from standing genetic variation. *Trends in Ecology & Evolution*, *23*(1), 38–44. https://doi.org/10.1016/j.tree.2007.09.008

Bei, M., Kratochwil, K., & Maas, R. L. (2000). BMP4 rescues a non-cell-autonomous function of Msx1 in tooth development. *Development (Cambridge, England)*, *127*(21), 4711–4718.

Bell, M. A. (2001). Lateral plate evolution in the threespine stickleback: Getting nowhere fast. *Genetica*, *112/113*, 445–461. https://doi.org/10.1023/A:1013326024547

Bell, M. A., & Foster, S. A. (Eds.). (1994). *The evolutionary biology of the threespine stickleback*. Oxford University Press.

Bessa, J., Tena, J. J., de la Calle-Mustienes, E., Fernández-Miñán, A., Naranjo, S., Fernández, A., Montoliu, L., Akalin, A., Lenhard, B., Casares, F., & Gómez-Skarmeta, J. L. (2009). Zebrafish enhancer detection (ZED) vector: A new tool to facilitate transgenesis and the functional analysis of *cis* -regulatory regions in zebrafish. *Developmental Dynamics*, *238*(9), 2409–2417. https://doi.org/10.1002/dvdy.22051

Biggs, L. C., & Mikkola, M. L. (2014). Early inductive events in ectodermal appendage morphogenesis. *Seminars in Cell & Developmental Biology*, *25–26*, 11–21. https://doi.org/10.1016/j.semcdb.2014.01.007

Boel, A., De Saffel, H., Steyaert, W., Callewaert, B., De Paepe, A., Coucke, P. J., & Willaert, A. (2018). CRISPR/Cas9-mediated homology-directed repair by ssODNs in zebrafish induces complex mutational patterns resulting from genomic integration of repair-template fragments. *Disease Models & Mechanisms*, *11*(10), dmm035352. https://doi.org/10.1242/dmm.035352

Byrne, S. M., Ortiz, L., Mali, P., Aach, J., & Church, G. M. (2015). Multi-kilobase homozygous targeted gene replacement in human induced pluripotent stem cells. *Nucleic Acids Research*, *43*(3), e21–e21. https://doi.org/10.1093/nar/gku1246

Carroll, S. B. (2008). Evo-Devo and an Expanding Evolutionary Synthesis: A Genetic Theory of Morphological Evolution. *Cell*, *134*(1), 25–36. https://doi.org/10.1016/j.cell.2008.06.030

Chan, Y. F., Marks, M. E., Jones, F. C., Villarreal, G., Shapiro, M. D., Brady, S. D., Southwick, A. M., Absher, D. M., Grimwood, J., Schmutz, J., Myers, R. M., Petrov, D., Jonsson, B., Schluter, D., Bell, M. A., & Kingsley, D. M. (2010). Adaptive Evolution of Pelvic Reduction in Sticklebacks by Recurrent Deletion of a Pitx1 Enhancer. *Science*, *327*(5963), 302–305. https://doi.org/10.1126/science.1182213

Chang, H. H. Y., Pannunzio, N. R., Adachi, N., & Lieber, M. R. (2017). Non-homologous DNA end joining and alternative pathways to double-strand break repair. *Nature Reviews. Molecular Cell Biology*, *18*(8), 495–506. https://doi.org/10.1038/nrm.2017.48

Cleves, P. A., Ellis, N. A., Jimenez, M. T., Nunez, S. M., Schluter, D., Kingsley, D. M., & Miller, C. T. (2014). Evolved tooth gain in sticklebacks is associated with a cis-regulatory allele of Bmp6. *Proceedings of the National Academy of Sciences*, *111*(38), 13912–13917. https://doi.org/10.1073/pnas.1407567111

Cleves, Phillip A., Hart, J. C., Agoglia, R. M., Jimenez, M. T., Erickson, P. A., Gai, L., & Miller, C. T. (2018). An intronic enhancer of Bmp6 underlies evolved tooth gain in sticklebacks. *PLOS Genetics*, *14*(6), e1007449. https://doi.org/10.1371/journal.pgen.1007449

Colosimo, P. F. (2005). Widespread Parallel Evolution in Sticklebacks by Repeated Fixation of Ectodysplasin Alleles. *Science*, *307*(5717), 1928–1933. https://doi.org/10.1126/science.1107239

Cresko, W. A., Amores, A., Wilson, C., Murphy, J., Currey, M., Phillips, P., Bell, M. A., Kimmel, C. B., & Postlethwait, J. H. (2004). Parallel genetic basis for repeated evolution of armor loss in Alaskan threespine stickleback populations. *Proceedings of the National Academy of Sciences of the United States of America*, *101*(16), 6050–6055. https://doi.org/10.1073/pnas.0308479101

Darwin, C. (1859). *On the Origins of Species by Means of Natural Selection, or the Preservation of Favoured Races in the Struggle for Life*.

Deplancke, B., Alpern, D., & Gardeux, V. (2016). The Genetics of Transcription Factor DNA Binding Variation. *Cell*, *166*(3), 538–554. https://doi.org/10.1016/j.cell.2016.07.012

Ellis, N. A., Glazer, A. M., Donde, N. N., Cleves, P. A., Agoglia, R. M., & Miller, C. T. (2015). Distinct developmental genetic mechanisms underlie convergently evolved tooth gain in sticklebacks. *Development*, *142*(14), 2442–2451. https://doi.org/10.1242/dev.124248

Ellis, Nicholas A., Donde, N. N., & Miller, C. T. (2016). Early development and replacement of the stickleback dentition: Stickleback tooth Patterning. *Journal of Morphology*, *277*(8), 1072–1083. https://doi.org/10.1002/jmor.20557

Erickson, P. A., Cleves, P. A., Ellis, N. A., Schwalbach, K. T., Hart, J. C., & Miller, C. T. (2015). A 190 base pair, TGF-β responsive tooth and fin enhancer is required for stickleback Bmp6 expression. *Developmental Biology*, *401*(2), 310–323. https://doi.org/10.1016/j.ydbio.2015.02.006

Erickson, P. A., Ellis, N. A., & Miller, C. T. (2016). Microinjection for Transgenesis and Genome Editing in Threespine Sticklebacks. *Journal of Visualized Experiments*, *111*, 54055. https://doi.org/10.3791/54055

Erickson, P. A., Glazer, A. M., Cleves, P. A., Smith, A. S., & Miller, C. T. (2014). Two developmentally temporal quantitative trait loci underlie convergent evolution of increased branchial bone length in sticklebacks. *Proceedings of the Royal Society B: Biological Sciences*, *281*(1788), 20140822. https://doi.org/10.1098/rspb.2014.0822

Erickson, P. A., Glazer, A. M., Killingbeck, E. E., Agoglia, R. M., Baek, J., Carsanaro, S. M., Lee, A. M., Cleves, P. A., Schluter, D., & Miller, C. T. (2016b). Partially repeatable genetic basis of benthic adaptation in threespine sticklebacks: REPEATABLE EVOLUTION IN BENTHIC STICKLEBACKS. *Evolution*, *70*(4), 887–902. https://doi.org/10.1111/evo.12897

Ferrer-Admetlla, A., Liang, M., Korneliussen, T., & Nielsen, R. (2014). On Detecting Incomplete Soft or Hard Selective Sweeps Using Haplotype Structure. *Molecular Biology and Evolution*, *31*(5), 1275–1291. https://doi.org/10.1093/molbev/msu077

Furlong, E. E. M., & Levine, M. (2018). Developmental enhancers and chromosome topology. *Science (New York, N.Y.)*, *361*(6409), 1341–1345. https://doi.org/10.1126/science.aau0320

Gasperini, M., Tome, J. M., & Shendure, J. (2020). Towards a comprehensive catalogue of validated and target-linked human enhancers. *Nature Reviews Genetics*, *21*(5), 292–310. https://doi.org/10.1038/s41576-019-0209-0

Gehring, W. (1998). *Master Control Genes in Development and Evolution: The Homeobox Story*. Yale University Press.

Glazer, A. M., Cleves, P. A., Erickson, P. A., Lam, A. Y., & Miller, C. T. (2014). Parallel developmental genetic features underlie stickleback gill raker evolution. *EvoDevo*, *5*(1), 19. https://doi.org/10.1186/2041-9139-5-19

Glazer, A. M., Killingbeck, E. E., Mitros, T., Rokhsar, D. S., & Miller, C. T. (2015). Genome Assembly Improvement and Mapping Convergently Evolved Skeletal Traits in Sticklebacks with Genotyping-by-Sequencing. *G3: Genes|Genomes|Genetics*, *5*(7), 1463–1472. https://doi.org/10.1534/g3.115.017905

Gross, H. P., & Anderson, J. M. (1984). Geographic Variation in the Gillrakers and Diet of European Threespine Sticklebacks, Gasterosteus aculeatus. *Copeia*, *1984*(1), 87. https://doi.org/10.2307/1445038

Hagen, D. W. (1967). Isolating Mechanisms in Threespine Sticklebacks ( *Gasterosteus* ). *Journal of the Fisheries Research Board of Canada*, *24*(8), 1637–1692. https://doi.org/10.1139/f67-138

Hagen, D. W., & Gilbertson, L. G. (1972). GEOGRAPHIC VARIATION AND ENVIRONMENTAL SELECTION IN *GASTEROSTEUS ACULEATUS* L. IN THE PACIFIC NORTHWEST, AMERICA. *Evolution*, *26*(1), 32–51. https://doi.org/10.1111/j.1558-5646.1972.tb00172.x

Hart, J. C. (2018). *Genetic and Genomic Bases of Evolved Increases in Stickleback Dentition* [University of California, Berkeley]. https://escholarship.org/uc/item/3dp2884n

Hart, J. C., & Miller, C. T. (2017). Sequence-Based Mapping and Genome Editing Reveal Mutations in Stickleback *Hps5* Cause Oculocutaneous Albinism and the *casper* Phenotype. *G3: Genes|Genomes|Genetics*, *7*(9), 3123–3131. https://doi.org/10.1534/g3.117.1125

Hermisson, J., & Pennings, P. S. (2005). Soft Sweeps: Molecular Population Genetics of Adaptation From Standing Genetic Variation. *Genetics*, *169*(4), 2335–2352. https://doi.org/10.1534/genetics.104.036947

Hisano, Y., Sakuma, T., Nakade, S., Ohga, R., Ota, S., Okamoto, H., Yamamoto, T., & Kawahara, A. (2015). Precise in-frame integration of exogenous DNA mediated by CRISPR/Cas9 system in zebrafish. *Scientific Reports*, *5*(1), 8841. https://doi.org/10.1038/srep08841

Hohenlohe, P. A., Bassham, S., Etter, P. D., Stiffler, N., Johnson, E. A., & Cresko, W. A. (2010). Population Genomics of Parallel Adaptation in Threespine Stickleback using Sequenced

RAD Tags. *PLoS Genetics*, *6*(2), e1000862. https://doi.org/10.1371/journal.pgen.1000862

Horsley, V., Aliprantis, A. O., Polak, L., Glimcher, L. H., & Fuchs, E. (2008). NFATc1 Balances Quiescence and Proliferation of Skin Stem Cells. *Cell*, *132*(2), 299–310. https://doi.org/10.1016/j.cell.2007.11.047

Hoshijima, K., Jurynec, M. J., & Grunwald, D. J. (2016). Precise Editing of the Zebrafish Genome Made Simple and Efficient. *Developmental Cell*, *36*(6), 654–667. https://doi.org/10.1016/j.devcel.2016.02.015

Huo, Y., Li, S., Liu, J., Li, X., & Luo, X.-J. (2019). Functional genomics reveal gene regulatory mechanisms underlying schizophrenia risk. *Nature Communications*, *10*(1), 670. https://doi.org/10.1038/s41467-019-08666-4

Huxley, J. (1942). *Evolution, the Modern Synthesis*. G. Allen and Unwin Limited.

Indjeian, V. B., Kingman, G. A., Jones, F. C., Guenther, C. A., Grimwood, J., Schmutz, J., Myers, R. M., & Kingsley, D. M. (2016). Evolving New Skeletal Traits by cis -Regulatory Changes in Bone Morphogenetic Proteins. *Cell*, *164*(1–2), 45–56. https://doi.org/10.1016/j.cell.2015.12.007

Innan, H., & Kim, Y. (2004). Pattern of polymorphism after strong artificial selection in a domestication event. *Proceedings of the National Academy of Sciences*, *101*(29), 10667–10672. https://doi.org/10.1073/pnas.0401720101

Irion, U., Krauss, J., & Nusslein-Volhard, C. (2014). Precise and efficient genome editing in zebrafish using the CRISPR/Cas9 system. *Development*, *141*(24), 4827–4830. https://doi.org/10.1242/dev.115584

Jacob, F., & Monod, J. (1961). Genetic regulatory mechanisms in the synthesis of proteins. *Journal of Molecular Biology*, *3*(3), 318–356. https://doi.org/10.1016/S0022-2836(61)80072-7

Jia, S., Zhou, J., Gao, Y., Baek, J.-A., Martin, J. F., Lan, Y., & Jiang, R. (2013). Roles of Bmp4 during tooth morphogenesis and sequential tooth formation. *Development*, *140*(2), 423–432. https://doi.org/10.1242/dev.081927

Jinek, M., Chylinski, K., Fonfara, I., Hauer, M., Doudna, J. A., & Charpentier, E. (2012). A Programmable Dual-RNA-Guided DNA Endonuclease in Adaptive Bacterial Immunity. *Science*, *337*(6096), 816–821. https://doi.org/10.1126/science.1225829

Jones, F. C., Grabherr, M. G., Chan, Y. F., Russell, P., Mauceli, E., Johnson, J., Swofford, R., Pirun, M., Zody, M. C., White, S., Birney, E., Searle, S., Schmutz, J., Grimwood, J., Dickson, M. C., Myers, R. M., Miller, C. T., Summers, B. R., … Kingsley, D. M. (2012). The genomic basis of adaptive evolution in threespine sticklebacks. *Nature*, *484*(7392), 55–61. https://doi.org/10.1038/nature10944

Kawakami, K. (2004). Transgenesis and gene trap methods in zebrafish by using the Tol2 transposable element. *Methods in Cell Biology*, *77*, 201–222. https://doi.org/10.1016/s0091-679x(04)77011-9

King, M. C., & Wilson, A. C. (1975). Evolution at two levels in humans and chimpanzees. *Science (New York, N.Y.)*, *188*(4184), 107–116. https://doi.org/10.1126/science.1090005

Kvon, E. Z., Kamneva, O. K., Melo, U. S., Barozzi, I., Osterwalder, M., Mannion, B. J., Tissières, V., Pickle, C. S., Plajzer-Frick, I., Lee, E. A., Kato, M., Garvin, T. H., Akiyama, J. A., Afzal, V., Lopez-Rios, J., Rubin, E. M., Dickel, D. E., Pennacchio, L. A., & Visel, A. (2016). Progressive Loss of Function in a Limb Enhancer during Snake Evolution. *Cell*, *167*(3), 633-642.e11. https://doi.org/10.1016/j.cell.2016.09.028

Lavin, P. A., & McPhail, J. D. (1986). Adaptive Divergence of Trophic Phenotype among Freshwater Populations of the Threespine Stickleback ( *Gasterosteus aculeatus* ). *Canadian Journal of Fisheries and Aquatic Sciences*, *43*(12), 2455–2463. https://doi.org/10.1139/f86-305

Lescak, E. A., Bassham, S. L., Catchen, J., Gelmond, O., Sherbick, M. L., von Hippel, F. A., & Cresko, W. A. (2015). Evolution of stickleback in 50 years on earthquake-uplifted islands. *Proceedings of the National Academy of Sciences*, *112*(52), E7204–E7212. https://doi.org/10.1073/pnas.1512020112

Liang, F., Han, M., Romanienko, P. J., & Jasin, M. (1998). Homology-directed repair is a major double-strand break repair pathway in mammalian cells. *Proceedings of the National Academy of Sciences of the United States of America*, *95*(9), 5172–5177. https://doi.org/10.1073/pnas.95.9.5172

Liu, J., Gong, L., Chang, C., Liu, C., Peng, J., & Chen, J. (2012). Development of Novel Visual-Plus Quantitative Analysis Systems for Studying DNA Double-Strand Break Repairs in Zebrafish. *Journal of Genetics and Genomics*, *39*(9), 489–502. https://doi.org/10.1016/j.jgg.2012.07.009

Mäkinen, H. S., Cano, J. M., & Merilä, J. (2006). Genetic relationships among marine and freshwater populations of the European three-spined stickleback (Gasterosteus aculeatus) revealed by microsatellites. *Molecular Ecology*, *15*(6), 1519–1534. https://doi.org/10.1111/j.1365-294X.2006.02871.x

Marques, D. A., Taylor, J. S., Jones, F. C., Di Palma, F., Kingsley, D. M., & Reimchen, T. E. (2017). Convergent evolution of SWS2 opsin facilitates adaptive radiation of threespine stickleback into different light environments. *PLOS Biology*, *15*(4), e2001627. https://doi.org/10.1371/journal.pbio.2001627

Mayr, E. (1982). *The growth of biological thought: Diversity, evolution, and inheritance*. Harvard Univ. Pr.

McDiarmid, T. A., Au, V., Loewen, A. D., Liang, J., Mizumoto, K., Moerman, D. G., & Rankin, C. H. (2018). CRISPR-Cas9 human gene replacement and phenomic characterization in *Caenorhabditis elegans* to understand the functional conservation of human genes and decipher variants of uncertain significance. *Disease Models & Mechanisms*, *11*(12), dmm036517. https://doi.org/10.1242/dmm.036517

McKinnon, J. S., & Rundle, H. D. (2002). Speciation in nature: The threespine stickleback model systems. *Trends in Ecology & Evolution*, *17*(10), 480–488. https://doi.org/10.1016/S0169-5347(02)02579-X

Mendel, G. (1865). Versuche ber Pflanzen-HyBriden. *Verh Naturforsch Ver Brnn*, *4*(347).

Miller, C. T., Beleza, S., Pollen, A. A., Schluter, D., Kittles, R. A., Shriver, M. D., & Kingsley, D. M. (2007). Cis-Regulatory Changes in Kit Ligand Expression and Parallel Evolution

of Pigmentation in Sticklebacks and Humans. *Cell*, *131*(6), 1179–1189. https://doi.org/10.1016/j.cell.2007.10.055

Miller, C. T., Glazer, A. M., Summers, B. R., Blackman, B. K., Norman, A. R., Shapiro, M. D., Cole, B. L., Peichel, C. L., Schluter, D., & Kingsley, D. M. (2014). Modular Skeletal Evolution in Sticklebacks Is Controlled by Additive and Clustered Quantitative Trait Loci. *Genetics*, *197*(1), 405–420. https://doi.org/10.1534/genetics.114.162420

Moore, J. K., & Haber, J. E. (1996). Cell cycle and genetic requirements of two pathways of nonhomologous end-joining repair of double-strand breaks in Saccharomyces cerevisiae. *Molecular and Cellular Biology*, *16*(5), 2164–2173. https://doi.org/10.1128/mcb.16.5.2164

Nath, S., Shaw, D. E., & White, M. A. (2021). Improved contiguity of the threespine stickleback genome using long-read sequencing. *G3 Genes|Genomes|Genetics*, *11*(2), jkab007. https://doi.org/10.1093/g3journal/jkab007

Nüsslein-Volhard, C., & Wieschaus, E. (1980). Mutations affecting segment number and polarity in Drosophila. *Nature*, *287*(5785), 795–801. https://doi.org/10.1038/287795a0

Orr, H. A., & Betancourt, A. J. (2001). Haldane's sieve and adaptation from the standing genetic variation. *Genetics*, *157*(2), 875–884.

Peichel, C. L., & Marques, D. A. (2017). The genetic and molecular architecture of phenotypic diversity in sticklebacks. *Philosophical Transactions of the Royal Society B: Biological Sciences*, *372*(1713), 20150486. https://doi.org/10.1098/rstb.2015.0486

Peichel, C. L., Sullivan, S. T., Liachko, I., & White, M. A. (2017). Improvement of the Threespine Stickleback Genome Using a Hi-C-Based Proximity-Guided Assembly. *Journal of Heredity*, *108*(6), 693–700. https://doi.org/10.1093/jhered/esx058

Pispa, J., & Thesleff, I. (2003). Mechanisms of ectodermal organogenesis. *Developmental Biology*, *262*(2), 195–205. https://doi.org/10.1016/s0012-1606(03)00325-7

Przeworski, M., Coop, G., & Wall, J. D. (2005). The signature of positive selection on standing genetic variation. *Evolution; International Journal of Organic Evolution*, *59*(11), 2312–2323.

Quammen, D. (2006). *The reluctant Mr. Darwin: An intimate portrait of Charles Darwin and the making of his theory of evolution* (1. ed). Atlas Books [u.a.].

Rebeiz, M., & Tsiantis, M. (2017). Enhancer evolution and the origins of morphological novelty. *Current Opinion in Genetics & Development*, *45*, 115–123. https://doi.org/10.1016/j.gde.2017.04.006

Reid, D. T., & Peichel, C. L. (2010). Perspectives on the genetic architecture of divergence in body shape in sticklebacks. *Integrative and Comparative Biology*, *50*(6), 1057–1066. https://doi.org/10.1093/icb/icq030

Roth, D. B., & Wilson, J. H. (1986). Nonhomologous recombination in mammalian cells: Role for short sequence homologies in the joining reaction. *Molecular and Cellular Biology*, *6*(12), 4295–4304. https://doi.org/10.1128/mcb.6.12.4295

Sabarís, G., Laiker, I., Preger-Ben Noon, E., & Frankel, N. (2019). Actors with Multiple Roles: Pleiotropic Enhancers and the Paradigm of Enhancer Modularity. *Trends in Genetics: TIG*, *35*(6), 423–433. https://doi.org/10.1016/j.tig.2019.03.006

Sabeti, P. C., Reich, D. E., Higgins, J. M., Levine, H. Z. P., Richter, D. J., Schaffner, S. F., Gabriel, S. B., Platko, J. V., Patterson, N. J., McDonald, G. J., Ackerman, H. C., Campbell, S. J., Altshuler, D., Cooper, R., Kwiatkowski, D., Ward, R., & Lander, E. S. (2002). Detecting recent positive selection in the human genome from haplotype structure. *Nature*, *419*(6909), 832–837. https://doi.org/10.1038/nature01140

Sansbury, B. M., Hewes, A. M., & Kmiec, E. B. (2019). Understanding the diversity of genetic outcomes from CRISPR-Cas generated homology-directed repair. *Communications Biology*, *2*(1), 458. https://doi.org/10.1038/s42003-019-0705-y

Schluter, D., Clifford, E. A., Nemethy, M., & McKinnon, J. S. (2004). Parallel evolution and inheritance of quantitative traits. *The American Naturalist*, *163*(6), 809–822. https://doi.org/10.1086/383621

Schluter, D., & McPhail, J. D. (1992). Ecological Character Displacement and Speciation in Sticklebacks. *The American Naturalist*, *140*(1), 85–108. https://doi.org/10.1086/285404

Schwartz, A. M., Demin, D. E., Vorontsov, I. E., Kasyanov, A. S., Putlyaeva, L. V., Tatosyan, K. A., Kulakovskiy, I. V., & Kuprash, D. V. (2017). Multiple single nucleotide polymorphisms in the first intron of the IL2RA gene affect transcription factor binding and enhancer activity. *Gene*, *602*, 50–56. https://doi.org/10.1016/j.gene.2016.11.032

Schwartz, J. (2008). *In pursuit of the gene: From Darwin to DNA*. Harvard University Press.

Shimizu, A., & Shimizu, N. (2013). Dual promoter expression system with insulator ensures a stringent tissue-specific regulation of two reporter genes in the transgenic fish. *Transgenic Research*, *22*(2), 435–444. https://doi.org/10.1007/s11248-012-9653-8

Smith, J. M., & Haigh, J. (1974). The hitch-hiking effect of a favourable gene. *Genetical Research*, *23*(1), 23–35.

Speidel, L., Forest, M., Shi, S., & Myers, S. R. (2019). A method for genome-wide genealogy estimation for thousands of samples. *Nature Genetics*, *51*(9), 1321–1329. https://doi.org/10.1038/s41588-019-0484-x

Square, T. A., Sundaram, S., Mackey, E. J., & Miller, C. T. (2021). Distinct tooth regeneration systems deploy a conserved battery of genes. *EvoDevo*, *12*(1), 4. https://doi.org/10.1186/s13227-021-00172-3

Vainio, S., Karavanova, I., Jowett, A., & Thesleff, I. (1993). Identification of BMP-4 as a signal mediating secondary induction between epithelial and mesenchymal tissues during early tooth development. *Cell*, *75*(1), 45–58. https://doi.org/10.1016/S0092-8674(05)80083-2

Voight, B. F., Kudaravalli, S., Wen, X., & Pritchard, J. K. (2006). A Map of Recent Positive Selection in the Human Genome. *PLoS Biology*, *4*(3), e72. https://doi.org/10.1371/journal.pbio.0040072

Walker, J. A. (1997). Ecological morphology of lacustrine threespine stickleback Gasterosteus aculeatus L. (Gasterosteidae) body shape. *Biological Journal of the Linnean Society*, *61*(1), 3–50. https://doi.org/10.1111/j.1095-8312.1997.tb01777.x

Walker, J. A., & Bell, M. A. (2000). Net evolutionary trajectories of body shape evolution within a microgeographic radiation of threespine sticklebacks (Gasterosteus aculeatus). *Journal of Zoology*, *252*(3), 293–302. https://doi.org/10.1111/j.1469-7998.2000.tb00624.x

Wang, Y., Li, L., Zheng, Y., Yuan, G., Yang, G., He, F., & Chen, Y. (2012). BMP Activity Is Required for Tooth Development from the Lamina to Bud Stage. *Journal of Dental Research*, *91*(7), 690–695. https://doi.org/10.1177/0022034512448660

Wray, G. A. (2007). The evolutionary significance of cis-regulatory mutations. *Nature Reviews Genetics*, *8*(3), 206–216. https://doi.org/10.1038/nrg2063

Wucherpfennig, J. I., Miller, C. T., & Kingsley, D. M. (n.d.). *Efficient CRISPR-Cas9 editing of major evolutionary loci in sticklebacks*. 26.

Xu, X.-R. S., Gantz, V. M., Siomava, N., & Bier, E. (2017). CRISPR/Cas9 and active genetics-based trans-species replacement of the endogenous Drosophila kni-L2 CRM reveals unexpected complexity. *ELife*, *6*, e30281. https://doi.org/10.7554/eLife.30281

Yoshimi, K., Kunihiro, Y., Kaneko, T., Nagahora, H., Voigt, B., & Mashimo, T. (2016). SsODN-mediated knock-in with CRISPR-Cas for large genomic regions in zygotes. *Nature Communications*, *7*(1), 10431. https://doi.org/10.1038/ncomms10431

Zhang, J.-P., Li, X.-L., Li, G.-H., Chen, W., Arakaki, C., Botimer, G. D., Baylink, D., Zhang, L., Wen, W., Fu, Y.-W., Xu, J., Chun, N., Yuan, W., Cheng, T., & Zhang, X.-B. (2017). Efficient precise knockin with a double cut HDR donor after CRISPR/Cas9-mediated double-stranded DNA cleavage. *Genome Biology*, *18*(1), 35. https://doi.org/10.1186/s13059-017-1164-8

# Chapter 2

## Evolved *Bmp6* enhancer alleles drive spatial shifts in gene expression during tooth development

Mark D. Stepaniak, Tyler A. Square, and Craig T. Miller

A version of this chapter was submitted to bioRxiv on 5/14/21

### 2.1 Abstract

Mutations in enhancers have been shown to often underlie natural variation but the evolved differences between enhancer activity can be difficult to identify *in vivo*. Threespine sticklebacks (*Gasterosteus aculeatus*) are a robust system for studying enhancer evolution due to abundant natural genetic variation, a diversity of evolved phenotypes between ancestral marine and derived freshwater forms, and the tractability of transgenic techniques. Previous work identified a series of polymorphisms within an intronic enhancer of the *Bone morphogenetic protein 6* (*Bmp6*) gene that are associated with evolved tooth gain, a derived increase in freshwater tooth number that arises late in development. Here we use a bicistronic reporter construct containing a genetic insulator and a pair of reciprocal two-color transgenic reporter lines to compare enhancer activity of marine and freshwater alleles of this *Bmp6* tooth enhancer. In older fish the two alleles drive partially overlapping expression in both mesenchyme and epithelium of developing teeth, but the freshwater enhancer drives a reduced mesenchymal domain and a larger epithelial domain relative to the marine enhancer. In younger fish, a time point before tooth number between the marine and freshwater population becomes significantly different, enhancer activity of the two alleles appear more similar. Last, we compare *Bmp6* expression by *in situ* hybridization in developing teeth of marine and freshwater fish. We find reduced mesenchymal and expanded epithelial *Bmp6* expression in freshwater teeth relative to marine teeth, consistent with the reporter gene results. Together, these data support a model in which the polymorphisms within this enhancer underlie evolved tooth gain by shifting the spatial expression of *Bmp6* during tooth development, and provide a general strategy to identify spatial differences in enhancer activity *in vivo*.

## 2.2 Introduction

The process of development is largely orchestrated by developmental regulatory genes whose spatial and temporal patterns of transcription are controlled by enhancers, *cis*-regulatory elements that bind transcription factors and promote transcription of target genes (Furlong & Levine, 2018; Gasperini et al., 2020). Most developmental regulatory genes are pleiotropic, and function repeatedly at different times and in different tissues during development (Sabarís et al., 2019). Thus, mutations in enhancers of developmental regulatory genes are often more tolerated than coding sequence mutations due to having fewer pleiotropic effects, as the impacts of enhancer mutations are more likely to be restricted in time and/or space, compared to the anatomically more widespread impacts of coding mutations (Carroll, 2008). The importance of enhancers in regulating morphological evolution, natural variation, and disease phenotypes in humans is well established (Rebeiz & Tsiantis, 2017; Rickels & Shilatifard, 2018). However, a growing need has emerged for methods and approaches to compare the activity of molecularly divergent enhancer alleles.

*Cis*-regulatory changes have been shown to underlie the evolution of multiple morphological traits in threespine stickleback fish (*Gasterosteus aculeatus*). Threespine sticklebacks live in both marine and freshwater environments in the Northern Hemisphere, repeatedly forming populations in rivers, streams, ponds, and lakes from ancestral marine populations (Bell & Foster, 1994; McKinnon & Rundle, 2002). Following a freshwater colonization event, a suite of traits has been observed to typically evolve such as reduction in armor (Bell & Foster, 1994; Colosimo, 2005; Cresko et al., 2004) and changes in body shape (Albert et al., 2008; Reid & Peichel, 2010; Walker, 1997; Walker & Bell, 2000). Other traits that typically evolve major differences are those associated with feeding morphology, likely an adaptation to different diets of larger prey in freshwater environments relative to marine ancestral environments (Bell & Foster, 1994; Gross & Anderson, 1984; Hagen, 1967; Lavin & McPhail, 1986; Schluter & McPhail, 1992). High resolution genetic mapping studies have implicated *cis*-regulatory changes as underlying several phenotypes that have evolved in freshwater, including the reduction of armor plates (Archambeault et al., 2020; Colosimo, 2005; Indjeian et al., 2016; O'Brown et al., 2015), pelvic spines (Chan et al., 2010), and pigmentation (Miller et al., 2007), and increases in branchial bone length (Erickson, et al., 2016), and pharyngeal tooth number (Cleves et al., 2014; Cleves et al., 2018).

Increases in pharyngeal tooth number have evolved independently in multiple freshwater stickleback populations (Ellis et al., 2015). Comparing lab-reared marine fish and freshwater fish from the benthic (bottom-dwelling) population of Paxton Lake, revealed that a divergence in tooth number occurs late in development (around ~20 mm standard length, when fish are juveniles and about half of their adult size). This difference in tooth number continues to increase and become more significantly different at adult stages (Cleves et al., 2014). Quantitative trait loci (QTL) mapping identified a large effect QTL that underlies this evolved tooth gain. An F2 cross between a low-toothed Japanese marine fish and a high-toothed benthic Paxton Lake freshwater fish identified a QTL peak on chromosome 21 that explained approximately 30% of the variance in tooth number within the cross. The peak contained the candidate gene *Bone morphogenetic protein 6* (*Bmp6*) which is dynamically expressed in developing teeth. *In situ* hybridization shows initial *Bmp6* expression early in the overlying inner, but not outer, dental epithelium (IDE and ODE respectively), as well as in underlying dental mesenchyme, followed by a decrease in expression in the epithelium before the tooth finally erupts into a functional tooth (Cleves et al., 2014; Ellis et al., 2016). Allele specific expression experiments identified

*cis*-regulatory changes in *Bmp6*. In tooth tissue from $F_1$ hybrids of high-toothed Paxton benthic fish and low-toothed marine fish, a 1.4 fold decrease in *Bmp6* expression from the high-tooth freshwater Paxton benthic allele compared to the marine allele was reported (Cleves et al., 2014). Work in mice and fish has demonstrated an essential role for BMPs in developing teeth (Bei et al., 2000; Cleves et al., 2018; Jia et al., 2013; Vainio et al., 1993; Wang et al., 2012), suggesting a possible causative role of *Bmp6* in evolved tooth gain.

Further refinement of the QTL interval identified a haplotype containing 10 single nucleotide polymorphisms (SNPs) within the intron 4 of *Bmp6* that vary concordantly with the presence or absence of the tooth QTL (Cleves et al., 2018). These variable positions define a high-tooth associated haplotype and low-tooth associated haplotype from the Paxton benthic freshwater and marine alleles, respectively. Six core SNPs lie within 468 bases upstream of the previously described minimally sufficient *Bmp6* intron 4 tooth enhancer (Figure S 2.1) (Cleves et al., 2018). We hypothesized that these core QTL-associated SNPs are modifying the spatial and/or temporal activity of the adjacent tooth enhancer.

Comparing expression patterns of two different alleles of an enhancer through reporter constructs in an organismal context presents two major problems: (1) comparisons of enhancer variants integrated in two different organisms are difficult to fully control for developmental time and genetic background differences and (2) aspects of reporter expression may in part reflect genomic integration site rather than actual enhancer activity. A single bicistronic transgenic construct that contains both enhancer/reporter pairings could address the first problem by providing a comparison within the same animal (and thus both enhancers being compared are at the same stage and in the same genotype). Furthermore, a single bicistronic construct simultaneously reduces the number of genomic integration sites to one and thus reduces position effects, partially addressing the second problem. The placement of a genetic insulator between the enhancer-reporter pairings can reduce cross talk of an enhancer with the opposite paired reporter, creating a more accurate expression profile. Genetic insulators have been shown to be effective in zebrafish (Bessa et al., 2009; Shimizu & Shimizu, 2013). A second alternative approach to a single bicistronic transgene is the use of doubly transgenic two-color lines that include both marine and freshwater enhancers paired with different reporters as parts of separate transgenes. This approach addresses the first problem by having both enhancers in the same animal. With this doubly transgenic two-color line approach, enhancers can be tested with reciprocal pairings (i.e. multiple transgenic reporter lines with different enhancers driving different fluorophores), to control for possible position effects. Here we use transgenic reporter assay experiments to test the hypothesis that the marine and freshwater *Bmp6* intron 4 enhancers have different spatial and/or temporal activity in developing fish embryos, larvae, and adults. We tested this hypothesis in two ways: first, by using a bicistronic enhancer transgene to compare activities of two enhancers in the same fish, and second, by comparing doubly transgenic two-color fish in which the marine and freshwater enhancers drive different fluorophores from different genomic integrations. Lastly, we tested whether the spatial shifts in enhancer activity between marine and freshwater enhancers are also observed for endogenous patterns of *Bmp6* expression during tooth development in marine and freshwater fish.

## 2.3 Materials and Methods

### Animal statement

All animal work was approved by UCB animal protocol #AUP-2015-01-7117-2. Fish were reared as previously described (Erickson et al., 2014).

### Insulator containing bicistronic construct

Gibson assembly was used to create bicistronic constructs to determine insulator efficiency in sticklebacks. Two enhancers with distinct expression domains were used: a 1.3kb fragment from the intron 4 of *Bmp6* (Cleves et al., 2018) and the stickleback ortholog of the R2 enhancer for *Col2a1a*, first identified in zebrafish and previously shown to drive similar embryonic expression in sticklebacks (Dale & Topczewski, 2011; Erickson et al., 2016). These two enhancers were placed on opposite sides of a genetic insulator, each with a different reporter gene, either mCherry (mCh) or enhanced GFP (eGFP). The mouse tyrosinase GAB insulator was amplified off the 2pC_GS plasmid (Bessa et al., 2009), while the R2 *Col2a1a* enhancer was PCR amplified from a previously used reporter plasmid (Erickson et al., 2016). The intron 4 enhancer of *Bmp6* was PCR amplified from a reporter plasmid containing either the freshwater allele from the benthic Paxton Lake population or the allele from the Little Campbell marine population (Cleves et al., 2018). All enhancers were PCR amplified simultaneously with the *Hsp70l* promoter as a single amplicon. eGFP and mCh were amplified from previously used reporter plasmids (O'Brown et al., 2015). Primers used and assembly steps are listed in the Supplemental Methods. All components were combined using a Gibson assembly reaction (New England Biolabs ref # E2611L) following the manufacturer's protocol and transformed into XL1 blue competent cells. Transformed cells were grown on ampicillin containing LB plates and colony inserts were sequence verified by colony PCR. Positive colonies were used to start 50 ml cultures, which were grown overnight. Plasmids were then isolated by Qiagen midi-prep (ref #12145), and Sanger sequence verified.

Tol2 transposase mRNA was transcribed using the plasmid pCS2-TP (Kawakami, 2004) that had been linearized with *Not*I. The linear plasmid was used as template for in vitro transcription using the mMessage SP6 kit (#AM1340). The resulting mRNA was purified using Qiagen RNeasy columns (#74104). Transgene plasmids were co-injected with Tol2 mRNA into newly in vitro fertilized one-cell embryos as described (Erickson et al., 2016). Approximately 200ng of plasmid in 1µl was combined with 1µl of 2M KCl, 0.5µl of 0.5% phenol red, and approximately 1µl of 350 ng/µl of Tol2 transposase mRNA, with water added to a final volume of 5µl, yielding a total concentration of ~40ng/µl of plasmid and 70ng/µl of mRNA. Embryos were generated from Rabbit Slough (Alaska) marine fish, and lines established and maintained by crossing to lab-reared fish from this same population.

### Generation of single color and doubly transgenic two-color reporter lines

The previously described ~1.3kb *Bmp6* intron 4 tooth enhancer (Cleves et al. 2018) was amplified from a Paxton Lake benthic fish and Little Campbell marine fish (Figure S 2.1) using the primer pairs MDS35/36 (GCCGGCTAGCGAGAGCATCCGTCTTGTGGG/GCCGGGATC CAGAGTCCTGATGGCCTCTCC) to create reporter plasmids containing the positive orientation (i.e. same 5' to 3' orientation as in endogenous locus) of the enhancer relative to the reporter gene or MDS27/28 (GCCGGCTAGCAGAGTCCTGATGGCCTCTCC/GCCGGGATC CGAGAGCATCCGTCTTGTGGG) to create reporter plasmids containing the negative orientation [i.e. the opposite 5' to 3' orientation as in the endogenous locus, and possibly more

similar to the orientation that an enhancer 3' to the promoter (e.g. an enhancer in intron 4) would be after looping to contact the promoter] of the enhancer. The fragments were then cloned in both possible 5' to 3' orientations into a Tol2 reporter construct upstream of the zebrafish *Hsp70l* promoter and either eGFP or mCherry using *BamH*I and *Nhe*I in the previously generated reporter constructs. Fish that were transgenic for both the marine and the freshwater reporter alleles were generated in one of two ways: (1) crossing of stable lines each containing a single transgene (2) injection of one reporter construct into a stable transgenic line of the opposite (i.e. different population and fluorophore) allele.

**Detecting enhancer activity by fluorescent microscopy**

Enhancer activity of the transgenic constructs was imaged by fluorescent microscopy. Previous work demonstrated a *cis*-regulatory difference in *Bmp6* expression between marine and freshwater alleles, with the difference arising late in development (Cleves et al., 2014). As both a divergence in tooth number attributed to the QTL and allele specific expression (ASE) differences arise late in development, post-20 mm total length (Cleves et al., 2014; Cleves et al., 2018), reporter positive fish were dissected at standard lengths pre- and post-tooth number divergence (20 mm total length) as previously described (Ellis & Miller, 2016). Tooth plates were then fixed in 4% PFA in 1x PBS for 60 minutes, washed through a graded series of 3:1, 1:1, 1:3 water and glycerol solutions into 100% glycerol, flat-mounted, and imaged. Comparisons were made across the different alleles and orientations on a Leica M165FC fluorescent dissecting microscope with filters GFP1 (#10447447) and RhodB (#10447360), and a Leica DM2500 compound microscope with filters GFP (#11532366) and TX2 (#11513885). To compare enhancer activity in fish before and after tooth divergence (20 mm standard length), ventral tooth plates and dorsal tooth plates were imaged and enhancer activity was assessed in the dental epithelium and mesenchyme of each tooth, in each of three pre-divergence sized fish (between 16 - 18.5 mm total length) and three post-divergence sized fish (between 30 – 48 mm total length) in two different sets of integrations and enhancer/reporter pairings. If the QTL-associated SNPs are responsible for the QTL peak and therefore tooth number differences observed late in development, as well as the ASE differences, we would expect the enhancers to have different activity in > 20 mm fish compared to < 20 mm fish. We would also expect the enhancers to have similar activity earlier in development, when allele specific expression was not significantly different between the freshwater and marine alleles (Cleves et al., 2014).

**Quantification of enhancer activity differences across tooth development**

As we hypothesized that the QTL associated intronic polymorphisms result in differential enhancer activity in the dental mesenchyme and/or epithelium, we characterized enhancer activity in both tissues across multiple tooth plates. The stage of each tooth was scored as either early (early bell stages in which mesenchyme has condensed under the epithelium but no mineralization has occurred), middle (mineralization of the forming tooth has started to occur, also called late bell stage) or late (a fully formed tooth has erupted, also called functional stage (Ellis et al., 2015)). The activity for each enhancer allele was recorded as either present or absent in the epithelium (early and middle stages) and mesenchyme. Additionally, we also recorded if either allele (marine or freshwater) drove more robust or extensive expression in each domain, indicating an allelic bias.

### *In situ* hybridization on sections

Stickleback adult (~40 cm standard length) pharyngeal tissues were prepared, sectioned, and assayed by ISH in parallel to compare the spatial distribution of *Bmp6* mRNA. Adults derived from marine (Rabbit Slough [RABS]) and freshwater (Paxton Benthic [PAXB]) populations were euthanized, and their pharyngeal tissues were fixed overnight in 4% formaldehyde (Sigma P6148) in 1x phosphate-buffered saline (PBS) at 4° C with heavy agitation, washed 3x 20 min with PBST on a nutator, then decalcified for 5 days in 20% ethylenediaminetetraacetic acid (EDTA, pH 8.0) at room temperature on a nutator. Marine and freshwater fish were always collected and prepared in parallel such that all storage and preparation intervals were equivalent. The *in situ* hybridization (ISH) for *Bmp6* was carried out as described previously (Square et al., 2021), with some modifications to ensure maximally comparable assays were carried out on marine and freshwater samples in parallel. A previously published *Bmp6* riboprobe was used in this study (Cleves et al., 2014; Square et al., 2021). The *Bmp6* riboprobe was synthesized with digoxygenin-labeled UTP and added at a concentration of ~300 ng/mL in 20 mL of hybridization buffer, split between 2 different LockMailer slide containers (Sigma-Aldrich), and agitated overnight in a rotating hybridization oven at 67° C. Slides from marine and freshwater fish were cohoused in the hybridization buffers to ensure equal exposure to the riboprobe between marine and freshwater samples. Hybridization buffer washes, blocking, and antibody incubation steps were as previously described (Square et al., 2021). Signal development was carried out for 2, 3, or 7 days to visualize mRNA localization. Marine and freshwater slides were developed in parallel (in the same solutions, in the same LockMailer containers), and only those sections that experienced the same coloration reaction were compared (i.e. we only directly compared sections that were prepared in parallel). To prepare slides for imaging, they were counterstained with DAPI, rinsed then washed 3x 5+ min with deionized $H_20$, coverslipped with deionized $H_20$, and imaged on a Leica DM2500 microscope. The procedure outlined in this section was replicated three times, each replication used two marine and two freshwater adults, for a total of n=6 fish from each background.

## 2.4 Results

### Two ways to compare enhancers in transgenic fish

We used two strategies to compare enhancer alleles in the same transgenic fish. First, we used a single bicistronic construct with a genetic insulator separating two enhancer/reporter pairs. Second, we used two separate transgenic constructs, independently integrated in the same fish line and each containing a single enhancer allele (marine or freshwater, Figure S 2.1) with a distinct fluorescent reporter (eGFP or mCherry), to generate doubly transgenic two-color fish.

### Insulator efficiency in $F_0$ fish

To test the first strategy of a bicistronic construct separated by an insulator, a bicistronic construct was generated using two enhancers that drive expression in non-overlapping domains. In sticklebacks, the *Col2a1a R2* enhancer drives expression in the developing notochord with expression seen by the third day post fertilization (dpf) (Erickson, Ellis, et al., 2016). By 8 dpf we observed *R2* reporter expression in the developing craniofacial skeleton, including Meckel's cartilage, the hyosympletic, and the ceratohyal (Figure S 2.2), similar to the reported enhancer activity in zebrafish (Dale & Topczewski, 2011). The *Bmp6* intron 4 tooth enhancer has not been reported to drive expression in the domains seen in the *R2 Col2a1a* enhancer. In addition, the previously described tooth and early fin domains (Cleves et al., 2018), as well as the presently

described late fin domains, are not domains in which the *Col2a1a* enhancer has been observed to drive expression. Thus, to our knowledge these two enhancers drive distinct and non-overlapping expression domains within these embryonic and larval tissues, providing multiple locations that can test for insulation within the construct.

Three clutches were injected with a *Col2a1a* enhancer/*Bmp6* tooth enhancer bicistronic construct (Figure 2.1A) for a total of 228 injected embryos, of which 92 were scoreable at 7 dpf. Four domains (left and right pectoral fins, median fin fold, and notochord) were scored for insulation efficiency (0-2 for no to complete insulation, see Supplemental Methods). Across all domains the average insulator score was 0.94 (Table S 2.1). Overall, the bicistronic construct using the mouse tyrosinase insulator element (GAB) moderately prevented reporter genes from being activated by nearby enhancers when placed between the elements. Within the same $F_0$ fish we observed both insulated and uninsulated domains, with insulation even varying within a domain (Figure 2.1B). For example, insulation was observed in the median fin and left pectoral fin, but not within some regions of the right pectoral fin of a 7 dpf embryo in which both mCherry and eGFP were observed. To control for enhancer/reporter pairing, the inverse construct was created, with the *Col2a1a* enhancer driving eGFP and the *Bmp6* tooth enhancer driving mCherry. A total of 154 fish were injected across two clutches, with 30 surviving to 7 dpf that were scoreable, with an average score of 0.64 (Table S 2.2). Overall, both insulator constructs demonstrate the ability to drive some degree of separate expression domains of two enhancers concurrently, consistent with results reported in zebrafish that showed insulators can block enhancer-promoter crosstalk (Bessa et al., 2009).

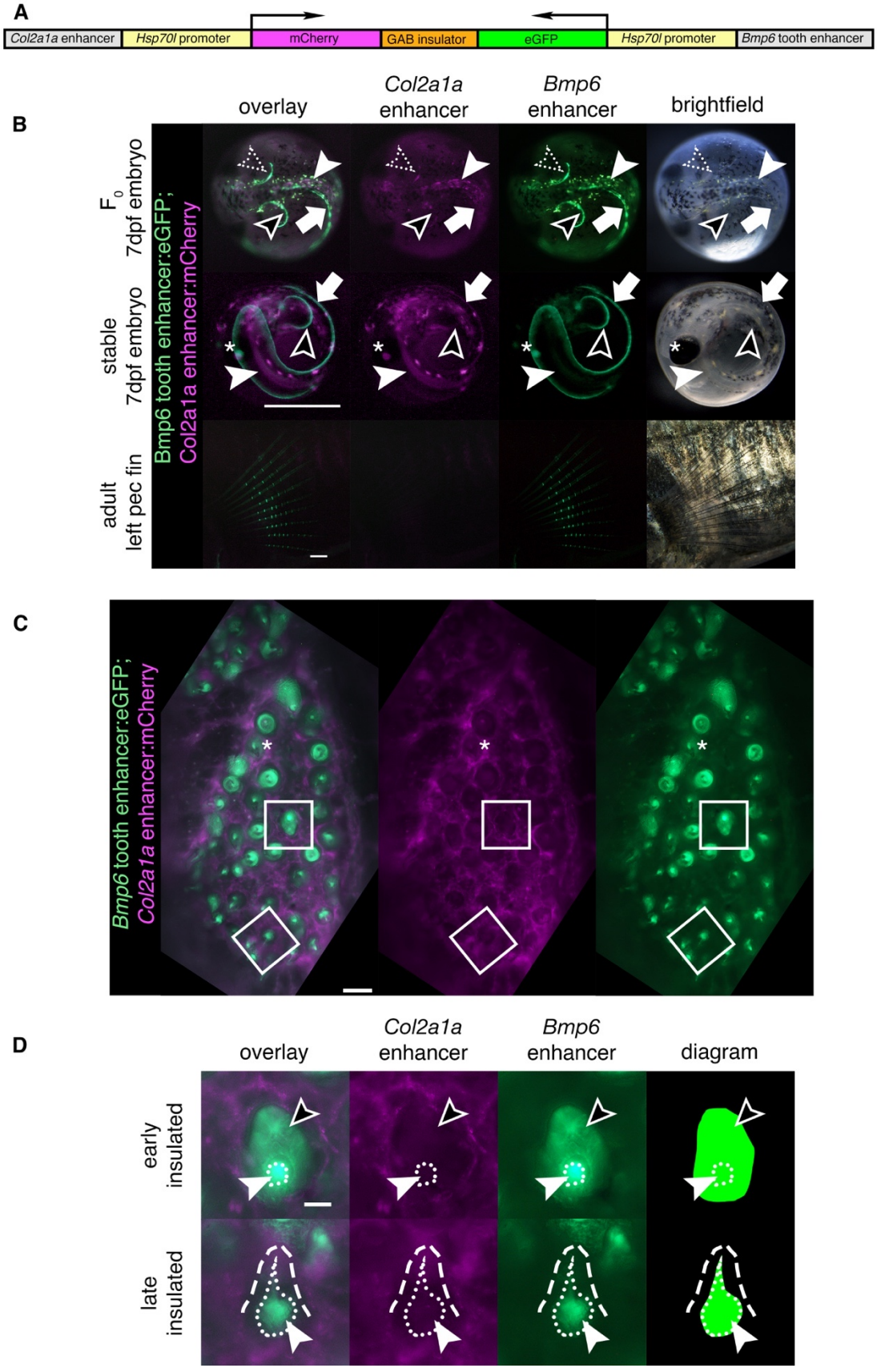
A
Col2a1a enhancer
Hsp70l promoter
mCherry
GAB insulator
eGFP
Hsp70l promoter
Bmp6 tooth enhancer
B
overlay
Col2a1a enhancer
Bmp6 enhancer
brightfield
F0 7dpf embryo
stable 7dpf embryo
adult left pec fin
Bmp6 tooth enhancer:eGFP;
Col2a1a enhancer:mCherry
C
Bmp6 tooth enhancer:eGFP;
Col2a1a enhancer:mCherry
D
overlay
Col2a1a enhancer
Bmp6 enhancer
diagram
early insulated
late insulated

**Figure 2.1 An insulated bicistronic construct reports separate expression patterns from two different enhancers. (A)** Bicistronic construct with a *Col2a1a* enhancer and *Hsp70l* promoter driving mCherry and the freshwater *Bmp6* intronic tooth enhancer and *Hsp70l* promoter driving eGFP, separated by the mouse tyrosinase insulator (GAB). **(B)** Transgenic fish show a separation of domains in red and green overlay, red channel only, green channel only, and brightfield (left to right). Top: In 7 days post fertilization (dpf) $F_0$ fish (dorsal view), insulation was observed in some but not all domains. Both mCherry and eGFP were observed in the same area in the right pectoral fin (dotted arrowhead), indicating incomplete or failed separation of domains, while in the other areas of the pectoral fin only eGFP was observed (black arrowhead). Within the notochord (solid white arrowhead), only mCherry was observed, while in the median fin (white arrow) only eGFP was observed, indicating insulation in both domains. Middle: In 7 dpf stable $F_1$ fish (lateral view), only eGFP was observed in the pectoral fins (black arrowhead) indicating successful insulation in those domains, while both fluorophores were detected in the median fin (white arrow) and in the notochord (solid white arrowhead) indicating a lack of insulation. Both fluorophores were detected in the lens of the eye (asterisk), a domain driven by the *Hsp70l* promoter. Bottom: in adult pectoral fins (lateral view), eGFP but not mCherry expression was detected. **(C-D)** Dorsal pharyngeal tooth plate (C) and representative teeth of early and late stages (D) from adult stable transgenic fish. (C) Insulator effectiveness was observed with eGFP restricted to predicted tooth domains and mCherry primarily present in the surrounding tissue. In some teeth, faint mCherry appeared to be expressed in the dental mesenchyme (asterisk). (**D**) eGFP expression was detected in the dental mesenchyme (solid arrowhead and extent of mesenchyme as white dotted line) and dental epithelium (black arrowhead) of developing teeth, while mCherry was expressed in the surrounding tissue (white dashed line outlines a mineralized tooth). Scale bars = 1mm **(B)**, 100μm **(C),** 25μm **(D).**

## Insulator effectiveness in stable fish

Variation in insulator effectiveness across an individual $F_0$ fish may be due to different genomic integrations of the bicistronic constructs. To determine the effectiveness of a single bicistronic transgene, $F_0$ fish were outcrossed to create stable $F_1$ individuals for the *Col2a1a R2*:mCherry; *Bmp6* tooth enhancer:eGFP bicistronic construct. In 7 dpf $F_1$ embryos, complete fin domains of the *Bmp6* enhancer were observed, with insulation apparent in some but not all domains (Figure 2.1B). In adults, *Bmp6* enhancer activity was observed in the intersegmental joints of fins (described below), however no mCherry was observed, suggesting effective insulation in that domain (Figure 2.1B). Insulator activity was also observed in pharyngeal teeth (Figure 2.1C). The *Bmp6* enhancer was observed to drive expression in the mesenchyme and inner dental epithelium (IDE) of pharyngeal teeth (Figure 2.1D), consistent with previous reports. mCherry was not observed in the tooth domains, suggesting effective insulation in adult teeth. Thus, in stable transgenic adults the insulator can separate the activity of the two enhancers, including within the dental epithelium and mesenchyme domains of the *Bmp6* enhancer.

## Bicistronic construct reveals spatial shifts in mesenchymal and epithelial activity of *Bmp6* enhancer alleles

Since the GAB genetic insulator can block enhancer-promoter crosstalk in bicistronic constructs, a bicistronic construct with both the marine and freshwater alleles (Figure 2.2A) was used to create a stable line as a first test for enhancer activity differences. The marine allele, paired with mCherry, appeared to drive a more robust mesenchymal domain compared to the freshwater allele (Figure 2.2B-C). In contrast, within the inner dental epithelium more GFP than mCherry signal was detected, suggesting an expanded epithelial domain driven by the freshwater enhancer

compared to the marine allele. Thus, in developing teeth from fish with this bicistronic transgene, the marine allele drove more robust expression in the mesenchyme while the freshwater allele drove more robust expression in the epithelium.

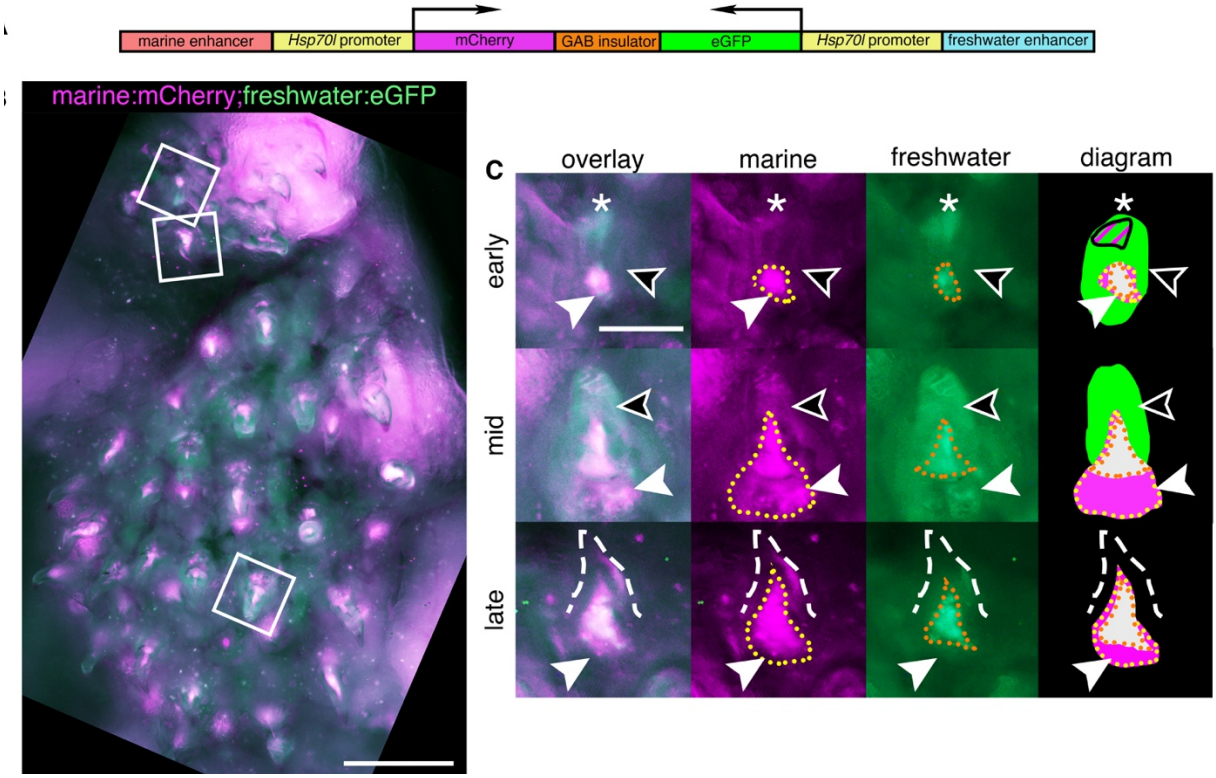


**Figure 2.2 A bicistronic construct using a genetic insulator separates the expression domains of the marine and freshwater alleles of the Bmp6 tooth enhancer. (A)** Bicistronic construct with the marine allele of the intron 4 *Bmp6* enhancer/*Hsp70l* promoter driving mCherry and the freshwater allele/*Hsp70l* promoter driving eGFP separated by the mouse tyrosinase GAB insulator. **(B)** Dorsal pharyngeal tooth plate from a fish transgenic with construct (A), and representative teeth (white boxes) from early, middle, and late stages (early bell, late bell, and functional, respectively) **(C)**. Early: epithelium expressed eGFP throughout (black arrowhead) while a concentrated tip (asterisk) was observed to contain both marine and freshwater activity. In the mesenchyme (white arrowhead) the marine allele had a more robust and larger expression domain (yellow dotted line) compared to the freshwater allele (orange dotted line). Middle: epithelium had freshwater expression while the marine allele continued to drive more robust expression in the mesenchyme compared to the freshwater allele. Late: As in the other stages the freshwater allele had a more restricted expression domain in mesenchyme of erupted mineralized teeth (dashed line). Scale bars = 200μm **(B)**, 50μm **(C)**.

### Doubly transgenic fish confirm expanded freshwater epithelial *Bmp6* enhancer activity in post-divergence fish

As a second method to compare the spatial and temporal activity of marine and freshwater enhancer alleles, we generated stable bi-color transgenic lines with the two different alleles of the *Bmp6* intron 4 tooth enhancer on separate constructs: freshwater:eGFP;marine:mCherry, in the opposite 5' to 3' direction as the endogenous locus, and freshwater:mCherry;marine:eGFP, in

the same 5' to 3' direction as the endogenous locus. In adult fish, both marine and freshwater enhancers were observed to drive dynamic expression in the IDE, more intensely at earlier stages, and diminishing as development of the tooth approaches eruption (Figure 2.3A-C, and Figure S 2.3 A-C), consistent with *Bmp6* expression detected by whole-mount in situ hybridization (Cleves et al., 2014; Ellis et al., 2016). In multiple tooth germs, a brighter focus was observed at the distal tip of the epithelium with both enhancers (Figure 2.3A-C & Figure S 2.3 A-C), a domain resembling the localized distal epithelial expression of *Fgf10* and putative enamel knot in shark embryos (Rasch et al., 2016). This distal epithelial domain was the last epithelial region to drive reporter expression prior to cessation in the epithelium. While both enhancers were observed to drive expression in the epithelium, the freshwater allele drove seemingly more robust expression of the reporter, both in terms of intensity as well as spatial extent of the domain (Figure 2.3B-C, Figure S 2.3 B-C).

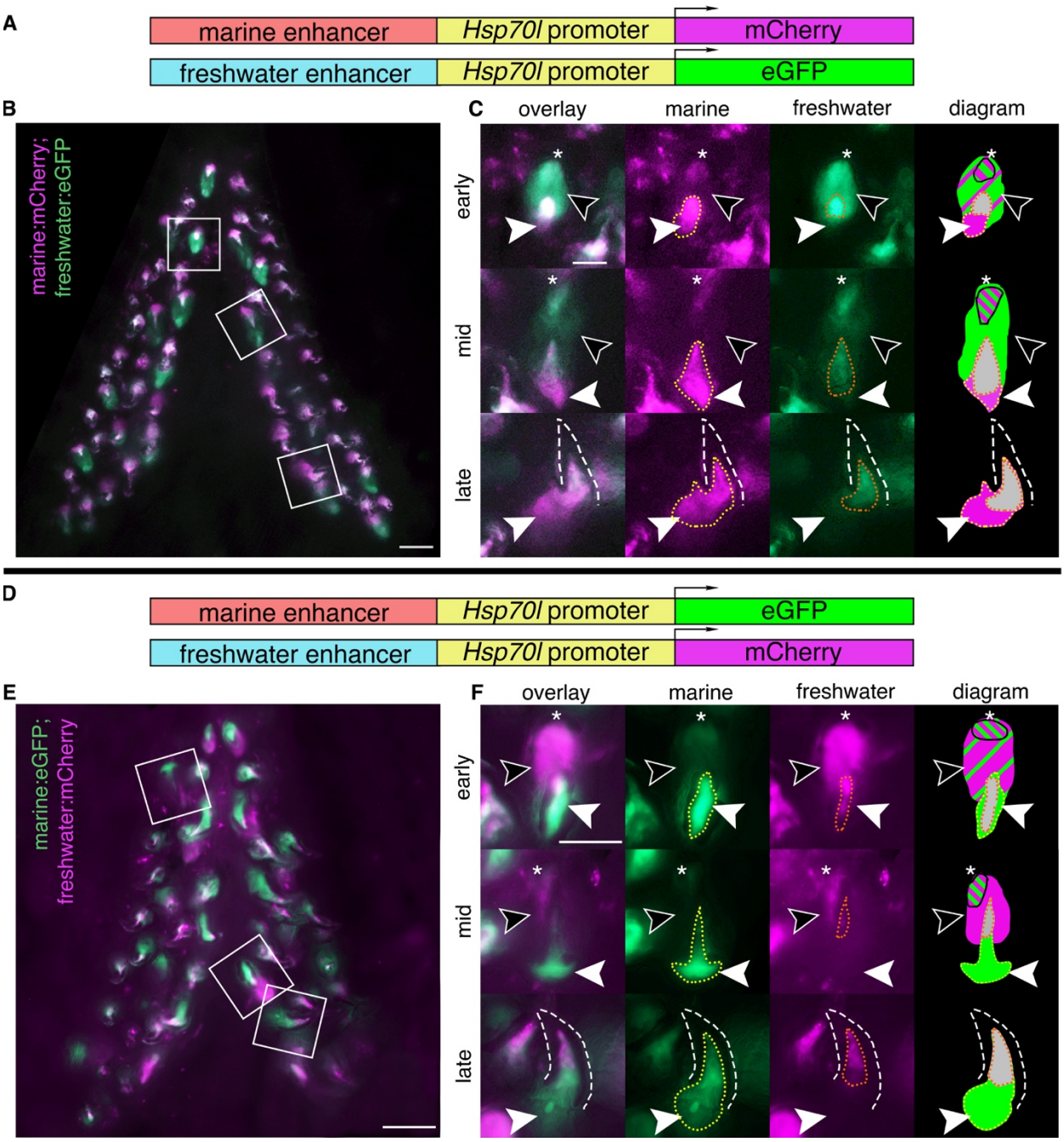


**Figure 2.3 Reduced mesenchymal and expanded epithelial expression of freshwater enhancer relative to marine enhancer in developing teeth.** Ventral pharyngeal tooth plates from fish doubly transgenic for two alleles of the *Bmp6* intron 4 enhancer driving two different reporter genes **(A,D)**: the marine enhancer driving mCherry with the freshwater enhancer driving eGFP **(B,C)** and the marine enhancer driving eGFP with the freshwater enhancing driving mCherry **(E,F)**. Bilateral ventral pharyngeal tooth plates **(B,E)** are shown, next to representative teeth from three stages **(C,F)**: early (early bell), middle (late bell), and late (functional) highlighted by white boxes in **B,E**. **(C,F)** Early: freshwater and marine enhancer drove expression in the epithelium (black arrowheads), with concentrated expression in the tip (asterisk), and more overall epithelial expression from the freshwater enhancer. Both enhancers also drove expression in the mesenchyme (solid white arrowhead) with a larger expression domain of the marine allele (yellow dotted line) compared to the freshwater allele (orange dotted line) seen in both

genotypes. Middle: freshwater allele still drove expression in the epithelium while marine allele had reduced or undetectable expression outside concentrated tip. The marine allele drove more robust mesenchymal expression compared to the freshwater allele. Late: marine allele drove robust expression in the mesenchyme compared to freshwater allele in mineralized tooth (dashed line). Diagram: summary of tooth epithelial and mesenchymal domains. The relative sizes of green and magenta hatched lines correspond to the approximate relative strength of expression in the epithelium. Overlapping mesenchyme domain is grey, and expanded marine mesenchyme is marked with white arrowhead. Scale bars = 100μm **(B,D)**, 50μm **(C, F)**.

**Doubly transgenic fish confirm reduced freshwater mesenchymal *Bmp6* enhancer activity in post-divergence fish**

Reporter expression from the two alleles appeared in the mesenchyme of teeth across all stages. In pre-eruption (early and middle stage) tooth germs, condensed mesenchyme was observed to show activity of both enhancers (Figure 2.3B-C and Figure S 2.3B-C). In fully formed, erupted, late-stage teeth, reporter expression was observed in the mesenchymal core, extending from the tip of the core down to the base of the tooth where expression widened. Deeper mesenchyme was observed to consistently display marine but not freshwater enhancer activity. The deeper, broader, and more robust mesenchymal expression domain driven by the marine allele compared to the freshwater allele was also observed in stages of tooth development prior to eruption (Figure 2.3B-C and Figure S 2.3B-C).

**Reciprocal reporter/enhancer pairing in second doubly transgenic two-color line support epithelial and mesenchymal shifts in enhancer activity**

To determine if the previous observations were artifacts due to factors such as transgene position effects, fluorophore used, or enhancer orientation, next we made constructs where each enhancer had an opposite enhancer orientation and drove the other fluorophore (Fig. 2.3D). These constructs were then randomly integrated by Tol2-mediated transgenesis, representing independent genomic integrations of oppositely oriented enhancers with alternate fluorophores, simultaneously controlling for genomic position effect, enhancer orientation, and fluorophore strength. Using these reciprocal constructs, we again observed the epithelial and mesenchymal differences seen in the bicistronic construct and the first double transgenic line, suggesting the freshwater SNPs reduce mesenchymal and expand epithelial enhancer activity (Figure 2.3E-F and Figure S 2.3E-F).

**Less pronounced enhancer activity differences in early fish**

Allele specific differences in the expression levels of the freshwater and marine alleles of *Bmp6*, as well as tooth number, have been shown to arise later in development (> 20 mm fish length). We hypothesized that if the SNPs found within the freshwater and marine haplotypes contribute to the allele specific expression differences, and subsequently tooth number differences, the differences in enhancer expression should be more pronounced in larger fish compared to smaller fish. Fish smaller than the tooth divergence point (~16-18.5 mm juveniles, see Methods) were dissected from each genotype and tooth plates were fixed and imaged (Figure 2.4). While the epithelial and mesenchymal expression differences observed in the older post-divergence stages were still present in both the dental epithelium and mesenchyme (Figure 2.4C,F), the enhancer differences were less pronounced. In multiple early and middle stage teeth the

epithelium showed similar activity from both alleles (Figure 2.4C,F), unlike the expanded freshwater epithelial domain that was observed in larger fish. Overall, the expression patterns of the two enhancers appeared more similar in pre-divergence fish, consistent with previous allele specific expression and tooth number results (Cleves et al., 2014).

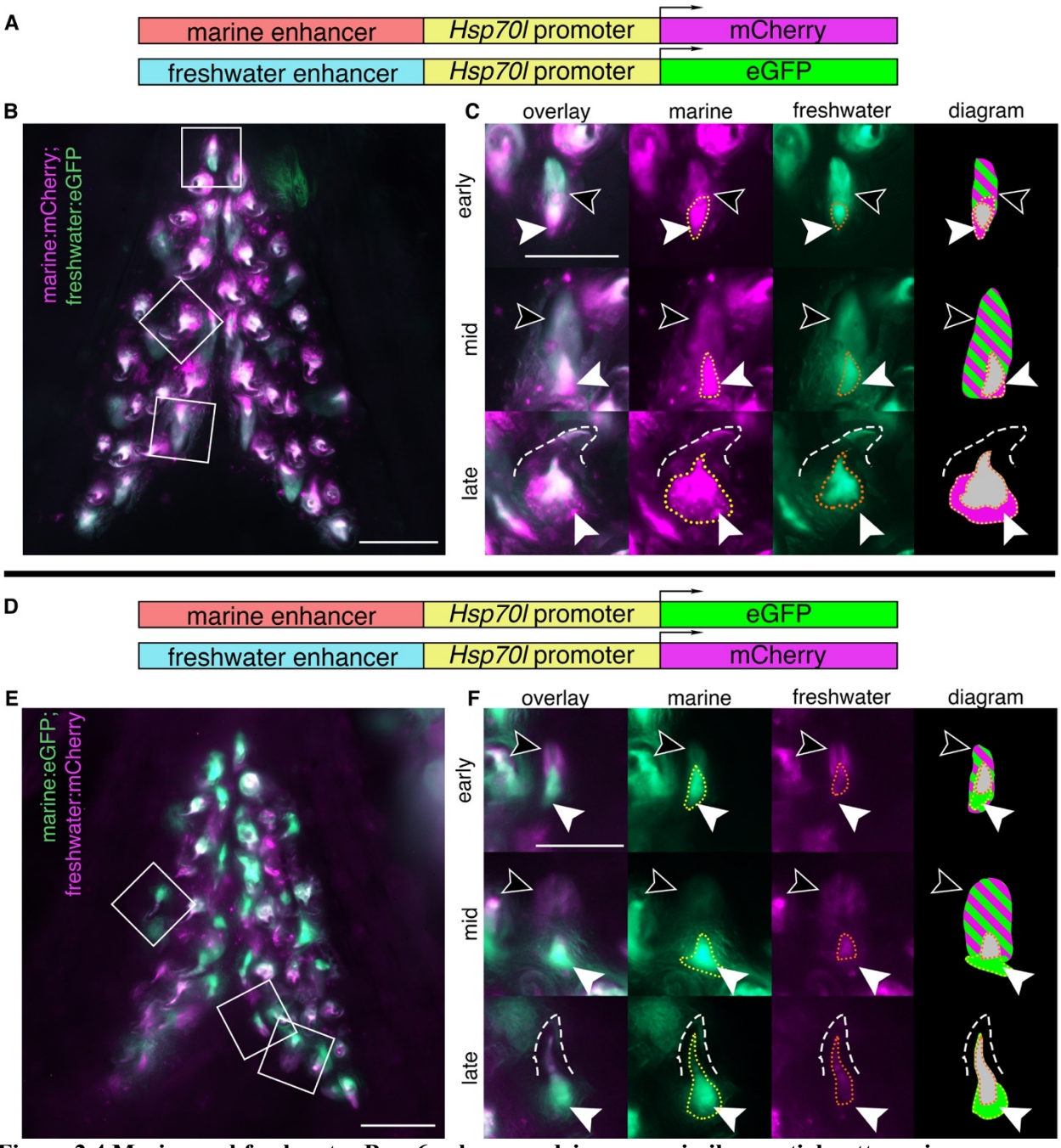


**Figure 2.4 Marine and freshwater Bmp6 enhancers drive more similar spatial patterns in younger fish.** Ventral pharyngeal tooth plates from < 20 mm (pre-tooth number divergence) fish doubly transgenic for two alleles of the *Bmp6* intron 4 enhancer driving two different reporter genes **(A,D)**: the marine enhancer driving mCherry with the freshwater enhancer driving eGFP **(B,C)** and the marine enhancer driving eGFP with the freshwater enhancing driving mCherry **(E,F)**. Bilateral ventral tooth plates **(B,E)**

are shown next to representative teeth from the three stages **(C,F)**: early, middle, and late highlighted by white boxes in **B,E**. Early: both freshwater and marine enhancer drove expression robustly in the epithelium (black arrowheads), while both enhancers drove expression in the mesenchyme (white arrowheads), the marine enhancer drove a broader domain (yellow dotted line) compared to the freshwater enhancer (orange dotted line). Middle: both enhancers continued to drive robust, apparently similar levels of expression in the epithelium (black arrows). In the mesenchyme (white arrowheads) the domain of the freshwater enhancer was reduced compared to the marine allele. Late: marine allele continued to drive a broader domain within the mesenchyme of mineralized teeth (dashed line). The relative sizes of green and magenta hatched lines correspond to the approximate relative strength of expression in the epithelium. Overlapping mesenchyme domain is grey, and expanded marine mesenchyme is marked with white arrowhead. Scale bars = 100μm **(B,E)**, 50μm **(C, F)**.

**Quantification of epithelial and mesenchymal expression patterns**

Quantification of epithelial and mesenchymal expression, and bias towards enhancer activity was scored for three tooth plates of each type (ventral and dorsal) at pre and post tooth number divergence (Supplemental Material). In post divergence fish activity of the freshwater enhancer was observed in the epithelium in both ventral and dorsal tooth plates in nearly all pre-eruption teeth (Figure 2.5A & Table S 2.3). The marine allele was detected in the epithelium of only a subset of pre-eruption teeth, from approximately 70-90% of pre-eruption teeth in pooled tooth plate data (Figure 2.5A). When combining tooth plate data for each genotype the marine enhancer was active in the epithelium in a higher percentage of early stage germs compared to middle stage (marine:mCherry;freshwater:eGFP early: 44/52 [84.6%], middle 39/51 [76.5%] and marine:eGFP;freshwater:mCherry early: 39/47 [83.0%], middle 30/40 [75%]). The pattern is still present when data is sorted by tooth plate and genotype (Supplemental Material). Therefore, while there does appear to be a stage effect, variation also exists within stages. Overall, the freshwater enhancer drove expression more frequently and more robustly in the epithelium of early and middle stage teeth compared to the marine allele in post divergence fish. However, in pre-divergence fish the epithelium of all pre-eruption teeth exhibited robust expression of both enhancers, across both genotypes and tooth plates (Figure 2.5A).

A bias towards the marine allele in the mesenchyme was observed in nearly every early or middle stage tooth germ, while the lack of bias, or entirely overlapping mesenchymal expression, was almost exclusively observed in late stage (erupted) tooth germs (Table S 2.4). The ventral tooth plates had an increased prevalence of marine enhancer bias in the mesenchyme of individual teeth compared to the dorsal tooth plates (marine:mCherry;freshwater:eGFP ventral: 146/167 [87.4%], dorsal: 102/149, [68.5%] and marine:eGFP;freshwater:mCherry ventral: 123/136 [90.4%], dorsal: 122/149 [81.9%]). In early and middle stage teeth, we observed a consistent marine bias in the mesenchyme of both the ventral and dorsal tooth plates. In fully formed erupted teeth a difference between the tooth plates became apparent. A larger proportion of erupted teeth were observed to have a marine bias in the mesenchyme in the ventral tooth plate compared to the dorsal tooth plate (Figure 2.5B-C).

There was a reduction in the proportion of erupted teeth with a marine bias when comparing post to pre divergence fish for all integrations and tooth plates (pre-divergence marine:mCherry;freshwater:eGFP ventral 54/80 [67.5%], dorsal 55/91 [60.4%] and marine:eGFP;freshwater:mCherry ventral 63/98 [64.3%], dorsal 51/103 [49.5%]) (Figure 2.5B) except for the dorsal tooth plates in the freshwater:eGFP;marine:mCherry genotype. Overall a

bias towards marine expression in the mesenchyme was observed, with a consistently larger proportion of late stage teeth demonstrating a bias in the ventral teeth compared to the dorsal teeth, with the difference between tooth plates becoming more drastic in larger fish. Thus, the trend in marine mesenchymal bias across dorsal versus ventral tooth plates mirrors the chromosome 21 tooth number QTL, which had a 28 LOD greater effect on ventral pharyngeal tooth number than dorsal pharyngeal tooth number (Miller et al., 2014). In addition, the difference in bias between pre-divergence and post-divergence fish is consistent with allele specific expression data in which early in development the marine and freshwater alleles of *Bmp6* are expressed at more similar levels, while in older fish there is a *cis*-regulatory reduction in expression of the freshwater allele (Cleves et al., 2014).

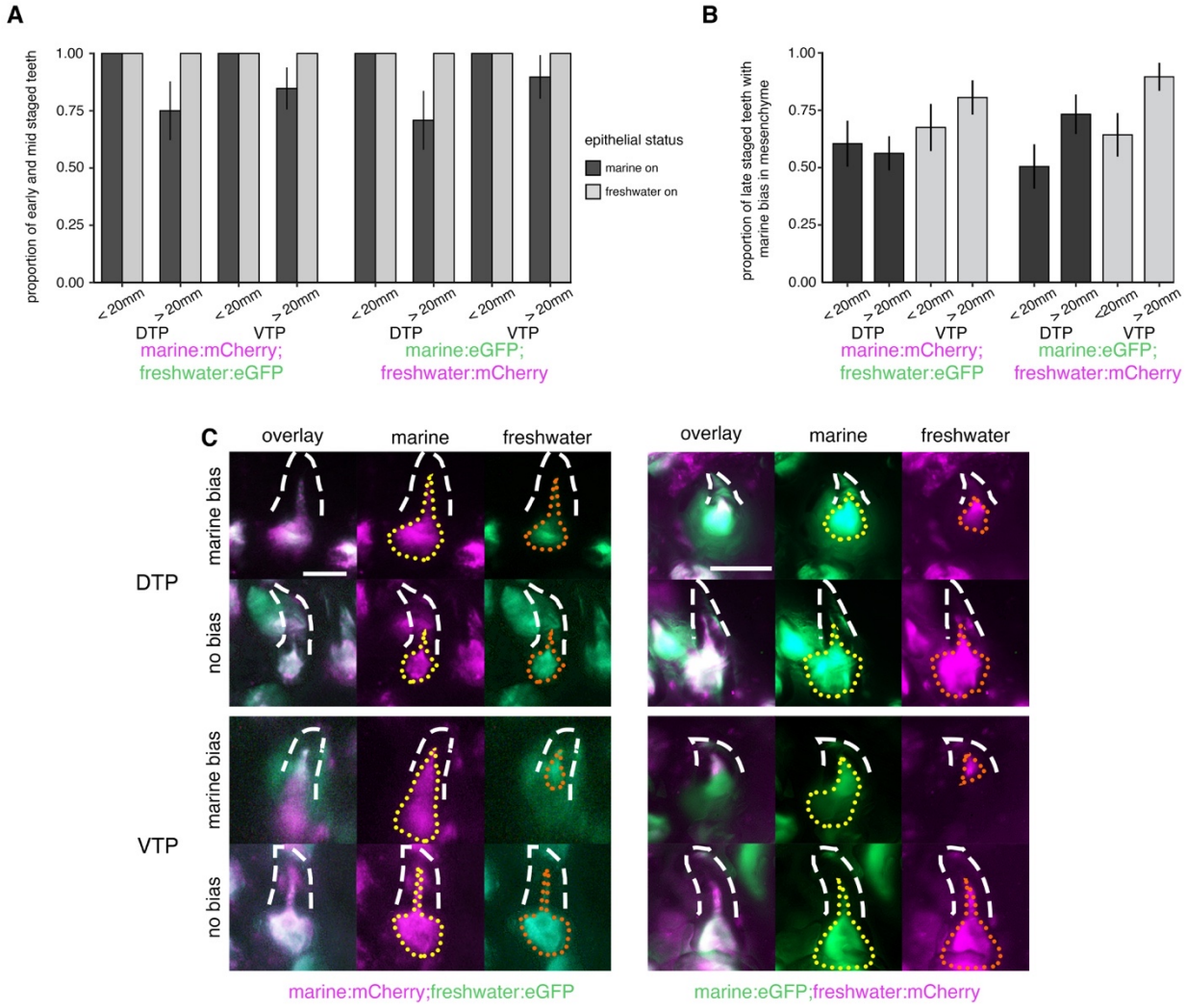


**Figure 2.5 Differences in enhancer activity vary based on dorsal vs. ventral tooth field, fish total length, and epithelial vs. mesenchymal domain. (A)** In < 20mm total length (pre-tooth number divergence) fish, the marine and freshwater alleles were expressed in the epithelium of all developing tooth germs regardless of genotype, while in > 20 mm total length (post-tooth number divergence) fish epithelial expression differences were consistent across tooth plates and genotypes. The freshwater allele consistently drove expression in all tooth germs scored, while the marine allele did not. **(B)** The

proportion of erupted teeth that demonstrated an observed mesenchymal bias of an expanded marine enhancer domain differed across dorsal and ventral tooth plates (DTP and VTP, respectively), with more bias ventrally than dorsally. **(C)** Examples of erupted teeth (white dashed lines) from both DTP and VTP that were scored as either having a marine bias in the mesenchyme [if the freshwater enhancer mesenchymal domain (orange dotted line) was more restricted compared to the marine enhancer domain (yellow dotted line)], or no bias if the freshwater enhancer mesenchymal domain was equivalent to the marine enhancer domain. Scale bars = 50μm **(C)**.

**Pectoral and caudal fin expression differences**

The *Bmp6* intron 4 enhancer was previously known to drive expression in the developing fin margins of the pectoral and caudal fins early in development, starting approximately 4 dpf (Cleves et al., 2018). In pre-hatching fish, 6 dpf, the domains of the two enhancers appear to be identical (Figure S 2.4A). We found that enhancer activity persists at later stages in both the pectoral and caudal fins, specifically in the intersegmental joints. The fin rays of all fins in sticklebacks consist of a series of repeated segments, made up of hemi-segments encasing a mesenchymal core like other teleosts (Haas, 1962; Santamaría et al., 1992). In the caudal fin of both genotypes (freshwater:eGFP;marine:mCherry and freshwater:mCherry;marine:eGFP), the freshwater enhancer was observed to have activity in multiple intersegmental joints, while the activity of the marine enhancer was detected in none or few joints (Figure S 2.4B). A similar pattern is observed in the pectoral fins (Figure S 2.4C). With both enhancers, more basal joints were observed to have expression, while fluorophore intensity diminished as the joints became more distal. Overall, across both fin types, the freshwater allele appeared to be active in a larger number of intersegmental joints. While more proximal intersegmental joints were more likely to have activity from both enhancers, the most proximal joint was observed to be lacking detectable reporter expression in some fin rays (Figure S 2.5A&B), suggesting a dynamic cycle of initial inactivity in newly formed, distal, intersegmental joints, followed by a period of activity in most joints as they adopt a more proximal identity, and a final transition to inactivity in the proximal most joints just prior to the ultimate fusion of basal most segment to the next segment.

***Bmp6* expression differences between marine and freshwater fish**

Given the consistent differences in reporter gene activity observed for the marine and freshwater enhancers, we next asked if endogenous *Bmp6* expression differed in tooth germs between marine and freshwater animals in a similar fashion. To answer this, we performed *in situ* hybridization (ISH) on thin sections of pharyngeal tissues from marine (Rabbit Slough) and freshwater (Paxton Benthic) adults (~40 mm standard length). Marine and freshwater samples were collected, prepared, and assayed in parallel to ensure maximal comparability of the resulting data (see Methods). While early bud and cap stage tooth germs did not show any consistent differences in gene expression, we did observe more widespread mesenchymal expression in marine tooth germs at early and late bell stages, and consistently widespread IDE expression in freshwater epithelium relative at late bell stages (Figure 2.6). These ISH results corroborate the reporter construct activity, suggesting that the regulation of *Bmp6* mRNA in tooth germs varies in the same direction as the variation in activity seen between the marine and freshwater *Bmp6* intron 4 enhancers.

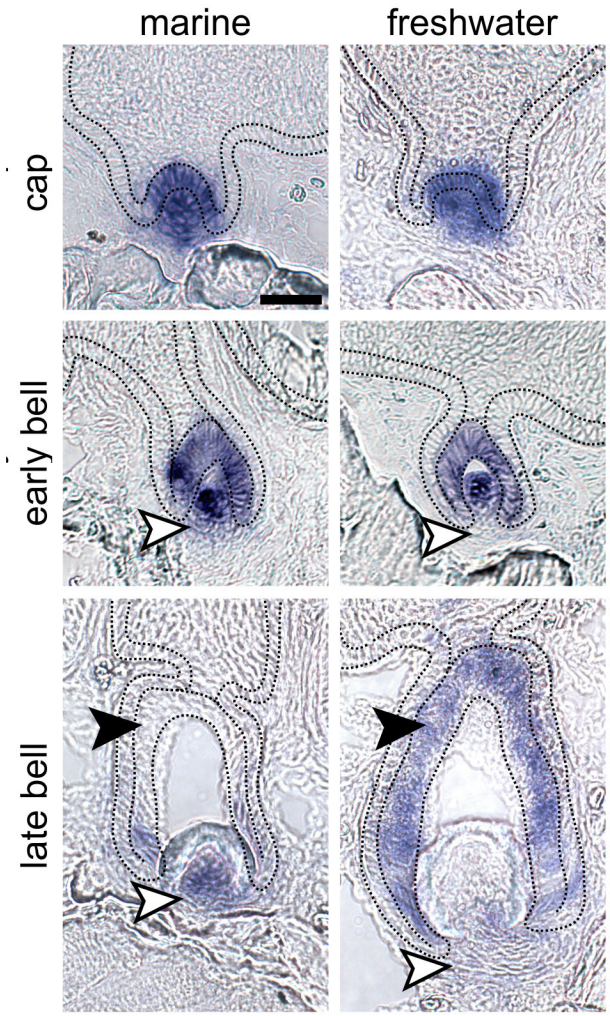


**Figure 2.6 In situ hybridization illustrates that Bmp6 expression shifts mirror enhancer activity differences in marine and freshwater backgrounds.** In situ hybridization (ISH) of *Bmp6* expression on thin sections of marine (left column) and freshwater (right column) homozygous backgrounds suggest that marine fish exhibit expanded mesenchymal expression at early and late bell stages (white arrowheads in middle and bottom rows, respectively), while freshwater fish exhibit relatively broader expression in the inner dental epithelium (IDE) of late bell stage teeth (black arrowheads in bottom row). No expression domain differences were observed in cap stage tooth germs (top row). Marine and freshwater strains are derived from  population in Rabbit Slough, AK, USA (RABS), and Paxton Lake, BC, Canada (PAXB), respectively. Black dotted lines demarcate the basalmost layer of epithelium, adjacent to the basement membrane, which includes the inner and outer dental epithelium. See Figure S 2.6 Figure S6 for DAPI counterstains and ISH images without markup. Scale bar = 20μm and applies to all panels.

## 2.5 Discussion

### Freshwater and marine alleles of *Bmp6* tooth enhancer drive expression differences in developing teeth

Throughout the development of a tooth, multiple pathways and signals, including BMPs, are involved in organ initiation and growth. Knocking out the receptor *Bmpr1a* in the dental

epithelium of mice leads to arrested development of the tooth at the bud stage, demonstrating a key activating role for BMP signaling during tooth development (Andl, 2004). Overexpressing *Noggin*, a BMP antagonist, in the epithelium also results in arrest at the placode stage (Wang et al., 2012). In addition, in *Msx1* mutant mice, exogenous *Bmp4* can rescue tooth development (Bei et al., 2000). Together, these results suggest a dynamic role of *Bmp* signaling in tooth development, both promoting and inhibiting tooth development at different stages. *Bmp6* is dynamically expressed during stickleback tooth development. Expression is detected early in the overlying inner dental epithelium (IDE) as well as in the condensing underlying odontogenic mesenchyme, with a subsequent cessation of expression in the epithelium, and continuous expression in the mesenchyme of the ossifying tooth (Cleves et al., 2014; Ellis et al., 2016). Freshwater sticklebacks homozygous for mutations in *Bmp6* have reductions in tooth number, showing *Bmp6* is required for aspects of tooth development in fish (Cleves et al., 2018).

A previously identified freshwater high-toothed associated haplotype within intron 4 of *Bmp6* underlies an evolved increase in tooth number. The haplotype is defined by six polymorphic sites in the 468 bp region upstream of a minimally sufficient *Bmp6* tooth enhancer, potentially modifying enhancer activity. Three lines of evidence (the bicistronic line, and two doubly transgenic lines) support the hypothesis that the associated polymorphisms upstream of the *Bmp6* tooth enhancer result in evolved spatial shifts in enhancer activity between the marine and freshwater alleles (Figures 2.1-2.4). Both alleles drove expression in the epithelium of early developing teeth, and in dental mesenchyme throughout development, similar to the expression pattern of the adjacent minimally sufficient 511 bp tooth enhancer previously reported (Cleves et al., 2018) as well as the reported expression of the endogenous *Bmp6* gene during tooth development (Cleves et al., 2014). In all three different transgenic comparisons, we observed the freshwater, high-toothed associated enhancer allele maintained a more robust expression domain in the overlying epithelium for a longer portion of a tooth's development compared to the marine, low-toothed associated allele in multiple independent lines. Conversely, the marine allele appeared to drive reporter expression in a larger domain in the underlying mesenchyme in a large proportion of teeth. We additionally found that marine and freshwater endogenous *Bmp6* gene expression domains differed in a manner that was consistent with the reporter gene results. Specifically, we observed larger mesenchymal domains in marine relative to freshwater fish, and expanded IDE domains in freshwater relative to marine fish, especially in late bell stage tooth germs. Together these data support the hypothesis that the intron 4 enhancer variants associated with tooth number differences drive *Bmp6* expression differences in tooth germs of >20 mm fish, which in turn leads to evolved tooth gain in freshwater fish (Figure 2.7). Outstanding questions include what these deep mesenchymal cells are and whether the expanded marine mesenchymal domain might include quiescent mesenchymal cells involved in tooth replacement. Other important questions include whether the differential expression of the endogenous *Bmp6* gene that occurs between marine and freshwater fish is at least partially driven by the two enhancer alleles, and if so, what the allelic effects are on tooth development and replacement, and which mutations are responsible for the expression differences.

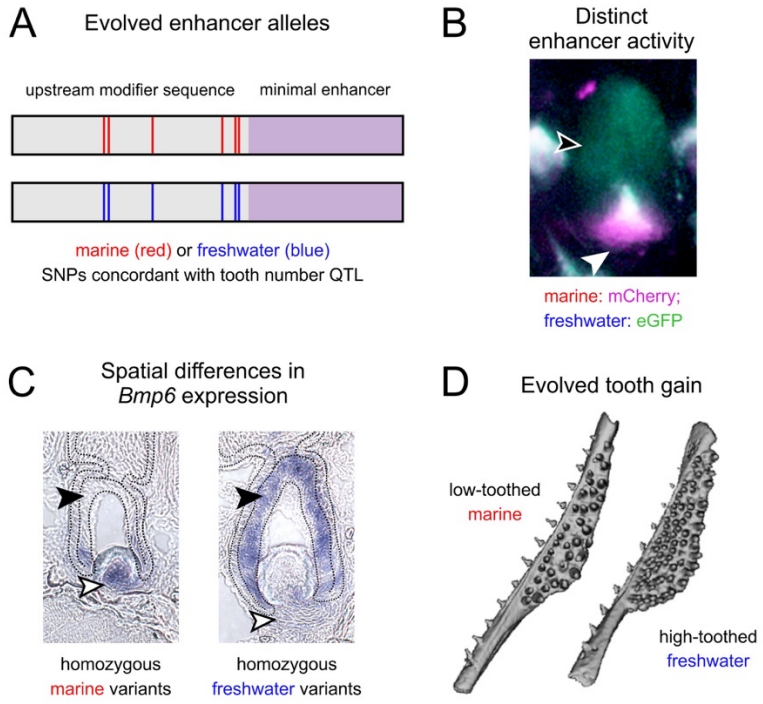


**Figure 2.7 A model for the role of *Bmp6 cis*-regulatory changes in underlying evolved tooth gain in sticklebacks. (A)** Quantitative trait loci (QTL) and fine mapping previously revealed variants in intron 4 of *Bmp6* that were associated with evolved tooth gain in freshwater fish (Cleves et al., 2014, 2018; Miller et al., 2014). These variants are adjacent to a previously characterized minimal enhancer (lavender) that was shown to drive expression in tooth epithelium and mesenchyme (Cleves et al., 2018). Six core single nucleotide polymorphisms (SNPs, depicted as red and blue lines within the modifier sequence), showed complete concordance with a large effect tooth number QTL (Cleves et al., 2018). **(B)** Marine and freshwater enhancers have different spatial activity, with the derived freshwater allele driving less mesenchymal expression, but more epithelial expression relative to the marine allele. **(C)** Consistent with the different enhancer activity, *Bmp6* expression by in situ hybridization is reduced in the mesenchyme but expanded in the epithelium in freshwater teeth relative to marine teeth. **(D)** We hypothesize that the enhancer alleles (A) have spatially shifted enhancer activity (B), resulting in shifts in *Bmp6* expression overall (C), and evolved tooth gain in freshwater fish (D).

Previous allele specific expression (ASE) experiments demonstrated a 1.4 fold reduction in the freshwater *Bmp6* allele compared to the marine in $F_1$ hybrid adult tooth tissue that included the entire ventral pharyngeal jaw, and thus both tooth epithelial and mesenchymal cells (Cleves et al., 2014). The mesenchymal biases in reporter expression are consistent with the ASE result, with more robust mesenchymal expression driven by the marine allele compared to the freshwater allele potentially responsible for the higher expression of the marine allele in the ASE experiments. In contrast, the expanded freshwater epithelial enhancer domain is not consistent with the overall ASE result in which freshwater alleles had *cis*-regulatory downregulation relative to marine alleles. Since the reduced mesenchymal domain in the freshwater enhancer relative to the marine enhancer was the most striking qualitative difference, it is possible that the epithelial bias, with a stronger signal driven by the freshwater enhancer, is quantitatively

canceled out by the bias in the mesenchyme, explaining the overall reduction of freshwater *Bmp6* expression compared to marine *Bmp6* expression in $F_1$ hybrids.

The enhancer expression differences appeared more pronounced in larger, post tooth number divergence fish compared to smaller, pre tooth number divergence fish. While the mesenchyme appeared to have a somewhat reduced difference of expression between the two alleles, the epithelium demonstrated less pronounced differences in activity between the alleles in pre-divergence fish. The observation is consistent with ASE results and the divergence in tooth number in marine and freshwater fish. While the mesenchymal difference was still observable early, it is possible there are other regulatory regions which act as repressors for the marine *Bmp6* allele or enhancers for the freshwater *Bmp6* allele early in development and so mask the mesenchymal bias of the marine intron 4 enhancer. For example, we previously reported a 5' *Bmp6* tooth enhancer that likely also contributes to the overall pattern of *Bmp6* in developing teeth (Erickson et al., 2015).

Future experiments to measure ASE in isolated tissues, with epithelium and mesenchyme separated could test whether opposing quantitative differences are present in dental epithelium vs. mesenchyme, as the new data presented here suggest. A quantitative method could be used to further test a hypothesis in which the two enhancers drive differing levels of expression, such as pyrosequencing (Wittkopp, 2012) with the two enhancers both driving identical fluorophores, with a single synonymous mutation distinguishing the two. Alternatively, single-cell RNA-seq (scRNA-seq) in the dental epithelium and mesenchyme, targeting the respective reporters of each enhancer, could determine if there are quantifiable expression differences between the two enhancers.

**QTL-associated sequence difference in alleles may underlie expression domain differences**

There are 14 point mutations and three indels distinguishing a low-toothed marine (Little Campbell) allele from the high-toothed Paxton Lake allele of the intron 4 enhancer in our reporter constructs. Previous experiments identified ten of these SNPs that co-occur consistently with the presence or absence of a tooth number QTL and of these ten, the core six are present in the enhancer reporter constructs tested here (Cleves et al., 2018). From our results we are unable to distinguish whether these six polymorphisms contribute to the expression differences we observed. While it is possible that the three indels or the eight non-QTL-associated SNPs may contribute, it is an attractive and parsimonious hypothesis that the same SNPs that co-occur with the tooth QTL are also responsible for the reporter expression differences, and the previously described allele specific expression results. Of the six QTL-associated SNPs tested here, of special interest is the second QTL-associated SNP (C←→T), which in the freshwater allele, creates a predicted NFATc1 binding site (Cleves et al., 2018). NFATc1 was shown to have importance in the balancing of quiescent and actively dividing stem cells in hair follicles (Horsley et al., 2008) which share homology with teeth (Ahn, 2015; Biggs & Mikkola, 2014; Pispa & Thesleff, 2003), and so a difference in NFATc1 binding may potentially play a role in the *Bmp6* allele specific expression and enhancer activity differences observed previously and here. Supporting this hypothesis, *Nfatc1b* expression was recently shown to be present in stickleback tooth germs and functional tooth mesenchyme (Square et al., 2021).

To better determine which polymorphisms may underlie the expression differences we observed, hybrid enhancers can be made. For example, if the creation of an NFATc1 binding site is at least partially responsible for the observed differences, a marine allele with the SNP converted to the freshwater identity, from a 'C' to a 'T', may recapitulate the freshwater

enhancer expression patterns. By creating and testing hybrid enhancers, future experiments could test which enhancer polymorphisms alone and in combination, contribute to the expression differences reported here.

**Fin expression differences**

In addition to the reporter expression differences driven by the two enhancers during tooth development, we observed distinct expression patterns in the pectoral and caudal fins. It was previously known that the minimal 511 base pair enhancer drove expression in the margins of early pectoral and median fins, but expression in adult fins had not been described. BMP signaling plays a role in fin regeneration, with BMP inhibition reducing osteoblast differentiation in new cells arising at the leading edge of the regenerating fin (Stewart et al., 2014). During zebrafish fin regeneration *bmp2b, bmp4,* and *bmp6* are expressed, and are thought to be important (Laforest et al., 1998; Murciano et al., 2002; Quint et al., 2002; Smith et al., 2006). While both alleles of the *Bmp6* enhancer drive expression in the pectoral and caudal fins of stickleback, the differing enhancer activities may result in developmental differences, through osteoblast function in the developing lepidotrichia and intersegmental joints, possibly leading to different fin morphologies and/or regenerative abilities. Differences in expression of *bmp2* have been observed in the regeneration of different rays of the caudal fin in cichlids (Ahi et al., 2017), as well as the expression of the gene *msxb*, which is downstream of *bmp* signaling in the regenerating zebrafish fin (Smith et al., 2006).

Multiple studies have identified habitat specific differences in fin morphology (Hendry et al., 2011; Kristjánsson et al., 2005; Taylor & McPhail, 1986). As the two enhancers are derived from populations with two distinct ecotypes, a benthic freshwater population, and a highly mobile anadromous population, it is possible this enhancer may influence pectoral and caudal fin size and shape in an adaptive manner. Characterization of fin morphology using fish from either a population in which the high-toothed and low-toothed associated haplotypes are segregating, or those from a control cross in which both alleles were present in the founding, could test whether there is a fin morphology difference associated with the different alleles.

**Bicistronic constructs and the use of genetic insulators**

Simultaneous comparison of two enhancer alleles in a single organism via a bicistronic construct is an attractive means to compare molecularly divergent enhancers (e.g. pairs of enhancers that contain sequence variation across populations to determine if there are population specific differences of enhancer activity). Previous work in zebrafish utilized genetic insulators as part of an enhancer trap as well as with two different tissue specific promoters and demonstrated the effectiveness of the technique (Bessa et al., 2009; Shimizu & Shimizu, 2013).

Here we used a bicistronic construct with a *Bmp6* enhancer and *Col2a1a* enhancer driving different fluorophores in mosaically transgenic $F_0$ fish to test whether the activities of two enhancers could be insulated from each other. Within the same $F_0$ individual, some domains demonstrated a high degree of insulator effectiveness while others did not. There are at least two possible explanations: 1) the insulated vs. non-insulated regions represent distinct and mosaic integration events, with the insulator effectiveness determined by the integration site in a particular subpopulation of cells, or 2) the same integration event can differ in insulator behavior stochastically or based on some context that differs from an insulated expression domain to an un-insulated domain. Regardless, examining enhancer activity in stable lines will still provide a

more complete picture of the role of the regulatory element and has advantages over mosaic $F_0$ analyses.

Genetic insulators have been reported to limit enhancer activity across the insulator boundary (Bessa et al., 2009; Shimizu & Shimizu, 2013) as well as protect against position effects (Chung et al., 1993), while other experiments show a lack of protection (Grajevskaja et al., 2013). The insulator used here, from the 5'end of the mouse tyrosinase locus, was reported to bind CTCF, like the β-globin 5'HS4 insulator from chicken, and is reported to prevent influences from nearby chromatin state and gene activity, the hallmarks of genetic insulators (Giraldo, 2003; Molto et al., 2009; Montoliu et al., 1996). As there are conflicting reports of the use of insulators to fully shield from nearby chromatin states and position effects, the combined use of a landing pad locus could help to further reduce these effects (Roberts et al., 2014). We recommend a multiple pronged approach utilizing multiple transgenic lines (e.g. either bicistronic constructs or multiple independent reciprocal two-color lines where each enhancer drives a different fluorophore in the same animal. Similar methods in doubly transgenic animals should allow future dissection of spatial differences in enhancer alleles, with the two methods acting as means of independent verification.

Changes in *cis*-regulation of developmental genes can be an important driver of morphological evolution, as well as human disease. The impact of mutations in *cis*-regulatory regions can be difficult to predict, and if the effect is subtle or slight, also to detect. The use of two enhancers in the same individual, either as parts of two independent transgenes or within a single bicistronic construct, can both control for the trans-environment and make even slight differences in expression activity apparent due to simultaneous imaging of reporter genes driven by both enhancers. Such an approach allows for directly comparing molecularly divergent regulatory elements, potentially identifying causal polymorphisms with important developmental and evolutionary implications.

ACKNOWLEDGEMENTS

We thank Phillip Cleves, James Hart, Priscilla Erickson and Ana Shaughnessy for helpful discussions, and Sophie Archameault and Alyssa Bormann for comments on the manuscript.

FUNDING

MDS was supported by an NSF-GRF; TAS was supported by NIH Fellowship F32-DE027871 to TAS and CTM; MDS, TAS, and CTM were supported by NIH Grant R01-DE021475 to CTM.

CONFLICTS OF INTEREST

None to report.

## 2.6 References

Ahi, E. P., Richter, F., & Sefc, K. M. (2017). A gene expression study of ornamental fin shape in Neolamprologus brichardi, an African cichlid species. *Scientific Reports*, *7*(1), 17398. https://doi.org/10.1038/s41598-017-17778-0

Ahn, Y. (2015). Signaling in Tooth, Hair, and Mammary Placodes. In *Current Topics in Developmental Biology* (Vol. 111, pp. 421–459). Elsevier. https://doi.org/10.1016/bs.ctdb.2014.11.013

Albert, A. Y. K., Sawaya, S., Vines, T. H., Knecht, A. K., Miller, C. T., Summers, B. R., Balabhadra, S., Kingsley, D. M., & Schluter, D. (2008). The genetics of adaptive shape shift in stickleback:

Pleiotropy and effect size. *Evolution; International Journal of Organic Evolution*, *62*(1), 76–85. https://doi.org/10.1111/j.1558-5646.2007.00259.x

Andl, T. (2004). Epithelial Bmpr1a regulates differentiation and proliferation in postnatal hair follicles and is essential for tooth development. *Development*, *131*(10), 2257–2268. https://doi.org/10.1242/dev.01125

Archambeault, S. L., Bärtschi, L. R., Merminod, A. D., & Peichel, C. L. (2020). Adaptation via pleiotropy and linkage: Association mapping reveals a complex genetic architecture within the stickleback *Eda* locus. *Evolution Letters*, *4*(4), 282–301. https://doi.org/10.1002/evl3.175

Bei, M., Kratochwil, K., & Maas, R. L. (2000). BMP4 rescues a non-cell-autonomous function of Msx1 in tooth development. *Development (Cambridge, England)*, *127*(21), 4711–4718.

Bell, M. A., & Foster, S. A. (Eds.). (1994). *The evolutionary biology of the threespine stickleback*. Oxford University Press.

Bessa, J., Tena, J. J., de la Calle-Mustienes, E., Fernández-Miñán, A., Naranjo, S., Fernández, A., Montoliu, L., Akalin, A., Lenhard, B., Casares, F., & Gómez-Skarmeta, J. L. (2009). Zebrafish enhancer detection (ZED) vector: A new tool to facilitate transgenesis and the functional analysis of *cis* -regulatory regions in zebrafish. *Developmental Dynamics*, *238*(9), 2409–2417. https://doi.org/10.1002/dvdy.22051

Biggs, L. C., & Mikkola, M. L. (2014). Early inductive events in ectodermal appendage morphogenesis. *Seminars in Cell & Developmental Biology*, *25–26*, 11–21. https://doi.org/10.1016/j.semcdb.2014.01.007

Carroll, S. B. (2008). Evo-Devo and an Expanding Evolutionary Synthesis: A Genetic Theory of Morphological Evolution. *Cell*, *134*(1), 25–36. https://doi.org/10.1016/j.cell.2008.06.030

Chan, Y. F., Marks, M. E., Jones, F. C., Villarreal, G., Shapiro, M. D., Brady, S. D., Southwick, A. M., Absher, D. M., Grimwood, J., Schmutz, J., Myers, R. M., Petrov, D., Jonsson, B., Schluter, D., Bell, M. A., & Kingsley, D. M. (2010). Adaptive Evolution of Pelvic Reduction in Sticklebacks by Recurrent Deletion of a Pitx1 Enhancer. *Science*, *327*(5963), 302–305. https://doi.org/10.1126/science.1182213

Chung, J. H., Whiteley, M., & Felsenfeld, G. (1993). A 5' element of the chicken beta-globin domain serves as an insulator in human erythroid cells and protects against position effect in Drosophila. *Cell*, *74*(3), 505–514. https://doi.org/10.1016/0092-8674(93)80052-g

Cleves, P. A., Ellis, N. A., Jimenez, M. T., Nunez, S. M., Schluter, D., Kingsley, D. M., & Miller, C. T. (2014). Evolved tooth gain in sticklebacks is associated with a cis-regulatory allele of Bmp6. *Proceedings of the National Academy of Sciences*, *111*(38), 13912–13917. https://doi.org/10.1073/pnas.1407567111

Cleves, Phillip A., Ellis, N. A., Jimenez, M. T., Nunez, S. M., Schluter, D., Kingsley, D. M., & Miller, C. T. (2014). Evolved tooth gain in sticklebacks is associated with a cis-regulatory allele of Bmp6. *Proceedings of the National Academy of Sciences*, *111*(38), 13912–13917. https://doi.org/10.1073/pnas.1407567111

Cleves, Phillip A., Hart, J. C., Agoglia, R. M., Jimenez, M. T., Erickson, P. A., Gai, L., & Miller, C. T. (2018). An intronic enhancer of Bmp6 underlies evolved tooth gain in sticklebacks. *PLOS Genetics*, *14*(6), e1007449. https://doi.org/10.1371/journal.pgen.1007449

Colosimo, P. F. (2005). Widespread Parallel Evolution in Sticklebacks by Repeated Fixation of Ectodysplasin Alleles. *Science*, *307*(5717), 1928–1933. https://doi.org/10.1126/science.1107239

Cresko, W. A., Amores, A., Wilson, C., Murphy, J., Currey, M., Phillips, P., Bell, M. A., Kimmel, C. B., & Postlethwait, J. H. (2004). Parallel genetic basis for repeated evolution of armor loss in Alaskan threespine stickleback populations. *Proceedings of the National Academy of Sciences of the United States of America*, *101*(16), 6050–6055. https://doi.org/10.1073/pnas.0308479101

Dale, R. M., & Topczewski, J. (2011). Identification of an evolutionarily conserved regulatory element of the zebrafish col2a1a gene. *Developmental Biology*, *357*(2), 518–531. https://doi.org/10.1016/j.ydbio.2011.06.020

Ellis, N. A., Glazer, A. M., Donde, N. N., Cleves, P. A., Agoglia, R. M., & Miller, C. T. (2015). Distinct developmental genetic mechanisms underlie convergently evolved tooth gain in sticklebacks. *Development*, *142*(14), 2442–2451. https://doi.org/10.1242/dev.124248

Ellis, Nicholas A., Donde, N. N., & Miller, C. T. (2016). Early development and replacement of the stickleback dentition: Stickleback tooth Patterning. *Journal of Morphology*, *277*(8), 1072–1083. https://doi.org/10.1002/jmor.20557

Ellis, Nicholas A., & Miller, C. T. (2016). Dissection and Flat-mounting of the Threespine Stickleback Branchial Skeleton. *Journal of Visualized Experiments*, *111*, 54056. https://doi.org/10.3791/54056

Erickson, P. A., Cleves, P. A., Ellis, N. A., Schwalbach, K. T., Hart, J. C., & Miller, C. T. (2015). A 190 base pair, TGF-β responsive tooth and fin enhancer is required for stickleback Bmp6 expression. *Developmental Biology*, *401*(2), 310–323. https://doi.org/10.1016/j.ydbio.2015.02.006

Erickson, P. A., Ellis, N. A., & Miller, C. T. (2016). Microinjection for Transgenesis and Genome Editing in Threespine Sticklebacks. *Journal of Visualized Experiments*, *111*, 54055. https://doi.org/10.3791/54055

Erickson, P. A., Glazer, A. M., Cleves, P. A., Smith, A. S., & Miller, C. T. (2014). Two developmentally temporal quantitative trait loci underlie convergent evolution of increased branchial bone length in sticklebacks. *Proceedings of the Royal Society B: Biological Sciences*, *281*(1788), 20140822. https://doi.org/10.1098/rspb.2014.0822

Erickson, P. A., Glazer, A. M., Killingbeck, E. E., Agoglia, R. M., Baek, J., Carsanaro, S. M., Lee, A. M., Cleves, P. A., Schluter, D., & Miller, C. T. (2016). Partially repeatable genetic basis of benthic adaptation in threespine sticklebacks: REPEATABLE EVOLUTION IN BENTHIC STICKLEBACKS. *Evolution*, *70*(4), 887–902. https://doi.org/10.1111/evo.12897

Furlong, E. E. M., & Levine, M. (2018). Developmental enhancers and chromosome topology. *Science (New York, N.Y.)*, *361*(6409), 1341–1345. https://doi.org/10.1126/science.aau0320

Gasperini, M., Tome, J. M., & Shendure, J. (2020). Towards a comprehensive catalogue of validated and target-linked human enhancers. *Nature Reviews Genetics*, *21*(5), 292–310. https://doi.org/10.1038/s41576-019-0209-0

Giraldo, P. (2003). Functional dissection of the mouse tyrosinase locus control region identifies a new putative boundary activity. *Nucleic Acids Research*, *31*(21), 6290–6305. https://doi.org/10.1093/nar/gkg793

Grajevskaja, V., Balciuniene, J., & Balciunas, D. (2013). Chicken β-globin insulators fail to shield the nkx2.5 promoter from integration site effects in zebrafish. *Molecular Genetics and Genomics*, *288*(12), 717–725. https://doi.org/10.1007/s00438-013-0778-0

Gross, H. P., & Anderson, J. M. (1984). Geographic Variation in the Gillrakers and Diet of European Threespine Sticklebacks, Gasterosteus aculeatus. *Copeia*, *1984*(1), 87. https://doi.org/10.2307/1445038

Haas, H. J. (1962). Studies on mechanisms of joint and bone formation in the skeleton rays of fish fins. *Developmental Biology*, *5*(1), 1–34. https://doi.org/10.1016/0012-1606(62)90002-7

Hagen, D. W. (1967). Isolating Mechanisms in Threespine Sticklebacks ( *Gasterosteus* ). *Journal of the Fisheries Research Board of Canada*, *24*(8), 1637–1692. https://doi.org/10.1139/f67-138

Hendry, A. P., Hudson, K., Walker, J. A., Räsänen, K., & Chapman, L. J. (2011). Genetic divergence in morphology-performance mapping between Misty Lake and inlet stickleback: Genetic divergence in morphology-performance mapping. *Journal of Evolutionary Biology*, *24*(1), 23–35. https://doi.org/10.1111/j.1420-9101.2010.02155.x

Horsley, V., Aliprantis, A. O., Polak, L., Glimcher, L. H., & Fuchs, E. (2008). NFATc1 Balances Quiescence and Proliferation of Skin Stem Cells. *Cell*, *132*(2), 299–310. https://doi.org/10.1016/j.cell.2007.11.047

Indjeian, V. B., Kingman, G. A., Jones, F. C., Guenther, C. A., Grimwood, J., Schmutz, J., Myers, R. M., & Kingsley, D. M. (2016). Evolving New Skeletal Traits by cis -Regulatory Changes in Bone Morphogenetic Proteins. *Cell*, *164*(1–2), 45–56. https://doi.org/10.1016/j.cell.2015.12.007

Jia, S., Zhou, J., Gao, Y., Baek, J.-A., Martin, J. F., Lan, Y., & Jiang, R. (2013). Roles of Bmp4 during tooth morphogenesis and sequential tooth formation. *Development*, *140*(2), 423–432. https://doi.org/10.1242/dev.081927

Kawakami, K. (2004). Transgenesis and gene trap methods in zebrafish by using the Tol2 transposable element. *Methods in Cell Biology*, *77*, 201–222. https://doi.org/10.1016/s0091-679x(04)77011-9

Kristjánsson, B. K., Skúlason, S., & Noakes, D. L. G. (2005). Unusual number of pectoral fin rays in an Icelandic population of threespine stickleback (Gasterosteus aculeatus) recently isolated in freshwater. *Evolutionary Ecology*, *18*(4), 379–384. https://doi.org/10.1007/s10682-004-2679-5

Laforest, L., Brown, C. W., Poleo, G., Géraudie, J., Tada, M., Ekker, M., & Akimenko, M. A. (1998). Involvement of the sonic hedgehog, patched 1 and bmp2 genes in patterning of the zebrafish dermal fin rays. *Development (Cambridge, England)*, *125*(21), 4175–4184.

Lavin, P. A., & McPhail, J. D. (1986). Adaptive Divergence of Trophic Phenotype among Freshwater Populations of the Threespine Stickleback ( *Gasterosteus aculeatus* ). *Canadian Journal of Fisheries and Aquatic Sciences*, *43*(12), 2455–2463. https://doi.org/10.1139/f86-305

McKinnon, J. S., & Rundle, H. D. (2002). Speciation in nature: The threespine stickleback model systems. *Trends in Ecology & Evolution*, *17*(10), 480–488. https://doi.org/10.1016/S0169-5347(02)02579-X

Miller, C. T., Beleza, S., Pollen, A. A., Schluter, D., Kittles, R. A., Shriver, M. D., & Kingsley, D. M. (2007). Cis-Regulatory Changes in Kit Ligand Expression and Parallel Evolution of Pigmentation in Sticklebacks and Humans. *Cell*, *131*(6), 1179–1189. https://doi.org/10.1016/j.cell.2007.10.055

Miller, C. T., Glazer, A. M., Summers, B. R., Blackman, B. K., Norman, A. R., Shapiro, M. D., Cole, B. L., Peichel, C. L., Schluter, D., & Kingsley, D. M. (2014). Modular Skeletal Evolution in Sticklebacks Is Controlled by Additive and Clustered Quantitative Trait Loci. *Genetics*, *197*(1), 405–420. https://doi.org/10.1534/genetics.114.162420

Molto, E., Fernandez, A., & Montoliu, L. (2009). Boundaries in vertebrate genomes: Different solutions to adequately insulate gene expression domains. *Briefings in Functional Genomics and Proteomics*, *8*(4), 283–296. https://doi.org/10.1093/bfgp/elp031

Montoliu, L., Umland, T., & Schütz, G. (1996). A locus control region at −12 kb of the tyrosinase gene. *The EMBO Journal*, *15*(22), 6026–6034. https://doi.org/10.1002/j.1460-2075.1996.tb00991.x

Murciano, C., Fernández, T. D., Durán, I., Maseda, D., Ruiz-Sánchez, J., Becerra, J., Akimenko, M. A., & Marí-Beffa, M. (2002). Ray–Interray Interactions during Fin Regeneration of Danio rerio. *Developmental Biology*, *252*(2), 214–224. https://doi.org/10.1006/dbio.2002.0848

O'Brown, N. M., Summers, B. R., Jones, F. C., Brady, S. D., & Kingsley, D. M. (2015). A recurrent regulatory change underlying altered expression and Wnt response of the stickleback armor plates gene EDA. *ELife*, *4*, e05290. https://doi.org/10.7554/eLife.05290

Pispa, J., & Thesleff, I. (2003). Mechanisms of ectodermal organogenesis. *Developmental Biology*, *262*(2), 195–205. https://doi.org/10.1016/s0012-1606(03)00325-7

Quint, E., Smith, A., Avaron, F., Laforest, L., Miles, J., Gaffield, W., & Akimenko, M.-A. (2002). Bone patterning is altered in the regenerating zebrafish caudal fin after ectopic expression of sonic hedgehog and bmp2b or exposure to cyclopamine. *Proceedings of the National Academy of Sciences*, *99*(13), 8713–8718. https://doi.org/10.1073/pnas.122571799

Rasch, L. J., Martin, K. J., Cooper, R. L., Metscher, B. D., Underwood, C. J., & Fraser, G. J. (2016). An ancient dental gene set governs development and continuous regeneration of teeth in sharks. *Developmental Biology*, *415*(2), 347–370. https://doi.org/10.1016/j.ydbio.2016.01.038

Rebeiz, M., & Tsiantis, M. (2017). Enhancer evolution and the origins of morphological novelty. *Current Opinion in Genetics & Development*, *45*, 115–123. https://doi.org/10.1016/j.gde.2017.04.006

Reid, D. T., & Peichel, C. L. (2010). Perspectives on the genetic architecture of divergence in body shape in sticklebacks. *Integrative and Comparative Biology*, *50*(6), 1057–1066. https://doi.org/10.1093/icb/icq030

Rickels, R., & Shilatifard, A. (2018). Enhancer Logic and Mechanics in Development and Disease. *Trends in Cell Biology*, *28*(8), 608–630. https://doi.org/10.1016/j.tcb.2018.04.003

Roberts, J. A., Miguel-Escalada, I., Slovik, K. J., Walsh, K. T., Hadzhiev, Y., Sanges, R., Stupka, E., Marsh, E. K., Balciuniene, J., Balciunas, D., & Muller, F. (2014). Targeted transgene integration overcomes variability of position effects in zebrafish. *Development*, *141*(3), 715–724. https://doi.org/10.1242/dev.100347

Sabarís, G., Laiker, I., Preger-Ben Noon, E., & Frankel, N. (2019). Actors with Multiple Roles: Pleiotropic Enhancers and the Paradigm of Enhancer Modularity. *Trends in Genetics: TIG*, *35*(6), 423–433. https://doi.org/10.1016/j.tig.2019.03.006

Santamaría, J. A., Marí-Beffa, M., & Becerra, J. (1992). Interactions of the lepidotrichial matrix components during tail fin regeneration in teleosts. *Differentiation*, *49*(3), 143–150. https://doi.org/10.1111/j.1432-0436.1992.tb00662.x

Schluter, D., & McPhail, J. D. (1992). Ecological Character Displacement and Speciation in Sticklebacks. *The American Naturalist*, *140*(1), 85–108. https://doi.org/10.1086/285404

Shimizu, A., & Shimizu, N. (2013). Dual promoter expression system with insulator ensures a stringent tissue-specific regulation of two reporter genes in the transgenic fish. *Transgenic Research*, *22*(2), 435–444. https://doi.org/10.1007/s11248-012-9653-8

Smith, A., Avaron, F., Guay, D., Padhi, B. K., & Akimenko, M. A. (2006). Inhibition of BMP signaling during zebrafish fin regeneration disrupts fin growth and scleroblast differentiation and function. *Developmental Biology*, *299*(2), 438–454. https://doi.org/10.1016/j.ydbio.2006.08.016

Square, T. A., Sundaram, S., Mackey, E. J., & Miller, C. T. (2021). Distinct tooth regeneration systems deploy a conserved battery of genes. *EvoDevo*, *12*(1), 4. https://doi.org/10.1186/s13227-021-00172-3

Stewart, S., Gomez, A. W., Armstrong, B. E., Henner, A., & Stankunas, K. (2014). Sequential and Opposing Activities of Wnt and BMP Coordinate Zebrafish Bone Regeneration. *Cell Reports*, *6*(3), 482–498. https://doi.org/10.1016/j.celrep.2014.01.010

Taylor, E. B., & McPhail, J. D. (1986). Prolonged and burst swimming in anadromous and freshwater threespine stickleback, *Gasterosteus aculeatus*. *Canadian Journal of Zoology*, *64*(2), 416–420. https://doi.org/10.1139/z86-064

Vainio, S., Karavanova, I., Jowett, A., & Thesleff, I. (1993). Identification of BMP-4 as a signal mediating secondary induction between epithelial and mesenchymal tissues during early tooth development. *Cell*, *75*(1), 45–58. https://doi.org/10.1016/S0092-8674(05)80083-2

Walker, J. A. (1997). Ecological morphology of lacustrine threespine stickleback Gasterosteus aculeatus L. (Gasterosteidae) body shape. *Biological Journal of the Linnean Society*, *61*(1), 3–50. https://doi.org/10.1111/j.1095-8312.1997.tb01777.x

Walker, J. A., & Bell, M. A. (2000). Net evolutionary trajectories of body shape evolution within a microgeographic radiation of threespine sticklebacks (Gasterosteus aculeatus). *Journal of Zoology*, *252*(3), 293–302. https://doi.org/10.1111/j.1469-7998.2000.tb00624.x

Wang, Y., Li, L., Zheng, Y., Yuan, G., Yang, G., He, F., & Chen, Y. (2012). BMP Activity Is Required for Tooth Development from the Lamina to Bud Stage. *Journal of Dental Research*, *91*(7), 690–695. https://doi.org/10.1177/0022034512448660

Wittkopp, P. J. (2012). Using Pyrosequencing to Measure Allele-Specific mRNA Abundance and Infer the Effects of Cis- and Trans-regulatory Differences. In V. Orgogozo & M. V. Rockman (Eds.), *Molecular Methods for Evolutionary Genetics* (Vol. 772, pp. 297–317). Humana Press. https://doi.org/10.1007/978-1-61779-228-1_18

## 2.7 Supplemental Materials

## Supplemental Figures

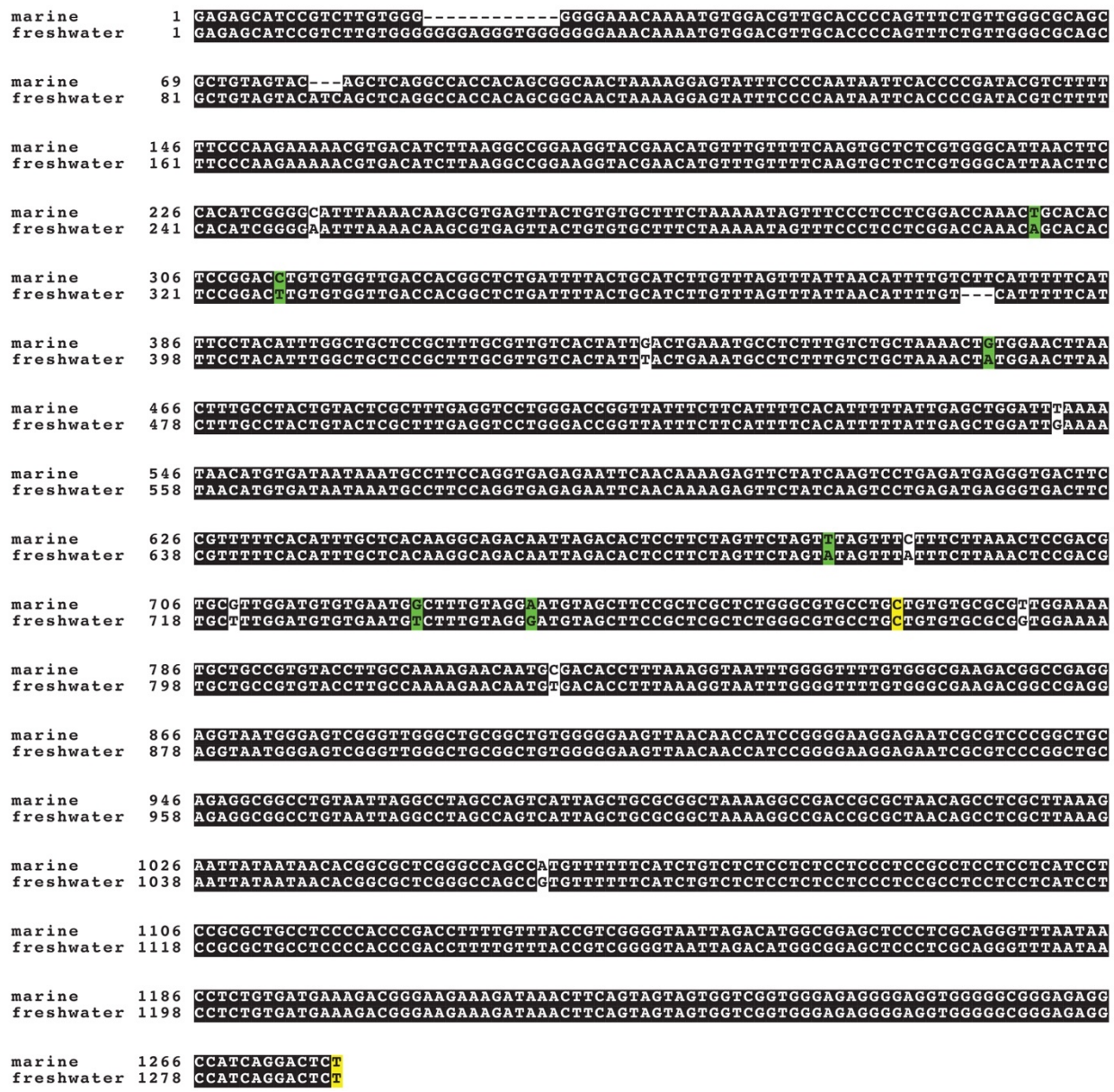


**Figure S 2.1 Sequence alignment of marine and freshwater alleles of *Bmp6* tooth enhancer.** Six core single nucleotide polymorphisms (green) concordant with the presence or absence of a large effect tooth number QTL lie upstream of a ~511 bp minimal *Bmp6* tooth enhancer (start and end in yellow). Other polymorphisms (white) are not concordant with the presence or absence of the tooth QTL (Cleves et al., 2018).

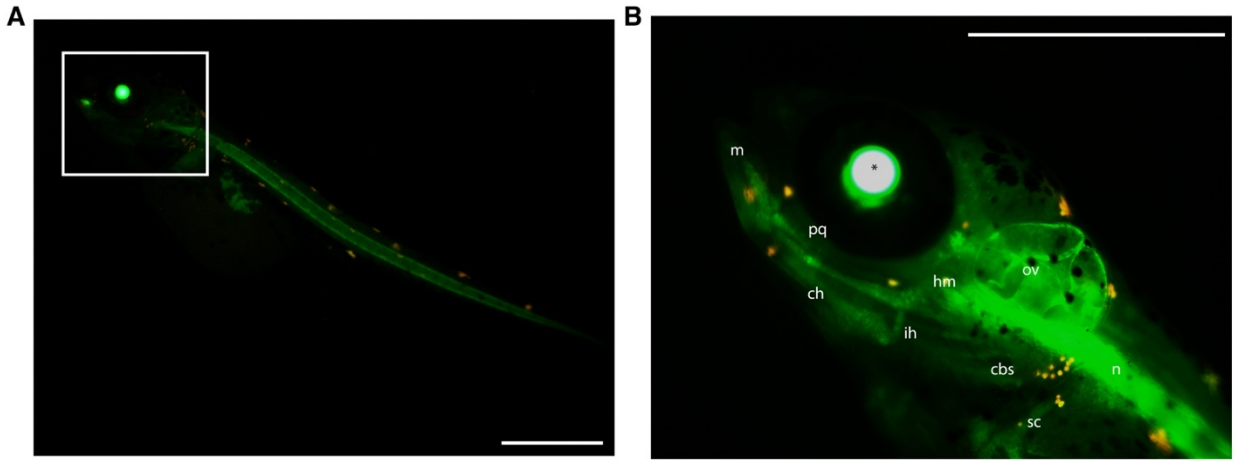


**Figure S 2.2 *Col2a1a* enhancer drives reporter expression in craniofacial cartilage and notochord in developing stickleback embryos. (A)** In a ten day post-fertilization embryo, reporter expression was observed in notochord (n) and **(B)** craniofacial cartilage including Meckel's (m), ceratohyal (ch), interhyal (ih), ceratobranchials (cbs), palatoquadrate (pq), and the hyosympletic (hm). Expression was also seen in the scapulocoracoid (sc), and otic vesicle (ov). Scale bars = 500μm **(A,B)**

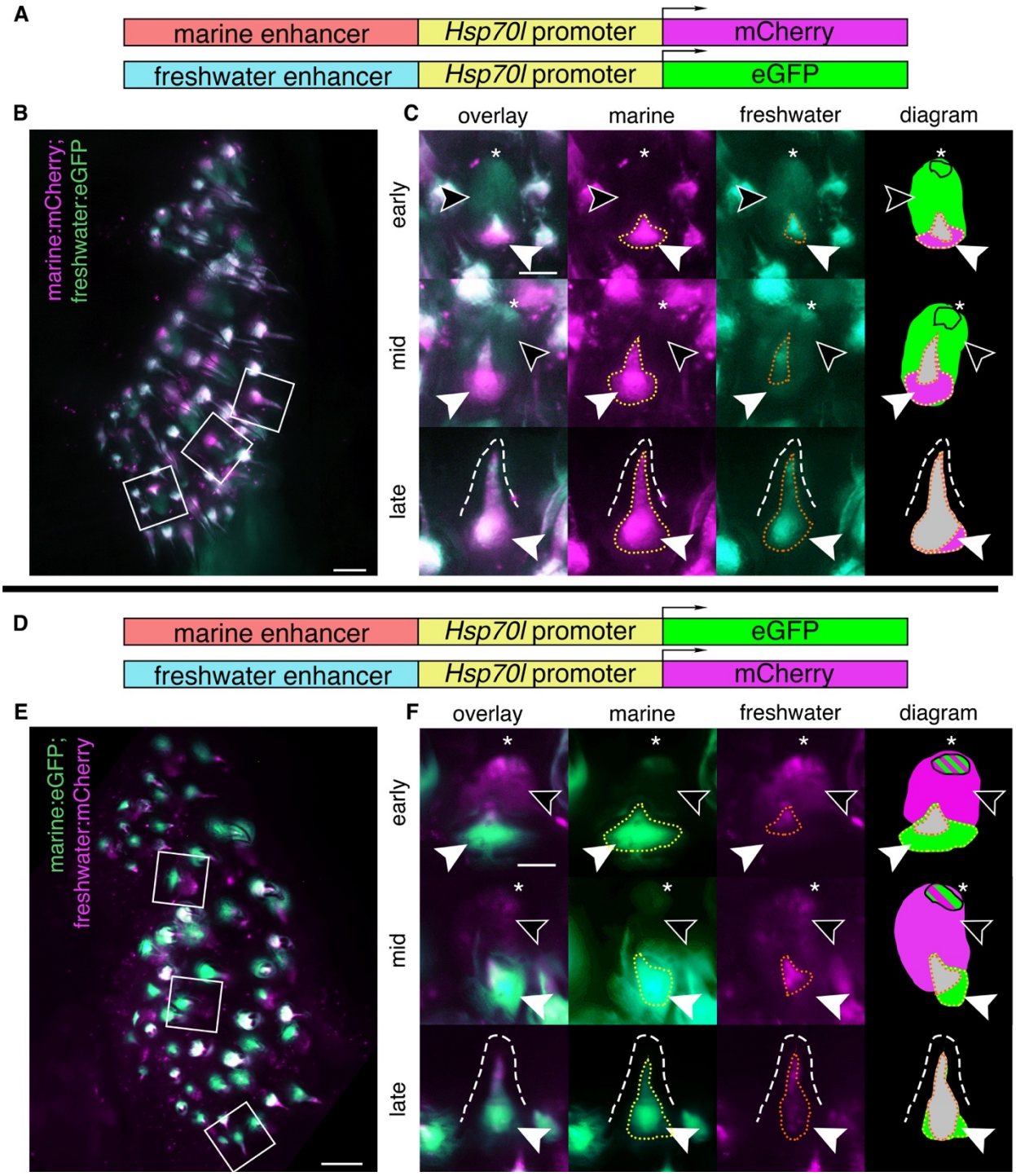


**Figure S 2.3 Marine and freshwater *Bmp6* enhancers drive different spatial patterns in dorsal pharyngeal replacement teeth.** Dorsal pharyngeal tooth plates from fish doubly transgenic for two alleles of the *Bmp6* intron 4 enhancer driving two different reporter genes **(A,D)**: the marine enhancer driving mCherry with the freshwater enhancer driving eGFP **(B,C)** and the marine enhancer driving eGFP with the freshwater enhancing driving mCherry **(E,F)**. Unilateral dorsal pharyngeal tooth plates **(B,E)** are shown, next to representative teeth from three stages **(C,F)**: early, middle, and late highlighted by white boxes in **B,E**. **(C,F)** Early: freshwater enhancer drove expression in the epithelium (black arrowheads), with concentrated expression in the tip (asterisk), while the marine enhancer did not reliably drive

expression in the epithelium, but was observed in the distal tip **(F)** in some instances. Both enhancers also drove expression in the mesenchyme (solid white arrowhead) with a larger expression domain of the marine allele (yellow dotted line) compared to the freshwater allele (orange dotted line). Middle: freshwater allele still drove expression in the epithelium while the marine allele was restricted to the distal tip. The marine allele drove more robust mesenchymal expression compared to the freshwater allele. Late: marine allele drives robust expression in the mesenchyme compared to freshwater allele in mineralized tooth (dashed line). Diagram: summary of tooth epithelial and mesenchymal domains. The relative sizes of green and magenta hatched lines correspond to the approximate relative strength of expression in the epithelium. Overlapping mesenchyme domain is grey, and expanded marine mesenchyme is marked with white arrowhead. Scale bars = 100μm **(B,E)**, 50μm **(C, F)**.

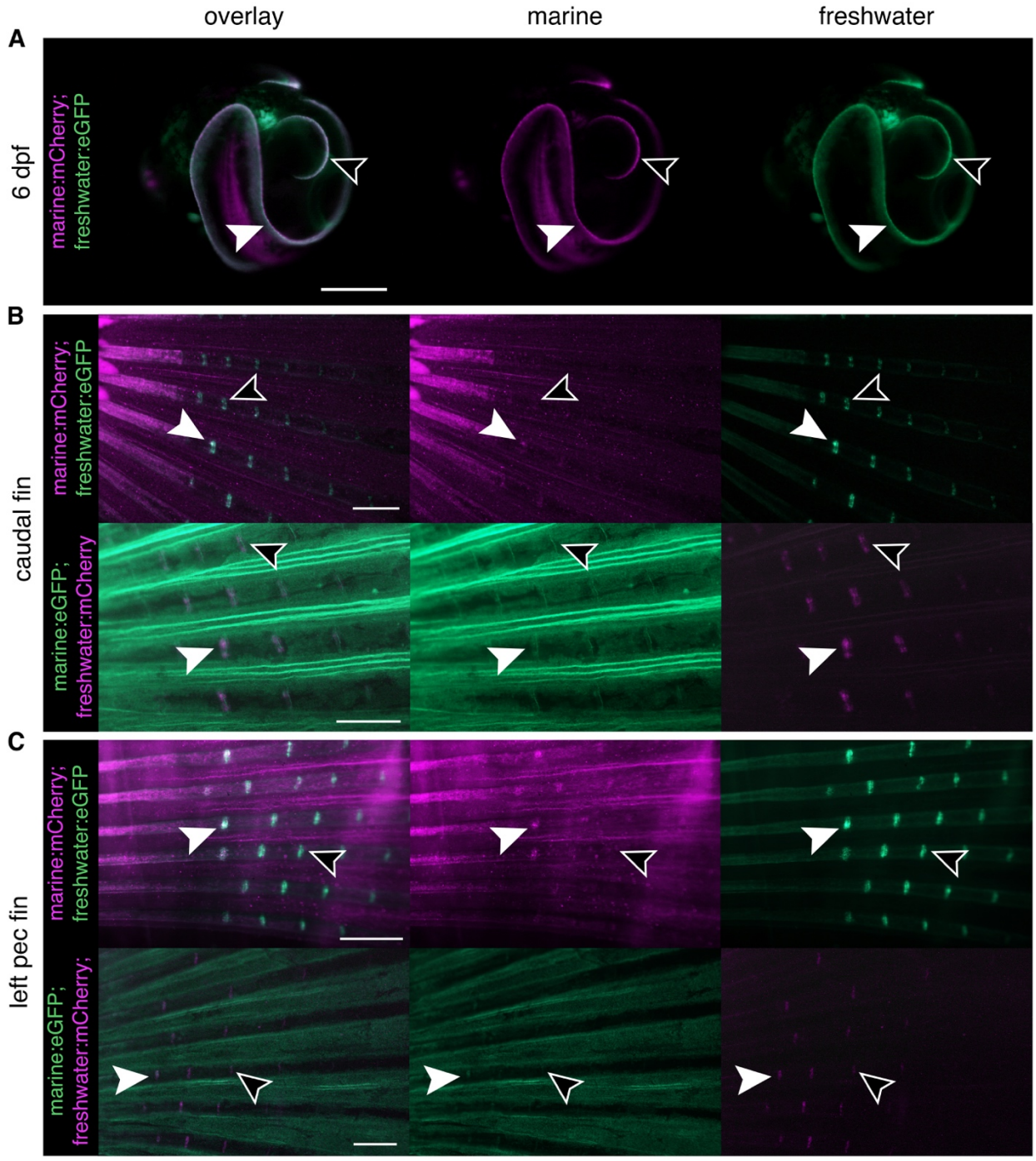


**Figure S 2.4 Freshwater allele drives expression in more intersegmental joints of both pectoral and caudal fins compared to the marine allele. (A)** In young, pre-hatching fish (6 dpf) the marine and freshwater enhancers drive expression in identical patterns in the developing fin margins of the pectoral fins (solid white arrowhead) and median fin (black arrowhead). **(B)** In adult caudal fins the more basal intersegmental joints were observed to have activity from both the marine and freshwater alleles (solid white arrowhead) while more distal joints were observed to only have freshwater enhancer activity (black arrowhead). The pattern was observed across both enhancer/reporter pairings. **(C)** Left pectoral fins from adults were observed to have activity from both enhancers in more basal intersegmental joints (solid

white arrowheads) while only the freshwater allele was observed to have activity in more distal joints (empty arrowheads). Scale bars = 0.5 mm.

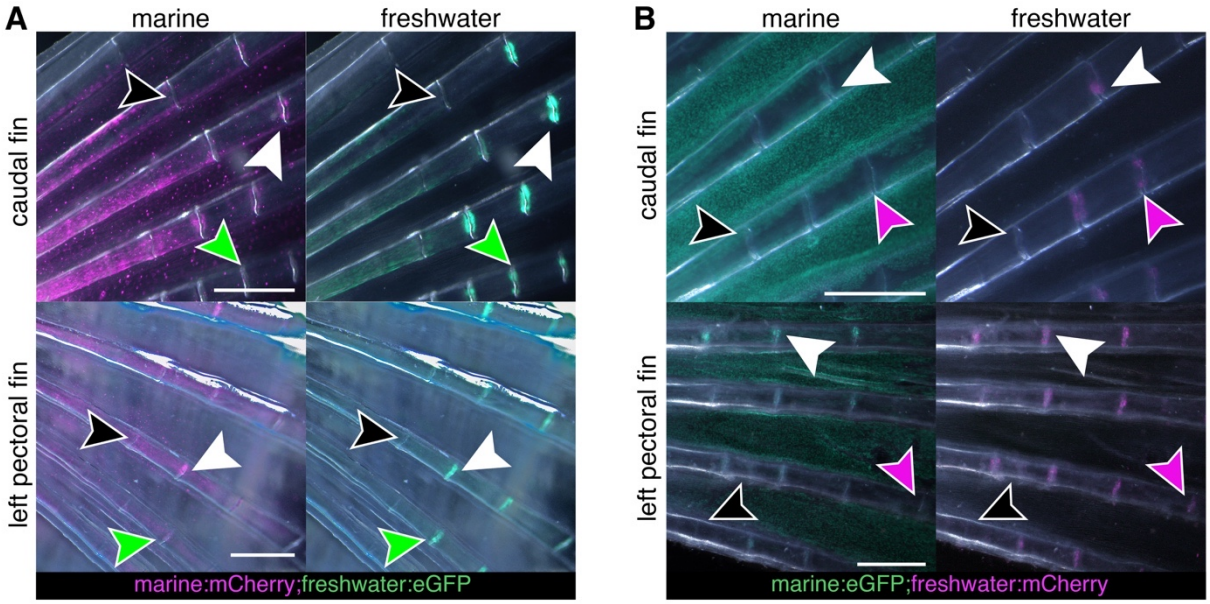


**Figure S 2.5 Fin expression patterns of both alleles change over developmental time**. **(A)** Caudal and pectoral fins with the freshwater enhancer driving eGFP and marine enhancer driving mCherry. Only the freshwater enhancer is active in more distal joints (green arrowhead) while in more basal joints both enhancers are active (solid white arrowhead). No enhancer activity was observed in the most basal joints (black arrowhead). **(B)** Caudal and pectoral fins with the freshwater enhancer driving mCherry and marine enhancer driving eGFP. Similar to **(A)**, the freshwater allele is active in more distal joints than the marine allele (purple arrowhead), more basal joints exhibit activity from both enhancers (solid white arrowhead). In the most basal joints, activity from either enhancer was not observed (black arrowhead). Scale bars = 0.5mm

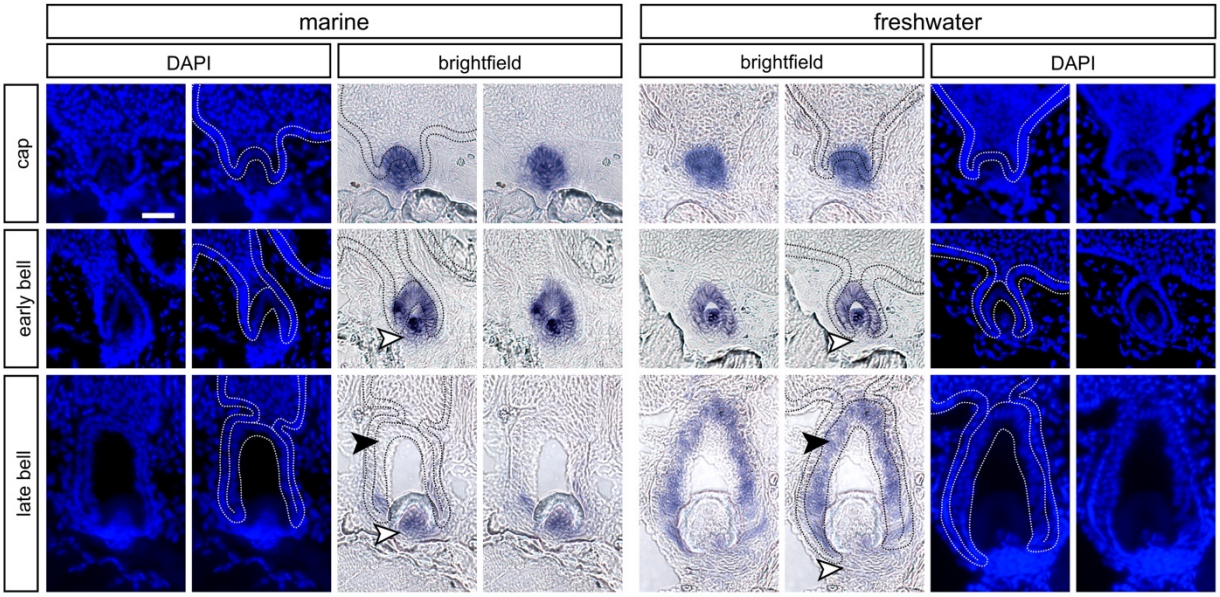


**Figure S 2.6 DAPI counterstain distinguishes between epithelial and mesenchymal tissues on thin sections.** Inner four columns show brightfield *in situ* hybridization (ISH) images for *Bmp6* expression on marine (left) and freshwater (right) backgrounds, innermost columns with no annotations, adjacent to the same images with annotations (as presented in Figure 6). The outermost four columns show DAPI counterstains of the same sections, again shown both with and without annotations. The first row shows a cap stage tooth, the second row shows an early bell stage tooth, and the third row shows a late bell stage tooth. All dotted lines (black in brightfield images, white in DAPAI images) demarcate the basalmost layer of epithelium in the tooth field, which is contiguous with the inner and outer dental epithelia of tooth germs. Regions where differences in expression were detected are marked with arrowheads: white arrowheads mark expanded mesenchymal expression in marine relative to freshwater, while black arrowheads mark expanded epithelial expression in freshwater relative to marine (as shown in Figure 8). Scale bar = 20 μm and applies to all panels.

## Supplemental Tables

| Domain | "0"- apparent no insulation | "1" – partial insulation observed | "2" – apparent complete insulation | Total fluorescence positive domains |
|---|---|---|---|---|
| Left pec fin | 24 | 13 | 28 | 65 |
| Right pec fin | 28 | 14 | 21 | 63 |
| Median fin | 34 | 23 | 29 | 86 |
| Notochord | 9 | 1 | 3 | 13 |
| Total | 95 | 51 | 81 | 227 |

**Table S 2.1 Insulator scores for each reporter positive domain in F0 fish with *Col2a1a*:mCh;*Bmp6* tooth enhancer:eGFP transgene.** For each reporter positive domain in $F_0$ fish with *Col2a1a*:mCh;Bmp6 tooth enhancer:eGFP transgene, a score of 0-2 was given for observed non, partial, or complete insulation.

| Domain | "0"- apparent no insulation | "1" – partial insulation observed | "2" – apparent complete insulation | Total fluorescence positive domains |
|---|---|---|---|---|
| Left pec fin | 12 | 2 | 4 | 18 |
| Right pec fin | 6 | 4 | 3 | 13 |
| Median fin | 15 | 4 | 3 | 22 |
| Notochord | 5 | 0 | 5 | 10 |
| Total | 38 | 10 | 15 | 63 |

**Table S 2.2 Insulator scores for each reporter positive domain in F0 fish with the *Col2a1a*:eGFP;*Bmp6* tooth enhancer:mCh transgene.** For each reporter positive domain in $F_0$ fish with *Col2a1a*:mCh;Bmp6 tooth enhancer:eGFP transgene, a score of 0-2 was given for observed non, partial, or complete insulation.

| tooth plate | time point | stage | freshwater positive (N/%) | marine positive (N/%) | total teeth in stage | genotype |
|---|---|---|---|---|---|---|
| DTP | pre-divergence | early | 20/100% | 20/100% | 20 | freshwater:eGFP;marine:mCherry |
| DTP | post-divergence | early | 29/100% | 24/82.8% | 29 | freshwater:eGFP;marine:mCherry |
| DTP | pre-divergence | mid | 16/100% | 16/100% | 16 | freshwater:eGFP;marine:mCherry |
| DTP | post-divergence | mid | 15/100% | 9/60.0% | 15 | freshwater:eGFP;marine:mCherry |
| VTP | pre-divergence | early | 19/100% | 19/100% | 19 | freshwater:eGFP;marine:mCherry |
| VTP | post-divergence | early | 23/100% | 20/87.0% | 23 | freshwater:eGFP;marine:mCherry |
| VTP | pre-divergence | mid | 22/100% | 22/100% | 22 | freshwater:eGFP;marine:mCherry |
| VTP | post-divergence | mid | 36/100% | 30/83.3% | 36 | freshwater:eGFP;marine:mCherry |
| DTP | pre-divergence | early | 13/100% | 13/100% | 13 | freshwater:mCherry;marine:eGFP |
| DTP | post-divergence | early | 24/100% | 18/75.0% | 24 | freshwater:mCherry;marine:eGFP |
| DTP | pre-divergence | mid | 16/100% | 16/100% | 16 | freshwater:mCherry;marine:eGFP |
| DTP | post-divergence | mid | 24/100% | 16/66.7% | 24 | freshwater:mCherry;marine:eGFP |
| VTP | pre-divergence | early | 16/100% | 16/100% | 16 | freshwater:mCherry;marine:eGFP |
| VTP | post-divergence | early | 23/100% | 21/91.3% | 23 | freshwater:mCherry;marine:eGFP |
| VTP | pre-divergence | mid | 13/100% | 13/100% | 13 | freshwater:mCherry;marine:eGFP |
| VTP | post-divergence | mid | 16/100% | 14/87.5% | 16 | freshwater:mCherry;marine:eGFP |

**Table S 2.3 Epithelial expression of enhancer by tooth plate, tooth stage, and genotype.** For each tooth field (dorsal or ventral tooth plate, DTP or VTP), stage (pre-divergence = <20 mm fish length, post-divergence = >20 mm fish length, tooth stage [early or middle (mid), see Methods], the number (N),

percentage (%) of detected epithelial expression are listed, along with total number of teeth and genotype of transgene.

| tooth plate | time point | stage | unbiased mesenchymal expression (N/%) | biased mesenchymal expression (N/%) | Total teeth in stage | genotype |
|---|---|---|---|---|---|---|
| DTP | pre-divergence | early | 3/15% | 17/85% | 20 | freshwater:eGFP;marine:mCherry |
| DTP | post-divergence | early | 1/3.4% | 28/96.6% | 29 | freshwater:eGFP;marine:mCherry |
| DTP | pre-divergence | mid | 2/12.5% | 14/87.5% | 16 | freshwater:eGFP;marine:mCherry |
| DTP | post-divergence | mid | 0/0% | 15/100% | 15 | freshwater:eGFP;marine:mCherry |
| DTP | pre-divergence | late | 36/39.6% | 55/60.4% | 91 | freshwater:eGFP;marine:mCherry |
| DTP | post-divergence | late | 46/43.8% | 59/56.2% | 105 | freshwater:eGFP;marine:mCherry |
| VTP | pre-divergence | early | 4/21.1% | 15/88.9% | 19 | freshwater:eGFP;marine:mCherry |
| VTP | post-divergence | early | 0/0% | 23/100% | 23 | freshwater:eGFP;marine:mCherry |
| VTP | pre-divergence | mid | 2/9.1% | 20/90.9% | 22 | freshwater:eGFP;marine:mCherry |
| VTP | post-divergence | mid | 0/0% | 36/100% | 36 | freshwater:eGFP;marine:mCherry |
| VTP | pre-divergence | late | 26/32.5% | 54/67.5% | 80 | freshwater:eGFP;marine:mCherry |
| VTP | post-divergence | late | 21/19.4% | 87/80.6% | 108 | freshwater:eGFP;marine:mCherry |
| DTP | pre-divergence | early | 0/0% | 13/100% | 13 | freshwater:mCherry;marine:eGFP |
| DTP | post-divergence | early | 0/0% | 24/100% | 24 | freshwater:mCherry;marine:eGFP |
| DTP | pre-divergence | mid | 1/6.3% | 15/93.7% | 16 | freshwater:mCherry;marine:eGFP |
| DTP | post-divergence | mid | 0/0% | 24/100% | 24 | freshwater:mCherry;marine:eGFP |
| DTP | pre-divergence | late | 51/49.5% | 52/50.5% | 103 | freshwater:mCherry;marine:eGFP |
| DTP | post-divergence | late | 27/26.7% | 74/73.3% | 101 | freshwater:mCherry;marine:eGFP |
| VTP | pre-divergence | early | 0/0% | 16/100% | 16 | freshwater:mCherry;marine:eGFP |
| VTP | post-divergence | early | 0/0% | 23 (2 Freshwater [8.7%], 21 Marine [91.3%]) | 23 | freshwater:mCherry;marine:eGFP |
| VTP | pre-divergence | mid | 0/0% | 13/100% | 13 | freshwater:mCherry;marine:eGFP |
| VTP | post-divergence | mid | 0/0% | 16/100% | 16 | freshwater:mCherry;marine:eGFP |
| VTP | pre-divergence | late | 35/35.7% | 63/64.3% | 98 | freshwater:mCherry;marine:eGFP |
| VTP | post-divergence | late | 10/10.3% | 87 (1 Freshwater [1%], 86 [88.7%] Marine) | 97 | freshwater:mCherry;marine:eGFP |

**Table S 2.4 Mesenchymal bias of enhancer expression by tooth plate, tooth stage, and genotype.** For each tooth field (dorsal or ventral tooth plate, DTP or VTP), stage (pre-divergence = <20 mm fish length, post-divergence = >20 mm fish length, tooth stage [early or middle (mid), see Methods], the number (N), percentage (%) of detected mesenchymal bias in expression are listed, along with total number of teeth and genotype of transgene.

## Supplemental Methods

Multiple fluorescent reporter transgenes were assembled using the methods and primers as described below. Component abbreviations below are as follows: *Hsp70l* = stickleback *Hsp70l* promoter (O'Brown et al., 2015); GAB = mouse tyrosinase insulator (Bessa et al., 2009); *Col2a1a* = *Col2a1a R2* enhancer (Dale & Topczewski, 2011).

### *Col2a1a* containing insulator construct #1
### *Col2a1a* enhancer/*Hsp70l*→mCh+GAB+eGFP←*Hsp70l*/*Bmp6* enhancer

The components of GAB, eGFP, and *Hsp70l*/*Bmp6* enhancer were amplified using primers MDS126/136, MDS137/89, and MDS90/131 respectively. The amplicons were combined with a modified plasmid (pT2He, modified to contain only polyclonal sites) linearized with *Nde*I and *BamH*I as well as Gibson Assembly master mix (NEB #E2611L) and incubated following the manufacturer's protocol. The resulting plasmid was digested with *Nde*I and *Bsu36*I and the fragments for the second half, *Col2a1a* enhancer/*Hsp70l* and mCherry, were amplified with MDS138/139 and MDS140/141 respectively. The plasmid and amplicons were combined with Gibson Assembly master mix and incubated following the manufacturer's protocol.

| primer name | primer sequence | description |
|---|---|---|
| MDS126 | cagataggcccctaaggactagtcatatgCTCACTATAGGGCGAATGGAGCTC | GAB forward |
| MDS136 | atgtggtatggctgatGCCGCCAGTGTGATGGATATC | GAB reverse |
| MDS137 | ccatcacactggcggcATCAGCCATACCACATTTGTAGAGG | eGFP forward |
| MDS89 | tgcagtcgacggtGGTCGCCACCATGGTGAG | eGFP reverse |
| MDS90 | catggtggcgaccACCGTCGACTGCAGGAAAAAAAAAC | *Bmp6*+*Hsp70l* forward |
| MDS131 | taaataaagattcattcaagatctggatccGAGAGCATCCGTCTTGTGGG | *Bmp6*+Hsp70l reverse |
| MDS138 | acacaggccagataggcccctaaggCGCTCCTTGAGGGTTTGAG | *Col2a1a* enhancer+*Hsp70l* forward |
| MDS139 | ggtggcgaccGTCGACTGCAGGAAAAAAAAAC | *Col2a1a* enhancer+*Hsp70l* reverse |
| MDS140 | tgcagtcgacGGTCGCCACCATGGTGAG | mCh forward |
| MDS141 | cattcgccctatagtgagcatatgATCAGCCATACCACATTTGTAGAGG | mCh reverse |

Primers used to amplify components of the Col2a1a:mCherry;Bmp6 tooth enhancer:eGFP insulator containing bicistronic construct

***Col2a1a* containing insulator construct #2**
***Col2a1a* enhancer/*Hsp70l*→eGFP+GAB+mCh←*Hsp70l*/*Bmp6* enhancer**
The assembly of the second *Col2a1a* containing bicistronic construct is nearly identical to the first. All steps are the same except primers MDS137/89 were used to amplify mCherry in the first assembly step and primers MDS140/141 were used to amplify eGFP in the second assembly step. Due to identical sequence at the transition from *Hsp70l* to mCherry/eGFP and at the 3' end of the SV40 polyA sequence for each reporter, the same primers can be used to amplify both off of the original reporter plasmids.

| primer name | primer sequence | description |
|---|---|---|
| MDS126 | cagataggcccctaaggactagtcatatgCTCACTATAGGGCGAATGGAGCTC | GAB forward |
| MDS136 | atgtggtatggctgatGCCGCCAGTGTGATGGATATC | GAB reverse |
| MDS137 | ccatcacactggcggcATCAGCCATACCACATTTGTAGAGG | mCh forward |
| MDS89 | tgcagtcgacggtGGTCGCCACCATGGTGAG | mCh reverse |
| MDS90 | catggtggcgaccACCGTCGACTGCAGGAAAAAAAAAC | *Bmp6+Hsp70l* forward |
| MDS131 | taaataaagattcattcaagatctggatccGAGAGCATCCGTCTTGTGGG | *Bmp6*+Hsp70l reverse |
| MDS138 | acacaggccagataggcccctaaggCGCTCCTTGAGGGTTTGAG | *Col2a1a* enhancer+*Hsp70l* forward |
| MDS139 | ggtggcgaccGTCGACTGCAGGAAAAAAAAAC | *Col2a1a* enhancer+*Hsp70l* reverse |
| MDS140 | tgcagtcgacGGTCGCCACCATGGTGAG | eGFP forward |
| MDS141 | cattcgccctatagtgagcatatgATCAGCCATACCACATTTGTAGAGG | eGFP reverse |

Primers used to amplify components of the Col2a1a:eGFP;Bmp6 tooth enhancer:mCherry insulator containing bicistronic construct

***Bmp6* intron 4 enhancer containing insulator construct**
**Marine *Bmp6* enhancer/*Hsp70l*→eGFP+GAB+mCh←*Hsp70l*/Freshwater *Bmp6* enhancer**
The first assembly step was the same as the previous two constructs, except the primer pair MDS90/131 was used to specifically amplify the freshwater *Bmp6* enhancer. Linearization of the plasmid and Gibson Assembly was completed as before. The resulting plasmid was digested with *Nde*I and *Bsu36*I and the fragments for the second half, Marine *Bmp6* enhancer/*Hsp70l* and mCherry, were amplified with MDS164/139 and MDS140/141 respectively. The newly digested plasmid and amplicons were combined with Gibson Assembly master mix and incubated following the manufacturer's protocol.

| primer name | primer sequence | description |
|---|---|---|
| MDS126 | cagataggcccctaaggactagtcatatgCTCACTATAGGGCGAATGGAGCTC | GAB forward |
| MDS136 | atgtggtatggctgatGCCGCCAGTGTGATGGATATC | GAB reverse |
| MDS137 | ccatcacactggcggcATCAGCCATACCACATTTGTAGAGG | eGFP forward |
| MDS89 | tgcagtcgacggtGGTCGCCACCATGGTGAG | eGFP reverse |
| MDS90 | catggtggcgaccACCGTCGACTGCAGGAAAAAAAAAC | Freshwater *Bmp6+Hsp70l* forward |
| MDS131 | taaataaagattcattcaagatctggatccGAGAGCATCCGTCTTGTGGG | Freshwater *Bmp6*+Hsp70l reverse |
| MDS164 | ctgaaacacaggccagataggcccctaagGAGAGCATCCGTCTTGTG | Marine *Bmp6* enhancer+*Hsp70l* forward |
| MDS139 | ggtggcgaccGTCGACTGCAGGAAAAAAAAAC | Marine *Bmp6* enhancer+*Hsp70l* reverse |
| MDS140 | tgcagtcgacGGTCGCCACCATGGTGAG | mCh forward |
| MDS141 | cattcgccctatagtgagcatatgATCAGCCATACCACATTTGTAGAGG | mCh reverse |

Primers used to amplify components of the Freshwater Bmp6 tooth enhancer:eGFP;marine Bmp6 tooth enhancer:mCherry insulator containing bicistronic construct

**Scoring effectiveness of insulators**
To assess insulator effectiveness, all surviving injected fish were raised to 7 days post fertilization. At this time point the *Bmp6* intronic enhancer drives robust reporter expression in

multiple domains including the distal edges of the median and pectoral fins, while the *Col2a1a* enhancer drives expression in the notochord (Cleves et al., 2018; Erickson et al., 2016). Four anatomical domains were scored for insulator effectiveness: the left and right pectoral fins, the median fin, and the notochord. Insulator efficiency was scored on a scale of 0 (apparent complete lack of insulation) to 2 (fully insulated enhancers) for each domain in which expression was observed. Insulation activity was only assessed for domains in which expression of at least a single fluorophore was present. Since effectiveness was scored in $F_0$ fish which are mosaic for the injected transgene, not all domains expressed a fluorophore.

## Supplemental Results

### Insulator effectiveness in bicistronic constructs

Insulator scores were not significantly different across injection clutches for the *Col2a1a R2*:mCherry; *Bmp6* tooth enhancer:eGFP construct (Kruskal-Wallis left pectoral fin $P = 0.075$, right pectoral fin $P = 0.52$, median fin fold $P = 0.116$, Wilcoxon rank sum notochord $P = 0.25$), nor the *Col2a1a R2*:eGFP; *Bmp6* tooth enhancer:mCherry construct (Wilcoxon rank sum left pectoral fin $P = 0.144$, right pectoral fin $P = 0.134$, median fin fold $P = 0.211$), suggesting that the inter-clutch variation did not have a significant impact on insulation scores. The left pectoral fin ($P = 0.036$) and the median fin fold ($P = 0.016$) were found to be significantly different between the two constructs while the right pectoral fin ($P = 0.68$) and notochord ($P = 0.29$) were not significantly different.

### Marine enhancer activity in the epithelium differs across tooth stage and fish size

In post-tooth number divergence fish activity of the freshwater enhancer was observed in the epithelium in both ventral and dorsal tooth plates in all pre-eruption teeth (marine:mCherry;freshwater:eGFP ventral: 59/59, dorsal: 44/44, and marine:eGFP;freshwater:mCherry ventral: 39/39, dorsal: 48/48), while the marine allele was observed in a subset of pre-eruption teeth (marine:mCherry;freshwater:eGFP ventral: 50/59 [84.7%], dorsal: 33/44 [75.0%], and marine:eGFP;freshwater:mCherry ventral: 35/39 [89.7%], dorsal: 34/48 [70.8%]). A higher percentage of early stage pre-eruption germs had marine activity in the epithelium compared to middle stage pre-eruption germs (marine:mCherry;freshwater:eGFP ventral: 20/23 [87.0%], dorsal: 24/29 [82.8%], and marine:eGFP;freshwater:mCherry ventral: 21/23 [91.3%], dorsal: 18/24 [75%]) than middle stage germs (marine:mCherry;freshwater:eGFP ventral: 30/36 [83.3%], dorsal: 9/15 [60.0%], and marine:eGFP;freshwater:mCherry ventral: 14/16 [87.5%], dorsal: 16/24 [66.7%]). In contrast to post-divergence, or > 20 mm total length, the marine enhancer in pre-divergence fish was active in every pre-eruption tooth germ (marine:mCherry;freshwater:eGFP ventral: 31/31, dorsal: 36/36, and marine:eGFP;freshwater:mCherry ventral: 29/29, dorsal: 29/29).

### Mesenchymal bias differs across tooth stage, plate, and fish size

Mesenchymal bias, in which one enhancer was observed to drive a broader domain within the mesenchyme, was scored for post divergence fish. In early and middle stage teeth, we observed a consistent marine enhancer bias in the ventral (marine:mCherry;freshwater:eGFP early: 23/23, middle: 36/36, marine:eGFP;freshwater:mCherry early: 21/23 [91.3%], middle: 16/16) and dorsal tooth plates (early: 28/29, 96.6%, middle:15/15, marine:eGFP;freshwater:mCherry early: 24/24, middle: 24/24)). A larger proportion of functional, erupted teeth were observed to have a marine bias in the mesenchyme in the ventral tooth plate (marine:mCherry;freshwater:eGFP 87/108 [80.6%], marine:eGFP;freshwater:mCherry 86/97 [88.7%]) compared to the dorsal tooth plate (marine:mCherry;freshwater:eGFP 59/105 [56.2%], marine:eGFP;freshwater:mCherry 74/101 [73.3%] (Figure 5B-C). There was a reduction in the proportion of erupted teeth with a marine bias when comparing post to pre divergence fish for all integrations and tooth plates (pre-divergence marine:mCherry;freshwater:eGFP ventral: 54/80 [67.5%] and marine:eGFP;freshwater:mCherry ventral: 63/98 [64.3%], dorsal pre: 51/103 [49.5%]) (Figure 5B) except for the dorsal tooth plates in the freshwater:eGFP;marine:mCherry genotype (pre: 55/91 [60.4%], post: 59/105[56.2%]).

# Chapter 3

## Replacement of population specific enhancer alleles in threespine stickleback using the CRISPR/Cas9 system

### 3.1 Abstract

The CRISPR/Cas9 system has given researchers new abilities to manipulate the genetics of their model organism. A common, though no-less powerful, use is to induce loss of function mutations in genes of interest, allowing researchers to probe the function of genes practically on-demand. Other uses for CRISPR/Cas9 include rescuing single nucleotide polymorphism mutants and knocking in reporter genes to create dynamic expression profiles of genes of interest. Recent work with the threespine stickleback has shown the system's amenability to gene editing. In order to probe the role of a *cis*-regulatory variant of the gene *Bmp6* I used the CRISPR/Cas9 system to replace the endogenous sequence of an enhancer with an alternate allele. Multiple approaches were used and successful replacement in $F_0$ animals, as well as propagation of an edited allele. The methods used here open up opportunities to test the function of *cis*-regulatory regions in sticklebacks. By creating chimeric chromosomes with replaced population specific *cis*-regulatory regions, the phenotypic contributions of the different alleles can be assessed.

### 3.2 Introduction

The threespine stickleback (*Gasterosteus aculeatus*) provides an ideal model system for studying enhancer evolution as it pertains to local adaptation. Marine sticklebacks have repeatedly colonized freshwater environments and typically evolve a suite of traits (Bell & Foster, 1994). While there is divergence in coding regions, a majority of sequence divergence between freshwater and marine populations fall within non-coding/regulatory regions (Jones et al., 2012). Changes in cis-regulation, through mutations in regulatory regions, have been shown to underlie multiple traits in stickleback evolution such as pelvic spine and armor plating reduction (Chan et al., 2010; Colosimo, 2005), and changes in pharyngeal tooth number (Cleves et al., 2014; Cleves et al., 2018). Within the stickleback system, the function of specific regulatory elements has been tested using reporter genes to determine the expression domain the element (Chan et al., 2010; Cleves et al., 2018; Erickson et al., 2015).

Previous work, using QTL mapping, fine mapping, and Tol2-mediated transgenesis/enhancer reporter experiments, has identified a haplotype just upstream of a tooth enhancer for the gene *Bone morphogenetic protein 6* (*Bmp6*) associated with evolved tooth gain in some freshwater populations (Cleves et al., 2014; Cleves et al., 2018). A series of single nucleotide polymorphisms (SNPs) were identified that varied concordantly with the presence or absence of a tooth number QTL peak from multiple crosses of freshwater (high tooth) by marine (low tooth) fish. Six of these polymorphisms lie upstream of a minimal tooth enhancer for the gene *Bmp6* which is a candidate thought to underlie evolved tooth gain due to the gene's expression in developing teeth and allele specific expression change. The six SNPs define either a high tooth-associated haplotype (freshwater allele) or a low tooth-associated haplotype (marine allele) first identified in QTL crosses. The haplotypes may modify the activity of the downstream *Bmp6* tooth enhancer through changes in transcription factor binding sites, thereby changing *Bmp6* expression and subsequently tooth development.

The CRISPR/Cas9 system allows for the introduction of double stranded breaks at precise locations in the genome using a flexible guide RNA system (Jinek et al., 2012). The Cas9

protein uses a short, approximately 20 bp, RNA sequence (sgRNA) to identify target sites on double stranded DNA and cleaves both strands of DNA. In addition, a protospacer adjacent motif (PAM), an NGG sequence, is required immediately proximal to the target region for successful recognition (Marraffini & Sontheimer, 2010). The introduction of double stranded breaks (DSB) stimulate repair pathways within the cell which can utilize multiple methods to repair the break: non-homologous end joining (NHEJ), microhomology-mediated end joining (MMEJ), and homology directed repair (HDR) (Davis & Chen, 2013; Liang et al., 1998; Wang & Xu, 2017). Repairs using NHEJ typically result in insertions or deletions at the cut site (Davis & Chen, 2013) which can result in knockouts of genes by targeting coding regions (Hoshijima et al., 2016). The CRISPR/Cas9 system can also induce mutations in regulatory elements, to determine the role specific elements or regions play (Hörnblad et al., 2021). CRISPR/Cas9 knockouts have been demonstrated to work in sticklebacks, recapitulating a spontaneous loss-of-function mutation (Hart & Miller, 2017).

More precise and constructive edits using double stranded breaks, such as knocking in a reporter (Hisano et al., 2015), or replacing a mutant SNP (Hoshijima et al., 2016), can be achieved as well, and relies on pathways in which a donor template is used to repair the damage, broadly labeled homology directed repair (HDR). Following the DSB, resection of the exposed 5' ends lead to single stranded 3' sequence which can then search for homology and invade a donor strand. Invasion results in a Holliday junction and resolution of the complex can lead to incorporation of donor sequence. (Jasin & Rothstein, 2013). In zebrafish, HDR has been successfully used to make gene knockout/reporter knock-ins (Hoshijima et al., 2016), rescue mutant alleles (Irion et al., 2014), knock in sequence precisely in-frame (Hisano et al., 2015), or modify individual sites (Boel et al., 2018).

The CRISPR/Cas9 system, through HDR, can help answer questions regarding the role specific regulatory sequences play in phenotypic evolution or how a gene has evolved in different lineages. For example, replacing an endogenous, long range, limb enhancer for the gene *Sonic hedgehog* in mice with the orthologous enhancer from different species of snake resulted in limb reduction, suggesting the sequence divergence in enhancers may underlie limb loss in snakes (Kvon et al., 2016). Replacement of orthologous sequence in regulatory elements has also been performed in *Drosophila* (Xu et al., 2017), while entire genes have been replaced with orthologs from different species in *Caenorhabditis elegans* (McDiarmid et al., 2018) while gene replacement of non-orthologous sequence has been performed in human iPS cells (Byrne et al., 2015).

Donor templates contain the desired replacement or knock-in sequence flanked by homology arms, extended sequences of homology matching the target locus. The homology arms are central to HDR and act as the starting sites for strand invasion, due to their high degree of sequence identity. Donor templates fall in three categories: linear double stranded DNA, circular double stranded DNA (plasmids), and single stranded oligo deoxynucleotides (ssODN). In zebrafish, a common approach for knock-in experiments and short sequence replacement is the use of a plasmid donor, with relatively large homology arms (approximately 1kb), which are flanked by target sites for a nuclease (either Cas9, TALEN, or I-sceI) so it can be linearized *in vivo* (Hoshijima et al., 2016; Irion et al., 2014). Alternatively, short homology arms to encourage MMEJ has proven to be highly efficient at knocking in sequence (Hisano et al., 2015; Wierson et al., 2020). Bai et al. (2020) tested each donor, with variations, for efficiency at rescuing an albino tyrosinase mutant, replacing a 25bp deletion with a wildtype allele. While ssODNs had the highest efficiency, plasmid donors also resulted rescue though at low percentages.

CRISPR/Cas9 and homology directed repair provide a means to directly test the phenotypic effect of specific alleles. By replacing the high-tooth associated haplotype in a freshwater background, Fishtrap Creek, with the low-tooth associated haplotype, the effects of the haplotypes can be determined. In addition, the reciprocal experiment can be performed, replacing a low-tooth allele with the high-tooth allele in a marine background. If replacement can occur in a gene edited fish, it can be outcrossed, and the progeny will be genetically similar to the original population except for the replaced haplotype. As the edited sequence will be the primary difference between the progeny with the high tooth haplotype and those without, any difference in tooth number is likely the result of the replacement.

## 3.3 Methods

### Animal statement

All animal work was approved by UCB animal protocol #AUGP-201501-7117-2. Fish were reared as previously described (Erickson et al., 2014).

### Cas9 and guide generation

Cas9 protein was purchased from the University of California, Berkeley QB3 MacroLab (https://qb3.berkeley.edu/facility/qb3-macrolab). Cas9 mRNA was prepared following a previously published protocol for generating mutant alleles in zebrafish (Talbot & Amacher, 2014). The pCS2-nCas9n (Addgene #47929) plasmid was linearized with *Not*I and the Invitrogen SP6 mMessage mMachine Kit (product #AM1340) was used to transcribe the mRNA which was purified using RNeasy Mini Kit (catalogue #74104) and diluted to a concentration of 400ng/µl.

Guides were designed following the previously stated protocol. Potential guides were first identified using the Zinc Finger Targeter (ZiFiT) tool (Sander et al., 2007, 2010). Multiple potential guides were selected based on their proximity to the target replacement sequence and restriction enzyme cut sites that could facilitate identification of Cas9-induced indels through gel electrophoresis of digested PCR products. Guide templates were created using the "short oligo method" described in Talbot & Amacher (2014). The templates were then used to generate sgRNAs with MAXIscript T7 kit and were diluted down to approximately 400ng/µl and stored at -80°C.

To test the guides 24 marine fish were injected with sgMDS11 (Table S1). The target site was amplified using MDS180/MDS169 and digested using *HpH*I. The diagnostic digest could not be interpreted but seven fish were chosen at random to genotype by sequencing. The target site for sgMDS11 was sequenced and deletions were found in all seven fish. Guide sgMDS4 was also tested for cleavage efficiency using a restriction digest of *Xma*I on a PCR product created with primers MDS160/161, as the PAM site of sgMDS4 is contained within an *Xma*I cut site. PCR products from 12 fish were digested using *Xma*I, resulting in nine that appeared to have some amount of uncut PCR products, suggesting Cas9 induced indels. Three fish were selected for sequencing, with all three containing indels at the sgMDS4 site.

### *Bmp6* intronic enhancer nomenclature

The high-tooth associated haplotype within intron 4 of *Bmp6* that was first identified in QTL experiments and refined through a 'genome sieve', in which previous lab members identified the polymorphisms that varied consistently with the presence or absence of the QTL peak, has been given the label of "D". It should be noted, the high-tooth associated haplotype is defined by a

series of six SNPs, which have been found in multiple populations with variation in the surrounding polymorphisms across and within the same population (see chapter three of this dissertation). The original "D allele" was identified on a Paxton Benthic chromosome, and the sequence used to create the donor plasmid for RABS is this PAXB specific "D allele". There are polymorphisms that differ between the Paxton "D allele" and the "D allele" found within the Fishtrap Creek stock fish. Through the remainder of the chapter I will use the term high-tooth associated haplotype and "D allele" interchangeably, specifying the Fishtrap Creek stock version as FTC-D. As "D" is defined by a haplotype using six positions, there are multiple possible "non-D" alleles that vary in polymorphic sites outside of the haplotype defining six. The FTC-D allele is segregating in the stock populations, and so the allele in the FTC stocks which does not contain the high-tooth associated haplotype will be referred to as FTC-nonD.

The donor sequence used in the FTC injection plasmid was amplified off of a plasmid that contained the sequence derived from a Little Campbell marine fish (LC28). In QTL crosses, this marine allele was associated with few numbers of teeth, thus this allele is referred to as the "low-tooth associated haplotype". As the origin of the replacement sequence was a marine fish, and is contrasted to the freshwater derived "D-allele", I will use the terms low tooth-associated haplotype and marine or LC28 allele interchangeably when referring to the donor sequence.

**Cas9, guide RNA, and donor plasmid injection approaches**

Three approaches were used to replace the high-tooth associated allele with the low tooth associated allele in Fishtrap Creek stock fish (Figure 3.1A). In all three approaches the same donor plasmid was used while the number of sgRNAs and the use of Cas9 protein or mRNA varied. The published stickleback injection protocol was followed (Erickson et al., 2016) for all three methods. Donor plasmids were co-injected with sgRNA into one-cell embryos. Approximately 1µl of 200ng/µl donor plasmid was combined with 1µl of 2M KCl, and 0.5µl of 0.5% phenol red for all microinjections. For approaches #1 and #3 approximately 400ng of each guide was added, along with 0.5µl of 40µM Cas9 protein for Approach #1 and 400 ng Cas9 mRNA for Approach #3 with water added to a final volume of 5µl resulting in a final concentration of 40 ng/µl of donor plasmid and approximately 80 ng/µl of each guide. In Approach #2, 0.5µl of 40µM Cas9 protein, approximately 1µl of 400 ng of sgMDS11, and water adding to a final volume of 5µl were combined, yielding a total concentration of 40ng/µl of plasmid and 80ng/µl of sgRNA.

| approach | guides used | Cas9 |
|---|---|---|
| 1 | sgMDS4, sgMDs11 | protein |
| 2 | sgMDS11 | protein |
| 3 | sgMDs4, sgMDS11 | mRNA |

**Table 3.1** Guide and Cas9 combinations used for allele replacement

**Donor template construction**

The six SNP defined haplotype and downstream tooth enhancer span an approximately 1.2kb stretch which is the central component of the donor template. Due to the overall size off the sequence to be replaced, a plasmid donor was selected as the type of replacement template. While circular plasmids have shown to be able to produce knock-ins and replacement (Hoshijima

et al., 2016), donors linearized, *in vivo*, have been demonstrated to yield higher efficiencies (Irion et al., 2014; Zheng et al., 2017) and so target sequence for sgMDS11 was added to the homology arms to linerize the plasmid after injection.

As the desired sequence to be replaced is the same locus from two different populations, the sequence divergence between the two alleles is less than similar experiments in which either orthologs from different species were replaced, or reporters were used to replace endogenous genes generating knockouts/knock-ins. There is a relatively high degree of homology, approximately 97%, along with multiple 100-230 bp stretches of complete homology, when comparing a high tooth allele identified from a Paxton Benthic fish, and a low tooth allele identified from a marine Little Campbell fish. The high sequence similarity, with a nearly 600 bp stretch of nearly 99% identity in the core of the target sequence, suggests that recombination is able to occur throughout the haplotype, reducing the likelihood that whole haplotype replacement would occur.

The donor plasmid for injecting into freshwater, Fishtrap Creek (FTC), fish was created with the 1.2 kb haplotype/enhancer sequence from a Little Campbell marine fish which contained the low-tooth associated haplotype which was initially used in a quantitative trait loci (QTL) mapping experiment (Cleves et al., 2014). The homology arms, which also contained the target sequences for the sgRNAs used, were cloned from stock FTC fish (cl.1793) to have as much shared sequence identity as possible with the recipient fish. Primers MDS199 and MDS189 were used to amplify the 5' upstream homology arm, while primers MDS190 and MDS201 were used to amplify the 3' downstream homology arm. Primers MDS199 and MDS201 contained sequence to add the sgMDS11 target to the arms. Both amplicons were cloned into a pBlueScript II SK plasmid. As the homology arms contained cut sites for both guides used, sgMDS4 and sgMDS11, the PAM sequences within the arms were changed to prevent cleavage of the donor. Primers MDS195/MDS196 and MDS202/MS203 were used in a site directed mutagenesis PCR protocol to change the first 'G' of each PAM site to a 'T' (NGG →NTG/CCN→CAN).

The polymorphisms which define the haplotype are clustered towards the 5' end of the 1.2 kb enhancer. To facilitate genotyping with easily amplified amplicons a shorter 5' homology arm of 458 bp was used. By creating a shorter upstream arm, a primer external to the sequence homologous to the construct in the genome could be placed closer to the informative sites, creating a shorter amplicon and that should not amplify off of donor plasmid, which would result in a deceptive sequence. Primers MDS215 and MDS189 were used to amplify a smaller homology arm off of the site direct mutagenesis treated 5' homology arm plasmid.

The donor plasmid was created using Gibson Assembly (Gibson et al., 2009). The NEBuilder Assembly tool (nebuilder.neb.com) from New England BioLabs was used to generate primer sequences for each of the homology arms and the 1.2kb enhancer sequence (primers MDS205-209 and MDS216). Once each component was amplified using the primers with overlapping sequence it was assembled using the NEB Gibson Assembly protocol (https://www.neb.com/protocols/2012/12/11/gibson-assembly-protocol-e5510). The final donor plasmid (Figure 3.1B) contains a 458 bp upstream homology arm, in which there is a target site for guide sgMDS11 with a modified PAM site, the 1278 bp marine enhancer sequence, and a 1216 bp downstream homology arm, which contains target site for guide sgMDS4 with a modified PAM site. The sequence is flanked by two added target sites for the guide sgMDS11 to linearize the plasmid *in vivo*.

A donor plasmid was also created to inject into a Rabbit Slough (RABS) marine background (Figure 3.1B), in an attempt to replace a marine allele with the high-tooth associated freshwater allele first identified in the Paxton Benthic (PAXB) population (Cleves et al., 2018). A nearly identical strategy was used to the previous plasmid, except homology arms were amplified initially from a marine, Rabbit Slough, stock fish. The haplotype containing 1290bp enhancer was amplified from a plasmid containing sequence from a Paxton Benthic fish initially used in the quantitative trait loci (QTL) mapping experiment (Cleves et al., 2018).

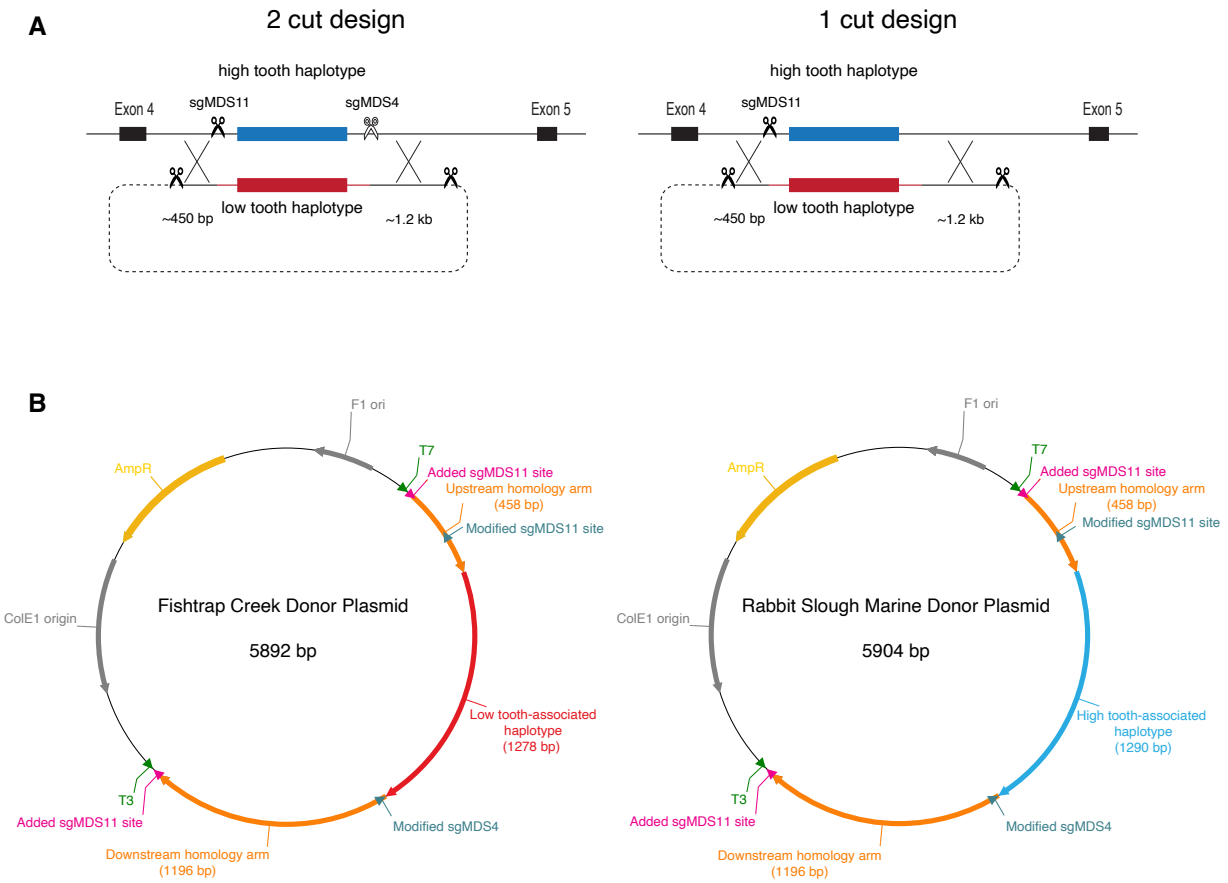


**Figure 3.1 Donor plasmids and injection schemes for both freshwater (Fishtrap Creek) and marine (Rabbit Slough) backgrounds. (A)** Two designs were used to generate a linear donor plasmid in vivo and inducing double stranded breaks at the endogenous locus. In the two cut approaches (using either Cas9 mRNA or protein) two sgRNAs were used, one upstream of the haplotype (sgMDS11) and one downstream of the haplotype (sgMDS4), while in the one cut approach (Cas9 protein) only sgMDS11 was used to cleave the endogenous locus. In both designs, sites for sgMDS11 were added to flank the donor sequence to allow the linearization in vivo. **(B)** Donor plasmids contained either the low tooth-associated haplotype (injected into FTC) or high tooth-associated haplotype (injected into RABS) flanked by two homology arms (458 bp and 1196 bp) amplified off of the same background the plasmid was injected into. The arms end with added target sequence for the sgRNA sgMDS11 to linearize in vivo. The target sequences for sgMDS11 and sgMDS4 that are contained within the donor plasmids have been modified to change the NGG PAM sequence to NTG, inhibiting cleavage of the donor by the co-injected guides. Arrows for each component point in the 5' to 3' genomic direction, while the arrowheads for sgMDS11 and sgMDS4 sites point towards the PAM site.

**Genotyping methods**

Of the polymorphisms that define the high-tooth associated haplotype, one falls within an *Ava*II restriction enzyme cut site. The site is tri-allelic, with the high-tooth associated, and a second allele in marine stocks, disrupting the recognition sequence. The reference allele, and the identity used in the Fishtrap Creek donor plasmid, creates an *Ava*II recognition site. Following amplification of the region with any of multiple primer pairs (MDS233/MDS234, MDS219/MDS220, MDS219/221, MDS213/JCH200) and digestion there is a consistent difference between the two haplotypes, with the high-tooth associated haplotype (D) generating a 197 bp band, while the marine or low tooth associated haplotype generates a 181 bp. While other bands are also generated the multiple *Ava*II sites are close enough together that any amplicon that spans from just 3' of the cutsite to outside the 5' homology arm will consistently generate either the 197 or 181 bp band. The 16 bp difference is resolvable on a 3% agarose gel. To screen $F_0$ injected fish for potential allele replacement genotyping by Sanger sequence and restriction fragment length polymorphism were used. As foreign DNA, both in linear and circular states, can amplify within injected embryos of other fish species (Stuart et al., 1988; Winkler et al., 1991) diagnostic primers were selected to prevent amplification off of the donor plasmid within $F_0$ fish. A forward primer outside of the upstream homology arm was paired with a reverse primer within the donor replacement sequence, meaning any amplified sequence must come from the genome of the injected fish and not the donor plasmid.

All fish to be genotyped were allowed to grow to at least four days post-fertilization (dpf) in brackish water (3.5g/L Instant Ocean salt, 0.217 ml/L 10% sodium bicarbonate) to ensure sufficient genomic DNA for genotyping. Whole embryos of injected $F_0$, uninjected controls, and $F_1$ fish were digested for 12 hours at 55°C in tail digestion buffer (10mM Tris pH 8.0, 100mM NaCl, 10 mM EDTA, 0.05% SDS, 2.5 µl Proteinase K (Ambion AM2546)), followed by phenol-chloroform extraction and rehydration in 50µl of water. DNA concentration was estimated via nanodrop and diluted to 20ng/µl.

**Genotyping $F_0$ injected fish**

Approximately 50 Fishtrap Creek stock one cell embryos were injected with sgMDS4, sgMDS11, Cas9 protein, and a donor plasmid (Approach #1). Surviving $F_0$ fish were genotyped using Sanger sequencing and *Ava*II digestion, followed by cloning of the targeted region to refine potentially Cas9/HDR induced alleles. As the high-tooth associated haplotype is not fixed in the Fishtrap Creek stock population three uninjected controls were also genotyped via sequencing to determine if any potential allele replacement positive fish were false positives.

PCR was first performed using the primer pair of MDS213/JCH200. Approximately 5µl of the resulting PCR product was then digested with *Ava*II for two hours to ensure digestion to completion and the digested reaction was then run on a 3% agarose gel. Sanger sequencing was performed on the remaining volume to characterize PAM sequences in injected individuals and the identities at variable sites in both injected and uninjected control samples. Due to a potentially high degree of mosaicism within each $F_0$ fish, cloning of the replacement target region into a plasmid was done in order to identify individual alleles. Primer pairs MDS219/MDS220 (containing the first three SNPS) and MDS219/MDS221 (containing all six SNPS) were used to amplify the region in fish identified to potentially contain marine allele. Amplification was followed by digestion with the restriction enzymes *Xba*I and *Xho*I. The amplicon was then ligated into pBlueScript II SK and was used to transform chemically competent DH5-α *E.coli* purchased from the University of California, Berkeley QB3 MacroLab

(https://qb3.berkeley.edu/facility/qb3-macrolab). Following an overnight incubation, colonies were then screen for inserts using a T3/JCH199 primer pair, with the resulting PCR run on a gel. Due to small percentage of colonies which appeared insert positive through the colony PCR protocol, it is difficult to estimate the relative proportion of alleles within each $F_0$ fish. Sanger sequencing was performed on all colonies which appeared to have the marine, low-tooth associated allele. The same procedure was used for the other approaches. Eight embryos of Approach #2, using a single sgRNA, were genotyped, while four for Approach #3, using two sgRNAs and Cas9 mRNA, were genotyped.

**Injection of high-tooth associated haplotype into a marine background**

Both approaches using Cas9 protein were applied using a marine background (RABS), with the objective of replacing the endogenous sequence with a high-tooth associated haplotype isolated from a Paxton Benthic fish containing the chromosome XXI tooth QTL (Cleves et al., 2014). Approximately 100 RABS embryos were injected with sgMDS4/sgMDS11, Cas9 protein, and a donor plasmid containing the high-tooth haplotype. 19 embryos survived to 5 dpf and were genotyped. *Ava*II digest was performed on a MDS213/JCH200 amplicon, with Sanger sequencing of individuals with banding patterns suggestive of replacement. In addition, 32 embryos injected with sgMDS11, Cas9 protein, and a donor plasmid (Approach #2) across three injection rounds were genotyped using *Ava*II and Sanger sequencing. Amplification of the region was done using primer pairs MDS230/MDS233, MDS213/173 (both clutch TG1682), MDS213/JCH200 (clutch TG1557), or MDS233/181 (clutch TG1649). TG1682 used a new left homology arm, in which a SNP 119bp upstream of the sgMDS11 target site was changed (A→G) to better match the recipient stock fish.

**Outcrossing and genotyping for transmission of mutant alleles in FTC**

In order to transmit potential mutant alleles, $F_0$ fish were either outcrossed to stock or in-crossed to other $F_0$ fish if available. As mutant fish are likely highly mosaic, with allele replacement relatively rare events, multiple offspring would need to be genotyped in order to detect successful transmission of mutant alleles. For crosses created with injected females at least eight offspring were genotyped using the same primers as for $F_0$ fish, but sequencing was restricted to sequence flanking the PAM site. Due to the presence of the non-D allele in Fishtrap Creek stocks, *Ava*II digest of $F_1$ fish would be significantly less informative initially, compared to first sequencing the PAM. Crosses between transgenic males and stock females were screened by genotyping the sperm prep of the male (see below), resulting in the entire potential clutch being genotyped with a single sequencing reaction.

**Outcrossing successful male**

An injected FTC male (MDS021221-1M), from TG1547, was outcrossed to a stock FTC female. The male had been injected with both sgMDS4/sgMDS11, and Cas9 mRNA. To genotype the outcross, 50µl of the sperm prep was used in lieu of fin tissue or embryo in the phenol chloroform genomic DNA extraction protocol. PCR with MDS219/MDS221 was performed and was genotyped by Sanger sequencing followed by digestion and ligation of the resultant amplicon into a plasmid to resolve individual alleles. Six colonies were verified to contain inserts and genotyped using *Ava*II digest, resulting in three potential low-tooth alleles and three potential high-tooth alleles. Each colony was used to start a 4 ml culture. Sanger sequencing using T3 as a sequencing primer was performed on each mini-prepped culture.

## 3.4 Results

### Cloning of the haplotype from uninjected Fishtrap Creek stock fish identifies unique polymorphisms to the stock population

Fish from the Fishtrap Creek stock population were genotyped for the haplotype via Sanger sequencing using primers MDS233/MDS234. The resulting amplicon was cloned into the pBlueScript II SK plasmid for refinement of the haplotype. Two sequences were clearly identified, a high-tooth associated haplotype allele and a low-tooth associated allele. Both alleles were identified in multiple fish with agreement for each polymorphic site and contained identities at multiple points that were unique to the stock population (Figure 2). The characterization of the alleles present within the stock population allows for the comparison to potentially modified chromosomes and the determination of replacement has occurred.

### Two guide RNAs and Cas9 protein injection resulted in multiple alleles in $F_0$ FTC fish

While approximately 50 embryos were initially injected using the first approach of two sgRNAs and Cas9 protein along with the donor plasmid, only nine survived to 4 dpf to be genotyped. In addition, three uninjected siblings were also genotyped to determine if any apparent replaced alleles represented likely homology directed repair driven replacement events. Three of the nine surviving injected fish, labeled as 3, 5, and 8, were genotyped as potentially containing modified alleles. *Ava*II digest of MDS213/JCH200 PCR products indicated both alleles at the enzyme cut site, suggesting at least partial replacement had occurred. Sanger sequencing indicated modified PAM sites in the same three fish.

Regions of the haplotype was cloned in Fish 3, 5, and 8. In each fish, apparent replacement had occurred (Figure 3.2). The entire haplotype appeared to have been replaced in both Fish 5 and Fish 8 (seqMDS290 and seqMDS293 respectively using primers MDS219/221), while only the first region of the haplotype was cloned in Fish 3 (seqMDS294). Multiple colonies that contained only the first half of the region (due to primers used) were sequenced for Fish 5, resulting in three that contained the high-tooth "D" allele (seqMDS284), one that contained the edited low-tooth allele (seqMDS259), and a difficult to categorize allele (seqMDS267), indicating a majority of chromosomes were unedited. While most polymorphic sites upstream of the genotyped PAM had the same identity across the cloned alleles, a combination of a singleton and different alleles at the PAM suggests multiple modified alleles were created through Cas9 and HDR mediated allele replacement.

As the "D" allele is segregating in the Fishtrap Creek stock population, it is possible the generated replacement alleles were simply the "non-D" allele present in the stock. To determine the likelihood of the apparent replacement alleles being false positives, three uninjected control fish were also sequenced. All three uninjected control fish were genotyped as homozygous for the high-tooth associated, "D", allele using Sanger sequencing, indicating the likelihood original genotype across the injected clutch is homozygous for the high-tooth associated allele, and the assumed modified alleles are likely to be the result of Cas9 HDR mediated allele replacement.

Two cloned alleles, one from Fish 3 and Fish 5, did not contain changes to the genotyped PAM site (seqMDS295 and seqMDS267 respectively). Due to a single polymorphic site unique to seqMDS295, it appears the two alleles are unique and may be the result of allele replacement. It is possible the PAM of the downstream target site, which was not genotyped in any $F_0$ fish, had been modified and therefore may explain the lack of change in the two un-modified-PAM alleles. Alternatively, seqMDS295 and seqMDS267 may represent an additional unedited allele at the locus and be a second low-tooth associated haplotype containing chromosome. The two

alleles contain two SNPs upstream of the target site with identities that are not observed together, with the site immediate 5' of the sgMDS11 site not having the marine identity in any other sequence amplified from a Fishtrap Creek animal, injected or uninjected. It is formally possible these two chromosomes may be another non-D allele segregating in the stocks and the single site that differs between them is a mutation introduced during the cloning process. Overall, due to the number of alleles present within the clutch, including those identified from injected fish and uninjected controls, it can be concluded that Cas9 mediated changes occurred, and generated multiple mutant alleles. For example, in Fish 5 (seqMDS267, seqMDS259/seqMDS290, and seqMDS284) and Fish 8 (seqMDS260, seqMDS261/seqMDS293), three distinct alleles were cloned, while Fish 3 has a unique allele not found in either of the other two (seqMDS295). A total of at least six alleles, including the high-tooth associated haplotype, were amplified from a single clutch. As the clutch would only contain a maximum of four if each parent had two unique alleles, it can be concluded replacement has occurred.

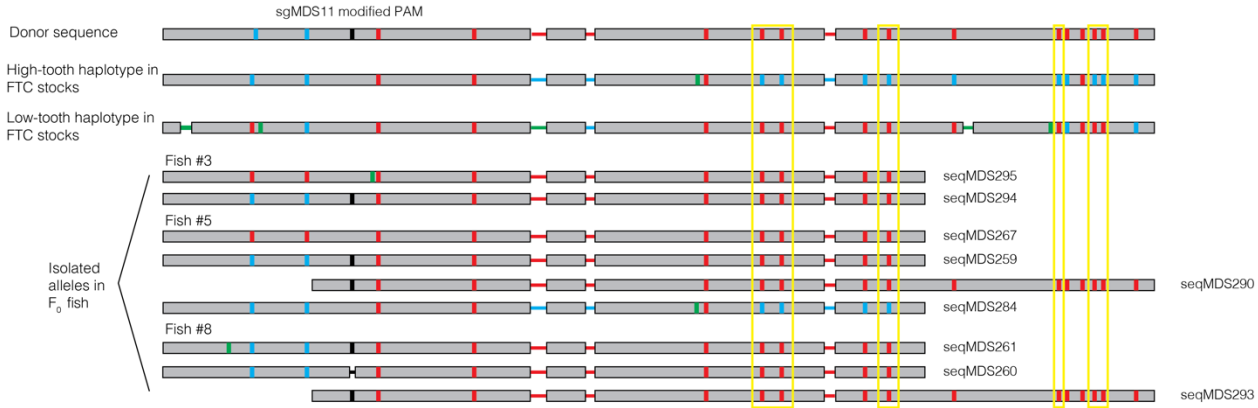


**Figure 3.2 Mutant alleles isolated from three $F_0$ injected Fishtrap Creek embryos demonstrate allele replacement using two guide RNAs and Cas9 protein.** Three embryos, labeled Fish #3, 5, and 8, were identified which contained the low-tooth associated haplotype through Sanger sequencing. Subsequent cloning of the region identified multiple mutant alleles for each fish indicating allele replacement has occurred after the 5' cut site when using two sgRNAs flanking the haplotype containing region. Grey regions indicate invariable sites, red, blue, and green vertical lines indicate single nucleotide polymorphisms with identities consistent with the marine/low-tooth haplotype or freshwater/high-tooth haplotype, or unique to the Fishtrap Creek background respectively. Indels are represented by horizontal lines. Modified PAM sequences are represented either by a black vertical line (single nucleotide change) or horizontal black line (indel). Haplotype defining positions are identified in yellow highlight. Shorter sequences were generated by cloning with MDS219/MDS220 while longer amplicons were created by cloning with MDS219/MDS221. Representative high-tooth and low-tooth associated haplotype containing chromosomes from the Fishtrap Creek stock fish shown above.

### Two guide RNA and Cas9 mRNA injection in FTC did not result in replacement in a small number of F0 animals

Only four Fishtrap Creek stock fish injected with guides sgMDS4/sgMDS11 and Cas9 mRNA were genotyped in order to preserve other $F_0$ individuals for future outcrossing. As one third of injected fish using two sgRNAs and Cas9 protein demonstrated allele replacement, four fish would likely contain a single replacement event if the two methods had similar efficiencies.

*Ava*II digest and Sanger sequencing of the variable sites of four injected fish and three uninjected controls revealed all seven fish appeared to be homozygous for the "D" allele. It is possible that the four injected fish were mosaic but the replacement allele was too rare to detect compared to the unedited allele. Overall it appeared the replacement was less likely to occur using Cas9 mRNA compared to protein though only a small number of $F_0$ fish were genotyped.

**Injection of single guide RNA and Cas9 protein results in multiple mutant alleles in $F_0$ embryos in FTC**

Ten 4dpf embryos were genotyped using the *Ava*II restriction digest. Two fish, TG1547 #6 and #7, appeared to be heterozygous and were selected for subsequent sequencing and sub-cloning using MDS219/MDS220 and MDS219/MDS221. At least six alleles were identified from TG1547 #7, while three were identified from TG1547 #6 (Figure 3.3). In addition, the male parent of clutch TG1547 was genotyped by sequencing as being homozygous for the high-tooth associated allele, matching the allele identified in uninjected controls from previous injection rounds. Two alleles from TG1547#6 contain individual SNPs that are not found in any other sequence from Fishtrap Creek stock fish nor are they found in 38 wild caught Fishtrap Creek genomes, suggesting they may be PCR induced mutations.

Multiple alleles present seem to be chimeric alleles between the endogenous sequence and the donor sequence. For example, the allele seqMDS466 shares perfect homology with the marine haplotype/donor until the last approximate hundred bases of the amplicon, in which the remaining SNPs become consistent with the known high-tooth haplotype in the stock population. This is contrasted to the allele seqMDS465 in which the entire sequence is consistent with the donor plasmid. The mutant chromosome of seqMDS466 likely used a large proportion of the donor as template before finding a region of sufficient homology, at which point a second Holliday junction potentially occurred, and the 3' remainder of the chromosome appeared unaffected, while the chromosome of seqMDS465 resolved the recombination further downstream, resulting in more polymorphisms captured. A similar pattern can be seen in comparing seqMDS451, seqMDS450, and seqMDS448, while seqMDS447 may either represent a very early resolution of HDR or a largely unedited, original allele. Interestingly, every sequenced PAM site indicates the replacement of the first guanine in the tri-nucleotide NGG component to the thymine as provided in the donor plasmid.

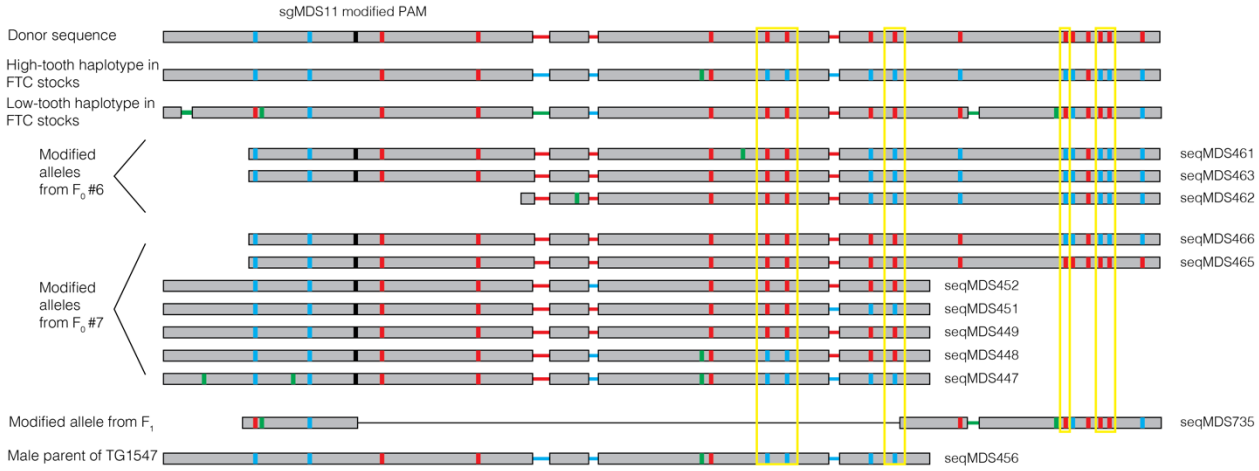


**Figure 3.3 Multiple mutant alleles were created from the injection of $F_0$ fish with a single guide**. After amplification of the region from two fish, TG1547 #6 and TG1547#7, were found to have a modified PAM site and marine identities at multiple positions. Cloning the region identified multiple alleles from each individual fish, indicating some form of Cas9 mediated mutagenesis occurred. Multiple clones matched the donor plasmid throughout the length of the clone (segMDS465 and seqMDS449), while others appeared to be the result of homology directed repair at different points throughout the haplotype, creating chimeric chromosomes with stretches consistent with the low tooth-associated and high tooth-associated alleles (seqMDS466, seqMDS463, seqMDS448). A low tooth-associated haplotype identified in the Fishtrap Creek stock contains polymorphic positions that are unique to the population, allowing distinction between the segregating allele in the stocks and a mutant allele, resulting from Cas9 induced homology directed repair (HDR). The sequencing of the FTC-D allele (seqMDS456 and the high tooth sequence identified previously) allows for the identification of likely termination points of recombination and HDR. Crossing of $F_0$ injected fish resulted in the transmission of a mutant chromosome containing a 665 bp deletion, spanning from the sgMDS11 cut site to just past the third haplotype defining SNP (seqMDS735). Grey regions indicate invariable sites, red, blue, and green vertical lines indicate single nucleotide polymorphisms with identities consistent with the marine allele, "D" allele from PAXB, or unique to the Fishtrap Creek background respectively. Indels are represented by horizontal lines. Modified PAM sequences are represented either by a black vertical line (single nucleotide change) or horizontal black line (indel). Haplotype defining positions are identified in yellow highlight. Shorter sequences were generated by cloning with MDS219/MDS220 while longer amplicons were created by cloning with MDS219/MDS221.

**Transmission of mutant alleles from F0 fish injected with a single sgRNA**

Injected fish were either outcrossed to stock fish or in-crossed to other injected individuals. A total of 15 $F_0$ FTC fish were crossed (Table 3.2), with nine having been outcrossed to stock fish and five $F_0$ females crossed to a single $F_0$ male. A total of ten clutches were created that had contained mutant sgMDS11 target sites containing indels genotyped by sequencing. No modified PAM sequence was found. Due to the segregating, non-D allele in Fishtrap Creek stocks, true replacement events were difficult to detect despite best efforts of genotyping stock parents and the FTC-nonD allele creating potential false positives. Sequencing did not reveal transmission of any replacement event in $F_1$ fish. Genotyping one cross, TG1566 female 4 x TG1566 male 1 (MDS022820-1M), did find two embryos with large, 665 bp deletions spanning the beginning of the haplotype, which resulted in the deletion of the first three haplotype defining SNPs (Figure 3.3). The remaining sequence on the mutant chromosome is consistent with the non-high-tooth

associated allele in the stock population. Deletions of the haplotype on a marine background have been generated in the lab previously, with no resulting phenotypic change. However, the different, freshwater, genetic background may uncover a mutant allele effect.

| cross/description | number of embryos genotyped | description |
|---|---|---|
| TG1749 | 13 | no change detected |
| TG1757 | 6 | possible lesion at cut site in 2/6 embryos |
| TG1765 | 10 | lesion in cut site in 5/10 embryos |
| TG1770 | 8 | no change detected |
| TG1566 female 1 x TG1566 male 1 (MDS022820-1M) | 8 | lesion at cut site in 1/8 |
| TG1566 female 2 x TG1566 male 1 (MDS022820-1M) | 8 | lesion at cut site in 1/8 |
| TG1566 female 3 x TG1566 male 1 (MDS022820-1M) | 8 | no change detected |
| TG1566 female 4 x TG1566 male 1 (MDS022820-1M) | 8 | large, 665 bp deletion, removing first 3 haplotype defining SNPS in 2/8 embryos |
| TG1566 female 5 x TG1566 male 1 (MDS022820-1M) | 8 | lesion at cut site in 1/8 |
| TG1566 female 6 x stock | 8 | no change detected |
| FTCAS 10/07/20 | 8 | no change detected |
| FTC AS MDS081220-1M x stock | 6 | no change detected |
| MDS011420-1M FTC AS | sperm prep genotyped | lesion at cut site |
| FTC AS female 4 | 8 | lesion at cut site in 1/8 |
| FTC AS female 5 | 8 | lesion at cut site in 4/8 |
| FTC AS female 6 | 8 | lesion at cut site in 1/8 |

**Table 3.2** Crosses of F0 injected Fishtrap Creek fish

### Transmission of replacement alleles from a single $F_0$ male injected with two sgRNAs and Cas9 mRNA

A male (MDS021221-1M) $F_0$ injected using Approach #3, with Cas9 mRNA, was outcrossed to a stock Fishtrap Creek fish. The sperm prep from male MDS021221-1M was genotyped by sequencing and a modified PAM was observed, with the C→A change that is in the donor plasmid, suggesting potential replacement on at least a subset of chromosomes within the gametes. Subsequent cloning and sequencing of clones revealed replacement throughout the haplotype, with multiple alleles present (Figure 3.4). As observed with the single sgRNA approach (Figure 3.3), chimeric chromosomes were present, while they were not observed with the two sgRNA/Cas9 protein approach (Figure 3.2). Five different alleles were sequenced from the gametes of the transgenic male, including those that matched the donor (seqMDS803), and the high-tooth associated allele (seqMDS804). One SNP distinguishes seqMDS804 from the known high-tooth allele in the FTC stocks, suggesting this allele is either an additional chromosome, or the result of PCR recombination (see discussion). Some alleles have unique combinations of identities (seqMDS799/802) that do not appear to be a possible result of either FTC sequence having undergone recombination with the donor allele at a single point. Instead the sequence appears to alternate between matching the donor and the endogenous sequence. The pattern may be due to PCR recombination or uncharacterized alleles within the stock population.

Overall, seqMDS803 and seqMDS800 appear to represent true complete and partial replacement events.

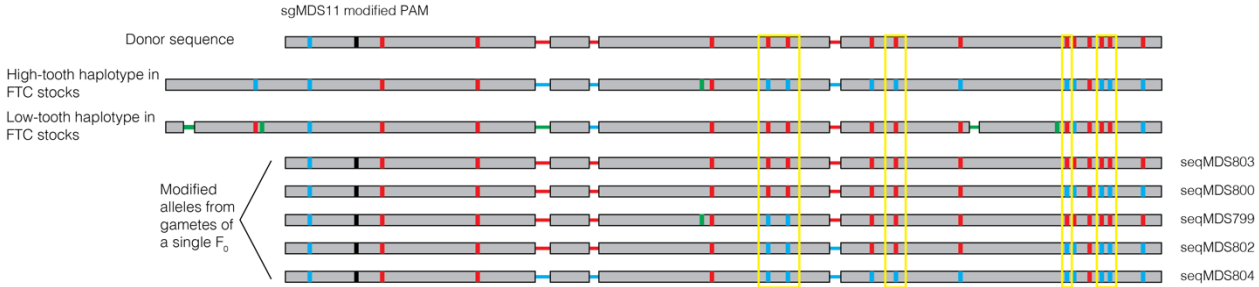


**Figure 3.4 Figure 3.4 Multiple alleles are present in the germline of an $F_0$ male injected with sgMDS11/sgMDS4 and Cas9 mRNA.** Cloning of the target region using DNA extracted from the sperm prep of an $F_0$ male (MDS021221-1M) revealed multiple different mutant alleles, indicating a highly mosaic gonad. Allele seqMDS803 appears to be a complete replacement of the target region, while the sequences of seqMDS800 and seqMDS799 suggest replacement at the beginning and end of the haplotype respectively, reflecting Cas9 cleavage and subsequent HDR starting at either sgMDS11 (upstream and pictured cut site) or sgMDS4 (downstream and not pictured). seqMDS804 may represent an original allele with only a modified PAM site for sgMDS11. The chimeric seqMDS802 contains a stretches consistent with the Fishtrap Creek high tooth- and low tooth-associated alleles alternating, suggesting PCR recombination. Grey regions indicate invariable sites, red, blue, and green vertical lines indicate single nucleotide polymorphisms with identities consistent with the marine/low-tooth haplotype or freshwater/high-tooth haplotype, or unique to the Fishtrap Creek background respectively. Indels are represented by horizontal lines. Modified PAM sequences are represented either by a black vertical line (single nucleotide change) or horizontal black line (indel). Haplotype defining positions are identified in yellow highlight. Shorter sequences were generated by cloning with MDS219/MDS220 while longer amplicons were created by cloning with MDS219/MDS221.

**Screening for allele replacement in Rabbit Slough Marine background**

19 fish injected using two sgRNAs and Cas9 protein were screened for allele replacement. *Ava*II digest indicated a single individual that may have experienced allele replacement. Subsequent sequencing of the sgMDS11 cut site revealed a small indel, disrupting the site. However, sequencing of the haplotype defining region showed no replacement. A total of 32 fish injected with a single sgRNA (sgMDS11) across three rounds of injection were genotyped, primarily through sequencing (Table 3.3). 11 out of 19 fish with sequencing data surrounding the sgMDS11 cut site showed lesions as evidence by the loss of the sequencing read, while one fish had an apparent integration of the modified based within the PAM which matches the donor plasmid. However, sequencing of six haplotype regions and 16 *Ava*II digests revealed no likely replacement events.

| clutch | number of fish genotyped | description |
|---|---|---|
| TG1557 | 16 *Ava*II digest, 3 sgMDS11 site sequenced, 3 haplotype sequenced (16 total) | 2 fish had disruptions at sgMDS11 site, including an apparent incorporation of a modified PAM site |
| TG1649 | 8 sgMDS11 site sequenced (8 total) | 4/8 contained a deletion within sgMDS11 target site |
| TG1682 | 8 sgMDS11 site sequenced, 3 haplotype sequenced (8 total) | 8/8 contained deletions at sgMDS11 cut site but no allele replacement |

**Table 3.3** Injection and replacement outcomes in a marine background

## 3.5 Discussion

### Homology directed repair in Fishtrap Creek fish results in whole and partial haplotype replacement

Three methods were used to replace the high tooth-associated haplotype in Fishtrap Creek stock fish with a donor, specifically a low tooth-associated allele sourced from a Little Campbell marine fish used in previous QTL experiments. All three approaches used the same donor, consisting of a shorter upstream homology arm (458 bp), a marine haplotype containing core (1278 bp), and a longer, downstream homology arm (1196 bp). Each homology arm was terminated with an added target site for the guide sgMDS11. Approaches varied in their use of one or two guide RNAs and Cas9 mRNA or protein.

$F_0$ injected individuals from two approaches (Cas9 protein and either one or two guide RNAs) yielded chromosomes that apparently contained replacement events. The use of two guides generated low tooth haplotype alleles in at least three of nine injected individuals. Using this approach complete replacement was observed in which all sites that distinguish the donor from endogenous sequence matched the donor identity (seqMDS259-261, seqMDS290, seqMDS294). Some amplified haplotypes either did not contain modified PAM sites at the 5' cut site (seqMDS267) or contained a unique polymorphism (seqMDS295). While it is possible these represent original genomic sequence, it is also possible the modified PAM was not integrated from the donor and the unique polymorphism was a PCR induced variant, as no other chromosome across all experiments contained a polymorphism at that site.

When using a single guide (sgMDS11), it can be predicted that multiple alleles would be created. Following the initial double stranded break, strand invasion would occur on the donor and continue until resulted in a large number of different alleles from a single $F_0$ injected fish, either through crossover resolution of a double Holliday junction (Jasin & Rothstein, 2013) or simply break induced replication (BIR) (Li & Heyer, 2008). As this process would vary cell to cell, it would be expected to result in multiple different alleles in which varying degrees of replacement has occurred. For example, seqMDS465 has the entire haplotype replaced, while seqMDS466 has resulted in the replacement of all but the 3' most set of SNPs, and seqMDS451 shows replacement of only the 5' most haplotype defining SNPs. Despite screening 17 $F_0$ adults, there was no transmission of replacement alleles from fish injected with a single guide and Cas9 protein, while a single large deletion allele was transmitted.

Outcrossing an $F_0$ that was injected with two sgRNAs and Cas9 mRNA resulted in the only apparent transmission of a replaced allele. Entire replacement was observed (seqMDS803) as well as partial replacement (seqMDS799/800). Interestingly, the two partial replacement alleles have similarities to those seen in $F_0$ fish when a single guide was used. Instead of HDR proceeding from only a single possible double stranded break (site of sgMDS11), it could proceed either from upstream or downstream of the haplotype (sgMDS11 or sgMDS4 targets

respectively) and so may explain the bi-directional replacement. It is possible this phenomenon would also have been seen in the two sgRNA/Cas9 protein $F_0$ fish upon further genotyping. It is not clear why the two sgRNA/Cas9 mRNA approach was the only one that resulted in transmission as edited alleles are present in the Cas9 protein $F_0$ at levels high enough to be easily detected through sequencing and cloning of specific alleles at the region. As the propagated replaced alleles were identified from a sperm prep two possible factors may have played a role:1) genotyping multiple alleles within a sperm prep is far easier and simpler as a single PCR could be done to amplify all present, while genotyping the $F_1$ offspring from a female $F_0$ requires multiple independent reactions and fewer possible alleles can be sampled and/or 2) due to development it is possible males may be more likely to transmit transgenes, for example if the male germline is set aside later in development which would provide a longer opportunity for allele replacement to occur in cells that will eventually give rise to gametes. Alternatively, Cas9 mRNA may simply be more effective when wanting to transmit replaced alleles.

**Outcrossing TG2127**

While replacement was observed in the germline of the Fishtrap Creek male MDS021221-1M, there appeared to be a very high degree of mosaicism, as evidenced by five separate alleles generated through cloning of the region. PCR recombination may be able to explain some of the chimeric alleles that were sequence, but there must still be multiple alleles transmitted and therefore only a fraction of the $F_1$ fish contain the replaced allele. Due to the number of cloned alleles, it can be estimated that approximately one fifth of the offspring of the male, clutch TG2127, contains the Cas9 mediated replaced allele. I caution against genotyping $F_1$ fish and then keeping those that appear to contain a desired allele. When screening the Fishtrap Creek stocks for those homozygous for the high-tooth allele prior to injections, fin clipping appeared to result in some loss of fish, and the squeezing of gravid females would occasionally be lethal the following day. As Fishtrap Creek fish appear to be more sensitive to handling than other stock fish, I recommend crossing fish as they become available and genotyping the transgenic parent post-fertilization to screen for the mutant allele.

In order to determine if there is a phenotypic effect of the haplotype replacement, an $F_1$ fish that contains the replaced allele should be crossed to a Fishtrap Creek stock fish that is homozygous for the high-tooth associated allele. This would create two potential genotypes in the $F_2$ generation: heterozygous with the replaced allele and homozygous for the high tooth allele. As the tooth QTL is additive, I would predict a phenotypic difference between the two genotypes if there is an effect on tooth number. Crossing to a heterozygous FTC stock fish, containing both the high tooth-associated allele (D) and the FTC non-high tooth-associated allele (non-D), would create four different genotypes: D/D, D/non-D, D/edited, and non-D/edited. If the haplotype underlies the tooth number QTL, I would predict the D/non-D and D/edited genotypes would have similar tooth numbers, as the non-D and edited alleles should have similar effects if the hypothesis is accurate.

**Chimeric chromosomes allow for the testing of specific SNPs**

The chromosomes isolated from the gametes of Fishtrap Creek male MDS021221-1M contain multiple alleles, including those that appear to contain stretches of sequence from the endogenous FTC-D allele and the donor, low tooth haplotype, allele. For example, the allele seqMDS799 contains the high tooth associated identity for the first two SNPs but the marine identity for the following four, while the allele seqMDS800 contains the marine identity for the

first three SNPs before reverting to the original FTC-D allele. The chimeric chromosomes may provide an opportunity to dissect the haplotype by position, allowing for the determination of the contributions of combinations of SNPs. Crossing a fish heterozygous for the seqMDS800 allele ($3^M3^D$/D) with a fish homozygous for the D allele would allow the direct comparison of effects of the first three SNPs as either marine or D identity on tooth number, generating homozygous high tooth haplotype and heterozygous ($3^M3^D$/D) fish. Alternatively, crossing the $3^M3^D$/D $F_1$ fish to a D/non-D het would generate $3^M3^D$/D, $3^M3^D$/non-D, D/non-D, D/D. Comparing the $3^M3^D$/D to either D/D or D/non-D fish would determine the effect of either the first three or last three SNPs being the high tooth allele, respectively.

**No evidence of replacement in Rabbit Slough background**

Multiple attempts were made to replace the marine, low tooth-associated allele, with the high tooth, "D" allele from the Paxton Benthic population. While screening of PAM sites for sgMDS11 showed some lesions were introduced, there was little evidence of haplotype replacement. A new homology arm was used after a polymorphic site was identified in the region in the RABS stock fish, however this did not appear to result in sequence exchange. It is possible that replacement had occurred in multiple $F_0$ fish, but was not detected, though the use of *Ava*II digest along with Sanger sequencing for a subset of RABS injected fish reduced the likelihood of a true replacement event being missed. $F_0$ fish that were injected with sgMDS11, a donor plasmid, and Cas9 protein can be outcrossed with the resulting clutch screened for replacement. As there will be fewer alleles present in $F_1$ than $F_0$ individuals, specific PAM disruption, through the change from NGG to NGT, would be easier to detect. The successful propagation of a replaced allele in FTC, using Cas9 mRNA and two sgRNAs, encourage the continued efforts of replacement in a RABS background using the same approach.

**Replacing individual polymorphisms through ssODN donors**

The effective use of single stranded oligo deoxynucleotides (ssODN) as donor templates for replacing or knocking in sequence been demonstrated in multiple experimental designs and model organisms, including zebrafish (Boel et al., 2018), mice (Yoshimi et al., 2016), and human cell lines (Richardson et al., 2016; Skarnes et al., 2019). ssODN as a donor can be especially effective when the objective is for a small number of nucleotides to be changed and are close to the PAM site and the ssODN is complementary to the non-targeting strand (Okamoto et al., 2019; Richardson et al., 2016). Knock in experiments have been able to use relatively large donor templates in mice, on the order of 1kb, to insert reporter transgenes (Yoshimi et al., 2016). Sequence replacement experiments in zebrafish has used shorter donors to replace individual SNPs, with optimum donor length of 120bp (Boel et al., 2018) and HDR efficiencies decreasing with larger, 180bp templates. Knocking in a short sequence in zebrafish, high rates of success have been seen with relatively larger, 300-500 bp, single strand donors (Bai et al., 2020). The use of single strand donors for small sequence knock in had much higher efficiency rates than other methods including linearized and circular plasmid donors. Further improvements to HDR efficiency has been demonstrated by covalently linking the donor ssODN to the Cas9 protein (Aird et al., 2018; Savic et al., 2018).

The haplotype defining polymorphisms span approximately 440 bp, with four of the six SNPs forming pairs that are separated by less than 15 bases. ssODN donor templates could be used to replace subsets of SNPs either individually or in small groups. Four templates would be sufficient to replace all polymorphisms in a stepwise manner. For example, the first two sites could be replaced initially, then the third could be replaced, which is approximately 135 bp

away, with a different donor template. This piece-by-piece approach would allow the creation of transgenic lines that contain specific chimeric chromosomes to test the effects of changing individual sites. While complete and partial replacement chromosomes have been propagated in the Fishtrap Creek background using a plasmid donor, the ssODN approach may provide a means of replacing the low tooth, marine allele in a Rabbit Slough background, which was not observed in the experiments performed here. The ssODN approach would also allow for the replacement of just the QTL associated positions, and not the other variants that are interspersed between the six sites. It is possible the other variable sites within the region, while not perfectly associated with the presence/absence of a QTL peak, may affect transcription factor binding to a lesser degree and therefore have a potential affect.

Of specific interest would be the NFATc1 binding site creating SNP (*Ava*II SNP). A PAM falls just four bases downstream of this SNP, allowing for a double strand break just 3' of the SNP of interest. A ssODN donor template should be able to easily replace either jut the NFATC1 SNP, or the position 12 bases 5' as well, since positions close to the PAM site are more amenable to replacement through HDR (Okamoto et al., 2019). In order to allow cleavage of the genomic target and prevent cleavage of both the donor and desired replaced/inserted sequence, mismatches or ablated PAM sites are typically incorporated in the donor template. When targeting coding sequences, synonymous substitutions can be used in the donor template, resulting in desired changes to the gene of interest as well as non-functional changes (Boel et al., 2018; Bottcher et al., 2014; Inui et al., 2015; Ran et al., 2013). As the region of interest in this instance is regulatory, non-coding, sequence, it is difficult to predict if induced mutations, used to disrupt targeting. Fortunately, the sites that differ between haplotypes fall within a potential sgRNA target. Mismatches between the sgRNA and target can negatively impact the ability of Cas9 to cleave the target, specifically those on the PAM proximal end and multiple mismatches can dramatically reduce the cutting ability of Cas9 (Anderson et al., 2015; Zheng et al., 2017). In the instance of the NFATc1/*Ava*II site, the position falls within the highly sensitive core of the target sequence that does not tolerate mismatches, while another, upstream, SNP would fall in the 5' PAM-distal end of the guide. While 5' PAM-distal mismatches are more well tolerated, the combination of two mismatches, even if one is 19 bases distal to the PAM, often greatly reduce the introduction of indels at a target site (Anderson et al., 2015). Therefore, following successful replacement through HDR with the alternate alleles at the two sites, subsequent cleavage and induced mutations through NHEJ are unlikely to occur simply due to the replaced sequence being sufficiently mismatched compared to the guide RNA used to induce breaks in the genomic sequence.

The third SNP of the haplotype is approximately 140 bp downstream of the previously described sgRNA target site, and so would not be well suited for replacement through the same ssODN donor as the first two positions. However, it is the first base within a potential sgRNA target, just 5' to an NGG PAM, which, while tolerated, should still reduce cutting efficiency once the allele replacement has occurred. The three remaining SNPs of the haplotype span approximately 50 bases, with the downstream most two separated by only nine bases and flank a possible sgRNA target, making them potential targets for a single guide/ssODN donor. The final SNP does not fall within a possible target site which makes replacement through a ssODN and Cas9 difficult. Other engineered Cas proteins have greatly reduced the PAM restriction and so provide more flexibility in selecting target sites (Walton et al., 2020), meaning it could be targeted with a double strand break nearby using a new Cas9 protein.

**Potential false positives**

There are three possible explanations for the alleles seen when amplifying the target region from $F_0$ injected FTC fish: 1) replacement has occurred, 2) marine, apparently replaced alleles, even those matching the donor template, represent the FTC-nonD allele segregating in the stock population, 3) what appear as amplicons showing successful replacement are the results of recombination during PCR.

1) Replacement has occurred
   Cloning using internal, in the replacement sequence and external, on the chromosome outside of the homology arms, primers to amplify the junction where replacement would be expected to begin has unveiled multiple possible alleles, including those with complete and partial sequence replacement. As the sequence in the donor template between the homology arms has areas of complete homology with the recipient genome, it is possible recombination can occur throughout the haplotype and generate partial replacement alleles, for example seqMDS799, seqMDS800, seqMDS463, and seqMDS451.

2) "Replaced" alleles are segregating FTC-nonD alleles
   The stock population used for injections, FTC 19x19, was founded by two individuals, meaning a maximum of four alleles could exist within the target region in the initial cross. Recombination could, over generations, create new haplotypes by recombining at different points along the haplotype, though it seems unlikely to have recombined multiple times within the small, less than 500 base pair window that contains the haplotype. In addition, the central part of chromosome XXI has a suppressed recombination rate (Glazer et al., 2015), further reducing the likelihood that the multiple alleles are the result of ancestral D and non-D alleles recombining.

3) PCR recombination
   PCR recombination occurs when incomplete elongation allows for partial amplicons from different alleles to anneal at sites of homology and act as starting points of elongation in the following cycle, creating chimeric alleles (Meyerhans et al., 1990). In this instance, it is possible two alleles within a heterozygous animal, the low tooth- and high tooth-associated alleles, could be combined and create unique chimeric sequences that have the appearance that HDR has occurred at different points. There are FTC stock specific polymorphisms, or those consistent with the Paxton, high-tooth allele, on the FTC-nonD chromosome (seqMDS472) that are not seen in the potential generated replacement alleles (seqMDS465). Chromosomes that contain large stretches that exclusively match the donor (seqMDS803, seqMDS800, seqMDS799) support true replacement as there are no polymorphic sites with FTC specific identities throughout those replaced stretches despite the FTC specific identities existing in the stock population and on the FTC-nonD chromosome. In order to generate chromosomes with the marine identity at all six sites from FTC-nonD chromosomes, FTC specific identities would also have to be incorporated (such as the FTC specific indel on the 3' end of seqMDS472). It is possible, and potentially even likely, chromosomes such as seqMDS802 were generated through PCR recombination in order to explain alternating stretches of high tooth identities and

low tooth identities. PCR recombination can be suppressed through low numbers of initial template and fewer cycles (Lahr & Katz, 2009). Assuming a maximum of 20 ng of genomic DNA was used in each reaction, a total of approximately $4x10^4$ copies would be present in the reaction. Using the polymerase Phusion, it has been shown even with $1x10^5$ copies of the template, at 30 PCR cycles, only 5% (+/- 8%) of eventual products are chimeric. While 35 cycles were used, it is unlikely that recombination through originally occurring haplotypes resulted in all of the multiple alleles identified. PCR recombination has occurred in CRISPR/Cas9 knock-in experiments (Won & Dawid, 2017), in which the injected construct, spanning the homology arms, has inserted elsewhere in the genome. The homology arm sequence allowed the initial amplicon from the desired insertion site and the inserted transgene to anneal and from deceptive amplicons that appear to indicate correct insertion. By amplifying using primers outside the transgene, the entire original locus can be genotyped and verify either correct insertion or replacement. If the donor is randomly inserted in the genome and is in fact creating the apparent replacement alleles, the reverse primer internal to the donor should only create initial amplicons that contain the donor haplotype. Therefore, alleles that result from knock-in/PCR recombination should only have the marine haplotype on the 3' end, while chromosomes like seqMDS451,seqMDS463, seqMDS466, and seqMDS799, begin matching the donor and transition to the FTC-D identity.

While there are different possible explanations for the multiple alleles generated through CRISPR/Cas9 injection the number observed, shared identity with the entire stretch of the donor plasmid across the sequenced window, and structure of partial replacement chromosomes all suggest that at least a subset of haplotypes identified are the result of homology directed repair and replacement using Little Campbell derived donor sequence. There are FTC-nonD alleles present in $F_0$ injected animals (likely seqMDS452), but there are population specific polymorphisms or combinations of polymorphisms that allow for the identification of unedited vs. edited alleles. Also, if insertion of donor template and PCR recombination underlie multiple alleles in the Fishtrap Creek background, it could be expected that the same should occur in the Rabbit Slough background, however there was no apparent replacement observed.

Often the replacement of genomic sequence with a donor template using CRISPR/Cas9 involves replacing a sequence with a non-homologous sequence, or orthologous sequence with less conservation than seen in these experiments. This chapter demonstrates the successful replacement of highly homologous sequence (97.9% shared sequence identity spanning from sgMDS11 to sgMDS4), with the expected result of partial replacement, as homology directed repair can use the donor template at multiple points across the provided haplotype. The work shown here provides: 1) proof of concept that enhancer replacement can occur in threespine sticklebacks, opening up the possibility of testing the role population specific regulatory regions that contain multiple polymorphisms, 2) the beginning of a transgenic line that founders of a contains Little Campbell Marine regulatory sequence on a freshwater background, allowing for the testing of a QTL associated haplotype, and 3) the possibility to identify the causative SNPs underlying the tooth number QTL through chimeric chromosomes.

## 3.6 References


Aird, E. J., Lovendahl, K. N., St. Martin, A., Harris, R. S., & Gordon, W. R. (2018). Increasing Cas9-mediated homology-directed repair efficiency through covalent tethering of DNA repair template. *Communications Biology*, *1*(1), 54. https://doi.org/10.1038/s42003-018-0054-2

Anderson, E. M., Haupt, A., Schiel, J. A., Chou, E., Machado, H. B., Strezoska, Ž., Lenger, S., McClelland, S., Birmingham, A., Vermeulen, A., & Smith, A. van B. (2015). Systematic analysis of CRISPR–Cas9 mismatch tolerance reveals low levels of off-target activity. *Journal of Biotechnology*, *211*, 56–65. https://doi.org/10.1016/j.jbiotec.2015.06.427

Bai, H., Liu, L., An, K., Lu, X., Harrison, M., Zhao, Y., Yan, R., Lu, Z., Li, S., Lin, S., Liang, F., & Qin, W. (2020). CRISPR/Cas9-mediated precise genome modification by a long ssDNA template in zebrafish. *BMC Genomics*, *21*(1), 67. https://doi.org/10.1186/s12864-020-6493-4

Bell, M. A., & Foster, S. A. (Eds.). (1994). *The evolutionary biology of the threespine stickleback*. Oxford University Press.

Boel, A., De Saffel, H., Steyaert, W., Callewaert, B., De Paepe, A., Coucke, P. J., & Willaert, A. (2018). CRISPR/Cas9-mediated homology-directed repair by ssODNs in zebrafish induces complex mutational patterns resulting from genomic integration of repair-template fragments. *Disease Models & Mechanisms*, *11*(10), dmm035352. https://doi.org/10.1242/dmm.035352

Bottcher, R., Hollmann, M., Merk, K., Nitschko, V., Obermaier, C., Philippou-Massier, J., Wieland, I., Gaul, U., & Forstemann, K. (2014). Efficient chromosomal gene modification with CRISPR/cas9 and PCR-based homologous recombination donors in cultured Drosophila cells. *Nucleic Acids Research*, *42*(11), e89–e89. https://doi.org/10.1093/nar/gku289

Jones, F. C., Grabherr, M. G., Chan, Y. F., Russell, P., Mauceli, E., Johnson, J., Swofford, R., Pirun, M., Zody, M. C., White, S., Birney, E., Searle, S., Schmutz, J., Grimwood, J., Dickson, M. C., Myers, R. M., Miller, C. T., Summers, B. R., … Kingsley, D. M. (2012). The genomic basis of adaptive evolution in threespine sticklebacks. *Nature*, *484*(7392), 55–61. https://doi.org/10.1038/nature10944

Byrne, S. M., Ortiz, L., Mali, P., Aach, J., & Church, G. M. (2015). Multi-kilobase homozygous targeted gene replacement in human induced pluripotent stem cells. *Nucleic Acids Research*, *43*(3), e21–e21. https://doi.org/10.1093/nar/gku1246

Chan, Y. F., Marks, M. E., Jones, F. C., Villarreal, G., Shapiro, M. D., Brady, S. D., Southwick, A. M., Absher, D. M., Grimwood, J., Schmutz, J., Myers, R. M., Petrov, D., Jonsson, B., Schluter, D., Bell, M. A., & Kingsley, D. M. (2010). Adaptive Evolution of Pelvic Reduction in Sticklebacks by Recurrent Deletion of a Pitx1 Enhancer. *Science*, *327*(5963), 302–305. https://doi.org/10.1126/science.1182213

Cleves, P. A., Ellis, N. A., Jimenez, M. T., Nunez, S. M., Schluter, D., Kingsley, D. M., & Miller, C. T. (2014). Evolved tooth gain in sticklebacks is associated with a cis-regulatory allele of Bmp6. *Proceedings of the National Academy of Sciences*, *111*(38), 13912–13917. https://doi.org/10.1073/pnas.1407567111

Cleves, Phillip A., Hart, J. C., Agoglia, R. M., Jimenez, M. T., Erickson, P. A., Gai, L., & Miller, C. T. (2018). An intronic enhancer of Bmp6 underlies evolved tooth gain in sticklebacks. *PLOS Genetics*, *14*(6), e1007449. https://doi.org/10.1371/journal.pgen.1007449

Colosimo, P. F. (2005). Widespread Parallel Evolution in Sticklebacks by Repeated Fixation of Ectodysplasin Alleles. *Science*, *307*(5717), 1928–1933. https://doi.org/10.1126/science.1107239

Davis, A. J., & Chen, D. J. (2013). DNA double strand break repair via non-homologous end-joining. *Translational Cancer Research*, *2*(3), 130–143. https://doi.org/10.3978/j.issn.2218-676X.2013.04.02

Erickson, P. A., Cleves, P. A., Ellis, N. A., Schwalbach, K. T., Hart, J. C., & Miller, C. T. (2015). A 190 base pair, TGF-β responsive tooth and fin enhancer is required for stickleback Bmp6 expression. *Developmental Biology*, *401*(2), 310–323. https://doi.org/10.1016/j.ydbio.2015.02.006

Erickson, P. A., Ellis, N. A., & Miller, C. T. (2016). Microinjection for Transgenesis and Genome Editing in Threespine Sticklebacks. *Journal of Visualized Experiments*, *111*, 54055. https://doi.org/10.3791/54055

Gibson, D. G., Young, L., Chuang, R.-Y., Venter, J. C., Hutchison, C. A., & Smith, H. O. (2009). Enzymatic assembly of DNA molecules up to several hundred kilobases. *Nature Methods*, *6*(5), 343–345. https://doi.org/10.1038/nmeth.1318

Glazer, A. M., Killingbeck, E. E., Mitros, T., Rokhsar, D. S., & Miller, C. T. (2015). Genome Assembly Improvement and Mapping Convergently Evolved Skeletal Traits in Sticklebacks with Genotyping-by-Sequencing. *G3: Genes|Genomes|Genetics*, *5*(7), 1463–1472. https://doi.org/10.1534/g3.115.017905

Hart, J. C., & Miller, C. T. (2017). Sequence-Based Mapping and Genome Editing Reveal Mutations in Stickleback *Hps5* Cause Oculocutaneous Albinism and the *casper* Phenotype. *G3: Genes|Genomes|Genetics*, *7*(9), 3123–3131. https://doi.org/10.1534/g3.117.1125

Hisano, Y., Sakuma, T., Nakade, S., Ohga, R., Ota, S., Okamoto, H., Yamamoto, T., & Kawahara, A. (2015). Precise in-frame integration of exogenous DNA mediated by CRISPR/Cas9 system in zebrafish. *Scientific Reports*, *5*(1), 8841. https://doi.org/10.1038/srep08841

Hörnblad, A., Bastide, S., Langenfeld, K., Langa, F., & Spitz, F. (2021). Dissection of the Fgf8 regulatory landscape by in vivo CRISPR-editing reveals extensive intra- and inter-enhancer redundancy. *Nature Communications*, *12*(1), 439. https://doi.org/10.1038/s41467-020-20714-y

Hoshijima, K., Jurynec, M. J., & Grunwald, D. J. (2016). Precise Editing of the Zebrafish Genome Made Simple and Efficient. *Developmental Cell*, *36*(6), 654–667. https://doi.org/10.1016/j.devcel.2016.02.015

Inui, M., Miyado, M., Igarashi, M., Tamano, M., Kubo, A., Yamashita, S., Asahara, H., Fukami, M., & Takada, S. (2015). Rapid generation of mouse models with defined point mutations by the CRISPR/Cas9 system. *Scientific Reports*, *4*(1), 5396. https://doi.org/10.1038/srep05396

Irion, U., Krauss, J., & Nusslein-Volhard, C. (2014). Precise and efficient genome editing in zebrafish using the CRISPR/Cas9 system. *Development*, *141*(24), 4827–4830. https://doi.org/10.1242/dev.115584

Jasin, M., & Rothstein, R. (2013). Repair of Strand Breaks by Homologous Recombination. *Cold Spring Harbor Perspectives in Biology*, *5*(11), a012740–a012740. https://doi.org/10.1101/cshperspect.a012740

Jinek, M., Chylinski, K., Fonfara, I., Hauer, M., Doudna, J. A., & Charpentier, E. (2012). A Programmable Dual-RNA-Guided DNA Endonuclease in Adaptive Bacterial Immunity. *Science*, *337*(6096), 816–821. https://doi.org/10.1126/science.1225829

Jones, F. C., Grabherr, M. G., Chan, Y. F., Russell, P., Mauceli, E., Johnson, J., Swofford, R., Pirun, M., Zody, M. C., White, S., Birney, E., Searle, S., Schmutz, J., Grimwood, J., Dickson, M. C., Myers, R. M., Miller, C. T., Summers, B. R., … Kingsley, D. M. (2012). The genomic basis of adaptive evolution in threespine sticklebacks. *Nature*, *484*(7392), 55–61. https://doi.org/10.1038/nature10944

Kvon, E. Z., Kamneva, O. K., Melo, U. S., Barozzi, I., Osterwalder, M., Mannion, B. J., Tissières, V., Pickle, C. S., Plajzer-Frick, I., Lee, E. A., Kato, M., Garvin, T. H., Akiyama, J. A., Afzal, V., Lopez-Rios, J., Rubin, E. M., Dickel, D. E., Pennacchio, L. A., & Visel, A. (2016). Progressive Loss of Function in a Limb Enhancer during Snake Evolution. *Cell*, *167*(3), 633-642.e11. https://doi.org/10.1016/j.cell.2016.09.028

Lahr, D. J. G., & Katz, L. A. (2009). Reducing the impact of PCR-mediated recombination in molecular evolution and environmental studies using a new-generation high-fidelity DNA polymerase: Research Reports. *BioTechniques*, *47*(4), 857–866. https://doi.org/10.2144/000113219

Li, X., & Heyer, W.-D. (2008). Homologous recombination in DNA repair and DNA damage tolerance. *Cell Research*, *18*(1), 99–113. https://doi.org/10.1038/cr.2008.1

Liang, F., Han, M., Romanienko, P. J., & Jasin, M. (1998). Homology-directed repair is a major double-strand break repair pathway in mammalian cells. *Proceedings of the National Academy of Sciences of the United States of America*, *95*(9), 5172–5177. https://doi.org/10.1073/pnas.95.9.5172

Marraffini, L. A., & Sontheimer, E. J. (2010). CRISPR interference: RNA-directed adaptive immunity in bacteria and archaea. *Nature Reviews Genetics*, *11*(3), 181–190. https://doi.org/10.1038/nrg2749

McDiarmid, T. A., Au, V., Loewen, A. D., Liang, J., Mizumoto, K., Moerman, D. G., & Rankin, C. H. (2018). CRISPR-Cas9 human gene replacement and phenomic characterization in *Caenorhabditis elegans* to understand the functional conservation of human genes and decipher variants of uncertain significance. *Disease Models & Mechanisms*, *11*(12), dmm036517. https://doi.org/10.1242/dmm.036517

Meyerhans, A., Vartanian, J. P., & Wain-Hobson, S. (1990). DNA recombination during PCR. *Nucleic Acids Research*, *18*(7), 1687–1691. https://doi.org/10.1093/nar/18.7.1687

Okamoto, S., Amaishi, Y., Maki, I., Enoki, T., & Mineno, J. (2019). Highly efficient genome editing for single-base substitutions using optimized ssODNs with Cas9-RNPs. *Scientific Reports*, *9*(1), 4811. https://doi.org/10.1038/s41598-019-41121-4

Ran, F. A., Hsu, P. D., Wright, J., Agarwala, V., Scott, D. A., & Zhang, F. (2013). Genome engineering using the CRISPR-Cas9 system. *Nature Protocols*, *8*(11), 2281–2308. https://doi.org/10.1038/nprot.2013.143

Richardson, C. D., Ray, G. J., DeWitt, M. A., Curie, G. L., & Corn, J. E. (2016). Enhancing homology-directed genome editing by catalytically active and inactive CRISPR-Cas9 using asymmetric donor DNA. *Nature Biotechnology*, *34*(3), 339–344. https://doi.org/10.1038/nbt.3481

Sander, J. D., Maeder, M. L., Reyon, D., Voytas, D. F., Joung, J. K., & Dobbs, D. (2010). ZiFiT (Zinc Finger Targeter): An updated zinc finger engineering tool. *Nucleic Acids Research*, *38*(Web Server), W462–W468. https://doi.org/10.1093/nar/gkq319

Sander, J. D., Zaback, P., Joung, J. K., Voytas, D. F., & Dobbs, D. (2007). Zinc Finger Targeter (ZiFiT): An engineered zinc finger/target site design tool. *Nucleic Acids Research*, *35*(Web Server), W599–W605. https://doi.org/10.1093/nar/gkm349

Savic, N., Ringnalda, F. C., Lindsay, H., Berk, C., Bargsten, K., Li, Y., Neri, D., Robinson, M. D., Ciaudo, C., Hall, J., Jinek, M., & Schwank, G. (2018). Covalent linkage of the DNA repair template to the CRISPR-Cas9 nuclease enhances homology-directed repair. *ELife*, *7*, e33761. https://doi.org/10.7554/eLife.33761

Skarnes, W. C., Pellegrino, E., & McDonough, J. A. (2019). Improving homology-directed repair efficiency in human stem cells. *Methods*, *164–165*, 18–28. https://doi.org/10.1016/j.ymeth.2019.06.016

Stuart, G. W., McMurray, J. V., & Westerfield, M. (1988). Replication, integration and stable germ-line transmission of foreign sequences injected into early zebrafish embryos. *Development (Cambridge, England)*, *103*(2), 403–412.

Talbot, J. C., & Amacher, S. L. (2014). A Streamlined CRISPR Pipeline to Reliably Generate Zebrafish Frameshifting Alleles. *Zebrafish*, *11*(6), 583–585. https://doi.org/10.1089/zeb.2014.1047

Walton, R. T., Christie, K. A., Whittaker, M. N., & Kleinstiver, B. P. (2020). Unconstrained genome targeting with near-PAMless engineered CRISPR-Cas9 variants. *Science*, *368*(6488), 290–296. https://doi.org/10.1126/science.aba8853

Wang, H., & Xu, X. (2017). Microhomology-mediated end joining: New players join the team. *Cell & Bioscience*, *7*, 6. https://doi.org/10.1186/s13578-017-0136-8

Wierson, W. A., Welker, J. M., Almeida, M. P., Mann, C. M., Webster, D. A., Torrie, M. E., Weiss, T. J., Kambakam, S., Vollbrecht, M. K., Lan, M., McKeighan, K. C., Levey, J., Ming, Z., Wehmeier, A., Mikelson, C. S., Haltom, J. A., Kwan, K. M., Chien, C.-B., Balciunas, D., … Essner, J. (2020). Efficient targeted integration directed by short homology in zebrafish and mammalian cells. *ELife*, *9*, e53968. https://doi.org/10.7554/eLife.53968

Winkler, C., Vielkind, J. R., & Schartl, M. (1991). Transient expression of foreign DNA during embryonic and larval development of the medaka fish (Oryzias latipes). *Molecular and General Genetics MGG*, *226–226*(1–2), 129–140. https://doi.org/10.1007/BF00273596

Won, M., & Dawid, I. B. (2017). PCR artifact in testing for homologous recombination in genomic editing in zebrafish. *PLOS ONE*, *12*(3), e0172802. https://doi.org/10.1371/journal.pone.0172802

Xu, X.-R. S., Gantz, V. M., Siomava, N., & Bier, E. (2017). CRISPR/Cas9 and active genetics-based trans-species replacement of the endogenous Drosophila kni-L2 CRM reveals unexpected complexity. *ELife*, *6*, e30281. https://doi.org/10.7554/eLife.30281

Yoshimi, K., Kunihiro, Y., Kaneko, T., Nagahora, H., Voigt, B., & Mashimo, T. (2016). SsODN-mediated knock-in with CRISPR-Cas for large genomic regions in zygotes. *Nature Communications*, *7*(1), 10431. https://doi.org/10.1038/ncomms10431

Zheng, T., Hou, Y., Zhang, P., Zhang, Z., Xu, Y., Zhang, L., Niu, L., Yang, Y., Liang, D., Yi, F., Peng, W., Feng, W., Yang, Y., Chen, J., Zhu, Y. Y., Zhang, L.-H., & Du, Q. (2017). Profiling single-guide RNA specificity reveals a mismatch sensitive core sequence. *Scientific Reports*, *7*(1), 40638. https://doi.org/10.1038/srep40638

## 3.7 Supplemental Materials

| guide name | target sequence | promoter | scaffold | total sequence ordered |
|---|---|---|---|---|
| sgMDS4 | GGAATCTGGGTCA GTAACCC | TAATACGA CTCACTAT A | GTTTTAGAGC TAGAAATAGC | GCGTAATACGACTCACTATAGGAATCTGGGTCA GTAACCCGTTTTAGAGCTAGAAATAGC |
| sgMDS11 | GGCGTCCCGAGTG GTGAGG | TAATACGA CTCACTAT A | GTTTTAGAGC TAGAAATAGC | GCGTAATACGACTCACTATAGGCGTCCCGAGTG GTGAGGGTTTTAGAGCTAGAAATAGC |

Sequences for guide RNAs flanking targeted region and fragments ordered for guide transcription

| primer | sequence | description |
|---|---|---|
| MDS189 | GCCGTCTAGACCCACAAGACGGATGCTCT | upstream homology arm R + Xba |
| MDS190 | GCCGCTCGAGTAGTAGTGGTCGGTGGGAGA | downstream homology arm F + xho (1.27 kb product, 1.18 kb homology arm) |
| MDS195 | CCGAGTGGTGAGGCTGAGAGGTCTTGATG | site directed mutagenesis F for sgMDS11 site |
| MDS196 | CATCAAGACCTCTCAGCCTCACCACTCGG | site directed mutagenesis R sgMDS11 site |
| MDS199 | GCCGTCTAGACCGCCTCACCACTCGGGACGCCATCAAACCCTA ATCCGCCCA | upstream homology arm F +xba +seq for sgMDS11 (1.42 kb product, 1.18kb homology arm) |
| MDS201 | GCCGTCTAGACCGCCTCACCACTCGGGACGCCCTCCCCTTCCTG CCTGTAAA | downstream arm R + xba +guide sequence for sgMDS11 |
| MDS202 | GGGTCAGTAACCCGTGGAGGAGGAAGGAG | site directed mutagenesis F sgMDS4 site |
| MDS203 | CTCCTTCCTCCTCCACGGGTTACTGACCC | site directed mutagenesis R sgMDS4 site |
| MDS205 | GACGGATGCTCTCCCCATCCCTCCTGTCCTC | left homology arm forward |
| MDS206 | CAGGAGGGATGGGGAGAGCATCCGTCTTGTG | haplotype/enhancer sequence forward |
| MDS207 | GGGAGGAGGAAGGAGAGAGTCCTGATGGCCTCTC | haplotype/enhancer sequence reverse |
| MDS208 | CCATCAGGACTCTCTCCTTCCTCCTCCCCGG | right homology arm forward |
| MDS209 | GAGCTCCACCGCGGTGGCGGCCGCTCCGCCTCACCACTCGGGA | right homology arm reverse |
| MDS215 | GGCGTCCCGAGTGGTGAGGCGGCCTGCATGACTTTTCCTCCA | left homology arm reverse |

Sequences for donor assembly primers

| primer | sequence | description |
|---|---|---|
| JCH199 | GCGTGAGTTACTGTGTGCTTTC | Inside haplotype forward |
| JCH200 | CCAGGACCTCAAAGCGAGTA | Inside haplotype reverse |
| MDS160 | CCTCTGTGATGAAAGACGGG | Cas9 screening primer for sgMDS4 cut forward |
| MDS161 | GTGAGACAAGATTGCAGCTCT | Cas9 screening primer for sgMDS4 cut reverse |
| MDS169 | TCCTTTTAGTTGCCGCTGTG | Cas9 screening primer for sgMDS11 cut reverse |
| MDS180 | CCCAGCCACTTGTCTTTGTC | Cas9 screening primer for sgMDS11 cut forward |
| MDS181 | ATATTTACACTCCCCGGCGT | Cas9 screening primer for sgMDS11 cut reverse |
| MDS213 | AGAACATCTCCTTCACTTTCTCA | Allele swap genotyping primer F |
| MDS219 | GCCGCTCGAGAGAACATCTCCTTCACTTTCTCA | Allele swap genotyping primer forward with xho cut site |
| MDS220 | GCCGTCTAGACCAGGACCTCAAAGCGAGTA | Allele swap genotyping primer reverse with xba cut site, first 3 SNPs |
| MDS221 | GCCGTCTAGACAAGGTACACGGCAGCATTT | Allele swap genotyping primer reverse with xba cut site, all SNPs |
| MDS233 | GCCGCTCGAGACCTGGGAAGCGATTTACCT | Allele swap genotyping primer forward with xho cut site |
| MDS234 | GCCGTCTAGATTGTTAACTTCCCCCACAGC | Allele swap genotyping primer reverse with xba cut site, all SNPs |

Sequences for genotyping and cloning PCR primers

# Chapter 4

## Population genetics of an adaptive *cis*-regulatory allele of the gene *Bmp6*

### 4.1 Abstract

Population genetic data can be used to find potential signals of selection in the genome, identifying candidate genes for adaptation. The approach has been applied repeatedly to threespine sticklebacks, finding regions that are commonly used in the colonization of freshwater habitats. The Fishtrap Creek, WA population is highly derived and contains *cis*-regulatory allele of the gene *Bmp6* that is associated with an increase in tooth number. Freshwater populations often experience evolved tooth gain, with Fishtrap Creek having an increase in tooth number compared to marine populations. Some population genetic metrics identify potential targets of selection within the haplotype while other metrics do not, likely due to the history of the allele in the population as standing genetic variation.

### 4.2 Introduction

**Derived features of the Fishtrap Creek threespine stickleback population**

The stickleback population of Fishtrap Creek, WA is highly derived and as such, represents an opportunity to study the genetics of local adaptation. Like other freshwater fish, the population of Fishtrap Creek is low plated, but it also has experienced a dramatic reduction in gill rakers and a deepening of the body, likely adaptations to the local environment (Hagen & Gilbertson, 1972). The nearby marine population, Little Campbell, conversely has a high number of gill rakers (Hagen, 1967), and due to the geographic proximity and what is known of stickleback freshwater colonization, likely represents an approximation of the founding population of Fishtrap Creek. Following colonization, sticklebacks can evolve a suite of traits for adaptation to their new freshwater environment, including the previously mentioned reduction in plating, but also changes in feeding morphology such as gill raker number, tooth number, and branchial bone length. (Cleves et al., 2014; Ellis et al., 2015; Erickson et al., 2016; McPhail, 1992; Miller et al., 2014; Schluter & McPhail, 1992).

The Fishtrap Creek population has evolved an increase in tooth number relative to marine populations. Previous work has identified *Bmp6* as the likely causative gene underlying the tooth gain (Hart, 2018). Quantitative trait loci mapping (QTL) identified a region on chromosome XXI that explains approximately 30% of variation in tooth number between a low-toothed marine population and a high-toothed Paxton Lake, Benthic population (Cleves et al., 2014). The QTL contains the gene *Bmp6* and allele specific expression data shows a cis-regulated reduction in expression of the gene for the high-toothed chromosome. Further fine mapping identified a haplotype that varies concordantly with the presence or absence of the tooth number QTL, with a set of six sites falling just upstream of a *Bmp6* tooth enhancer (Cleves et al., 2018). Further mapping and sequencing experiments identified a tooth number QTL in the same region and the haplotype in multiple freshwater populations including Fishtrap Creek (Hart, 2018). An evolved increase in tooth number and the presence of the haplotype in the population provides an opportunity to test the hypothesis that natural selection has acted on the haplotype, favoring an increase in tooth number in response to a new environment. I hypothesize the haplotype modifies expression of the *Bmp6* tooth enhancer, with some of the allele specific expression result stemming from the difference in function between the marine/low-tooth associated allele and the freshwater/high-tooth associated allele. The differences in expression may give rise to the

evolved phenotype of increased tooth number. If the haplotype underlies evolved tooth gain that is adaptive, signatures of selection should be detectable surrounding the haplotype.

**Geologic history and human shaping of Fishtrap Creek**

During the last glaciation event, the Fraser Glaciation, the region now containing Fishtrap Creek was covered by the Cordilleran Ice Sheet, stretching south, well past Seattle, Washington (Thorson, 1980). The Puget Lobe of the sheet reached a maximum southern extent and began retreating north approximately 17,000 yr B.P. (Porter & Swanson, 1998). Following the initial retreat of the ice sheet, the region containing now Fishtrap Creek underwent a series of changes. It was initially covered in ice, then submerged under an expanding ocean, and re-covered by the advancing Sumas ice sheets. The region was finally uncovered from both ice and ocean by the early Holocene, approximately 10,000 yr B.P and the Nooksack River likely formed, which Fishtrap Creek feeds (Kovanen et al., 2020). Fishtrap Creek is therefore likely approximately 10,000 years old and no older than approximately 13,000-15,000 years old.

Fishtrap Creek drains approximately 36 square miles, 14.4 square miles in Washington state, with the remaining area in Canada and feeds the Nooksack river just south of Lynden, WA. The watershed has a high percentage of agricultural usage and increases in impermeable surfaces, which have resulted in water quality concerns. A majority of area of the watershed is made up of agricultural crop land (70.5%) and developed surfaces (20.1%). A small percentage of the watershed is farmstead (4.2%) or natural space (5.3%). Upstream of Lynden, WA the creek is considered a 303(d) stream stretch for pH, low dissolved oxygen, bacteria, and temperature, meaning the region is a state listed impaired or threatened water (Whatcom Conservation District, 2020). In addition, within the city and downstream, the creek has elevated levels of organochloride pesticides. The creek has been physically altered as well due to dredging and channelizing. Overall, the creek has experienced changes in water quality, flow, and physical structure in its recent history, which likely has had an effect on the resident stickleback population.

**Selective sweeps and methods for detecting natural selection**

Natural selection can leave "footprints" within the genome that population data can reveal, helping identify regions, genes, or even specific sites involved in adaptation. As an adaptive allele increases in frequency it will carry with it flanking, or "hitchhiking", sites which can eventually "sweep" to fixation (Smith & Haigh, 1974). In a so called selective sweep, if an allele increases in frequency sufficiently quicker than recombination can shuffle the flanking polymorphic sites, certain measurements will show deviation from an expected, neutral model. For example, a reduction in variation or an increase in linkage disequilibrium can occur around a site experiencing strong selection (Nielsen, 2005). Methods just as Tajima's D (Tajima, 1989) summarize the site frequency spectrum and generates a score that can be interpreted as representing different demographic histories. Following the reduction in diversity through the hitchhiking of flanking sites, singleton new mutations arise on the low diversity background which generates a higher than predicted proportion of rare alleles. Tajima's D captures information about the excess or reduction of rare alleles, characteristic of different demographic scenarios and types of selection (Biswas & Akey, 2006).

Selective sweeps can either be "hard" or "soft" based on factors such as the origin of the adaptive allele in the population and the timing of the onset of selection. In a hard sweep, the adaptive alleles coalesce to a single ancestor, typically before the onset of selection and are

usually the result of de novo mutations, while in soft sweeps the adaptive allele is present on multiple genetic backgrounds prior to the onset of selection, for example as standing genetic variation (Messer & Petrov, 2013). In the specific case of Fishtrap Creek and the high-tooth associated haplotype, geographic distribution of the haplotype suggests the haplotype was present as standing genetic variation in the ancestral marine population, and so represents a soft sweep scenario. The history of the adaptive allele determines what metrics are better able to detect the sweep. In a hard sweep there is a dramatic reduction of diversity around the adaptive site with a high frequency of derived alleles and singletons (Fay & Wu, 2000; Kim & Stephan, 2002; Smith & Haigh, 1974). Looking for areas with a reduction of diversity underlies most early tests for selection.

In a soft sweep there are multiple haplotypes at the adaptive locus, meaning there may not be a reduction in the local diversity, therefore approaches such as Tajima's D have limited ability to detect soft sweeps (Innan & Kim, 2004; Przeworski et al., 2005). If there is a reduction of diversity, it will be both narrower, due to more recombination in the history of the adaptive allele, and shallower as there are multiple backgrounds on which the adaptive allele can be (Barrett & Schluter, 2008; Hermisson & Pennings, 2005). Different approaches are better equipped to identify regions underlying soft sweeps, for example, through haplotype based methods (see below) and a focus on linkage disequilibrium.

**Haplotype based methods for detecting natural selection**

Selective sweeps can create stretches of extended haplotype homozygosity. As the adaptive allele increases in frequency it carries with it flanking polymorphisms, creating a region of homozygosity surrounding the adaptive allele, which results in a reduction in haplotype diversity. Extended haplotype homozygosity (EHH) and integrated haplotype score (iHS) are two main tests to detect potential selective sweeps. Starting at a central polymorphic site and proceeding outward, EHH effectively measures the likelihood of randomly selecting two haplotypes that match given the same identity of the central position (Sabeti et al., 2002). Since genome wide EHH would be represented as a series of values across a given window for each position in the genome, making comparisons across the genome is difficult. By integrating the curve generated by both allelic identities at the position and comparing them, the integrated haplotype score (iHS) is able to generate a single value for each position of the genome, allowing researchers to identify statistical outliers (Voight et al., 2006).

One benefit of both tests is the ability to focus on single polymorphisms instead of windows of the genome. As the high-toothed associated haplotype contains a series of SNPs, EHH and iHS allows for the comparison of each site, potentially identifying causative positions, or at least distinguish those that are potentially experiencing selection. Both EHH and iHS have been used to identify adaptive mutations in sticklebacks, specifically alleles of the opsin gene SWS2. EHH showed larger regions of haplotype homozygosity for both identities of the position based on the environment, with the reference allele having a larger footprint in the ancestral dark water lake environment with the alternate having a larger footprint in a transplanted clear water pond environment (Marques et al., 2017).

Another, more recently developed test also uses linkage between sites to identify sites potentially undergoing natural selection. nSL measures haplotypes, extending from individual sites, based on the number of sites, rather than by sequence length, and is therefore more robust to local variation in recombination and mutation rates than either iHS or EHH and can detect both hard and soft sweeps (Ferrer-Admetlla et al., 2014). The method has been used to identify

coding changes associated with adaptation to high elevations in humans (Eichstaedt et al., 2017), pesticide resistance in flies (Schmidt et al., 2017), as well as polymorphisms in enhancers in humans (Moon et al., 2019). The metric's use in sticklebacks has been demonstrated in comparing specie pairs and regions undergoing selection for benthic and limnetic populations (Wang, 2018).

**Ancestral recombination graphs as tools for detecting selection**

Ancestral recombination graphs (ARGs) recreate the ancestry of a population by combining the coalescence and recombination events that have occurred in the evolution of a population (Hejase et al., 2020). In short, using sequence data from multiple individuals, a history can be inferred by coalescing the polymorphisms backwards through time through modeling (Kingman, 1982). Upon this framework, information regarding recombination events can be applied to better explain the final diversity of haplotypes, or combinations of polymorphisms. ARGs can help characterize multiple aspects of the history of a population such as divergence times, effective population sizes, gene flow, and the age of alleles or the potential role of selection on an allele (Hubisz et al., 2019; Rasmussen et al., 2014; Skov et al., 2018). One tool that uses ARGs to estimate the effect of selection on a locus is the program Relate (Speidel et al., 2019). Relate recreates a local genealogy for each SNP in the genome, first creating a distance matrix and then reconstructs ancestral haplotypes from other samples, creating potential "hybrid" or coalesced haplotypes. The timing of events and branch lengths of the genealogies are then estimated. The tool can then ask if a lineage carrying a derived allele diversified and spread faster than a lineage with the ancestral allele, and if so, did the derived allele spread faster than expected under neutral conditions, indicating potential selection. ARGs are an additional tool for detecting selection and use a different framework for identifying loci of interest compared to metrics such as iHS or Tajima's D, therefore potentially being able to detect signals that would otherwise be missed.

**Selection on standing genetic variation**

Marine populations of stickleback act as a reservoir for colonization of freshwater habitats (Bell & Foster, 1994). As such, alleles that underlie adaptation to the freshwater environment likely exist within the ancestral marine population as standing genetic variation, meaning alleles that are present, though not necessarily adaptive, in the ancestral population. Once the allele is introduced into the new environment, selection can act, increasing the frequency. The role of standing genetic variation has been shown in multiple stickleback populations, allowing for rapid adaptation to new environments (Bassham et al., 2018; Erickson et al., 2016; Hohenlohe et al., 2010; Marques et al., 2018). In perhaps one of the most well-known examples of selection on standing variation, the alleles underlying plate loss have been re-used in multiple, independently derived freshwater populations (Colosimo, 2005). Barret & Schluter (2008) outline three ways to distinguish standing genetic variants from de novo mutations: 1) the signature of selection differs between the two, 2) the presence of the allele in an ancestral population, and 3) a phylogeny or inferred history to determine the origin or age of the allele. In the instance of the high-tooth associated haplotype the presence of the allele in multiple independent freshwater populations indicates point #2, the presence in an ancestral population, is likely true.

**Geographic distribution of high-tooth associated haplotype**
Previous work from the lab identified multiple populations in which at least six positions had the high-toothed associated identity within the haplotype (Erickson et al., 2016; Hart, 2018). Polymorphic positions associated with the tooth QTL were first identified in fish from Paxton Lake, Texada Island, British Columbia (Cleves et al., 2018) and further work expanded the populations which contain the haplotype to include another on Texada Island, Priest Lake, (Erickson et al., 2016), Enos Lake on nearby Vancouver Island, and mainland populations in Washington state: Fishtrap Creek, just south of the Canadian border, and Connor Creek on the Olympic peninsula (Hart, 2018).These previously known populations create a triangle in the Pacific Northwest with a total area of approximately 8270 $mi^2$ and the largest distance being between Connor Creek and the Texada Island populations, approximately 180 miles. Previous sequence data of multiple marine populations, Japanese Marine and Rabbit Slough, and Little Campbell, all lack the haplotype, as does the California population of El Cerrito Creek.

**High tooth associated haplotype presence in Little Campbell Marine population**
As the high tooth associated haplotype has been found in multiple, independently derived, freshwater populations, with no obvious means of gene flow between them, the haplotype is likely an example of standing genetic variation. One means of determining if an allele is derived from standing genetic variation is by identifying the allele in the ancestral population (Barrett & Schluter, 2008). While it may not be known what specific ancestral population gave rise to Fishtrap Creek, nearby Little Campbell serves as a reasonable proxy and sequencing these fish can provide insight into the history of the allele.

**Haida Gwaii**
The Haida Gwaii archipelago lies approximately 40 miles of the coast of British Columbia and provides an opportunity to examine the geographical distribution of the haplotype. The archipelago consists of approximately 150 islands with two main islands, Graham Island in the north and Moresby Island in the south. Haida Gwaii contains multiple, isolated stickleback populations, that colonized the chain following the glacial retreat approximately 12,000 years ago (Moodie & Reimchen, 1976) an occupy a diverse range of habitats with different conditions, such as predator regime (Bell & Foster, 1994; Moodie, 1972) and biophysical features (Moodie & Reimchen, 1976). Populations have been found to vary in multiple traits including defensive armor, in the form of pelvic and dorsal spines or lateral plates, gill raker number (Reimchen, 1980; Reimchen et al., 1985; Reimchen & Nosil, 2002, 2004), nuptial color (Moodie, 1972), and sensitivity to different wavelengths of light (Marques et al., 2017). A previous re-sequencing experiment (Marques et al., 2017) created an easily accessible dataset of genomes that may provide information on the geographic distribution of the high-toothed associated haplotype.

## 4.3 Methods

**Resequencing of wild caught marine and freshwater threespine stickleback**
Wild fish were collected from Fish Trap Creek[FTC] (Washington) or the anadromous run of the Little Campbell River [LITC] (British Columbia) under a collection permit from the Washington Department of Fish and Wildlife (permit #08-284) or the British Columbia Ministry of the Environment (permit #SU08-44549). DNA was extracted from caudal or pectoral fins from FTC fish using the Qiagen 96 well DNeasy Blood and Tissue Kit or via phenol chloroform extraction for LITC samples. DNA that was prepared via phenol chloroform extraction was also cleaned via

Zymo Clean and Concentrator column (cat# 11-302C). Concentration of DNA was determined via nanodrop.

The libraries for the FTC samples were prepared with the Nextera DNA Library Prep kit (ref 15028212) and custom dual-matched indexing primers ordered from IDT, to reduce index hopping. The manufacturer's provided protocol was followed, with an input quantity of 50 ng of genomic DNA. Libraries for LITC samples were prepared using the Nextera Library Flex Kit (ref 20018704), again with custom dual-matched indexing primers and following the provided protocol, with an input quantity of approximately 500 ng of genomic DNA.

Sequencing was performed on an Illumina Hiseq 4000 with 150 base paired-end reads on all samples. Fish were pooled, with the aim of obtaining approximately 6x coverage per sample. Four total sequencing runs were performed, two lanes of 20 FTC samples, one lane of 20 LITC samples, and one lane of 16 LITC samples resulting in an average of 16.9 M paired-reads per fish (7.8M to 28M, std 4.5 M). Raw reads were analyzed with FastQC (Andrews, 2010) to determine insert size and adapter content prior to trimming. All fasta files were trimmed using Trimmomatic (Bolger et al., 2014) to remove Nextera adapter sequences if present, creating both paired and unpaired output files containing trimmed reads.

Trimmed reads were aligned to an improved assembly of the stickleback reference genome (Glazer et al., 2015) using bowtie2 v2.1.0 (Langmead & Salzberg, 2012), as paired reads using local alignment and standard settings. After alignment, read groups were assigned using the picard tools AddOrReplaceReadGroups function (http://broadinstitute.github.io/picard). Bam files were sorted using samtools (Li et al., 2009) then duplicates were marked, again by picard tools (MarkDuplicates function). Previously identified indels were used to realign reads using the indel realignment tool (RealignerTarget Creater and Indel Realigner) from the Genome Analysis Toolkit (v 3.8) (McKenna et al., 2010). In addition, previously identified variants were used to recalibrate reads using the Base Quality Score Recalibration tool.

The initial sequencing work identified a third identity of one of the core polymorphic sites in both the marine and freshwater populations. Downstream applications were known to discard tri-allelic sites. In order to retain the position in the data set individuals with the lowest frequency identity were discarded, resulting in 71 individuals retained, 38 from Fishtrap Creek and 33 from Little Campbell, Marine. After realignment and recalibration bam files were fed through Qualimap v2.2.1(Okonechnikov et al., 2015) to determine average coverage and mapping quality. Combining all post-realignment and post-recalibration samples yielded 2,552.7 M reads, with 2,457.4M reads successfully aligned, resulting in a total of 96.3% of all reads aligning. An average of 33.7 M reads were aligned per sample. Overall, the sequencing resulted in an average coverage of approximately 10x. The percent of the genome with at least 6x coverage from each fish was averaged over the entire dataset, resulting in an average of 71% of the genome covered to 6x or greater.

**Variant Calling**

Once reads were processed, variants were called using the GenomeAnalysisToolkit HaplotypeCaller function (heterozygosity=0.0035 and indel_heterozygosity=0.00075, (Feulner et al., 2013; Hohenlohe et al., 2010)) creating intermediate gVCF files for each individual. Joint genotyping was performed with the preceding gVCF files and the GenotypeGVCFs tool to identify all variant positions, including those that are fixed in either population as an alternate allele. Indels and SNPS were split into separate files. After splitting the variants indels and SNPs were filtered (SNPs: QD < 2.0 || MQ < 40.0 || FS > 60.0 || SOR > 3.0 || MQRankSum<-12.5 ||

ReadPosRankSum < -8.0 and Indels: QD < 2.0 || ReadPosRankSum < -20.0 || Inbreeding < -0.8 || FS > 200.0 || SOR > 10.0) following the Broad's recommended hard filtering cutoffs. Next, positions were retained if they contained at least four reads of the alternate allele across all samples using bcftools (Li et al., 2009), and any individual genotype with a depth of less than four were converted to non-calls using vcftools (Danecek et al., 2011).

**Phasing haplotypes**

SNPs were then split into population specific partitions. Any position with more than 50% missing data was removed from further analysis, as were positions with more than two alleles. These steps resulted in 7,120,255 sites in the LITC set and 7,106,123 sites in the FTC data set with a total of 13.0% of genotypes missing in the LITC dataset and 11.5% of genotypes missing in the FTC data set, which were later imputed. Phasing was performed using Shapeit's read aware phasing feature on only bi-allelic SNPs (Delaneau et al., 2013) and within each population on a by chromosome basis, with only female fish in the chromosome XIX data set. Read supported phasing covered 9.5% of heterozygous sites in the FTC set and 11.3% of heterozygous sites in the LITC data set. Missing genotypes were imputed via Shapeit, with 0.54% of genotypes imputed at monomorphic sites in LITC and 0.834% of genotypes imputed at monomorphic sites in FTC. The two data sets were then merged, with missing positions for each population converted to the reference allele using bcftools (Li et al., 2009).

**Testing for population structure**

To characterize potential population structure within the Fishtrap Creek data set phased chromosomes were first converted to plink .bed format and then used with the program ADMIXTURE (Alexander et al., 2009). ADMIXTURE requires an initial number of clusters (K) or potential ancestral populations. By varying K and selecting the value with the lowest cross-validation score, a reasonable estimation of the initial parameter can be identified.

**Scans for selection**

**Window based calculations of genetic diversity and Tajima's D**

Natural selection can leave signatures in the genome surrounding adaptive sites. Nucleotide diversity is predicted to decrease near adaptive alleles that increase in frequency quickly over time, "pulling along" neighboring sites (Smith & Haigh, 1974), affecting the site frequency spectrum as well (Biswas & Akey, 2006). To test the hypothesis the high-tooth associated haplotype has reduced diversity in the surrounding region nucleotide diversity, $\pi$, was calculated for both the Little Campbell and Fishtrap Creek phased data sets using vcftools (Danecek et al., 2011) with 10kb sliding windows and a 2 kb step on each individual chromosome.

Tajima's D (Tajima, 1989) was also calculated across the genome. Following strong directional selection, Tajima's D becomes negative, indicating an excess of rare alleles (Pavlidis & Alachiotis, 2017; Tajima, 1989). Alternatively, a positive score can indicate balancing selection, population structure, or bottlenecks due to an excess of intermediate frequency alleles (Biswas & Akey, 2006). The metric was also calculated using vcftools with 10kb windows. A step function is not available for Tajima's D in vcftools and so was not included.

**EHH, iHS, and nSL calculations for SNPs across the genome**

Selscan (Szpiech & Hernandez, 2014) was used to calculate EHH (Sabeti et al., 2002), iHS (Voight et al., 2006), and nSL (Ferrer-Admetlla et al., 2014). EHH, iHS, and nSL tests were

calculated for FTC samples using phased data, which increases the power of the tests. A previously created genetic map was converted to the new assembly (Glazer et al., 2015) with the genetic positions for each physical position generated using the predictGMAP function (https://github.com/szpiech/predictGMAP). iHS and nSL values were normalized in 1% frequency bins using the provided *norm* program. In addition to iHS and nSL values for individual sites, 20kb bins were created with the proportion of sites within each bin with absolute values greater than the default critical value of the *norm* program, iHS and nSL > 2, which is approximately the 95$^{th}$ quantile for the genome wide average of the dataset for each metric.

**Relate: an Ancestral Recombination Graph (ARG) method for detecting selection**

An alternative method for detecting natural selection centers on ancestral recombination graphs, modeling the evolutionary history of a site and inferring selection based on allele frequencies through time. The program Relate estimates genome wide genealogies and ancestral changes to identify potential areas under selection (Speidel et al., 2019). The program models coalescence and recombination events over time, starting with contemporary genomes and working back to a modeled ancestral genome.

One requirement of the program is knowledge of derived and ancestral states for polymorphic sites. In highly divergent populations, ancestral states for polymorphic sites may be inferred based on the geographic distribution of alleles. Freshwater stickleback populations, in general, are typically thought to be derived from marine colonizers (Bell & Foster, 1994). As the Little Campbell marine population is geographically near Fishtrap Creek, and whole genome sequence data has been collected for dozens of individuals, allele frequencies in Little Campbell was used to infer ancestral vs. derived states for polymorphic sites. As the reference genome for the threespine stickleback assembly is from a derived freshwater population, Bear Paw Lake (Jones et al., 2012), the assumption that reference alleles are ancestral and alternate alleles are derived is not consistent with the natural history of the species.

Whole genome site allele frequencies were calculated for the genotyped and phased Little Campbell data set. In instances were a site had an alternate allele frequency of 75% or greater, the alternate allele was assumed to be the ancestral. If the allele is in high frequency in the current population, it is more likely to have been at a high frequency when the Fishtrap Creek population was established, and therefore, present in the founding population. While the current Little Campbell population is not the original source of the founders for Fishtrap Creek, it is the closest dataset available based on geography and what is known of stickleback colonization. A total of 691,090 sites with alternate allele frequencies of 75% or greater were identified in the Little Campbell data. These sites were then used to create a "Little Campbell reference" genome, in which the alternate identities at each site was overlaid on the Bear Paw Lake reference genome using GATK (McKenna et al., 2010), creating a new genome in which the 691,090 sites had exchanged the reference and alternate allele. The bcftools norm function (Li et al., 2009) was then used to re-align the variants to the new "Little Campbell reference genome". Relate also requires an estimation for the current effective population size ($N_e$). Smc++ was used to infer population size for Fishtrap Creek (Terhorst et al., 2017) and was estimated at approximately $N_e$ = 3000. All phased, Little Campbell reference-realigned, chromosomes were used except for chrXIX. A mutation rate of $6.8x10^{-8}$ was assumed (Roesti et al., 2015).

In order to test the haplotype SNPs for potential signals of selection, the recommended workflow outlined for Relate (https://myersgroup.github.io/relate/index.html) was followed. Phased vcf files were first converted to the haps/sample format. For all steps that required

mutation rates and generation times, an estimated mutation rate of $6.8x10^{-8}$ and generation time of one year were used. To first create marginal trees and position specific information (.anc and .mut files respectively), the genotype and sample information, as well as genetic maps from Glazer et al. (2015) were used for each chromosome with the Relate command. The resulting files are then used to generate a coalescence (.coal) file with the EstimatePopulationSize command (threshold --0). Finally the original .anc and .mut files, along with the .coal file were used with the DetectSelection command. This is a deviation from the workflow outlined in the manual for the program. EstimatePopulationSize outputs new updated .anc and .mut files with revised branch lengths. Sites of interest were lost in the new .anc and .mut files. An alternative is to use the resulting .coal file and the original .anc and .mut files with the DetectSelection command, in which the .coal file is then used to re-estimate branch lengths. Relate's DetectSelection command calculates a $\log_{10}(p)$ value based on the likelihood an allele would reach the current frequency based on neutral processes using on the recombination and coalescence history from previous steps. In addition to a *P* value for potential evidence of selection, the ancestral trees for each position can be generated. The shape of the tree can be informative as adaptive alleles can amplify descending lineages quickly, with rapid branching, while non-adaptive alleles are less likely to have clusters of branching events in close succession (Speidel et al., 2019).

**Identifying the high-tooth haplotype in Haida Gwaii populations**

To identify the haplotype in other populations, a Haida Gwaii dataset was used from Marques (2017). Reads were downloaded from the NCBI Sequence Read Archive, project SRP100209, aligned, filtered, and phased in the same process as above, with phasing performed within a separate Haida Gwaii data set partition. The resulting dataset contained 35 genomes from 27 different populations in addition to 23 genomes from a transplantation experiment, in which 100 fish from Mayer Lake (12 genomes), were transplanted to Roadside Pond (11 genomes). A total of 18 watersheds were represented, with most populations located on the northern Graham Island. Variants within the haplotype were visualized with the program haplostrips (Marnetto & Huerta-Sánchez, 2017).

## 4.4 Results

**Genome wide variation**

When examining genome wide variants population differences were observed. Since the marine and freshwater fish were genotyped as a single data set, there are sites that are polymorphic in one population, but fixed in the other, either as the reference or alternative alleles. Within the marine data set a total of $1.69x10^6$ monomorphic sites were genotyped, either fixed reference or alternate, leaving $5.35x10^6$ sites as polymorphic (76%). While in the freshwater data set only 55.6% of potential variant positions were polymorphic ($3.12x10^6$ monomorphic, $3.91x10^6$ polymorphic).

Within the polymorphic positions there were more singleton SNPs in the Little Campbell set ($1.20x10^6$) compared to the Fishtrap Creek set ($4.75x10^5$) (Table 4.1). The minor allele frequency was calculated for each polymorphic position. Overall, the marine data set consisted of a larger number and proportion of low frequency or rare alleles, while the freshwater population, not only showed fewer total polymorphic sites, but also contained a smaller number and proportion of low frequency alleles (Figure 4.1). For example, in terms of sites with a minor allele frequency of less than 0.1, the marine set had nearly twice as many sites, and the sites

constituted a nearly 20% larger proportion of the total population data set. A larger number of polymorphic sites, as well as a larger number and proportion of low frequency alleles is consistent with previous findings of marine populations of sticklebacks being representing large, diverse populations. Conversely, freshwater populations often experience bottleneck events due to founder's effect, and see a reduction in rare alleles (Jones et al, 2012, Terekhanova et al. 2014). The folded site frequency spectrum across the entire genome is consistent with these two predictions.

| minor allele frequency | Little Campbell/marine | Fishtrap Creek/freshwater |
|---|---|---|
| total variable sites | $5.35 \times 10^6$ | $3.91 \times 10^6$ |
| singletons | $1.20 \times 10^6$ (22.4%) | $4.75 \times 10^5$ (12.1%) |
| less than 10% | $3.15 \times 10^6$ (58.8%) | $1.60 \times 10^6$ (40.9%) |
| less than 25% | $4.33 \times 10^6$ (81.0%) | $2.67 \times 10^6$ (68.1% |
| less than 45% | $5.16 \times 10^6$ (96.4%) | $3.71 \times 10^6$ (94.9%) |

**Table 4.1** Minor allele frequencies of Little Campbell and Fishtrap Creek populations

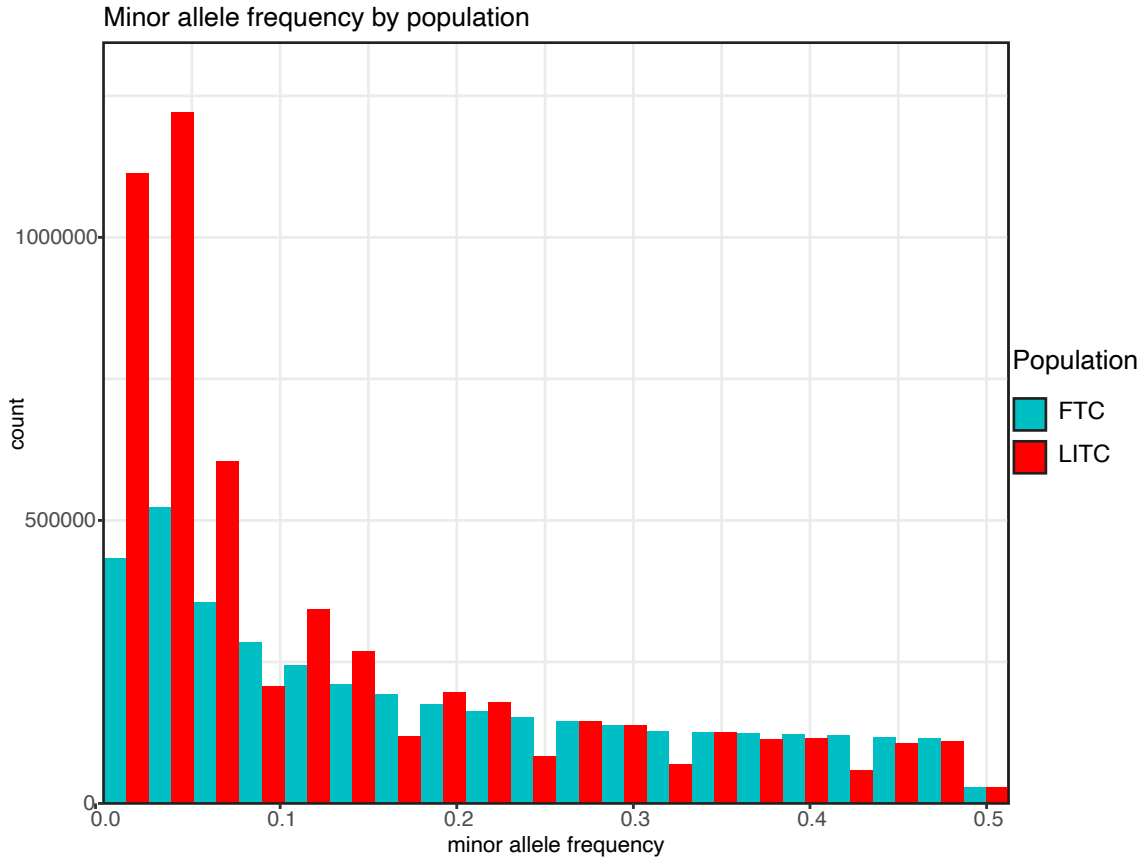


**Figure 4.1 Marine and freshwater populations show differing levels of overall genetic diversity.** Minor allele frequency spectrum of Fishtrap Creek (FTC) and Little Campbell (LITC) show patterns consistent with freshwater and marine populations. The Little Campbell population has a higher number and higher proportion of low frequency alleles compared to Fishtrap Creek.

**High-tooth associated haplotype in Fishtrap Creek**

It was known the high-tooth associated haplotype of intron four of *Bmp6* is segregating in Fishtrap Creek. Previously collected fish were genotyped using a restriction fragment length polymorphism (RFLP) assay and were found to have the following genotype and allele frequencies:

| genotype/allele | count | frequency |
|---|---|---|
| homozygous high-toothed associated haplotype | 11 | 0.46 |
| heterozygous | 11 | 0.46 |
| homozygous low-toothed associated haplotype | 2 | 0.083 |
| high-toothed associated haplotype | 33 | 0.6875 |
| low-toothed associated haplotype | 15 | 0.3125 |

**Table 4.2** Allele and genotype frequencies of the high-tooth associated haplotype in previously genotyped Fishtrap Creek fish

Original genotyping for the initial estimate was performed using primer pairs JCH 115/JCH116 (JCH115: GCCGGCAGCCAAGCGTGAGTTACTGTGTGC/ JCH116: GGAGCAGCCAAATGTAGGAA). A defining SNP within the haplotype creates or destroys an *Ava*II restriction cutsite (GGWCC). Amplicons with the high-toothed associated allele (GGWCT) at the position remain uncut at the site and remain a larger amplicon, while those with the low-toothed associated allele (GGWCC) are able to be cleaved at the *Ava*II site, resulting in the production of smaller fragments. This method was used with primer pairs JCH199 and JCH 200 to identify genotypes of DNA-prepped fish and to select proportions of genotypes representative of previous data to be sequenced.

Six polymorphic positions are used designate the high-tooth associated haplotype, with all six segregating in the Fishtrap Creek population. Recombination has occurred within the haplotype resulting in the haplotype being broken up across its length. Due to the recombination, allele frequency estimates for the entire haplotype from *Ava*II digest do not offer an accurate estimate, as only one position is actually genotyped. Allele frequency was calculated for each position using VCFtools (Danecek et al., 2011) (Table 4.3).

| chromosome | position | alleles | chromosomes (n) | reference | alternate |
|---|---|---|---|---|---|
| chrXXI | 8000155 | 2 | 76 | T:0.460526 | A:0.539474 |
| chrXXI | 8000169 | 2 | 76 | C:0.460526 | T:0.539474 |
| chrXXI | 8000312 | 2 | 76 | G:0.368421 | A:0.631579 |
| chrXXI | 8000538 | 2 | 76 | T:0.368421 | A:0.631579 |
| chrXXI | 8000582 | 2 | 76 | G:0.368421 | T:0.631579 |
| chrXXI | 8000592 | 2 | 76 | A:0.368421 | G:0.631579 |

**Table 4.3** Allele frequency for each position within the haplotype

The tool haplostrips (Marnetto & Huerta-Sánchez, 2017) was used to visualize the haplotype within the population, using the parameters of a minor allele frequency cutoff of 0.02

and sorting method 1 (sorting relative to a reference haplotype). 10kb and 20kb windows were centered at the midpoint of the six polymorphic sites (Figure 4.3 and 4.4). It appears that chromosomes containing the high tooth associated haplotype have less variation compared to those that do not have the haplotype. When drawing a distance tree, the branch length for chromosomes containing the haplotype appear overall reduced, and in some cases, greatly reduced, which would be consistent with a haplotype that increased in frequency rapidly in a population due to natural selection. Clustering of chromosomes, in the 20kb window, suggests there are multiple alleles of the high tooth associated haplotype in the population, as seen by high frequency polymorphisms that are common across some but not all chromosomes with the haplotype, for example, at positions 7991543, 7992273, 7992338, 7997093, and 7997503. While recombination can create multiple alleles of the same haplotype, the variation across chromosomes with the haplotype would also support multiple ancestral chromosomes with the high tooth associated allele, consistent with the model in which the haplotype was present as standing variation in the ancestral population, with multiple genetic backgrounds (Barrett & Schluter, 2008; Hermisson & Pennings, 2005).

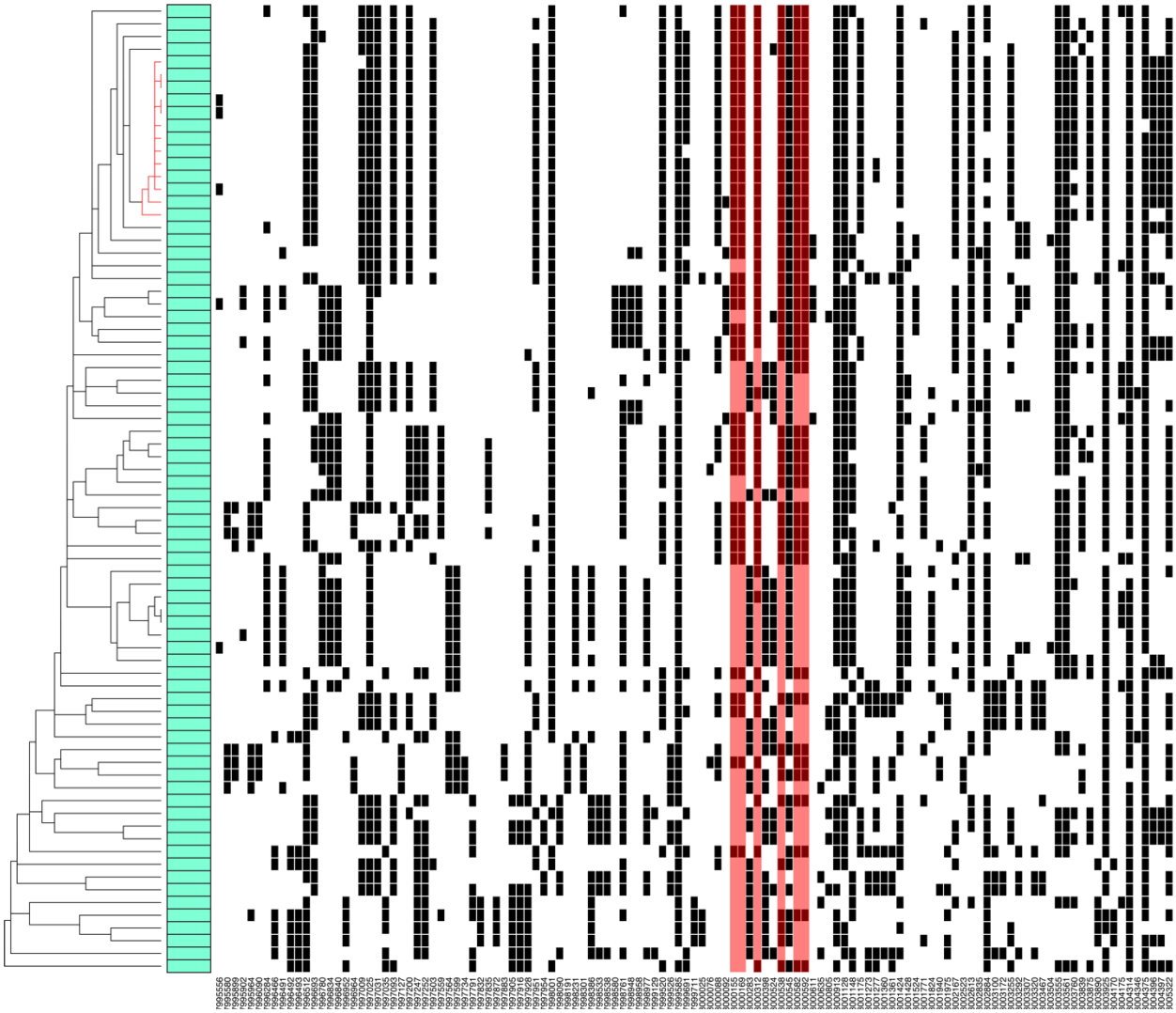

**Figure 4.2 Chromosomes contained within the Fishtrap Creek population show differing patterns of nearby variation relative to the high tooth or non-high tooth associated haplotype.** 10kb of each sequenced chromosome is represented by a horizontal line, centered on the haplotype on chromosome XXI. Columns represent polymorphic sites, with black rectangles representing the alternate allele, while white rectangles represent the reference allele. The six haplotype defining positions are highlighted by red columns. Branch length on the left is proportional to sequence distance between haplotypes. Chromosomes with the haplotype tend to cluster together, with very short branch length for some subclusters (red branches), indicating a high degree of similarity, especially in comparison to branch length for non-haplotype containing chromosomes.

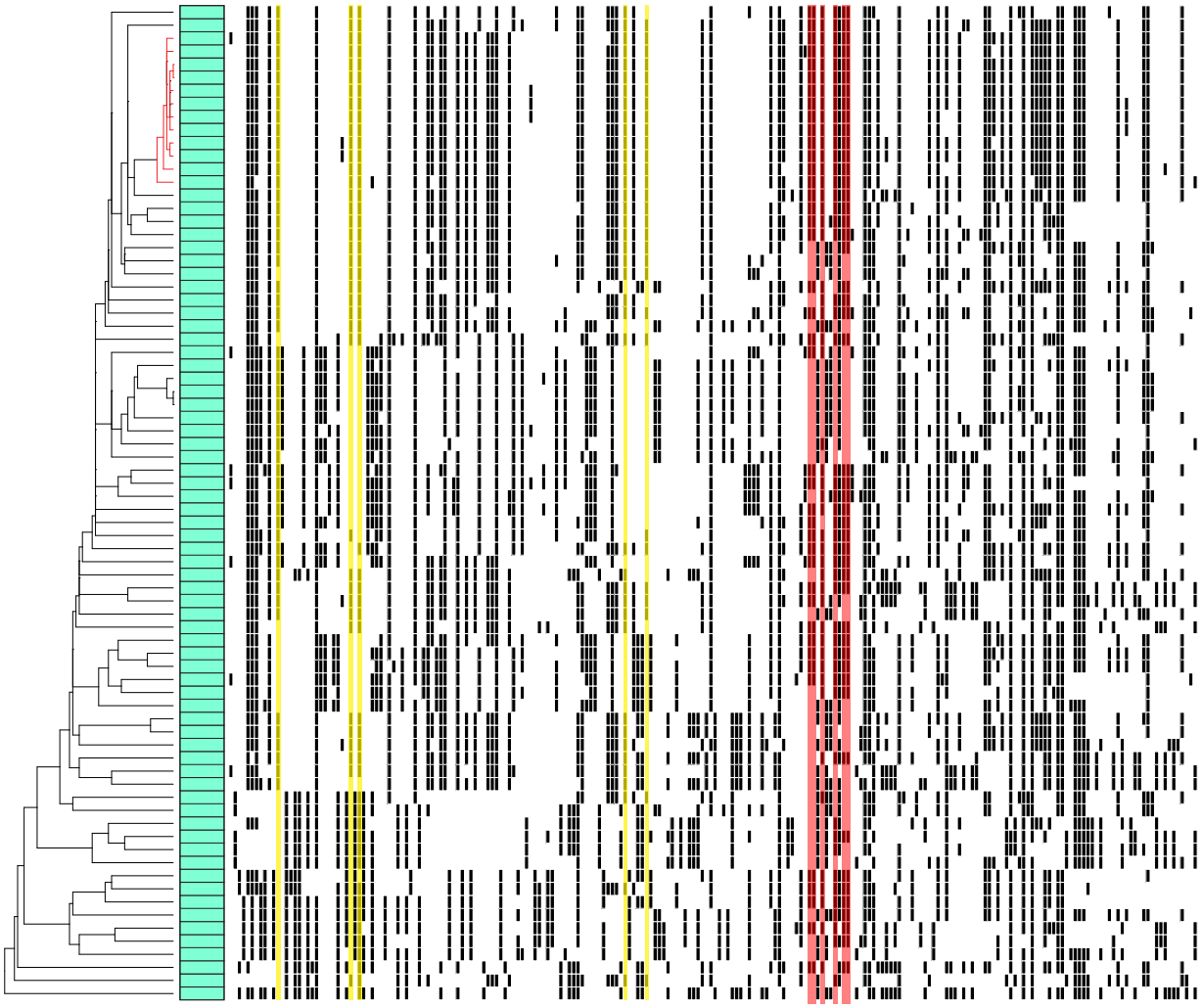

**Figure 4.3 20kb window of chromosome XXI in Fishtrap Creek continues to show clustering of chromosomes with the high tooth associated haplotypes.** The reduction polymorphisms surrounding the haplotype also persists in the chromosomes with the high tooth haplotype compared to chromosomes without. Yellow highlights label positions that are common for some chromosomes with the haplotype but missing in others, suggesting multiple ancestral chromosomes in the founding population.

**No observed population structure in Fishtrap Creek**

Following recommendations within the ADMIXTURE manual, the initial cluster number, K, was varied and the program was run with K=1 to K=5. CV scores were extracted for each run (Table 4.4). Overall the K value with the lowest CV score was K=1. This result indicates there is likely no population structure within the Fishtrap Creek data set.

| K value | CV error score |
|---|---|
| 1 | 0.57045 |
| 2 | 0.62775 |
| 3 | 0.72606 |
| 4 | 0.84882 |
| 5 | 0.96858 |

**Table 4.4** K values and resulting CV error scores from the program ADMIXTURE for Fishtrap Creek

**Genetic diversity and Tajima's D genome wide and around intron 4 of *Bmp6***

Genome wide calculations for genetic diversity, π, and Tajima's D (Figure 4.4A,B) were performed on Little Campbell and Fishtrap Creek phased data. Consistent with a previous observation that the marine data set had more low frequency and rare alleles, the genome wide level of genetic diversity was greater in Little Campbell (mean $\pi = 0.00242$) than Fishtrap Creek (mean $\pi = 0.00239$). While the difference in genetic diversity is expected as it is seen in other marine and freshwater population pairs, the magnitude is less than expected (Jones et al., 2012). Within the window which contains the haplotype, there appears to be little difference between the populations, however just upstream of *Bmp6* there is greater diversity in Fishtrap Creek (Figure 4.4C).

Tajima's D was also calculated across the entire genome, with a specific focus on the fourth intron of *Bmp6*. The genome wide average for Little Campbell, -0.371, could indicate population expansion. However, while the score is negative, indicating the excess of rare alleles, it is of relatively small magnitude and so may not be as meaningful as if it was a larger magnitude. Fishtrap Creek has a positive genome wide average Tajima's D score, 0.709, which indicates a reduction of rare alleles, which could result from a bottleneck event or balancing selection (Biswas & Akey, 2006). The window which contains the haplotype is consistent with genome wide scores (Figure 4.4D), a negative value in Little Campbell, -0.719, and positive in Fishtrap Creek, 0.639. Overall, the nucleotide diversity and Tajima's D scores for the region containing the haplotype do not indicate selection having occurred in the region. Either a decrease in diversity or a relatively large negative Tajima's D score (~ -2) would have indicated selection, which were not observed in the Fishtrap Creek data. These two metrics are typically not able to detect soft or incomplete sweeps, in which the adaptive allele exists on multiple backgrounds, or has not reached fixation. As the haplotype in Fishtrap Creek is not fixed, and likely entered the population as standing genetic variation, on multiple chromosomal backgrounds, there would need to be strong selection on the haplotype for it to be detected through these metrics.

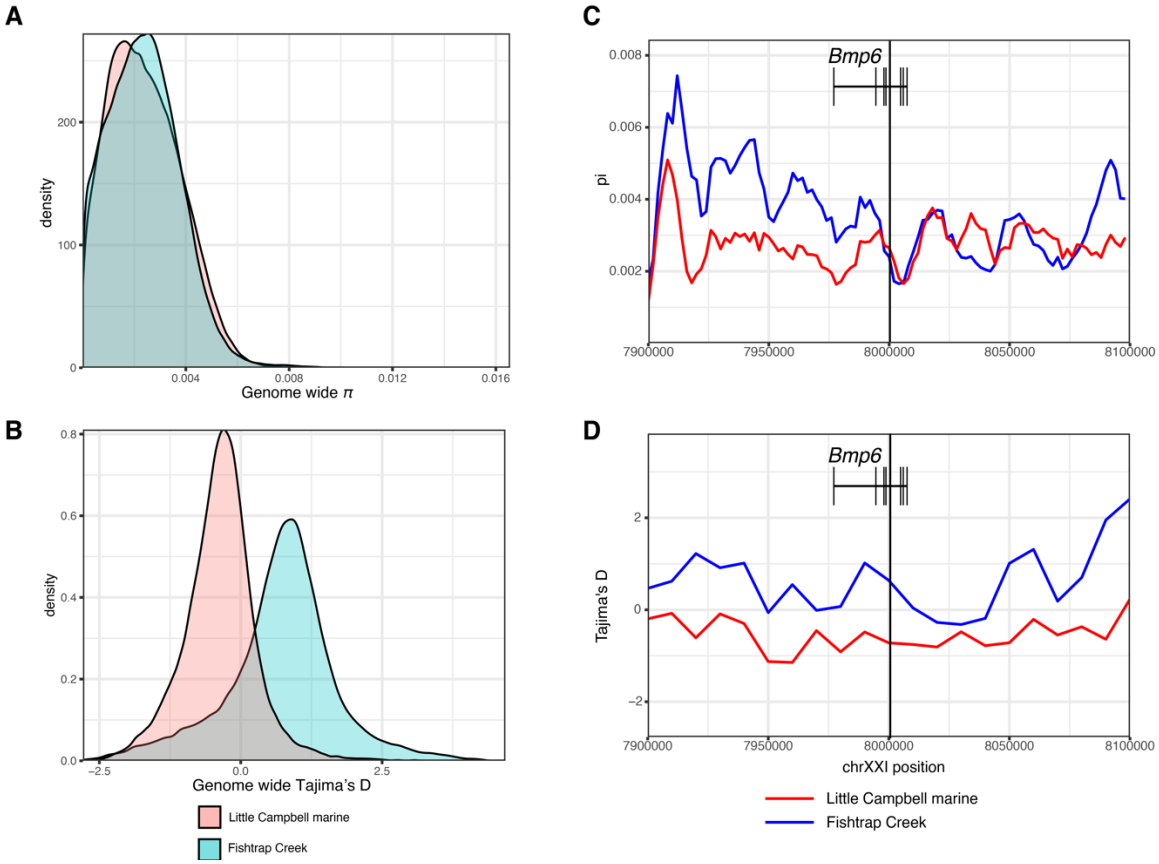


**Figure 4.4 Population specific differences exist in nucleotide diversity and Tajima's D. (A)** A density plot of sliding windows of genetic diversity calculations along the genome show the Little Campbell marine population has a slightly higher overall genetic diversity compared to Fishtrap Creek. **(B)** A genome wide calculation of Tajima's D also showed population specific differences, with Little Campbell having an average of -0.719 while Fishtrap Creek had a higher, positive average of 0.639. **(C)** Inspection of the area surrounding *Bmp6* does not show a reduction in diversity in the Fishtrap Creek population, as would be expected if the haplotype is experiencing strong selection. **(D)** Tajima's D calculations in the same region also indicate a lack of strong selection, which would be illustrated by large, negative scores for Fishtrap Creek.

## EHH for SNPs within the haplotype

Examining the six haplotype associated positions within the Fishtrap Creek dataset revealed differences in both EHH shape and iHS values. The EHH pattern of the first three positions, chrXXI: 8000155, 8000169, 8000312, showed a wider footprint of haplotype homozygosity for the high-tooth associated allele at each position compared to the reference allele or low-tooth associated allele (FIGURE 4.5). Alternatively, the last three positions, chrXXI:8000538, 8000582, 8000592, either had similar patterns for each allele, or had wider patterns of homozygosity for the low-tooth associated allele. The results suggest that in the first three positions, selection may have favored the high-tooth associated allele, while in last three were not favored by selection, indicating what positions of the haplotype may underlie the evolved tooth gain. The EHH results are consistent with the model in which the SNP at position 8000169, which creates an NFATc1 site in the high tooth associated allele, is at least partially responsible

for the QTL signal, and therefore, evolved tooth gain. Position 8000155 is in near perfect LD with position 8000169 and the similar EHH graphs are consistent with the observation.

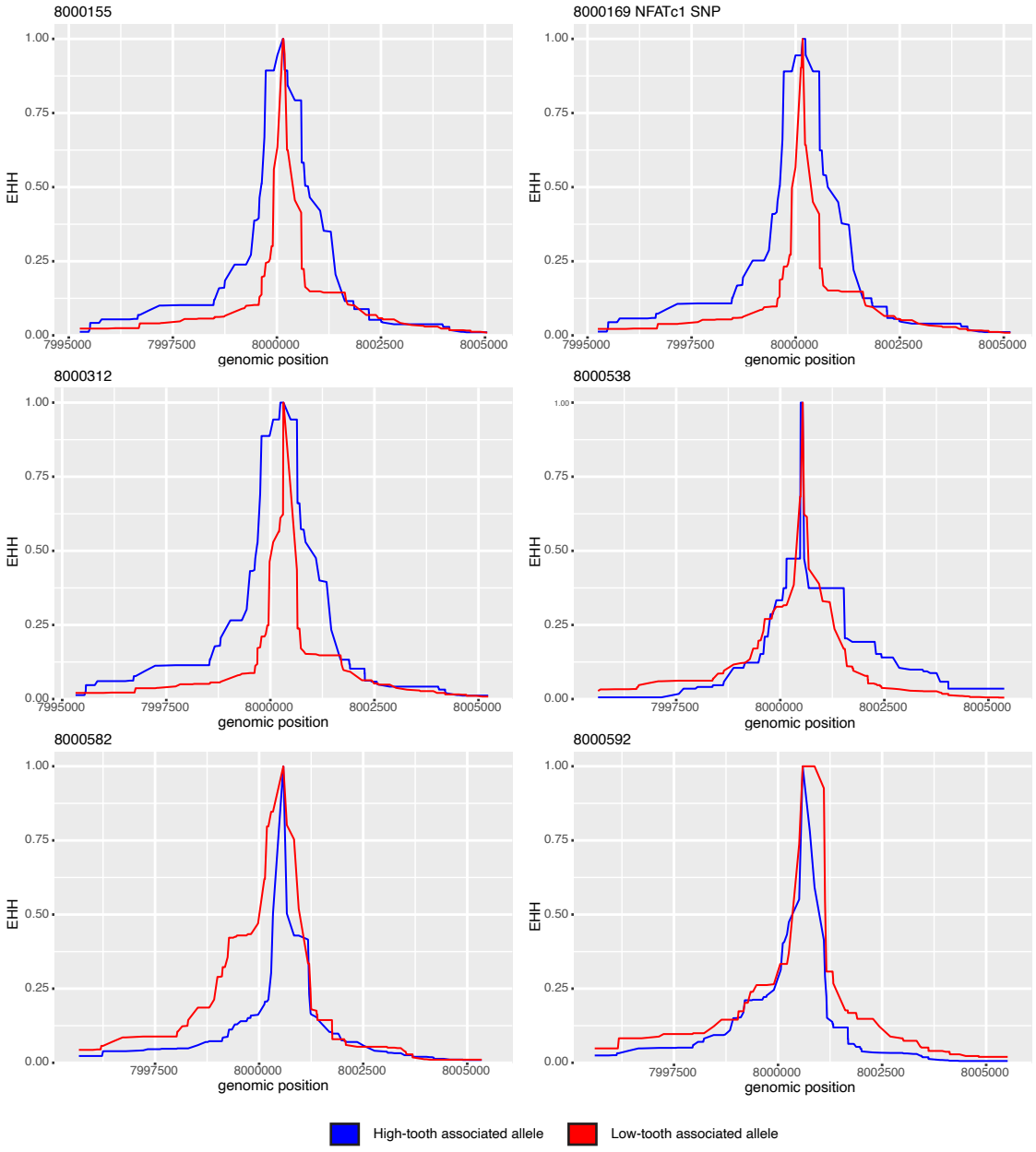


**Figure 4.5 Extended haplotype homozygosity (EHH) graphs for each of the six haplotype defining sites.** For positions chrXXI:8000155, 8000169, and 8000312 the high tooth associated allele (blue) had a wider stretch of haplotype homozygosity compared to the reference allele (red). For positions 8000538, 8000582, and 8000592, the high tooth allele no longer had a wider footprint than the reference allele.

### iHS and nSL scores surrounding *Bmp6* and within the intron

While iHS and nSL scores are calculated on a site by site basis, general patterns can be identified through binning sites. 20kb windows were created with the proportion of sites exceeding a

critical value of 2 for |iHS| or |nSL|. The proportion was normalized across the genome by number of polymorphic sites within each window. Overall, the window that contains the haplotype (8000000-8002000) does have a slightly elevated proportion of sites exceeding the critical threshold for both statistics (~20%), but is not a genome wide outlier (Figure 4.6A). When plotting individual site scores it is revealed all sites with iHS or nSL scores exceeding a value of 2 are further downstream than the six haplotype defining positions (Figure 4.6B). Overall the six haplotype defining positions are not genome-wide outliers nor elevated compared to surrounding sites.

As expected from the EHH results, the SNPs within the haplotype did not all share |iHS| scores. The first two positions, chrXXI:8000155 and 8000169, had identical scores (0.794224) and had a higher score than the other four positions (Figure 4.6 B&C). However, the two higher scores were still relatively low compared to the rest of the genome, falling within the 59.4% percentile. Interestingly, there are two positions within the haplotype that have higher scores than any position within the haplotype, chrXXI:8000283 and 8000398. iHS scores can either be positive or negative, with a negative score indicating the reference allele has a larger average haplotype compared to the alternate allele. At positions 8000283 and 8000398, the reference allele appears to be linked to the high-tooth associated identities (alternate alleles) at the haplotype defining positions (Figure 4.3), suggesting a connection between the negative iHS scores at these two inner positions and the positive scores at the haplotype defining positions.

When using the |nSL| metric, a similar pattern is observed, with the 8000155 and 8000169 having scores of 0.8996 and 0.8999 respectively. Similar to the iHS scores, while positions 8000155 and 8000169 have scores higher than the rest of the haplotype (Figure 4.6 B&C), they are low compared to the rest of the variants scored, falling in the 63.4% percentile. Positions chrXXI: 8000283 and 8000398 also have higher scores than any position in the haplotype, but the same explanation for the elevated iHS scores can be applied for the position's nSL scores as well. Overall, none of the six positions within the haplotype appear elevated using iHS or nSL metrics, which have been shown to be sensitive to soft sweeps. However, if the strength of selection is low enough, the haplotype may not be remarkable compared to other sites within the genome. Also, as the haplotype was present as standing genetic variation in ancestral marine populations, it likely has multiple chromosomal backgrounds and so has greater variation flanking the haplotype and is difficult to detect with these methods which rely on stretches of linkage disequilibrium.

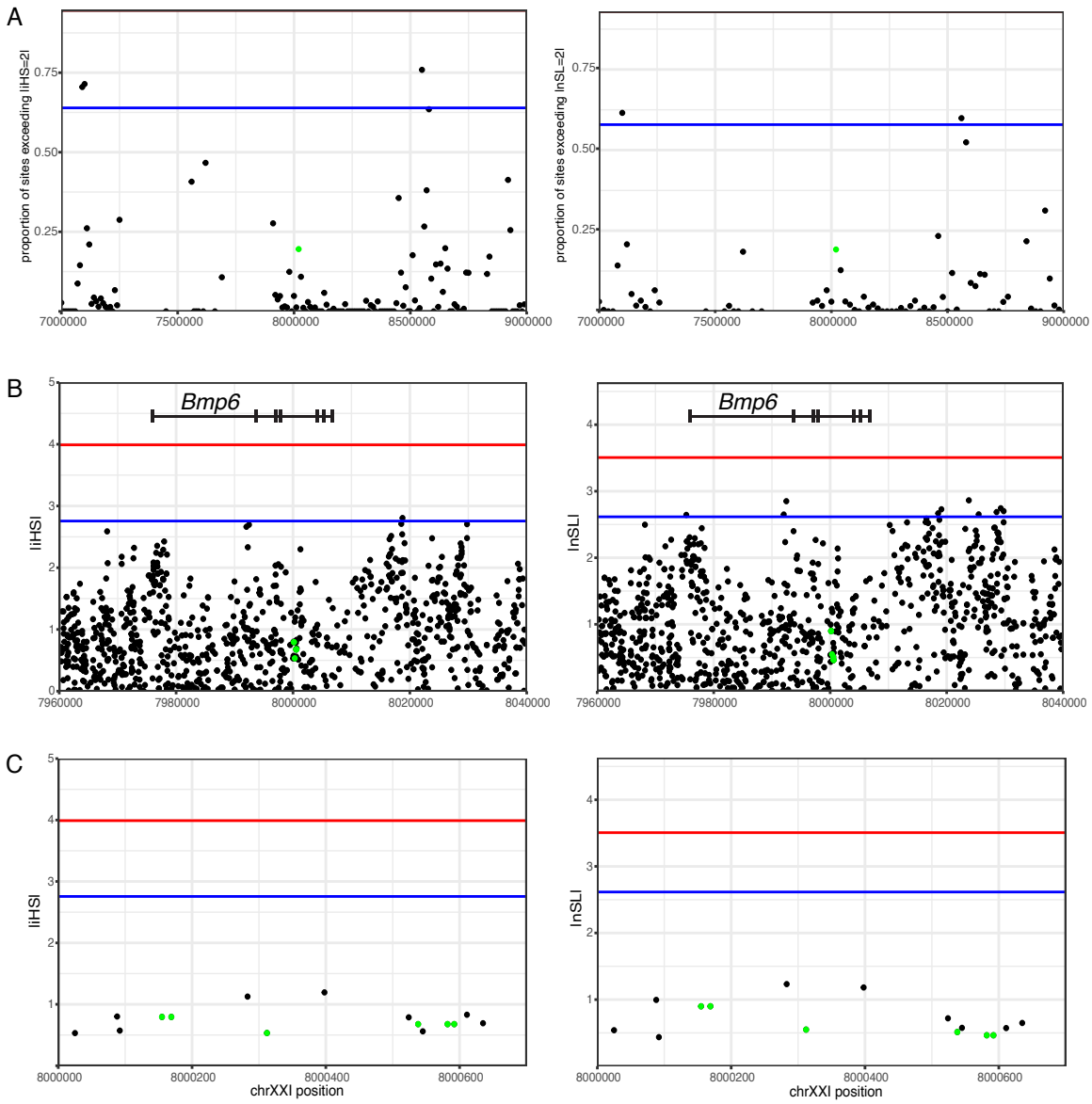


**Figure 4.6 iHS and nSL values in the haplotype show differences across positions. (A)** Calculating iHS and nSL in 20kb, normalized windows results in approximately 20% of sites within the haplotype containing window having scores higher than the a critical score of iHS or nSL of 2 (approximately 95$^{th}$ percentile for both). **(B)** Calculating the absolute value of the scores for individual sites revealed the positions exceeding the critical score are in the second half of the 8000000-8002000 window and are not the haplotype defining positions. **(C)** The first two positions of the haplotype have higher scores than any of the other four, while two positions within the haplotype span have still higher iHS and nSL scores. As the plotted scores are the absolute values, the high iHS scores for positions 8000283 and 8000398 are the result of, compared to the surrounding sites, relatively large negative scores. Haplotype defining SNPs highlighted in green. Blue line is the 99$^{th}$ percentile and red line is the 99.9$^{th}$ percentile for the genome for each statistic.

**Multiple hypothesis testing correction for Relate DetectSelection**

Relate's DetectSelection tool generates *P* values, as -log(*p*) scores, for evidence of selection at each position, based on the SNP's frequency and number of lineages through time compared to the contemporary dataset. In short, the tool asks whether neutral processes can account for changes in frequency and lineages over time, if lineages with the derived allele increased more quickly than lineages with the ancestral allele. Relate evidence of selection *P* values were calculated for every SNP within the genome except for those on chromosome XIX. Sites with derived allele frequencies that never increased to higher than 2 are assigned a $-\log_{10}(p)$ value of 1 and were removed. In addition, other sites were lost, such as chrXXI:8000312, due to default filtering criteria. A total of 3,145,454 sites were retained with 2,597,132 sites remaining after removing those with a $-\log_{10}(p)$ value of 1. As the program tests each individual SNP that passes through a filtering process, an incredibly large number of *P* values is generated. A density plot of the initial -log(*p*) scores (Figure 4.7A) shows a large proportion of sites, ~22.9%, having a score of less than -1.3, which translates to a *P* value of 0.05. This suggests a possible overestimation of significance for all sites. A Q-Q plot for the raw *P* values was generated using the qqman R library (D. Turner, 2018) (Figure 4.7B). As the observed *P* values deviated from expected rather dramatically, *P* value adjustments for multiple hypothesis testing was performed. Both Bonferonni and Benjamini-Hochberg (Benjamini & Hochberg, 1995) corrections were performed using the R function p.adjust and Q-Q plots of both adjusted sets of *P* values still showed elevated scores relative to expected values (Figure 4.7B). The Benjamini-Hochberg method yielded a plot with a smaller slope of observed vs. expected when compared to the Bonferonni graph or raw *P* value graph. In addition, a smaller portion of sites, 7.8%, had scores less than -1.3, closer to the expected 5%. For subsequent analysis the Benjamini-Hochberg adjusted *P* values were used but it should be noted the *P* values are likely still overestimates of the signal of selection and conclusions should be interpreted with that in mind.

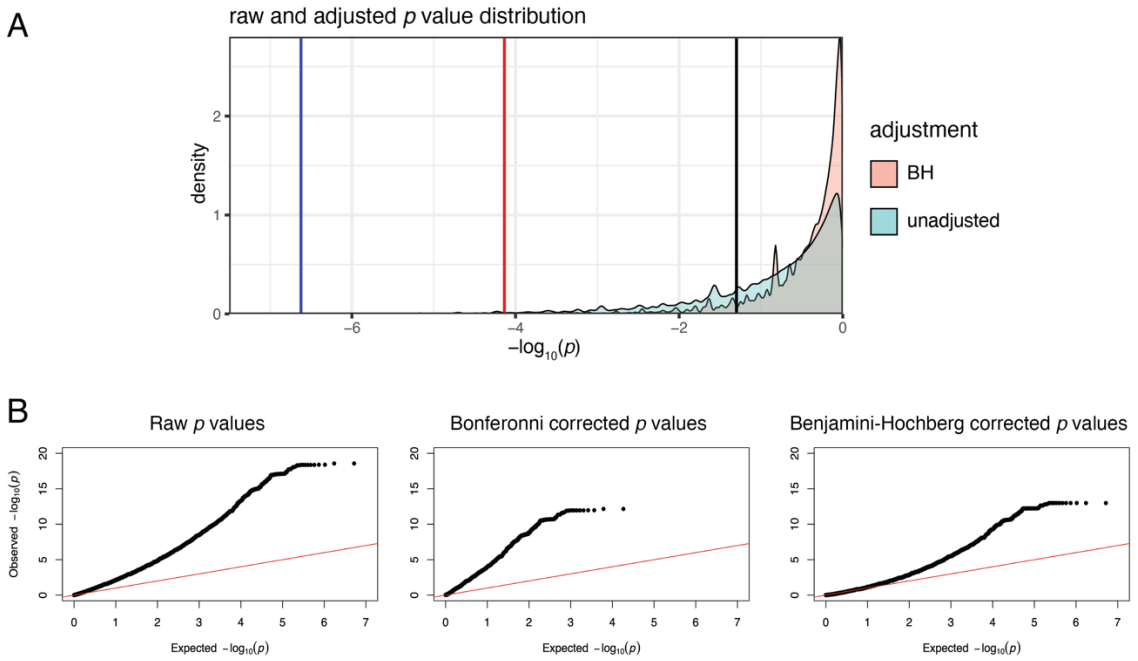


**Figure 4.7 Distribution of *P* values suggests an overestimation of selection.** A density plot of unadjusted *P* values and Benjamini-Hochberg (BH) adjusted *P* values (**A**) have similar distributions, however the unadjusted *P* value set has a larger proportion of values less than the significance threshold (-1.3, $P = 0.5$, black line) compared to the adjusted values. In both data sets the chrXXI:8000169 NFATc1 SNP are outliers (red line: BH adjusted value, blue line: unadjusted *P* value). Q-Q plots (**B**) show higher than expected $-\log_{10}(p)$ values for unadjusted scores, Bonferonni corrected scores, and Benjamini-Hochberg corrected scores. A slope of 1 (red line) represents complete agreement between observed and expected values.

**Elevated Relate *p* values for the haplotype defining positions within intron 4**

Benjamini-Hochberg corrected *p* values within the haplotype exhibit similar patterns to the values calculated using iHS and nSL. Both chrXXI:8000155 and chrXXI:8000169 had high $-\log_{10}(p)$ values (-4.137), while the downstream most sites, chrXXI:8000582 and chrXXI:8000592 had lower scores (-1.638), and chrXXI:8000538 had the lowest of the haplotype defining positions (-0.957) and did not reach a significant *P* value (Figure 4.8A). The differing scores by position suggests that each position has experienced different strengths of selection or ancestral events. The marginal tree for positions chrXXI:8000155/8000169 shows a rapid spreading of the derived allele in relatively recent generations as does the tree for chrXXI:8000582/8000592, but to a somewhat lesser degree (Figure 4.8B). Other sites near the haplotype can have less dramatic marginal trees, despite being at similar frequencies to the high-tooth associated alleles and being nearby (Figure 4.10). Position chrXXI:8000538 shows a less rapid increase in frequency as well. The markedly different projected histories of the sites within the haplotype, differing nSL, iHS, and Relate scores, and presence of multiple partial haplotypes within the wild population suggests a history in which the sites have been separated and experienced selection independently, resulting in the differing signals for each site.

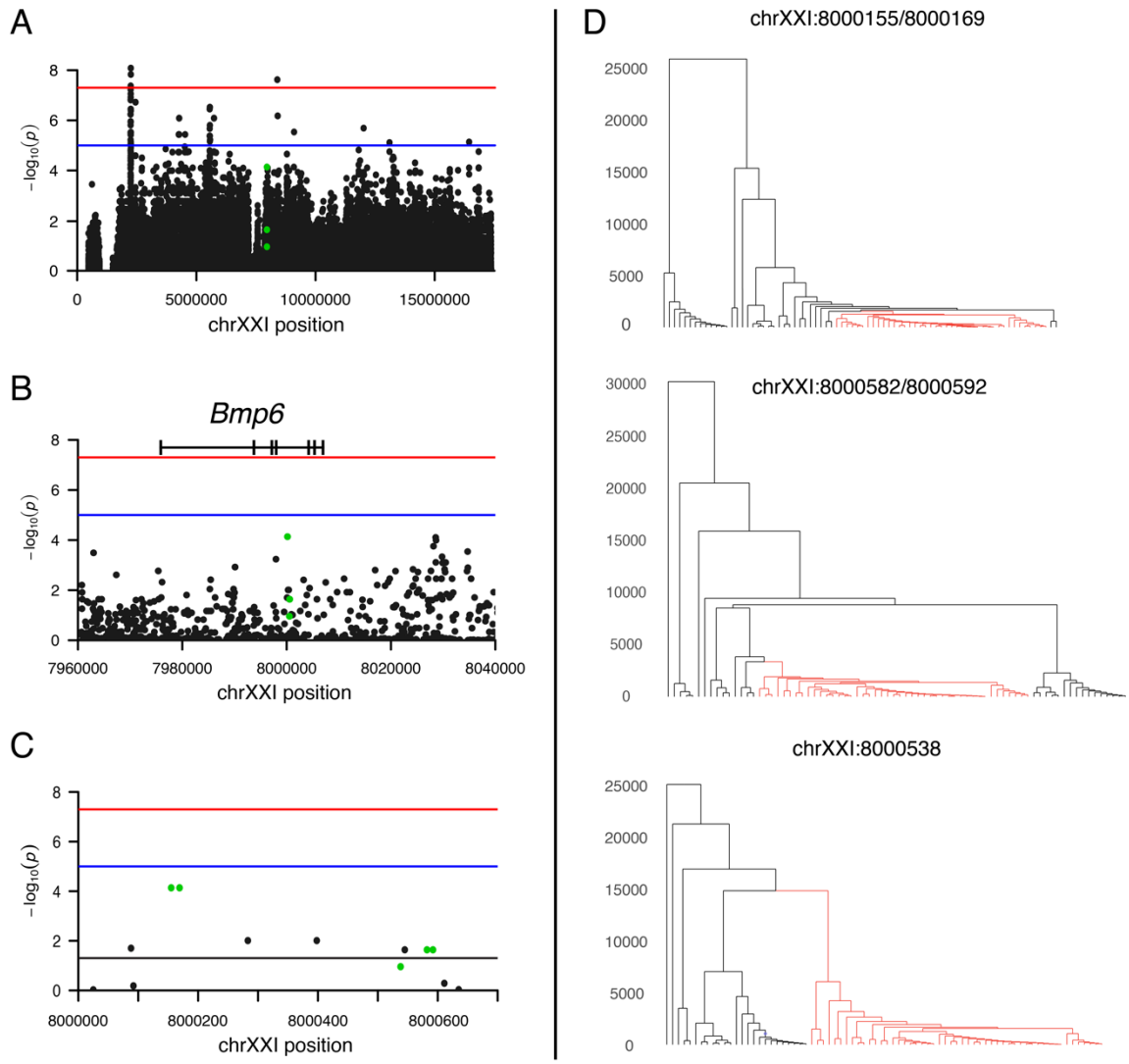


**Figure 4.8 Positions within the haplotypes differ in their Relate Evidence of Selection *P* scores and shape of marginal trees.** The sites within the haplotype are elevated compared to most other sites along the chromosome **(A)** and are high for their local region as well **(B)**, with four sites exceeding the significance threshold **(C)** and the first two, containing the NFATc1 site, having the highest scores of the haplotype. **(D)** The shapes of the marginal trees are consistent with alleles that have spread rapidly over time, with both the 8000155/8000169 and 8000582/8000592 pairs having a more recent, rapid spread than 8000538, suggesting those positions may play key roles in the haplotype-containing enhancer's evolution.

## Elevated iHS, nSL, and Relate scores downstream of *Bmp6* are contained within a previously identified branchial bone length QTL

A 1MB window centered on the fourth intron of *Bmp6* revealed a peak in the iHS, nSL, and Relate evidence of selection data sets further downstream (Figure 4.9). Expanding upon the peak identified a series of sites that have elevated scores. Nine positions over approximately 5.5kb have values above the 99$^{th}$ percentile for iHS (Figure 4.9A) and 12 positions over a 3.5kb span have scores above the 99$^{th}$ percentile for nSL values, with one site surpassing the 99.9$^{th}$

percentile (Figure 4.9B). The *P* value adjusted scores from Relate for 18 positions have values exceeding the 99$^{th}$ percentile over an approximately 40 kb span (chrXXI:8433610 to chrXXI:8473482), while there are four that exceed the 99.9$^{th}$ percentile over a 16kb span (chrXXI: 8433738 to chrXXI:8450234) (Figure 4.9C). The region corresponds to a bone length QTL previously identified in both a Paxton benthic and Fishtrap Creek cross (Erickson et al, 2014, Erickson et al., 2018). The QTL region in the Paxton benthic cross spans approximately 155kb, from chrXXI:8344512 to 8500043, and contained the genes *Tfap2a, Tmem14b, Mak, Plcxd2, Phldb2, Tmem56, ENSGACG00000002373,* and *Bco1*. Gene expression data as well as knockouts of the gene support *Tfap2a* as the candidate underlying the bone length QTL. Knockouts resulted in severe craniofacial malformations and defects and as with *Bmp6*, allele specific expression was observed between marine and freshwater populations. The highest scoring positions for each test are not at the same site but fall within less than 15kb of each other (chrXXI:8447569 for nSL, chrXXI:8448301 for iHS, chrXXI:8433738 for Relate). The highest iHS site is also the second highest nSL site, has an elevated Relate adjusted *P* value (*P* = 6e -4, -$\log_{10}(P)$= -3.22), and a marginal tree shape that suggests rapid spread (Figure 4.10). None of the highest value sites fall within the *Tfap2a* gene or highly conserved sequence but each are either contained within introns of the predicted gene *Phldb2* (nSL and iHS) or is intergenic (Relate). Two sites tie for the second highest scoring rank for the Relate test, and are within 2kb of the nSL and iHS outliers (chrXXI:8450230 and 8450234). The observation the high scores fall within non-coding sequence suggests a hypothesis in which the some of the high scoring sites may reside within an enhancer of the gene *Tfap2a* and could underlie the allele specific expression result.

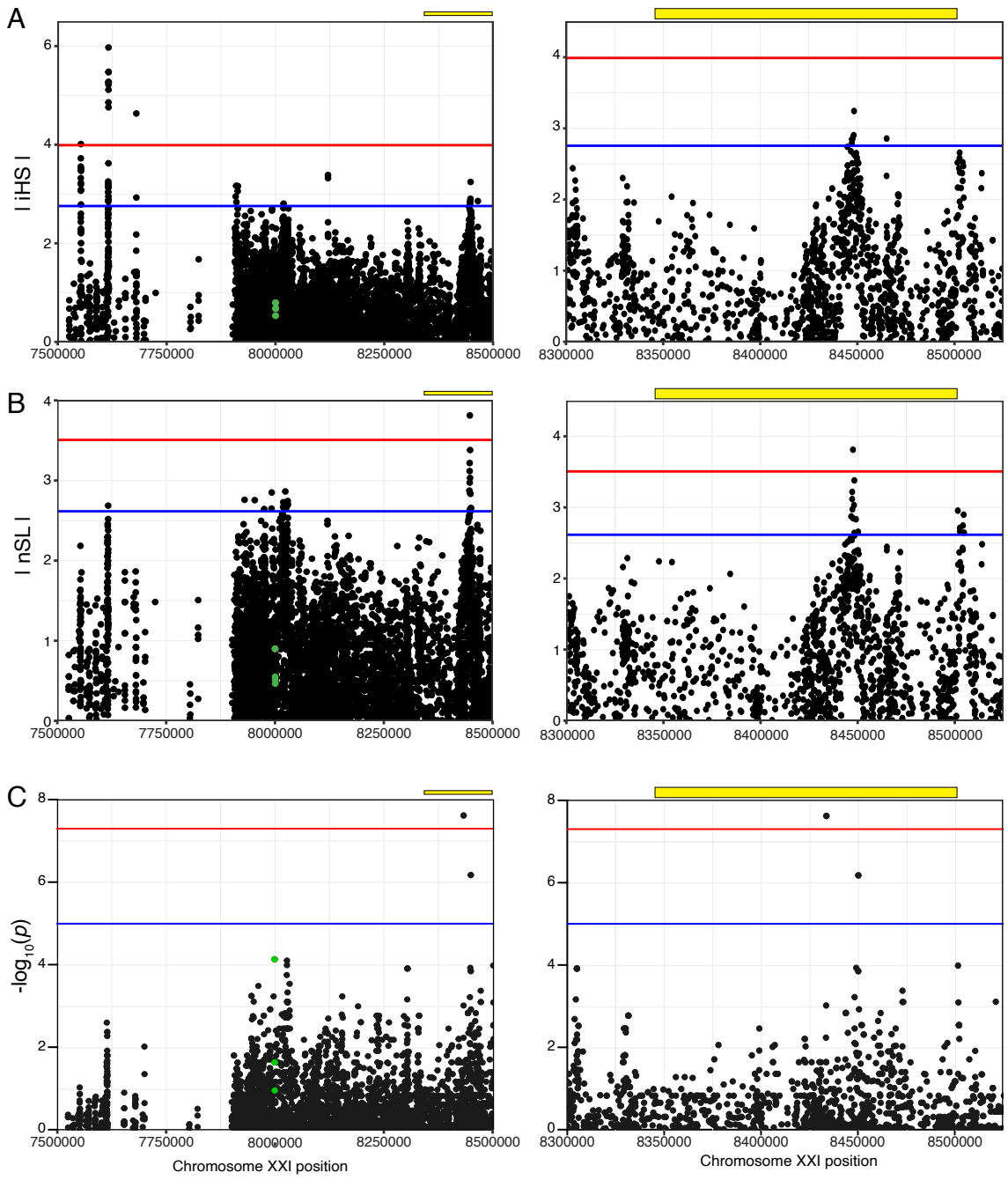


**Figure 4.9 Elevated scores for three metrics fall within a previously identified bone length QTL window.** Approximately 0.5mb downstream of the haplotype defining positions (green points, elevated iHS **(A)**, nSL **(B)**, and Relate's DetectSelection *P* value **(C)** scores fall within a previously identified QTL window for branchial bone length (yellow bar). In both iHS **(A)** and nSL **(B)** multiple sites have scores higher than the 99$^{th}$ percentile (blue line), while in the nSL scores, points approach and surpass the 99.9$^{th}$ percentile (red line). **(C)** The *P* values generated by Relate contains a small number of points exceeding $1x10^{-5}$ (blue line, 5) and $5x10^{-8}$ (red line, 7.3) in significance.

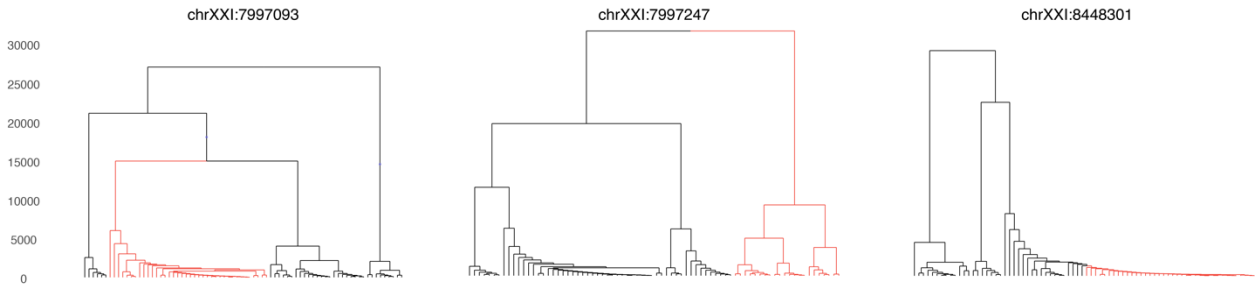


**Figure 4.10 Marginal trees for a site near the haplotype and within a branchial bone length QTL window display differing patterns.** Positions chrXXI:7997093 and chrXXI:7997247 are both near the haplotype defining sites and both have intermediate derived allele frequencies, similar to the haplotype defining sites. The sites do not appear closely linked with the high-tooth associated allele and so likely represent older mutations. The marginal trees for the sites show an older initial introduction (7997093 and 7997247) or a more gradual spread (7997247), unlike chrXXI:8000169 or 8000592. ChrXXI:844830 shows a rapid spread of the derived allele, consistent with an adaptive site and the elevated iHS and nSL scores. Lineages carrying the ancestral allele in black and derived allele in red.

**Geographic distribution of the high-tooth associated haplotype**

After combining fish previously sequenced by the Miller lab and aligning, calling variants, and phasing sequencing data from freshwater stickleback populations on Haida Gwaii, the high-tooth associated haplotype was found in multiple populations in the Pacific Northwest (Figure 4.11A). The allele had previously been identified in Paxton Lake (Canada), Enos Lake (Canada), Priest Lake (Canada), Connor Creek (WA), and Fishtrap Creek (WA). Within the Haida Gwaii archipelago, the six SNP allele was found in Mayer, Rouge, Serendipity, and Solstice Lakes. Recombinants were also identified in Silver, Spence, and Woodpile Lakes. The populations that contain the allele in Haida Gwaii are contained in multiple watersheds (FIGURE 4.11B), which limits the potential for gene flow between the populations, and supports the hypothesis the haplotype was present in the fish that independently colonized the lakes. Incorporation of the Haida Gwaii populations greatly expanded the geographic distribution of the allele and the number of populations in which it is contained.

Sequencing of 36 Little Campbell fish revealed a single chromosome which contained the high-tooth associated haplotype (Figure 4.12). If the 36 genomes are representative of the population as a whole, the haplotype is segregating within the Little Campbell marine population at a frequency of approximately 1.4%. Similar to results from Fishtrap Creek, a recombinant chromosome was also identified, containing the last four SNPs of the haplotype. The observation that the allele is present in a marine population within the Pacific Northwest, near multiple freshwater populations in which the allele is found, supports the hypothesis the allele was present as standing genetic variation in the marine fish that founded the individual freshwater populations.

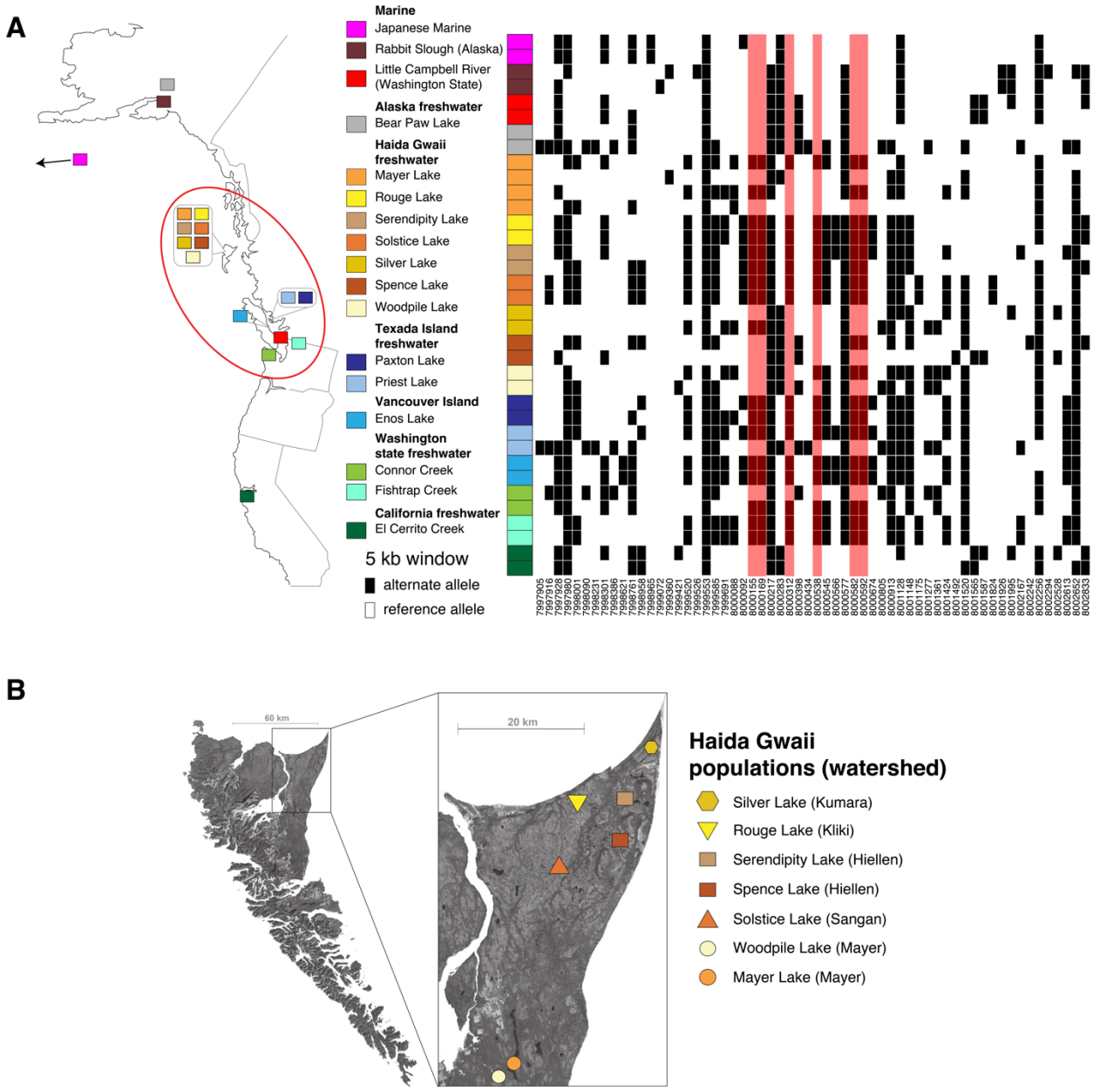


**Figure 4.11 Geographic distribution of the high-tooth associated haplotype in the Pacific Northwest reveals an expanded range. (A)** The high-tooth associated haplotype (positions highlighted in red) is found in multiple, independently-derived, freshwater populations in the Pacific Northwest that appears to be restricted a region between northern Washington State up the west coast of British Columbia (red circle). The haplotype was not identified in either Alaska or California freshwater populations or multiple marine populations. **(B)** Populations containing the haplotype, or portions of the haplotype, in the Haida Gwaii archipelago fall in different watersheds, suggesting independent colonization and a reduced likelihood of geneflow. Map modified from Deagle et al, 2013.

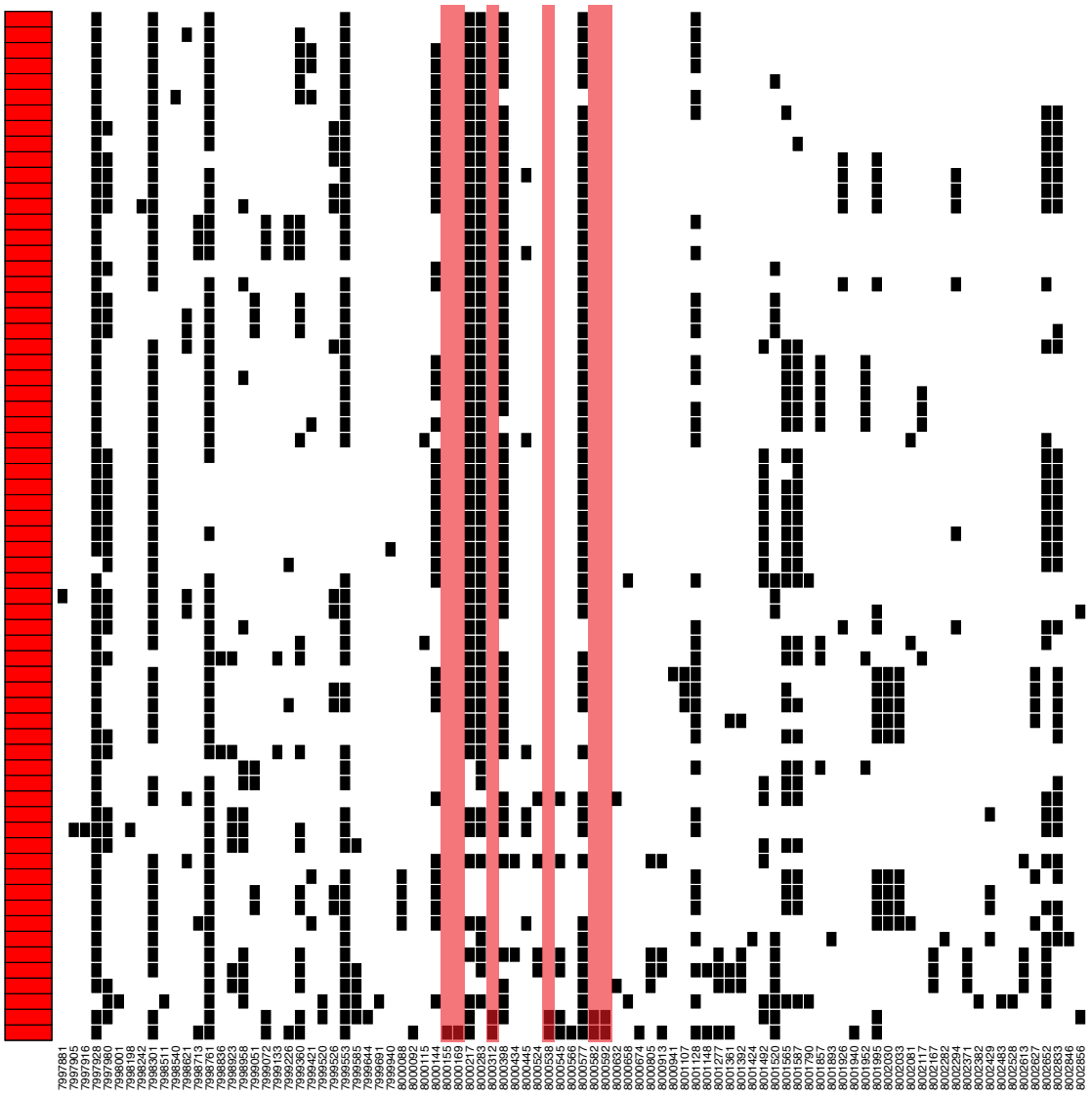


**Figure 4.12 The high tooth associated haplotype is segregating in the Little Campbell marine population.** A single chromosome (bottom) was found to contain the high tooth associated haplotype in the marine population of Little Campbell. The figure was generated using a 10kb window centered on the haplotype with a minor allele frequency cutoff of 0.01 to maintain the singleton SNPs in the first two positions of the haplotype.

## 4.5 Conclusion

### Genetic diversity and Tajima's D

The overall genetic diversity of the Fishtrap Creek and Little Campbell populations is reduced compared to previous estimates of diversity in other populations (Hohenlohe et al., 2010; Marques et al., 2018; Nelson & Cresko, 2018). The reduction in Fishtrap Creek is not surprising, as likely has a relatively small effective population size due to the size of the body of water. In addition, barriers such as manmade structures or a reduction of water level, preventing movement of individuals, can impede gene flow, reducing variation in river or creek dwelling sticklebacks (Raeymaekers et al., 2008). Therefore, it could be expected that a reduction in diversity would be observed in Fishtrap Creek, however the diversity of Little Campbell is surprising. Typically, marine populations have higher levels of genetic diversity and large effective population sizes. The lower level observed here may indicate a high degree of relatedness of the fish sampled or too harsh of filtering methods. A high proportion of polymorphic sites within the Little Campbell data set are relatively rare alleles in the population, as would be expected. As the filtering criteria used here relies on multiple occurrences and a certain number of total sequencing reads to verify a genotype, it is possible very rare alleles failed to pass the filters and were removed.

Using Tajima's D, the Fishtrap Creek population was found to have a genome wide average score of 0.709, in which a score of approximately 0 indicates a population only experiencing neutral effects. A positive score indicates a reduction of rare alleles, or increase in moderate frequency alleles, resulting from bottleneck events, balancing selection, or population structure (Biswas & Akey, 2006). As there is no evidence of structure within the Fishtrap Creek population (see below), the other explanations are more likely the underlying cause. Due to the history of the creek itself, including human development and use for irrigation, decreasing water flow, a bottleneck is reasonable. Further refinement of effective population size results over time from programs like SMC++ (Terhorst et al., 2017) or Relate (Speidel et al., 2019) can help identify potential bottlenecks. Other methods exist for specifically detecting balancing selection (Bryan et al., 2009; Siewert & Voight, 2020). Using what is known about other populations, I would have predicted the haplotype to be a high frequency in a shallow creek, in which benthic food items are likely to be the primary prey of sticklebacks, like Fishtrap Creek. However the intermediate allele frequency of the haplotype, as well as intermediate tooth number compared to other freshwater populations (Hart, 2018) creates an attractive hypothesis of balancing selection, for some purpose, maintaining the non-high-tooth associated haplotype in the population.

### A lack of structure in Fishtrap Creek population

The population in Fishtrap Creek did not appear to be structured, representing a single, panmictic population. Other stickleback populations have exhibited population structure associated with niche specific morphology (McPhail, 1992). It is formally possible the segregating high-tooth associated haplotype may be associated with niche partitioning within the creek, with the fish containing the haplotype having more teeth and therefore better able to exploit other resources compared to those without the high-tooth associated haplotype. The results from the program ADMIXTURE suggests that there is no niche partitioning structure within the population and it represents a single interbreeding genepool.

**EHH, iHS, nSL implicate the same sites within the haplotype**

Metrics such as Tajima's D and nucleotide diversity ($\pi$) have been able to identify regions of selection in other stickleback populations (Hohenlohe et al., 2010; Marques et al., 2017; Nelson & Cresko, 2018) but have little power in soft sweeps from standing genetic variation (Innan & Kim, 2004; Przeworski et al., 2005). Other methods such as EHH, iHS, and nSL, use haplotype homozygosity instead of changes in overall diversity in a region and are more robust in detecting soft sweeps (Ferrer-Admetlla et al., 2014; Nielsen, 2005; Sabeti et al., 2002; Voight et al., 2006). While these methods do provide more power in detecting selection in the scenario I hypothesize the high-tooth associated haplotype has experienced, none of the metrics suggested the haplotype as likely having experienced selection.

There are two obvious possible explanations for the lack of signal focused on the haplotype: 1) the haplotype is either not adaptive or is adaptive in other populations but has not experienced selection in Fishtrap Creek or 2) the strength of selection is low enough to drive the signal from these metrics too low to stand out against the genome wide average. Other populations provide opportunities to address the first possible explanation as the allele has been found in multiple other populations. If selection is too low to detect against the genome wide background, other methods, such as the use of Ancestral Recombination Graphs (ARGs) may provide a means to identify a signal. Alternatively, it is possible the genome wide averages for the scores are artificially inflated due to technical and methodical issues in the pipeline, essentially creating too much "static" to detect a clean "signal" of selection through. Reconsidering the pipeline, including filtering parameters, phasing methods, and using other tools to implement the tests may refine the output.

The six sites that define the haplotype had results for the three methods that ranged across the haplotype. Consistently, the first two SNPs, chrXXI:8000155 and 8000169, had the highest scores (iHS and nSL) or the largest tracks of homozygosity for the derived allele (EHH) compared to the other four positions of the haplotype. Previous work had identified a potential NFATc1 binding site created by the high-tooth associated allele at the chrXXI:8000169 position (Cleves et al., 2018). The transcription factor is known to be important in balancing the quiescence and activity of stem cells in hair follicles (Horsley et al., 2008), which share homology with teeth (Ahn, 2015; Biggs & Mikkola, 2014; Pispa & Thesleff, 2003). In addition, *Nfatc1b* has been shown to be present in stickleback tooth germs and functional tooth mesenchyme (Square et al., 2021). It is possible the NFATc1 binding site is responsible for evolved tooth gain and has experienced selection, while the other sites within the haplotype are linked, but are not related to the phenotype. ChrXXI:8000155 is in perfect linkage disequilibrium with chrXXI:8000169 and so may have elevated scores simply due to proximity, as would the other sites in the haplotype that have some linkage with 8000169.

**Ancestral recombination graphs reveals selection may be acting on the haplotype**

A relatively new set of approaches for detecting signals of selection are ancestral recombination graphs, which recreate the gene trees for given regions or sites and can detect selection through the topology of the trees (Hejase et al., 2020). Relate (Speidel et al., 2019) is one such method. Like iHS and nSL, scores are calculated for each SNP, estimating the likelihood an allele would reach its current frequency through neutral processes. Also like iHS and nSL, chrXXI:8000169 had the most significant score of the haplotype and was even elevated compared to the rest of the genome. Ancestral recombination graphs attempt to infer ancestral processes and states using modeling, and therefore the reliability of the results are contingent on the quality of the data

provided and the appropriateness of the tools/parameters. Relate has demonstrated reliability with human data (Speidel et al., 2019) but not in other systems. The program generates coalescent trees to infer ancestral events, so the test for selection is not based on observed patterns within the genome, but rather a created model, which should carry caveats. Agreement between measurements was observed in certain patterns, specifically the rank order of the SNPs within the haplotype, but a broader, genome-wide comparison would further bolster confidence the result. A sibling tool to Relate, CLUES, can take output from Relate and estimate the strength of selection and so is another potential continuation for this project (Stern et al., 2021).

**Elevated iHS, nSL, and Relate scores within a branchial bone length QTL**

Three methods, iHS ,nSL, and Relate's DetectSelection tool, identified elevated scores within a previously identified branchial bone length QTL (Erickson et al., 2018). While iHS and nSL are conceptually similar, in their focus on haplotype homozygosity, Relate's utilization of Ancestral Recombination Graphs to test for selection allows for an independent means to identify positions of interest. The result of different tests identifying signals within the same region likely indicates a true signal of selection. Previous work suggested the gene *Tfap2a* likely underlies the QTL due to craniofacial disruption in homozygous knockouts and allele specific expression data that showed a reduction of expression of a freshwater allele compared to a marine allele. Interestingly, Fishtrap Creek fish heterozygous for a mutant allele exhibited both an increase and decrease in size of different branchial bones, suggesting a complex role of the gene on craniofacial development and evolution(Erickson et al., 2018).

The ASE result, as well as a lack of concordant coding changes, indicate a *cis*-regulatory difference between the two alleles likely underlies the QTL peak. While the elevated scores for the metrics used here are greater than 15kb away from *Tfap2a*, enhancers can be hundreds of kb away from the genes they regulate (Anderson et al., 2014; Schoenfelder & Fraser, 2019), and so the signals detected may represent selection on regulatory elements for *Tfap2a*. Subcloning of potential regulatory regions has led to the identification of enhancers within sticklebacks (Cleves et al., 2018; Erickson et al., 2015). Future researchers, wanting to further dissect the branchial bone length QTL, could test differing regions of the QTL for enhancer activity, led by the iHS, nSL, and Relate outliers. Both the allele specific expression (ASE) result and the effect of the QTL were observed relatively early in development, with ASE differences arising as early as 9 days post-fertilization (dpf) and the QTL affecting bone length by 20 dpf. Therefore, if there are enhancers within subclones of the region, and differences in expression between a freshwater and marine allele, they would become apparent early in development through the use of tol2 reporter assays. If enhancers with differential gene expression are identified within the regions, using the signals of selection as guides, it would illustrate the use of *cis*-regulation through identified population specific enhancers in local adaptation.

**High tooth associated haplotype presence in Haida Gwaii**

Prior to incorporating the Haida Gwaii data set, distribution of the haplotype was restricted to the triangle straddling the US-Canada border. After calling variants from Haida Gwaii samples, multiple populations of the archipelago were observed to contain six of the haplotype-defining SNPs, including the NFATc1 associated position. Incorporating the new sequence increases the furthest distance between the two furthest haplotype-containing populations to nearly 600 miles, dramatically increasing the total range of the haplotype.

Within the Haida Gwaii archipelago four populations (Mayer Lake, Rouge Lake, Serendipity Lake, and Solstice Lake) were observed to contain the core six haplotype-defining SNPs, while three others (Silver Lake, Spence Lake, and Woodpile Lake) contained no more than three haplotype defining SNPs. Of the four populations that contain the entire six SNP haplotype, each population resides in a separate watershed (Deagle et al., 2013).

The Haida Gwaii re-sequencing data set provides the opportunity to scan multiple populations for the presence or absence of the haplotype, with representatives from a total of 28 populations on the island chain. However, most populations (23) are represented by a single individual, reducing the power to observe the haplotype in these populations. Of the populations in which the entire set of six polymorphisms was observed, three out of four were represented by a single fish. Silver and Woodpile Lakes were also only represented by a single individual, while the Spence Lake data contained four genomes. Of the four populations which contain the haplotype, the samples from three (Rouge Lake, Serendipity Lake, and Solstice Lake) were homozygous for all six sites, however, it cannot be determined if the haplotype is fixed in these populations due to sample size. In the most well represented population, Mayer Lake, a single individual out of twelve was observed to be heterozygous for the haplotype, while another only contained a subset of the SNPs.

Mayer Lake is a highly derived population, having an extremely large adult length and are highly melanistic, which is thought to be an adaptation to the tannin stained water of the lake (Moodie, 1972). Zooplankton constitutes the dominant component of Mayer Lake sticklebacks, which are well adapted to the niche with a high number of gill rakers. In 1993, 100 Mayer lake fish were transplanted to Roadside Pond, a small, shallow, clearwater environment, with little zooplankton and a larger number of benthic invertebrates. After 19 years of natural selection in the new environment, multiple traits in the sticklebacks of Roadside Pond had evolved consistent with a transition to a radically different habitat, including changes in predator regime and niche (Marques et al., 2017, Marques et al., 2018). Melanism decreased, consistent with a change in water opacity, as had the overall standard length of the fish, pelvic and dorsal spine length, plate number and plate size. Feeding morphology also changed, with an increase in raker spacing and lower jaw length and a decrease in raker number and length, consistent with a transition from a zooplankton diet to a larger, benthic invertebrate-based diet (Leaver & Reimchen, 2012). While multiple traits were characterized, including some feeding structures, pharyngeal teeth were not. The direction of change for the other traits, as well as the natures of the source lake versus the recipient pond, would predict an increase in pharyngeal tooth number, associated with a change in diet from zooplankton to benthic invertebrates. In other populations of sticklebacks, adaptation to a benthic niche has resulted in similar changes in feeding morphologies (McPhail, 1992; Schluter & McPhail, 1992), and later analysis of pharyngeal teeth in the same populations have also shown a change in phenotype, with an increase in tooth number (Cleves et al., 2014; Erickson et al., 2016).

Surprisingly, the high tooth-associated haplotype was observed in Mayer Lake, a limnetic population and source for the transplant experiment, but not in Roadside Pond, a shallow, benthic feeding population, and recipient habitat. There are three possible explanations: 1) the haplotype was not present in the initial 100 fish that were transplanted from Mayer Lake and Roadside Pond, 2) the haplotype was present in the 100 fish that were transplanted but was subsequently lost in Roadside Pond, or 3) the haplotype is present in Roadside Pond but not present in the fish sequenced in the experiment.

1) Due to the low number of individuals sequenced, it is difficult to estimate the frequency of the haplotype in Mayer Lake. In the dozen fish sequenced, only a single individual contained the haplotype and was heterozygous, resulting in an allele frequency of approximately 4%. Therefore, it is highly unlikely the allele was not present in the 100 fish transferred to Roadside Pond.
2) Once the haplotype was transferred to Roadside Pond, the allele was under new selective pressures associated with the new habitat. There are multiple lines of evidence that the allele is adaptive for benthic feeding fish, specifically the covariation with a QTL that is responsible for 30% of evolved tooth gain (Cleves et al., 2018), presence in multiple, independently derived populations (Erickson et al., 2016), and significance in the Relate program's Detect Selection module. However, the strength of selection has not been estimated, but since classic methods for detecting signals of selection are unable to detect the haplotype, it coefficient of selection is not believed to be large. It is possible, if the allele was present in the transplant population at a sufficiently low frequency and the coefficient of selection was also low, the allele could be lost due to genetic drift, which can have a considerable impact on small populations.
3) It is possible that even if the allele is present in Roadside Pond it may not have been sampled in the 11 fish collected. With no other information, this possible explanation is the most difficult to address. While 22 chromosomes would likely not provide an exhaustive depiction of the total variation for the genomic region in the population, after experiencing a bottleneck event 19 years prior, the data set should contain most alleles, with only very rare alleles absent.

Of the remaining three populations on Haida Gwaii in which the haplotype has been found, two, Rouge and Serendipity Lake, are relatively small and shallow (2m depth for both and 1.2 and 3.0 hectares area respectively), with an extremely low pH due to the high amount of tannins from the surrounding sphagnum moss. In both populations reduction or loss of defensive armor, either in the form of lateral plates, pelvic spines, or dorsal spines, have evolved (Reimchen, 1984). Solstice Lake, conversely, is much larger and deeper, with a depth of approximately 15m and total area of 51 hectares, but a reduction in defensive armor has also evolved (Reimchen, 1983). While Rouge and Serendipity Lake represent likely benthic ecotypes due to the shallowness of the lakes, there is no data available on gill raker number nor pharyngeal tooth numbers. It can be hypothesized that the high-tooth associated haplotype in these populations may contribute to an increase in tooth number and therefore adaptation to the shallow environment. Without phenotype data the hypothesis cannot be tested and without additional genotypes it is difficult to even estimate the prevalence of the haplotype in the population. The presence of the haplotype in both Solstice Lake and Mayer Lake may be due to founder's effect or admixture. Mayer Lake is connected to multiple creeks with phenotypically distinct ecotypes which have reductions in rakers compared to the lake population, likely due to an adaptation to benthic invertebrates (Deagle et al., 2012), and, I would predict, have an increase in pharyngeal tooth number.

Overall, the Haida Gwaii sequencing data from Marques et al. (2017) provides a look into the genetic variation in the archipelago and expands the geographic distribution of the high-toothed associated haplotype. Other populations in which the haplotype has been found have evolved tooth gain relative to marine populations (Hart, 2018), such as Fishtrap Creek and Paxton Lake, Benthic. Phenotype data, in the form of tooth counts, have not been collected for

any population on the Haida Gwaii archipelago, but the presence of the haplotype in populations suggests there may be an evolved tooth gain, using similar genetic mechanisms in multiple independent populations on the archipelago, and is worth further exploration.

**Future Directions**

Stickleback population genetic data, either through the use of RAD tag or whole genome sequencing, has been used to identify regions and genes undergoing selection, (Jones et al., 2012; Catchen et al., 2013; Chan et al., 2010; Hohenlohe et al., 2010; Marques et al., 2017), and in some cases specific sites (Marques et al., 2017). An appeal of using a large data set is it allows for an unbiased sampling and view of what genes may underlie adaptation. This thesis was focused on a specific haplotype and while whole genome sequencing data was collected to answer that question, the remainder of the data has been largely unused besides as acting as a comparison point.

As the Fishtrap Creek population exhibits highly derived phenotypes (Hagen, 1967; Hagen & Gilbertson, 1972; Hart, 2018) and the creek itself has experienced drastic changes in the recent history (Dickes, 1992; Whatcom Conservation District, 2020), there are likely regions in the genome associated with the evolution of the derived body shape, gill raker and defensive armor reduction, and physiological adaptations to the local environment. For example, *Eda* has been implicated in repeated reduction of lateral plates (Colosimo, 2005), as well being linked to multiple body shape features, including aspects of the head (Albert et al., 2007). Multiple candidates have also been identified that may underlie the reduction in raker number through QTL crosses, specifically including Fishtrap Creek fish (Glazer et al., 2014). Candidates from these experiments provide regions of interest the metrics generated here can characterize, scanning for signals of selection, connecting quantitative genetics through QTL mapping to population genetics, and potentially even identifying causative regions or mutations. Utilizing the data generated here and extending it through the use of additional tools can help further develop an understanding of what genes have been the targets of selection in Fishtrap Creek and allowed for adaptation to that environment.

This work used the Vincent J. Coates Genomics Sequencing Laboratory at UC Berkeley, supported by NIH S10 OD018174 Instrumentation Grant.

## 4.6 References

Ahn, Y. (2015). Signaling in Tooth, Hair, and Mammary Placodes. In *Current Topics in Developmental Biology* (Vol. 111, pp. 421–459). Elsevier. https://doi.org/10.1016/bs.ctdb.2014.11.013

Albert, A. Y. K., Sawaya, S., Vines, T. H., Knecht, A. K., Miller, C. T., Summers, B. R., Balabhadra, S., Kingsley, D. M., & Schluter, D. (2007). THE GENETICS OF ADAPTIVE SHAPE SHIFT IN STICKLEBACK: PLEIOTROPY AND EFFECT SIZE. *Evolution*, *0*(0), 071115145922005-??? https://doi.org/10.1111/j.1558-5646.2007.00259.x

Alexander, D. H., Novembre, J., & Lange, K. (2009). Fast model-based estimation of ancestry in unrelated individuals. *Genome Research*, *19*(9), 1655–1664. https://doi.org/10.1101/gr.094052.109

Anderson, E., Devenney, P. S., Hill, R. E., & Lettice, L. A. (2014). Mapping the *Shh* long-range regulatory domain. *Development*, *141*(20), 3934–3943. https://doi.org/10.1242/dev.108480

Andrews, S. (n.d.). *FastQC: a quality control tool for high throughput sequence data*. Babraham Bioinformatics, abraham Institute, Cambridge, United Kingdom. https://www.bioinformatics.babraham.ac.uk/projects/fastqc/

Barrett, R., & Schluter, D. (2008). Adaptation from standing genetic variation. *Trends in Ecology & Evolution*, *23*(1), 38–44. https://doi.org/10.1016/j.tree.2007.09.008

Bassham, S., Catchen, J., Lescak, E., von Hippel, F. A., & Cresko, W. A. (2018). Repeated Selection of Alternatively Adapted Haplotypes Creates Sweeping Genomic Remodeling in Stickleback. *Genetics*, *209*(3), 921–939. https://doi.org/10.1534/genetics.117.300610

Bell, M. A., & Foster, S. A. (Eds.). (1994). *The evolutionary biology of the threespine stickleback*. Oxford University Press.

Benjamini, Y., & Hochberg, Y. (1995). Controlling the False Discovery Rate: A Practical and Powerful Approach to Multiple Testing. *Journal of the Royal Statistical Society: Series B (Methodological)*, *57*(1), 289–300. https://doi.org/10.1111/j.2517-6161.1995.tb02031.x

Biggs, L. C., & Mikkola, M. L. (2014). Early inductive events in ectodermal appendage morphogenesis. *Seminars in Cell & Developmental Biology*, *25–26*, 11–21. https://doi.org/10.1016/j.semcdb.2014.01.007

Biswas, S., & Akey, J. M. (2006). Genomic insights into positive selection. *Trends in Genetics*, *22*(8), 437–446. https://doi.org/10.1016/j.tig.2006.06.005

Bolger, A. M., Lohse, M., & Usadel, B. (2014). Trimmomatic: A flexible trimmer for Illumina sequence data. *Bioinformatics*, *30*(15), 2114–2120. https://doi.org/10.1093/bioinformatics/btu170

Broad Institute Genome Sequencing Platform & Whole Genome Assembly Team, Jones, F. C., Grabherr, M. G., Chan, Y. F., Russell, P., Mauceli, E., Johnson, J., Swofford, R., Pirun, M., Zody, M. C., White, S., Birney, E., Searle, S., Schmutz, J., Grimwood, J., Dickson, M. C., Myers, R. M., Miller, C. T., Summers, B. R., … Kingsley, D. M. (2012). The genomic basis of adaptive evolution in threespine sticklebacks. *Nature*, *484*(7392), 55–61. https://doi.org/10.1038/nature10944

Bryan, A. W., Menke, M., Cowen, L. J., Lindquist, S. L., & Berger, B. (2009). BETASCAN: Probable β-amyloids Identified by Pairwise Probabilistic Analysis. *PLoS Computational Biology*, *5*(3), e1000333. https://doi.org/10.1371/journal.pcbi.1000333

Catchen, J., Bassham, S., Wilson, T., Currey, M., O'Brien, C., Yeates, Q., & Cresko, W. A. (2013). The population structure and recent colonization history of Oregon threespine stickleback determined using restriction-site associated DNA-sequencing. *Molecular Ecology*, *22*(11), 2864–2883. https://doi.org/10.1111/mec.12330

Chan, Y. F., Marks, M. E., Jones, F. C., Villarreal, G., Shapiro, M. D., Brady, S. D., Southwick, A. M., Absher, D. M., Grimwood, J., Schmutz, J., Myers, R. M., Petrov, D., Jonsson, B., Schluter, D., Bell, M. A., & Kingsley, D. M. (2010). Adaptive Evolution of Pelvic

Reduction in Sticklebacks by Recurrent Deletion of a Pitx1 Enhancer. *Science*, *327*(5963), 302–305. https://doi.org/10.1126/science.1182213

Cleves, P. A., Ellis, N. A., Jimenez, M. T., Nunez, S. M., Schluter, D., Kingsley, D. M., & Miller, C. T. (2014). Evolved tooth gain in sticklebacks is associated with a cis-regulatory allele of Bmp6. *Proceedings of the National Academy of Sciences*, *111*(38), 13912–13917. https://doi.org/10.1073/pnas.1407567111

Cleves, Phillip A., Hart, J. C., Agoglia, R. M., Jimenez, M. T., Erickson, P. A., Gai, L., & Miller, C. T. (2018). An intronic enhancer of Bmp6 underlies evolved tooth gain in sticklebacks. *PLOS Genetics*, *14*(6), e1007449. https://doi.org/10.1371/journal.pgen.1007449

Colosimo, P. F. (2005). Widespread Parallel Evolution in Sticklebacks by Repeated Fixation of Ectodysplasin Alleles. *Science*, *307*(5717), 1928–1933. https://doi.org/10.1126/science.1107239

D. Turner, S. (2018). qqman: An R package for visualizing GWAS results using Q-Q and manhattan plots. *Journal of Open Source Software*, *3*(25), 731. https://doi.org/10.21105/joss.00731

Danecek, P., Auton, A., Abecasis, G., Albers, C. A., Banks, E., DePristo, M. A., Handsaker, R. E., Lunter, G., Marth, G. T., Sherry, S. T., McVean, G., Durbin, R., & 1000 Genomes Project Analysis Group. (2011). The variant call format and VCFtools. *Bioinformatics*, *27*(15), 2156–2158. https://doi.org/10.1093/bioinformatics/btr330

Deagle, B. E., Jones, F. C., Absher, D. M., Kingsley, D. M., & Reimchen, T. E. (2013). Phylogeography and adaptation genetics of stickleback from the Haida Gwaii archipelago revealed using genome-wide single nucleotide polymorphism genotyping. *Molecular Ecology*, *22*(7), 1917–1932. https://doi.org/10.1111/mec.12215

Deagle, B. E., Jones, F. C., Chan, Y. F., Absher, D. M., Kingsley, D. M., & Reimchen, T. E. (2012). Population genomics of parallel phenotypic evolution in stickleback across stream–lake ecological transitions. *Proceedings of the Royal Society B: Biological Sciences*, *279*(1732), 1277–1286. https://doi.org/10.1098/rspb.2011.1552

Delaneau, O., Howie, B., Cox, A. J., Zagury, J.-F., & Marchini, J. (2013). Haplotype Estimation Using Sequencing Reads. *The American Journal of Human Genetics*, *93*(4), 687–696. https://doi.org/10.1016/j.ajhg.2013.09.002

Dickes, B. (1992). *Water Quality Screening in the Dakota, Bertrand, and Fishtrap Creek Watersheds, Whatcom County, Washington* (No. 92-e14).

Eichstaedt, C. A., Pagani, L., Antao, T., Inchley, C. E., Cardona, A., Mörseburg, A., Clemente, F. J., Sluckin, T. J., Metspalu, E., Mitt, M., Mägi, R., Hudjashov, G., Metspalu, M., Mormina, M., Jacobs, G. S., & Kivisild, T. (2017). Evidence of Early-Stage Selection on EPAS1 and GPR126 Genes in Andean High Altitude Populations. *Scientific Reports*, *7*(1), 13042. https://doi.org/10.1038/s41598-017-13382-4

Ellis, N. A., Glazer, A. M., Donde, N. N., Cleves, P. A., Agoglia, R. M., & Miller, C. T. (2015). Distinct developmental genetic mechanisms underlie convergently evolved tooth gain in sticklebacks. *Development*, *142*(14), 2442–2451. https://doi.org/10.1242/dev.124248

Erickson, P. A., Baek, J., Hart, J. C., Cleves, P. A., & Miller, C. T. (2018). Genetic Dissection of a Supergene Implicates *Tfap2a* in Craniofacial Evolution of Threespine Sticklebacks. *Genetics*, *209*(2), 591–605. https://doi.org/10.1534/genetics.118.300760

Erickson, P. A., Cleves, P. A., Ellis, N. A., Schwalbach, K. T., Hart, J. C., & Miller, C. T. (2015). A 190 base pair, TGF-β responsive tooth and fin enhancer is required for stickleback Bmp6 expression. *Developmental Biology*, *401*(2), 310–323. https://doi.org/10.1016/j.ydbio.2015.02.006

Erickson, P. A., Glazer, A. M., Killingbeck, E. E., Agoglia, R. M., Baek, J., Carsanaro, S. M., Lee, A. M., Cleves, P. A., Schluter, D., & Miller, C. T. (2016). Partially repeatable genetic basis of benthic adaptation in threespine sticklebacks: REPEATABLE EVOLUTION IN BENTHIC STICKLEBACKS. *Evolution*, *70*(4), 887–902. https://doi.org/10.1111/evo.12897

Fay, J. C., & Wu, C. I. (2000). Hitchhiking under positive Darwinian selection. *Genetics*, *155*(3), 1405–1413.

Ferrer-Admetlla, A., Liang, M., Korneliussen, T., & Nielsen, R. (2014). On Detecting Incomplete Soft or Hard Selective Sweeps Using Haplotype Structure. *Molecular Biology and Evolution*, *31*(5), 1275–1291. https://doi.org/10.1093/molbev/msu077

Feulner, P. G. D., Chain, F. J. J., Panchal, M., Eizaguirre, C., Kalbe, M., Lenz, T. L., Mundry, M., Samonte, I. E., Stoll, M., Milinski, M., Reusch, T. B. H., & Bornberg-Bauer, E. (2013). Genome-wide patterns of standing genetic variation in a marine population of three-spined sticklebacks: GENOMIC VARIATION IN MARINE STICKLEBACKS. *Molecular Ecology*, *22*(3), 635–649. https://doi.org/10.1111/j.1365-294X.2012.05680.x

Glazer, A. M., Cleves, P. A., Erickson, P. A., Lam, A. Y., & Miller, C. T. (2014). Parallel developmental genetic features underlie stickleback gill raker evolution. *EvoDevo*, *5*(1), 19. https://doi.org/10.1186/2041-9139-5-19

Glazer, A. M., Killingbeck, E. E., Mitros, T., Rokhsar, D. S., & Miller, C. T. (2015). Genome Assembly Improvement and Mapping Convergently Evolved Skeletal Traits in Sticklebacks with Genotyping-by-Sequencing. *G3: Genes|Genomes|Genetics*, *5*(7), 1463–1472. https://doi.org/10.1534/g3.115.017905

Hagen, D. W. (1967). Isolating Mechanisms in Threespine Sticklebacks ( *Gasterosteus* ). *Journal of the Fisheries Research Board of Canada*, *24*(8), 1637–1692. https://doi.org/10.1139/f67-138

Hagen, D. W., & Gilbertson, L. G. (1972). GEOGRAPHIC VARIATION AND ENVIRONMENTAL SELECTION IN *GASTEROSTEUS ACULEATUS* L. IN THE PACIFIC NORTHWEST, AMERICA. *Evolution*, *26*(1), 32–51. https://doi.org/10.1111/j.1558-5646.1972.tb00172.x

Hart, J. C. (2018). *Genetic and Genomic Bases of Evolved Increases in Stickleback Dentition* [University of California, Berkeley]. https://escholarship.org/uc/item/3dp2884n

Hejase, H. A., Dukler, N., & Siepel, A. (2020). From Summary Statistics to Gene Trees: Methods for Inferring Positive Selection. *Trends in Genetics*, *36*(4), 243–258. https://doi.org/10.1016/j.tig.2019.12.008

Hermisson, J., & Pennings, P. S. (2005). Soft Sweeps: Molecular Population Genetics of Adaptation From Standing Genetic Variation. *Genetics*, *169*(4), 2335–2352. https://doi.org/10.1534/genetics.104.036947

Hohenlohe, P. A., Bassham, S., Etter, P. D., Stiffler, N., Johnson, E. A., & Cresko, W. A. (2010). Population Genomics of Parallel Adaptation in Threespine Stickleback using Sequenced RAD Tags. *PLoS Genetics*, *6*(2), e1000862. https://doi.org/10.1371/journal.pgen.1000862

Horsley, V., Aliprantis, A. O., Polak, L., Glimcher, L. H., & Fuchs, E. (2008). NFATc1 Balances Quiescence and Proliferation of Skin Stem Cells. *Cell*, *132*(2), 299–310. https://doi.org/10.1016/j.cell.2007.11.047

Hubisz, M. J., Williams, A. L., & Siepel, A. (2019). *Mapping gene flow between ancient hominins through demography-aware inference of the ancestral recombination graph* [Preprint]. Evolutionary Biology. https://doi.org/10.1101/687368

Innan, H., & Kim, Y. (2004). Pattern of polymorphism after strong artificial selection in a domestication event. *Proceedings of the National Academy of Sciences*, *101*(29), 10667–10672. https://doi.org/10.1073/pnas.0401720101

Kim, Y., & Stephan, W. (2002). Detecting a local signature of genetic hitchhiking along a recombining chromosome. *Genetics*, *160*(2), 765–777.

Kingman, J. F. C. (1982). The coalescent. *Stochastic Processes and Their Applications*, *13*(3), 235–248. https://doi.org/10.1016/0304-4149(82)90011-4

Kovanen, D. J., Haugerud, Ralph A., & Easterbrook, Don J. (n.d.). *Geomorphic map of western Whatcom County, Washington* (Scientific Investigations Map 3406, Pamphlet 42 p. Scale 1:50,000,). U.S. Geological Survey. https://pubs.er.usgs.gov/publication/sim3406

Langmead, B., & Salzberg, S. L. (2012). Fast gapped-read alignment with Bowtie 2. *Nature Methods*, *9*(4), 357–359. https://doi.org/10.1038/nmeth.1923

Leaver, S. D., & Reimchen, T. E. (2012). Abrupt changes in defence and trophic morphology of the giant threespine stickleback ( *Gasterosteus* sp.) following colonization of a vacant habitat: Abrupt Morphological Shifts in Stickleback. *Biological Journal of the Linnean Society*, *107*(3), 494–509. https://doi.org/10.1111/j.1095-8312.2012.01969.x

Li, H., Handsaker, B., Wysoker, A., Fennell, T., Ruan, J., Homer, N., Marth, G., Abecasis, G., Durbin, R., & 1000 Genome Project Data Processing Subgroup. (2009). The Sequence Alignment/Map format and SAMtools. *Bioinformatics (Oxford, England)*, *25*(16), 2078–2079. https://doi.org/10.1093/bioinformatics/btp352

Marnetto, D., & Huerta-Sánchez, E. (2017). *Haplostrips*: Revealing population structure through haplotype visualization. *Methods in Ecology and Evolution*, *8*(10), 1389–1392. https://doi.org/10.1111/2041-210X.12747

Marques, D. A., Jones, F. C., Di Palma, F., Kingsley, D. M., & Reimchen, T. E. (2018). Experimental evidence for rapid genomic adaptation to a new niche in an adaptive radiation. *Nature Ecology & Evolution*, *2*(7), 1128–1138. https://doi.org/10.1038/s41559-018-0581-8

Marques, D. A., Taylor, J. S., Jones, F. C., Di Palma, F., Kingsley, D. M., & Reimchen, T. E. (2017). Convergent evolution of SWS2 opsin facilitates adaptive radiation of threespine stickleback into different light environments. *PLOS Biology*, *15*(4), e2001627. https://doi.org/10.1371/journal.pbio.2001627

McKenna, A., Hanna, M., Banks, E., Sivachenko, A., Cibulskis, K., Kernytsky, A., Garimella, K., Altshuler, D., Gabriel, S., Daly, M., & DePristo, M. A. (2010). The Genome Analysis Toolkit: A MapReduce framework for analyzing next-generation DNA sequencing data. *Genome Research*, *20*(9), 1297–1303. https://doi.org/10.1101/gr.107524.110

McPhail, J. D. (1992). Ecology and evolution of sympatric sticklebacks ( *Gasterosteus* ): Evidence for a species-pair in Paxton Lake, Texada Island, British Columbia. *Canadian Journal of Zoology*, *70*(2), 361–369. https://doi.org/10.1139/z92-054

Messer, P. W., & Petrov, D. A. (2013). Population genomics of rapid adaptation by soft selective sweeps. *Trends in Ecology & Evolution*, *28*(11), 659–669. https://doi.org/10.1016/j.tree.2013.08.003

Miller, C. T., Glazer, A. M., Summers, B. R., Blackman, B. K., Norman, A. R., Shapiro, M. D., Cole, B. L., Peichel, C. L., Schluter, D., & Kingsley, D. M. (2014). Modular Skeletal Evolution in Sticklebacks Is Controlled by Additive and Clustered Quantitative Trait Loci. *Genetics*, *197*(1), 405–420. https://doi.org/10.1534/genetics.114.162420

Moodie, G. E. E. (1972). Morphology, life history, and ecology of an unusual stickleback ( *Gasterosteus aculeatus* ) in the Queen Charlotte Islands, Canada. *Canadian Journal of Zoology*, *50*(6), 721–732. https://doi.org/10.1139/z72-099

Moodie, G. E. E., & Reimchen, T. E. (1976). Phenetic Variation and Habitat Differences in Gasterosteus Populations of the Queen Charlotte Islands. *Systematic Zoology*, *25*(1), 49. https://doi.org/10.2307/2412778

Moon, J. M., Capra, J. A., Abbot, P., & Rokas, A. (2019). Signatures of Recent Positive Selection in Enhancers Across 41 Human Tissues. *G3 (Bethesda, Md.)*, *9*(8), 2761–2774. https://doi.org/10.1534/g3.119.400186

Nelson, T. C., & Cresko, W. A. (2018). Ancient genomic variation underlies repeated ecological adaptation in young stickleback populations. *Evolution Letters*, *2*(1), 9–21. https://doi.org/10.1002/evl3.37

Nielsen, R. (2005). Molecular Signatures of Natural Selection. *Annual Review of Genetics*, *39*(1), 197–218. https://doi.org/10.1146/annurev.genet.39.073003.112420

Okonechnikov, K., Conesa, A., & García-Alcalde, F. (2015). Qualimap 2: Advanced multi-sample quality control for high-throughput sequencing data. *Bioinformatics*, btv566. https://doi.org/10.1093/bioinformatics/btv566

Pavlidis, P., & Alachiotis, N. (2017). A survey of methods and tools to detect recent and strong positive selection. *Journal of Biological Research-Thessaloniki*, *24*(1), 7. https://doi.org/10.1186/s40709-017-0064-0

Pispa, J., & Thesleff, I. (2003). Mechanisms of ectodermal organogenesis. *Developmental Biology*, *262*(2), 195–205. https://doi.org/10.1016/s0012-1606(03)00325-7

Porter, S. C., & Swanson, T. W. (1998). Radiocarbon Age Constraints on Rates of Advance and Retreat of the Puget Lobe of the Cordilleran Ice Sheet during the Last Glaciation. *Quaternary Research*, *50*(3), 205–213. https://doi.org/10.1006/qres.1998.2004

Przeworski, M., Coop, G., & Wall, J. D. (2005). The signature of positive selection on standing genetic variation. *Evolution; International Journal of Organic Evolution*, *59*(11), 2312–2323.

Raeymaekers, J. A. M., Maes, G. E., Geldof, S., Hontis, I., Nackaerts, K., & Volckaert, F. A. M. (2008). Modeling genetic connectivity in sticklebacks as a guideline for river restoration. *Evolutionary Applications*, *1*(3), 475–488. https://doi.org/10.1111/j.1752-4571.2008.00019.x

Rasmussen, M. D., Hubisz, M. J., Gronau, I., & Siepel, A. (2014). Genome-Wide Inference of Ancestral Recombination Graphs. *PLoS Genetics*, *10*(5), e1004342. https://doi.org/10.1371/journal.pgen.1004342

Reimchen, T. E. (1980). Spine deficiency and polymorphism in a population of *Gasterosteus aculeatus*: An adaptation to predators? *Canadian Journal of Zoology*, *58*(7), 1232–1244. https://doi.org/10.1139/z80-173

Reimchen, T. E. (1983). STRUCTURAL RELATIONSHIPS BETWEEN SPINES AND LATERAL PLATES IN THREESPINE STICKLEBACK ( *GASTEROSTEUS ACULEATUS* ). *Evolution*, *37*(5), 931–946. https://doi.org/10.1111/j.1558-5646.1983.tb05622.x

Reimchen, T. E. (1984). Status of Unarmored and Spine-deficient Populations (Charlotte Unarmoured Stickleback) of Threespine stickleback, Gasterosteus sp., on the Queen Charlotte Islands, British Columbia. *Canadian Field Naturalist*, *98*(1), 120–126.

Reimchen, T. E., & Nosil, P. (2002). TEMPORAL VARIATION IN DIVERGENT SELECTION ON SPINE NUMBER IN THREESPINE STICKLEBACK. *Evolution*, *56*(12), 2472–2483. https://doi.org/10.1111/j.0014-3820.2002.tb00172.x

Reimchen, T. E., & Nosil, P. (2004). VARIABLE PREDATION REGIMES PREDICT THE EVOLUTION OF SEXUAL DIMORPHISM IN A POPULATION OF THREESPINE STICKLEBACK. *Evolution*, *58*(6), 1274–1281. https://doi.org/10.1111/j.0014-3820.2004.tb01706.x

Reimchen, T. E., Stinson, E. M., & Nelson, J. S. (1985). Multivariate differentiation of parapatric and allopatric populations of threespine stickleback in the Sangan River watershed, Queen Charlotte Islands. *Canadian Journal of Zoology*, *63*(12), 2944–2951. https://doi.org/10.1139/z85-441

Roesti, M., Kueng, B., Moser, D., & Berner, D. (2015). The genomics of ecological vicariance in threespine stickleback fish. *Nature Communications*, *6*(1), 8767. https://doi.org/10.1038/ncomms9767

Sabeti, P. C., Reich, D. E., Higgins, J. M., Levine, H. Z. P., Richter, D. J., Schaffner, S. F., Gabriel, S. B., Platko, J. V., Patterson, N. J., McDonald, G. J., Ackerman, H. C., Campbell, S. J., Altshuler, D., Cooper, R., Kwiatkowski, D., Ward, R., & Lander, E. S. (2002). Detecting recent positive selection in the human genome from haplotype structure. *Nature*, *419*(6909), 832–837. https://doi.org/10.1038/nature01140

Schluter, D., & McPhail, J. D. (1992). Ecological Character Displacement and Speciation in Sticklebacks. *The American Naturalist*, *140*(1), 85–108. https://doi.org/10.1086/285404

Schmidt, J. M., Battlay, P., Gledhill-Smith, R. S., Good, R. T., Lumb, C., Fournier-Level, A., & Robin, C. (2017). Insights into DDT Resistance from the Drosophila melanogaster Genetic Reference Panel. *Genetics*, *207*(3), 1181–1193. https://doi.org/10.1534/genetics.117.300310

Schoenfelder, S., & Fraser, P. (2019). Long-range enhancer–promoter contacts in gene expression control. *Nature Reviews Genetics*, *20*(8), 437–455. https://doi.org/10.1038/s41576-019-0128-0

Siewert, K. M., & Voight, B. F. (2020). BetaScan2: Standardized Statistics to Detect Balancing Selection Utilizing Substitution Data. *Genome Biology and Evolution*, *12*(2), 3873–3877. https://doi.org/10.1093/gbe/evaa013

Skov, L., Macià, M. C., Lucotte, E., Cavassim, M. I. A., Castellano, D., Mailund, T., Schierup, M. H., & Munch, K. (2018). *Strong selective sweeps before 45,000BP displaced archaic admixture across the human X chromosome* [Preprint]. Genomics. https://doi.org/10.1101/503995

Smith, J. M., & Haigh, J. (1974). The hitch-hiking effect of a favourable gene. *Genetical Research*, *23*(1), 23–35.

Speidel, L., Forest, M., Shi, S., & Myers, S. R. (2019). A method for genome-wide genealogy estimation for thousands of samples. *Nature Genetics*, *51*(9), 1321–1329. https://doi.org/10.1038/s41588-019-0484-x

Square, T. A., Sundaram, S., Mackey, E. J., & Miller, C. T. (2021). Distinct tooth regeneration systems deploy a conserved battery of genes. *EvoDevo*, *12*(1), 4. https://doi.org/10.1186/s13227-021-00172-3

Stern, A. J., Speidel, L., Zaitlen, N. A., & Nielsen, R. (2021). Disentangling selection on genetically correlated polygenic traits via whole-genome genealogies. *The American Journal of Human Genetics*, *108*(2), 219–239. https://doi.org/10.1016/j.ajhg.2020.12.005

Szpiech, Z. A., & Hernandez, R. D. (2014). selscan: An Efficient Multithreaded Program to Perform EHH-Based Scans for Positive Selection. *Molecular Biology and Evolution*, *31*(10), 2824–2827. https://doi.org/10.1093/molbev/msu211

Tajima, F. (1989). Statistical method for testing the neutral mutation hypothesis by DNA polymorphism. *Genetics*, *123*(3), 585–595.

Terekhanova, M.V., Logacheva, M.D., Penin, A.A., Neretina, T.V., Barmintseva, A.E., Bazykin, G.A., Kondrashov, A.S., & Mugue, N.S. (2014). Fast Evolution from Precast Bricks: Genomics of young Freshwater Populations of Threespine Stickleback Gasterosteus aculeatus. PLoS Genetics, 10(10), e1004696. https://doi.org/10.1371/journal.pgen.1004696

Terhorst, J., Kamm, J. A., & Song, Y. S. (2017). Robust and scalable inference of population history from hundreds of unphased whole genomes. *Nature Genetics*, *49*(2), 303–309. https://doi.org/10.1038/ng.3748

Thorson, R. M. (1980). Ice-Sheet Glaciation of the Puget Lowland, Washington, during the Vashon Stade (Late Pleistocene). *Quaternary Research*, *13*(3), 303–321. https://doi.org/10.1016/0033-5894(80)90059-9

Voight, B. F., Kudaravalli, S., Wen, X., & Pritchard, J. K. (2006). A Map of Recent Positive Selection in the Human Genome. *PLoS Biology*, *4*(3), e72. https://doi.org/10.1371/journal.pbio.0040072

Wang, M. (2018). *The Genetic Basis of Adaptation and Speciation in Benthic and Limnetic Threespine Stickleback (Gasterosteus aculeatus)* [Universität Tübingen]. https://doi.org/10.15496/PUBLIKATION-25212

Whatcom Conservation District. (2020). *NRCS National Water Quality Initiative (NWQI) Watershed Assessment: Fishtrap Creek Watershed*.